

University of Alberta

**Interactions of Designed Transmembrane α -Helical Model
Peptides with Phospholipid Bilayer Model Membranes**

By

Feng Liu



**A thesis submitted to the Faculty of Graduate Studies and
Research in partial fulfillment of the requirements for the
degree of Doctor of Philosophy**

Department of Biochemistry

Edmonton, Alberta

Fall 2004



Library and
Archives Canada

Bibliothèque et
Archives Canada

Published Heritage
Branch

Direction du
Patrimoine de l'édition

395 Wellington Street
Ottawa ON K1A 0N4
Canada

395, rue Wellington
Ottawa ON K1A 0N4
Canada

Your file *Votre référence*
ISBN: 0-612-95972-4
Our file *Notre référence*
ISBN: 0-612-95972-4

The author has granted a non-exclusive license allowing the Library and Archives Canada to reproduce, loan, distribute or sell copies of this thesis in microform, paper or electronic formats.

L'auteur a accordé une licence non exclusive permettant à la Bibliothèque et Archives Canada de reproduire, prêter, distribuer ou vendre des copies de cette thèse sous la forme de microfiche/film, de reproduction sur papier ou sur format électronique.

The author retains ownership of the copyright in this thesis. Neither the thesis nor substantial extracts from it may be printed or otherwise reproduced without the author's permission.

L'auteur conserve la propriété du droit d'auteur qui protège cette thèse. Ni la thèse ni des extraits substantiels de celle-ci ne doivent être imprimés ou autrement reproduits sans son autorisation.

In compliance with the Canadian Privacy Act some supporting forms may have been removed from this thesis.

Conformément à la loi canadienne sur la protection de la vie privée, quelques formulaires secondaires ont été enlevés de cette thèse.

While these forms may be included in the document page count, their removal does not represent any loss of content from the thesis.

Bien que ces formulaires aient inclus dans la pagination, il n'y aura aucun contenu manquant.

Canada

To my daughter Grace for all the happiness she has brought us.

To my wife Wei for her understanding and support

To my mother Ai-Hua and in memory of my father Zhao-Rong

ACKNOWLEDGEMENTS

I am deeply indebted to my supervisor, Dr. Ronald McElhaney, for his excellent supervision, guidance, support and encouragement throughout this work.

My sincere thanks are due to Dr. Ruthven Lewis for his patience and invaluable support in many of the experimental and data analysis processes, and to Dr. David Mannock for his inspirations and many helpful suggestions.

I would also like to thank Dr. Elmar Prenner for helpful suggestions, and Mrs. Monica Kiricsi and Dr. Thomas Abraham for their encouragement.

I am grateful to Dr. Robert Hodges for his direction and for the synthesis of the transmembrane peptides and to Dr. Brian Sykes for his direction and for the generous availability of time on the NMR spectrometer.

Finally, I would like to thank the Department of Biochemistry, Faculty of Medicine and Dentistry, the University of Alberta, and the Canadian Institute of Health Research for financial support during my studies.

TABLE OF CONTENTS

	Page
Chapter I. General Introduction1
Functions of Membranes1
Composition and Structure of Membranes2
Membrane Lipid Structures4
Biophysical Techniques for the Study of Lipid Phase Behavior and Organization7
Membrane Lipid Phase Properties9
Membrane Proteins	...12
Protein-Lipid Interactions	...14
Studies of Protein-Lipid Interactions by Model Transmembrane Peptide	...18
References	...26
Chapter II. Effect of Variations in the Structure of a Polyleucine-Based α - Helical Transmembrane Peptide on Its Interaction with Phosphatidylcholine Bilayers	
Introduction	...40
Materials and Methods	...44
Results	...46
Thermotropic Phase Behavior of Phosphatidylcholine Bilayers in the Absence of Peptide	...47
The Effect of Peptide Incorporation on the Pretransition	...48
The Effect of Peptide Incorporation on the Main Transition	...49
Fourier Transform Infrared Spectroscopy Studies of Peptide- Containing PC Bilayers	...52
Discussion	...55
References	...65

Chapter III. Effect of Variations in the Structure of a Polyleucine-Based α -Helical Transmembrane Peptide on Its Interaction with Phosphatidylglycerol Bilayers

Introduction	...84
Materials and Methods	...89
Results	...90
Thermotropic Phase Behavior of PG Bilayers in the Absence of Peptide	...90
The Effect of Peptide Incorporation on the Pretransition	...91
The Effect of Peptide Incorporation on the Main Transition	...92
Fourier Transform Infrared Spectroscopic Studies of Peptide- Containing PG Bilayers	...95
Discussion	...99
References	..105

Chapter IV. Effect of Variations in the Structure of a Polyleucine-Based α -Helical Transmembrane Peptide on Its Interaction with Phosphatidylethanolamine Bilayers

Introduction	..122
Materials and Methods	..127
Results	..128
Thermotropic Phase Behavior of PE Bilayers in the Absence of Peptides	..130
Thermotropic Phase Behavior of Various PE Bilayers in the Presence of L ₂₄	..130
Thermotropic Phase Behavior of PE Bilayers in the Presence of Various Peptides	..134
Fourier Transform Infrared Spectroscopic Studies of Peptide- Containing PE Bilayers	..137

Discussion	..139
References	..148
Chapter V. A Differential Scanning Calorimetric and ³¹ P-NMR Spectroscopic Study of the Effect of Transmembrane α -Helical Peptides on the Lamellar/Reversed Hexagonal Phase Transition of Phosphatidylethanolamine Model Membranes	
Introduction	..166
Materials and Methods	..171
Results	..172
Discussion	..179
References	..185
Chapter VI. General Discussion	
Hydrophobic Mismatch between Peptides and Phospholipids	..203
H-bonding and Electrostatic Interactions between Peptides and Lipids	..205
Are L ₂₄ and Its Analogues Good Transmembrane Model Peptides?	..207
Role of Lysine Snorkeling in Peptide-Lipid Interactions	..210
Role of Interfacially-localized Tryptophan Residues in Peptide-Lipid Interactions	..212
Effects of Peptides on the L _{α} /H _{II} Phase Transition of DEPE Matrix	..216
Future Directions	..218
References	..221
Appendix 1. Differential Scanning Calorimetry and ² H-Nuclear Magnetic Resonance and Fourier Transform Infrared Spectroscopy Studies of the Effects of Transmembrane α -Helical Peptides on the Organization of Phosphatidylcholine Bilayers	
	..226

LIST OF TABLES

Table II-1. Hydrophobic thickness of bilayers formed by various phosphatidylcholines.

Table IV-1. Hydrophobic thickness of bilayers formed by various phosphatidylethanolamines.

LIST OF FIGURES

Figure I-1. Representative structures for selected membrane lipids.

Figure I-2. The time-averaged distributions of the principle structural groups of dioleoylphosphatidylcholine, together with the resulting polarity profile

Figure I-3. Polymorphic phases and molecular shapes for some membrane lipids.

Figure I-4. ^{31}P -NMR characteristics of phospholipids in various phases.

Figure II-1. Effect of L_{24} on the DSC heating thermograms of a series of *n*-saturated diacyl-PCs varying in hydrocarbon chain length.

Figure II-2. Illustration of the results of the curve-fitting procedure used to resolve the components of the DSC heating thermograms exhibited by mixtures of L_{24} with PC bilayers.

Figure II-3. Effect of L_{24} concentration on the peak temperature of the two components of the DSC thermograms exhibited by the mixtures of L_{24} and the *n*-saturated diacyl-PCs studied.

Figure II-4. Plot of the differences of the transition temperatures of the peptide-associated and the bulk lipids versus the mean hydrophobic thickness of the lipid bilayer at a peptide concentration of 3.3 mol %.

Figure II-5. Effect of L_{24} concentration on the transition enthalpies of the two components of the DSC thermograms exhibited by mixtures of peptides and *n*-saturated diacyl PCs.

Figure II-6. Effect of L_{24} concentration on the cooperativity ($\Delta T_{1/2}$) of the broad component of the DSC thermograms of the various PCs studied.

Figure II-7. Comparison of the effects of variations in the concentration of L₂₄, L₂₄DAP and W-L₂₂-W on the cooperativity ($\Delta T_{1/2}$) of the broad component of the DSC thermograms in the mixtures of peptide and 17:0 PC.

Figure II-8. Combined plots of CH₂ symmetric stretch, peptide amide I band, and DSC thermograms as a function of temperature for systems of L₂₄/13:0, 15:0, 17:0, and 19:0 PC.

Figure II-9. Combined plots of CH₂ symmetric stretch, peptide amide I band, and calorimetric thermograms as a function of temperature for systems of L₂₄, L₂₄DAP, W-L₂₂-W and 19:0 PC.

Figure II-10. Amide I band contours exhibited by the peptides L₂₄, L₂₄DAP and W-L₂₂-W incorporated into 19:0 PC bilayers.

Figure III-1. Effect of L₂₄ on the DSC thermograms of a series of *n*-saturated diacyl-PGs.

Figure III-2. Illustration of the curve-fitting procedure used to resolve the components of the DSC heating thermograms.

Figure III-3. Effects of L₂₄ concentration on the peak temperatures of the two components of the DSC thermograms exhibited by the mixtures of L₂₄ and the *n*-saturated diacyl-PGs.

Figure III-4. Plot of the differences of the transition temperatures of the peptide-associated and the peptide-poor PGs versus the hydrophobic chain length of the lipid bilayer at a peptide concentration of 3.3 mol%.

Figure III-5. Effects of L_{24} concentration on the transition enthalpies of the two components of the DSC thermograms exhibited by mixtures of L_{24} and n -saturated diacyl-PGs.

Figure III-6. Comparison of the effects of L_{24} concentration on the transition enthalpies of $L_{24}/15:0$ PG mixture with that on the transition enthalpies of $L_{24}/15:0$ PC mixture.

Figure III-7. Effect of NaCl concentration on the phase behaviors of $L_{24}/16:0$ PG mixtures at a peptide concentration of 3.3 mol%.

Figure III-8. FTIR spectra of gel and the liquid-crystalline phase formed by a mixture of L_{24} with 16:0 PG at a peptide concentration of 3.3 mol%.

Figure III-9. Combined plots of CH_2 symmetric stretch, peptide amide I band, and calorimetric thermograms as a function of temperature for systems of $L_{24}/16:0$ PG at a peptide concentration of 3.3 mol%.

Figure III-10. (A). The asymmetrical phosphate stretching regions of infrared spectra of 16:0 PG alone in the gel and the liquid-crystalline phases. (B) The asymmetrical phosphate stretching regions of infrared spectra of pure 16:0 PG, $L_{24}/16:0$ PG, $L_{24}DAP/16:0$ PG and $WL_{22}W/16:0$ PG at a peptide concentration of 3.3 mol%.

Figure IV-1. Effect of L_{24} on the DSC thermograms of a series of n -saturated diacyl-PEs.

Figure IV-2. Effects of L_{24} concentration on the peak temperatures of the two components of the DSC thermograms exhibited by the mixtures of L_{24} and the n -saturated diacyl-PEs.

Figure IV-3. Hydrocarbon chain length dependence of the differences (ΔT) between the transition temperatures of the peptide-rich and the peptide-poor PE components of

DSC thermograms exhibited by L₂₄/PE mixtures at a peptide concentration of 3.3 mol%. To facilitate comparison, comparable data obtained from studies of L₂₄ with PC bilayers are also shown.

Figure IV-4. Peptide-concentration dependent changes in the enthalpy of the thermotropic transitions exhibited by L₂₄-containing PE bilayers.

Figure IV-5. A comparison of the effects of L₂₄, L₂₄DAP and WL₂₂W on the DSC thermograms of 16:0 PE.

Figure IV-6. Hydrocarbon chain length dependence of the differences (ΔT) between the transition temperatures of the peptide-rich and the peptide-poor PE components of DSC thermograms exhibited by Peptide/PE mixtures at a peptide concentration of 3.3 mol%.

Figure IV-7. Effects of L₂₄, WL₂₂W, and L₂₄DAP concentration on the total transition enthalpies of 12:0, 14:0, 16:0, and 18:0 PE bilayers.

Figure IV-8. Plot of the transition width versus the hydrophobic chain length of the lipid bilayer at a peptide concentration of 3.3 mol%.

Figure IV-9. The C=O stretching and amide-I bands of the FTIR spectra exhibited by L₂₄-containing PE bilayers.

Figure IV-10. The C=O stretching and amide-I bands of the FTIR spectra exhibited by peptide-containing 16:0 PE bilayers.

Figure V-1. DSC heating and cooling thermograms illustrating the thermotropic phase behavior of aqueous dispersions of DEPE in the absence of peptides.

Figure V-2. DSC heating thermograms illustrating the effect of incorporation of the peptide L₂₄ on the L _{β} -L _{α} phase transition of DEPE.

Figure V-3. DSC heating (A) and cooling (B) thermograms illustrating the effect of the incorporation of peptide L₂₄ on the L_α-H_{II} phase transition of DEPE.

Figure V-4. Effect of peptide concentration on the enthalpy of the L_α-H_{II} phase transition of DEPE.

Figure V-5. Effects of peptide concentration on the L_α-H_{II} phase transition temperature of DEPE.

Figure V-6. Effect of the incorporation of peptide P₁₆ on the L_α-H_{II} phase transition of DEPE. Panel A shows DSC heating thermograms of the L_α-H_{II} phase transitions exhibited by vesicles composed of DEPE and the peptide P₁₆. Panel B shows a comparison of the concentration dependent changes in the T_h of DEPE induced by the peptides P₁₆ and L₂₄.

Figure V-7. Effects of peptide incorporation on the L_α-H_{II} phase transition of DPEPE. Panel A shows DSC heating thermograms of the L_α-H_{II} phase transitions exhibited by vesicles composed of DPEPE and the peptide W-L₂₂-W. Panel B shows a comparison of the peptide-induced depression in the T_h of DPEPE and DEPE.

Figure V-8. DSC heating (A) and cooling (B) thermograms illustrating the effect of scan rate on the L_α-H_{II} phase transitions that were examined.

Figure V-9. Effect of scan rate on the L_α-H_{II} phase transition temperatures of peptide-free and peptide-containing DEPE vesicles.

Figure V-10. Proton decoupled ³¹P-NMR spectra exhibited by peptide-free (A) and peptide-containing (B and C) DEPE preparations.

LIST OF ABBREVIATIONS

Phospholipids

PC	phosphatidylcholine, where the number before the colon represents the total number of carbon atoms in the hydrocarbon chains and the number after the colon represents the number of double bonds.
PG	phosphatidylglycerol
PE	phosphatidylethanolamine
PS	phosphatidylserine
DEPE	dielaidoylphosphatidylethanolamine (di-18:1 _t PE)
DPEPE	dipalmitelaidoylphosphatidylethanolamine (di-16:1 _t PE)
POPC	1-palmitoyl-2-oleoyl-phosphatidylcholine (16:0/18:1 _c PC)

Amino acids and peptides

DAP	L-2,3-diaminopropionic acid
P ₂₄	acetyl-Lys ₂ -Gly-Leu ₂₄ -Lys ₂ -Ala-amide
P ₁₆	acetyl-Lys ₂ -Gly-Leu ₁₆ -Lys ₂ -Ala-amide
L ₂₄	acetyl-Lys ₂ -Leu ₂₄ -Lys ₂ -amide
L ₂₄ -DAP	acetyl-DAP ₂ -Leu ₂₄ -DAP ₂ -amide
W-L ₂₂ -W	acetyl-Lys ₂ -Trp-Leu ₂₂ -Trp-Lys ₂ -amide;
(LA) ₁₂	acetyl-Lys ₂ -(Leu-Ala) ₁₂ -Lys ₂ -amide

A ₂₄	acetyl-Lys ₂ -Ala ₂₄ -Lys ₂ -amide
WALP	acetyl-Gly-Trp ₂ -(Leu-Ala) _n -Trp ₂ -Ala-ethanolamine
KALP	acetyl-Gly-Lys ₂ -(Leu-Ala) _n -Lys ₂ -Ala-ethanolamine

Phase properties

P _β '	rippled gel phase with tilted hydrocarbon chains
L _β '	lamellar gel phase with tilted hydrocarbon chains
L _β	lamellar gel phase with untilted hydrocarbon chains
L _α	lamellar liquid crystalline phase
H _{II}	inverted hexagonal phase
Q _{II}	cubic phase

Techniques

DSC	differential scanning calorimetry
FTIR	Fourier transform infrared
ESR	electron spin resonance
³¹ P-NMR	phosphorous-31 nuclear magnetic resonance
² H-NMR	deuterium nuclear magnetic resonance
CD	circular dichroism
T _m	gel/liquid-crystalline phase transition temperature
T _h	lamellar liquid-crystalline to inverted hexagonal phase transition temperature

ΔH phase transition enthalpy

$\Delta T_{1/2}$ the width of transition at half height

ΔT the shift of the T_m of the broad component relative to that of the sharp component

CHAPTER I. General Introduction

Functions of membranes

Biological membranes play many central and indispensable roles in the structure and function of all living cells (1). The plasma or limiting membranes give prokaryotic and eukaryotic cells their individuality by defining the cell boundary and by separating cells from their environment. In eukaryotic cells, internal membrane systems define the various organelles and compartments which make up these more complex cell types. The functional specialization of eukaryotic cells in the course of evolution has been closely linked to the formation of specialized intracellular organelles and compartments. In fact a key step in the emergence of life was likely the development of a membranous structure which enclosed a discrete compartment of aqueous solution containing the requisite suite of organic components required for the chemical evolution of living systems (2).

Biological membranes, in addition to defining the cell, also control the passive or active flow of material and information between cells and their environment or between different compartments in eukaryotic cells (1). Thus membranes act as both a highly selective filter and as a device for the active transport of various biochemical compounds and ions; they control the entry of nutrients and the exit of waste products; and they generate differences in the ion concentrations between the interior and exterior of the cell. Plasma membranes also function as both a sensor and a generator of chemical and physical signals. Thus membranes play a central role in modulating interactions between the cell and its environment and, especially in multicellular organisms, in modulating the interactions between different cell types.

Many important enzymes are attached to or are associated with biological membranes, particularly those involved in cellular signaling and the biosynthesis of membrane lipids and fat-soluble vitamins and hormones. Other enzymes which catalyze reactions in which water must be excluded are embedded in the membrane lipid bilayer, which presumably provides a hydrophobic medium in which such interactions can occur more efficiently. The two most important energy conversion processes in biological systems, oxidative phosphorylation and photosynthesis, are carried out by membrane systems (3). Since in both cases these processes depend on generating an electrochemical proton gradient between two compartments, the involvement of a membrane barrier in such a process is mandatory. Moreover, the lateral organization and vectorial orientation of various membrane proteins in the lipid bilayer is crucial to the functions of these and other energy transduction systems, as is the semipermeable nature of the lipid bilayer itself to protons and other ions.

Composition and structure of membranes

The two major components of membranes are lipids and proteins. Carbohydrates may also be present although they are almost exclusively in the form of glycolipid or glycoprotein. The relative mass ratios of lipids and proteins varies widely, from about 4:1 in relatively biologically inactive, insulating membranes such as myelin, to about 1:4 in biologically active membranes like the mitochondrion inner membrane (4). Plasma membranes typically have approximately equal amounts by weight of lipid and protein, meaning that the lipid-to-protein mole ratio in such membranes is about 100:1. Of course the particular spectra of lipid and protein molecular species present in each membrane system is quantitatively and often qualitatively unique, not only from one species to

another, but in multicellular organisms, from one type of cells to another, and in eukaryotic cells, from one membrane system to another within the same cell.

Biological membranes are generally sheetlike structures with a thickness between 60Å and 100Å that form closed boundaries between different compartments (5). Because the two faces of biological membranes encounter different environments, they are usually quite different in lipid and protein composition. For example, in human erythrocyte membranes, phosphatidylcholine (PC) and sphingomyelin are largely found on the outer leaflet, while phosphatidylethanolamine (PE) and phosphatidylserine (PS) are largely found on the inner leaflet of the bilayer (6). In addition, most biological membranes are electrically polarized, with the inside negative (typically –60 milivolts), which plays a key role in transport, energy conversion, and excitability (7).

All biological membranes are noncovalent assemblies of lipids and proteins. In 1972, Singer and Nicholson (8) proposed a fluid-mosaic model for the overall membrane organization and the interplay between lipids and proteins in biological membranes. In this model, the membrane phospholipids, glycolipids, and sterols are organized in a bilayer that serves both as a solvent for membrane proteins and as a permeability barrier. A proportion of membrane lipids are in contact with membrane proteins and are essential for their functions. The membrane lipids and proteins were proposed to move freely, both laterally and rotationally, in the lipid matrix, but not to flip-flop from one side of the membrane to the other. However, in the following years, biophysical studies indicated that the diffusion of membrane proteins in the fluid lipid bilayer is far from being unrestricted and some evidence indicates the formation of lateral microdomains in biological membranes, such as membrane rafts that are highly enriched in sphingolipids,

cholesterol and lipid-modified proteins (9). However, the evidence which has been reported to support the existence of membrane rafts in the biological membranes is considered unconvincing by many workers and questions concerning their nature, or even their existence, remain (10-12).

Membrane lipid structures

Glycerophospholipids are the major structural components in the majority of animal and bacterial cell membranes. Glycerophospholipids consist of a glycerol backbone, two fatty acids that are attached to the first and second carbons of glycerol through an ester linkage, and a highly polar and charged group that is attached through a phosphodiester linkage to the third carbon of glycerol backbone (Figure 1). The phosphate group in turn is usually linked by an ester linkage to one of several polar alcohols, including choline, ethanolamine, serine and glycerol. PC and PE have choline and ethanolamine as their polar headgroups, respectively, and are both zwitterionic. PC and PE are the major lipid components found in animal cell membranes (13), although PE can also be a major lipid component of some bacterial membranes as well (14). Phosphatidylglycerol (PG) and PS contain glycerol and serine as their polar headgroups and are both anionic. PS is usually the major anionic lipid component of animal cell membranes (13), while PG is the predominant (and often the only) anionic lipid component of bacterial membranes (14).

Glycerophospholipids generally have an amphipathic structure in which the lipid polar headgroups are hydrophilic and the lipid hydrocarbon chains are hydrophobic. The time-averaged positions of the principal structural groups of dioleoylphosphatidylcholine in a liquid-crystalline bilayer are shown in Figure 2 (15). A plot of the charge density distribution across the bilayer shows that the hydrocarbon chains form a uniformly

apolar environment in the interior of the bilayer, whereas the polar headgroup and glycerol backbone separate the hydrophobic membrane interior from the bulk water phase. The polarity of the hydrocarbon core is negligible, but polarity rises sharply in the interfacial region. Therefore, in the interfacial region, a small change in position relative to the bilayer center may result in a large change in polarity.

Typically glycerophospholipids contain even-numbered acyl chains with a wide range of chain structures and with chain lengths ranging from 14 to 24 carbon atoms. Many phospholipid molecules contain one saturated and one unsaturated chain. In animal cells and most bacteria, the saturated fatty acid is usually linked to the first carbon of the glycerol backbone and the unsaturated chain to the second carbon of glycerol backbone, both through an ester linkage (16). Bacteria contain only monounsaturated fatty acids but eukaryotes contain polyunsaturated fatty acids as well. The most common unsaturated fatty acyl chains in eukaryotes are 18:1 (oleic acid), 18:2 (linoleic acid), 18:3 (linolenic acid), and 20:4 (arachidonic acid), where the first number is the number of carbon atoms and the second one is the number of double bond). The double bonds found in natural phospholipids are nearly always *cis* rather than *trans*, which imparts a permanent kink or bend to the hydrocarbon chains. In some bacterial membranes, the glycerophospholipids may contain branched or cyclic fatty acyl chains, which play a similar role in chain packing to *cis*-double bonds by increasing the lipid molecular area and decreasing the chain-melting phase transition temperature.

Besides glycerophospholipids, biological membranes contain many other lipid species with different polar headgroups (Figure 1). Glycoglycerolipids possess a polar headgroup consisting of one or two sugar molecules which are attached through a

glycosidic linkage to the third carbon of glycerol, with two fatty acyl chains attached to the first and second carbons of the glycerol backbone. These are the predominant lipids in many bacteria and in chloroplast and plant cell membranes (14,17). Sphingolipids consist of the long-chain amino alcohol sphingosine, one long-chain fatty acid linked to sphingosine by an amide bond, and one polar headgroup, either a phosphorylated alcohol or one or more sugar molecules, that is linked to sphingosine either by a phosphodiester linkage or by a glycosidic linkage, respectively. Sphingolipids are normally the second largest class of polar membrane lipids in eukaryotic cells (13). Sterols are the major nonpolar structural lipids found in highest quantities in the plasma membranes of plant, animal, and eukaryotic microbial membranes, but are absent from prokaryotes. Sterols consist of a rigid steroid nucleus containing four fused rings, three with six carbons and one with five, and an alkyl side chain of 8-10 carbon atoms. Cholesterol is the most abundant sterol in animal tissues. It is a weakly amphipathic molecule with a small polar hydroxyl group and a large nonpolar hydrocarbon region (the steroid nucleus and hydrocarbon side chain). It may constitute 30% of the mass of the membrane lipids of some animal cell plasma membranes (18).

It is obvious from the above that membrane lipids contain a wide range of polar headgroups and hydrocarbon chains. To date, it still remains largely unknown why so many different kinds and molecular species of lipids are required to form a functional membrane. Several studies have shown that specific interactions may occur between membrane lipids and integral membrane proteins, indicating that membrane lipids are necessary for membrane protein stability and function (19-21). In addition, a number of biophysical techniques have been applied to elucidate the structural and physical

properties of individual lipid component from biological membranes and their relationship to membrane function.

Biophysical techniques for the study of lipid phase behavior and organization

Differential scanning calorimetry (DSC)

DSC is a thermodynamic technique which has proven of exceptional value in the study of the lipid phase behavior (22). In a DSC instrument there are two cells, the sample cell containing a suspension of lipid or membrane in aqueous buffer, and the reference cell containing buffer alone. Both cells are heated at the same rate and their temperature is monitored continuously. The temperatures of the sample and reference cells initially increase linearly with time and the temperature difference between them is maintained at zero. If the sample undergoes a thermally induced event, such as a phospholipid chain-melting phase transition, the heat capacity of the sample cell increases dramatically, thus more heat is required to maintain the same temperature in the two cells. This energy is recorded as the excessive specific heat as a function of temperature. A number of important thermodynamic parameters can be directly determined from a DSC curve: (i) T_m refers to the phase transition temperature where the excessive specific heat reaches the maximum; (ii) $\Delta T_{1/2}$ represents the intermolecular cooperativity of the lipid phase transition and is defined as the width of the DSC curve at half height; and (iii) ΔH represents the enthalpy of the transition and is determined by the area under the curve. DSC may also be used to study the thermal unfolding or denaturation of peptides or proteins in aqueous buffer or in model lipid or in biological membranes. Since the model peptides utilized in this work do not experience any

significant conformational change in the temperature range examined, DSC will be only utilized here to the study of lipid phase behavior.

Fourier transform infrared (FTIR) spectroscopy

FTIR spectroscopy is a non-perturbing technique to determine the conformational state and organization of phospholipid bilayers (23). Briefly, FTIR spectroscopy is based on the vibrational modes of particular chemical moieties which will undergo a transition between two vibrational states upon absorption of radiation at a given frequency. The transitions of different chemical bonds exhibit unique spectral band frequency maxima. In addition, changes in the conformation and the environment can also affect the absorption frequency and the bandwidth. In solution FTIR experiments, a number of different bands work well as spectroscopic probes of phospholipid bilayers (23). The CH₂ symmetric stretching band near 2850 cm⁻¹ is widely used to monitor the state of the rotational isomeric disorder of the lipid hydrocarbon chains. The ester carbonyl stretching bands near 1735 cm⁻¹ and the O-P-O asymmetrical stretching bands nears 1215 cm⁻¹ can be used to monitor changes in the hydration and/or polarity of the polar/apolar interfacial region and the phosphate polar headgroup of the lipid bilayer, respectively. Moreover, FTIR spectroscopy can also be used to determine peptide secondary structure by monitoring the conformationally sensitive amide I band near 1650 cm⁻¹ (24).

³¹P-nuclear magnetic resonance (³¹P-NMR)

³¹P-NMR is a convenient tool to study the phase state of phospholipids (25). In brief, a nuclear spin acts like a tiny bar magnet and may have two or more favorable orientations (spin states) in the presence of an applied magnetic field. A transient radiofrequency pulse is then used to induce a net transition between different spin states,

which will then decay back to equilibrium over time. From this relaxation process, information on both molecular order and motional rates can be derived. In the case of ^{31}P -NMR, the magnetic field experienced by the phosphorous nuclear spin is reduced by the bonding electrons. If the electron density is not isotropic, the chemical shielding will be the smallest (largest) along the molecular axis with the lowest (highest) electron density. Depending on the orientation of the phosphate, and thus the orientation of the lipid bilayer to the magnetic field, the resonance frequency varies between -23 and $+12$ parts per million. The polar headgroups of phospholipids in different phases have different rates and range of motions and thus have distinct ^{31}P -NMR spectra (see next section).

Membrane lipid phase properties

The lipids of biological membranes are usually organized as a lamellar liquid-crystalline lipid bilayer under physiologically relevant conditions. However, when isolated from biological membranes, individual lipids can form many different phases in aqueous buffer, depending primarily on the temperature and the effective shape of the lipid molecule. When the cross-sectional area of the polar headgroup of a lipid is almost equal to that of the hydrocarbon chains, such as with PC, the lipid molecule has a cylindrical shape and forms a lamellar phase. When the cross-sectional area of the polar headgroup of a lipid is smaller or larger than that of the hydrocarbon chains, the lipid molecule is cone-shaped or inverted-cone-shaped and forms either cubic or inverted-hexagonal and normal micellar phases, respectively (Figure 3) (25).

Lamellar gel phase (L_{β})

This two-dimensional phase is formed at lower temperatures in those lipids which form the lamellar structure. In this phase, the polar headgroups of the lipids face the

aqueous phase on both sides of the bilayer and the hydrocarbon chains oppose each other inside the lipid bilayer. In this phase, the hydrocarbon chains of the lipid are in an all-*trans* configuration and are much more ordered than in the lamellar liquid-crystalline phase. Therefore, the lipids in the L_{β} phase are packed more tightly together and have a smaller cross-sectional area per molecule and a greater hydrophobic thickness than in the lamellar liquid-crystalline phase. In the gel phase, the motional rate of hydrocarbon chains is much lower than that of the liquid-crystalline phase. The rates of lateral and rotational diffusion of phospholipids in the plane of the membrane are decreased by about two or three orders of magnitude compared with those in the liquid-crystalline phase.

Lamellar liquid-crystalline phase (L_{α})

This two-dimensional fluid phase is the form adopted by lipids in biological membranes under physiologically relevant conditions. In this phase, the polar headgroups of the lipids face the aqueous phase on both sides of the bilayer and the hydrocarbon chains oppose each other inside the lipid bilayer. In this phase, the lipid hydrocarbon chains contain a number of *gauche* rotational conformers. Therefore, the lipids are packed less tightly and have a larger cross-sectional area and a thinner hydrophobic thickness than in the L_{β} phase. The motional rates of the lipid molecule are much higher in liquid-crystalline phase than in L_{β} phase. Generally, the lipids diffuse freely laterally and rotationally in the liquid-crystalline phase, but lipid transverse diffusion or flip-flop is slow. The ^{31}P -NMR spectrum of L_{α} phase consists of a lower field shoulder and a higher field peak (Figure 4).

Inverted-hexagonal phase (H_{II})

The lipids in the three-dimensional H_{II} phase are in the form of cylinders which are packed in a hexagonal pattern. In this phase, the hydrocarbon chains face the outside, while the polar headgroups face the inside, where there is a column of water. The lipid hydrocarbon chains are in a disordered liquid-crystalline state. Biological membranes contain a significant portion of lipids, such as PE, that favor the H_{II} phase when isolated from other membrane components. The ^{31}P -NMR spectrum of H_{II} phase consists of a lower field peak and a higher field shoulder with a spectral width which is half that of the L_{α} phase (Figure 4).

Cubic phase (Q_{II})

This three-dimensional phase has structural characteristics that are intermediate between a lamellar phase and a H_{II} phase. There are two distinct classes of cubic phases (26). One is bicontinuous and consists of two sets of short tubes that are intertwined and unconnected. There are three different bicontinuous cubic phases with different surfaces of minimal area: the primitive, the gyroid, and the diamond. The other is discontinuous and consists of discrete micellar or inverted micellar aggregates. In the cubic phase, phospholipids experience all possible orientations on a relatively short time scale. Therefore, in ^{31}P -NMR spectra, cubic phases behave as an isotropic phase (Figure 4).

Micelles

This phase is formed by glycosphingolipids, lysophosphatidylcholines and many detergents. The lipids in the micellar phase are in the form of aggregates with a spherical or globular shape. In a micelle, the polar headgroups face the outside and are in contact with water while the hydrocarbon portions fill the interior of the sphere. The micellar

phase can be considered a one-dimensional phase in excess water, since the lipid micelles can diffuse and tumble rapidly in the water phase.

Lipid phase transitions

Membrane lipids can exist in a variety of different kinds of organized structures, particularly when fully hydrated. The particular structure which predominates depends on not only the structure of the lipid molecular itself but also on variables such as temperature, pressure, ionic strength, and pH. The most extensively studied lipid phase transitions are those between the L_{β} and L_{α} phases. In this chain-melting phase transition, the hydrocarbon chains are converted from an ordered all-*trans* conformation in the L_{β} phase to a less ordered conformation in the L_{α} phase in which the hydrocarbon chains contain a number of *gauche* conformers. Therefore, the L_{β}/L_{α} phase transition is accompanied by a pronounced lateral expansion and a concomitant decrease in the thickness of the bilayers. Thermodynamically, the L_{β}/L_{α} phase transitions occur when the entropic reduction in free energy arising from chain isomerism counterbalances the decrease in bilayer cohesive energy arising from the lateral expansion and from the energy of creating *gauche* conformers in the hydrocarbon chains.

Another intensively studied lipid phase transition is that between the two-dimensional L_{α} phase to the three-dimensional H_{II} phase. This phase transition is much less energetic and has slower kinetics than the L_{β}/L_{α} phase transition. However, the mechanism by which the conversions between the L_{α} and the H_{II} phases takes place is poorly understood to date.

Membrane proteins

Although the lipid bilayers form the fundamental structural scaffold of biological membranes, most specific membrane functions are carried out by associated or embedded membrane proteins. Membrane proteins can thus be divided into two broad structural groups: peripheral and integral proteins. Peripheral proteins are bound to membrane surfaces through electrostatic and H-bonding interactions with the polar headgroups of membrane lipids or with the hydrophilic domains of other membrane proteins, or through one or more covalently linked fatty acids or isoprenoid chains that insert into the lipid bilayer, such as myristic (14:0) or palmitic (16:0) acids, farnesyl or geranylgeranyl groups, or glycosylated derivatives of phosphatidylinositol (27). For example, annexins are a class of peripheral membrane proteins that can bind to the surface of bilayers containing anionic phospholipids (27). Integral or transmembrane proteins are very firmly associated with the membrane through one or more mainly hydrophobic transmembrane segments. Although about one-third of all proteins are integral membrane proteins, only relatively a few of protein structures deposited in the Protein Data Bank are integral membrane proteins (28). This is because of the difficulties in both the expression of membrane proteins in large quantities *in vitro* and the structural determination of membrane proteins in a membrane environment by NMR, X-ray diffraction, and other biophysical methods.

The integral membrane proteins can in turn be divided into two structural classes. Some integral proteins in the outer membranes of prokaryotes contain β -barrels, in which 20 or more transmembrane segments form β -sheets that traverse the lipid bilayer. For example, the porin FhuA of the *Escherichia coli* outer membrane contains a β -barrel

composed of 22 antiparallel β -sheets which form a transmembrane channel for iron ions bound to the carrier ferrichrome (29). However, most of integral membrane proteins are composed of transmembrane α -helices. Among them, type I and II integral membrane proteins contain only one transmembrane α -helix with the amino-terminus outside and inside the cell, respectively. Type III and IV integral membrane proteins contain multiple transmembrane α -helices. The best-studied integral membrane protein is the light-driven proton-pump bacteriorhodopsin (30). This protein contains seven transmembrane hydrophobic α -helical segments. Each of these α -helices contains about 20 hydrophobic residues, which is just long enough to allow an α -helix to span the hydrophobic core of the fluid lipid bilayer of a cell membrane. These seven α -helices are oriented roughly perpendicular to the membrane plane and are clustered together to form a transmembrane channel for proton movement.

Protein-lipid interactions

It goes without saying that the protein-lipid interactions are essential for the structure and stability of integral membrane proteins. Virtually all integral membrane proteins require a full complement of “boundary” lipids for their maximum activities and stabilities. Important insights into protein-lipid interactions have resulted from biophysical studies of some representative integral proteins in model membrane systems.

Lipid phase state and fluidity

The maximum activities and stabilities of most integral membrane proteins require the L_{α} rather than the L_{β} state of the host lipid bilayer. For example, the $(\text{Na}^+, \text{Mg}^{2+})$ -ATPase from *Acholeplasma laidlawii* B is active only in L_{α} lipids (31). This is understandable, since L_{β} phase lipid bilayers are too rigid to accommodate the necessary

conformational changes required for protein function and are too thick to accommodate the transmembrane segments of membrane proteins (see below). Moreover, the fluidity of the host lipid bilayer in the L_{α} phase can also affect the stability and activity of membrane proteins. Most membrane proteins have their maximum activities at an optimal fluidity (32), while some others have their activities increase continuously with an increase of the membrane fluidity, such as the $(\text{Na}^+, \text{K}^+)\text{-ATPase}$ from dog kidney (33).

Lipid bilayer thickness

Hydrophobic interactions between proteins and lipids play a major role in stabilizing membrane structure. Because any exposure of the hydrophobic segments of proteins or lipids to water is energetically unfavorable, one could predict that the length of the lipid-exposed hydrophobic segment of a transmembrane α -helix should be almost equal to the hydrophobic thickness of the lipid bilayer. This principle of protein-lipid hydrophobic matching was best illustrated in the “mattress” model of biological membranes first introduced by Bloom and Mouritsen in 1984 (34). For example, in eukaryotic cells, the concentration of cholesterol and sphingolipids increases along the secretory pathway, from the endoplasmic reticulum to the Golgi to the plasma membrane, suggesting a concomitant increase in membrane thickness. In line with this idea, the average length of the transmembrane domains of plasma membrane proteins (about 20 amino acid residues) is five amino acids longer than the average length of proteins from the Golgi (about 15 residues) (35). In addition, many studies have shown that the activities of membrane proteins are sensitive to the mismatch between the hydrophobic length of their transmembrane segments and the hydrophobic thickness of the host lipid bilayer. When

reconstituted in mono-unsaturated PC bilayers of varying chain length, the $(\text{Ca}^{2+}, \text{Mg}^{2+})$ -ATPase (36) and $(\text{Na}^+, \text{K}^+)$ -ATPase (37) from sarcoplasmic reticulum show an optimal activity at a lipid-chain length of about 18 carbons, whereas shorter or longer acyl chains support lower activity. A similar chain length dependence of enzyme activity has also been reported for the $(\text{Na}^+, \text{Mg}^{2+})$ -ATPase from *A.laidlawii* B (38).

Surface charge density

The bilayer surface charge density imparted by charged phospholipid headgroups may affect the activities of some membrane proteins. For example, the activity of $(\text{Na}^+, \text{Mg}^{2+})$ -ATPase from *A. laidlawii* B was inhibited when phospholipases were used to hydrolyze the endogenous anionic PG bilayers in the native membrane (39). In addition, *in vitro* studies showed that small to moderate amounts of anionic phospholipids, in the presence of large amounts of neutral lipids, are required for the maximal activities of the $(\text{Na}^+, \text{Mg}^{2+})$ -ATPase from *A. laidlawii* B (38). Moreover, the potassium channel KcsA from *Streptomyces lividans* also requires the presence of certain anionic phospholipids for its optimal function (40).

Nonlamellar phase-forming lipids

Some integral membrane proteins require the presence of nonlamellar phase-forming lipids for their maximum activity. It has been suggested that the unfavorable packing of these nonlamellar phase-forming lipids in a planar lipid bilayer can provide the curvature stress that is necessary for the conformational changes of membrane proteins or that inverted cone-shaped lipid molecules may be required for optimal packing around irregularly shaped membrane proteins. For example, the presence of nonlamellar phase-forming lipids can shift the human visual pigment rhodopsin from MI to MII state (41)

and increase the activity of the membrane-bound form of protein kinase C (42). Whether or not normal micelle-forming lipids play complementary roles in biological membranes has not been determined.

Cholesterol

The presence of cholesterol in the host lipid bilayer may be required for the optimal activity of some membrane proteins. For example, cholesterol is required to activate the plasma membrane acetylcholine receptor (43). The effects of cholesterol on membrane proteins are usually manifested through its effects on the thickness, fluidity, and/or the surface charge density of the host lipid bilayer. However, some integral membrane proteins may contain specific binding sites for cholesterol and interact directly with cholesterol, such as the band 3 protein of the human erythrocyte (44).

Lipid requirements for membrane protein structures

A number of X-ray diffraction studies of integral membrane proteins include bound lipids in their published structures. For example, the structure of bacteriorhodopsin contains as many as 18 archaeal lipids (45). The structure of cytochrome *c* oxidase contains up to 14 phospholipids (PEs, PCs and PGs) (46). The formate dehydrogenase-N from *E. coli* contains a bound cardiolipin molecule (47). Moreover, these lipids are often found at the interface between monomers in a multimeric structure, suggesting a significant role of membrane lipids in forming the contact surface between closely associated protein subunits in the membrane.

The flanking residues of transmembrane α -helical segments

Statistical analysis shows that the hydrophobic cores of the transmembrane α -helices of integral membrane proteins are normally flanked on both sides by aromatic residues

like tryptophans or tyrosines (48). The preference of aromatic residues for regions corresponding to the nonpolar/polar interfacial region of the lipid bilayer was also found to be one common feature shared by many integral membrane proteins with known three-dimensional structures, such as the potassium channel KcsA (21) and the bacteriophage M13 major coat protein (49). Aromatic residues have been suggested to act as membrane “anchors” to determine the precise position of transmembrane α -helices in membrane bilayers (50), and some evidence for this idea has come from studies of synthetic α -helical peptides flanked by tryptophan residues (51-53). Moreover, positively-charged residues such as arginine or lysine are frequently found to flank the aromatic residues at the ends of the α -helical transmembrane segments, where they can interact with the negatively-charged phosphate moieties of the lipid polar headgroups. For example, in potassium channel KcsA, the hydrophobic transmembrane α -helices are flanked by broad girdles of arginine residues that are located outside the narrow girdles of tryptophan residues (21).

Studies of protein-lipid interactions by model transmembrane peptides

As discussed above, the activities and stabilities of many integral membrane proteins are influenced by the phase state, fluidity, thickness, surface charge density, and the lamellar/nonlamellar phase-forming propensity of the host lipid bilayer. However, the molecular mechanisms by which various membrane protein functions, and thus presumably also membrane protein structure and dynamics, are modulated by the composition, structure and phase properties of the host lipid bilayer are largely unknown. This is partly because most integral membrane proteins are relatively large, multidomain macromolecules of complex and often unknown three-dimensional structure and

topology that can interact with lipid bilayers in complex, multifaceted ways (54-56). To overcome this problem, this laboratory and others have studied lipid-protein interactions at the molecular level by carrying out various biophysical studies on simple, well-defined model membrane systems consisting of single phospholipid molecular species and synthetic polypeptide models of the hydrophobic transmembrane α -helical segments of integral membrane proteins (51,57-59).

The lead peptide that this laboratory and others have studied has the structure acetyl-K₂-G-L₂₄-K₂-A-amide (P₂₄) (57-59). The long stretch of leucine residues was designed to form a stable α -helix that will partition strongly into the hydrophobic core of the lipid bilayer. The dilysine caps at the N- and C- termini of the model peptide were designed to anchor the ends of this peptide to the polar surface of the lipid bilayer and to inhibit its lateral aggregation. Indeed, circular dichroism (57) and FTIR spectroscopic (58,60,61) studies have shown that P₂₄ adopts a very stable α -helical conformation in lipid bilayers. X-ray diffraction (62), fluorescence quenching (63), and FTIR spectroscopic (58,60,61) studies confirm that P₂₄ and its analogues adopt a transbilayer orientation with the N- and C- termini exposed to the aqueous buffer and the hydrophobic core embedded in the hydrocarbon core of the lipid bilayer when reconstituted in various PC systems. These results clearly demonstrate that P₂₄ and its analogues are excellent models of transmembrane α -helices of integral membrane proteins.

To further explore the principles of peptide-lipid interactions, this laboratory has systematically changed the phospholipid fatty acid chain length and structure and the structure, charge, and the H-bonding capacity of the phospholipid polar headgroup, as well as the structure of the central α -helical region of the model peptides. The effects of

variations in polypeptide structure on the thermotropic phase behavior of the host lipid bilayer were studied by DSC, and the organization and conformation of the phospholipid polar headgroups and hydrocarbon chains in L_{β} and L_{α} phase were studied by electron-spin resonance (ESR), deuterium nuclear magnetic resonance ($^2\text{H-NMR}$) and FTIR spectroscopy. Similarly, the effect of variations in both the physical properties of the host lipid bilayer, and in the amino acid sequence of the synthetic model peptide, on peptide conformation and stability in the lipid bilayer were studied by FTIR spectroscopy. As well, the dynamics and state of aggregation of the model peptides in the lipid bilayer were monitored by ESR spectroscopy. In this way the nature and magnitude of the various electrostatic, H-bonding, van der Waals and hydrophobic interactions occurring between the phospholipid bilayers and the incorporated bilayer-spanning polypeptides could be determined, providing new insights into the molecular mechanisms whereby the structure and physical properties of the lipid bilayers of biological membranes modulate the enzymic, transport and receptor functions of the integral membrane proteins embedded in them.

This laboratory has studied the interactions of P_{24} with n -saturated PCs and PEs by high-sensitivity DSC and FTIR spectroscopy (58,60,64). Previous DSC studies showed that the incorporation of P_{24} progressively decreases the temperature and cooperativity of the L_{β}/L_{α} phase transitions in both PC and PE bilayers (58,64). Moreover, FTIR studies show that P_{24} adopts a very stable α -helical conformation in PE bilayers as in PC bilayers (64). Qualitatively similar results were observed in the studies of the interactions of a P_{24} derivative, acetyl- K_2 -(LA) $_{12}$ - K_2 -amide [(LA) $_{12}$], with the n -saturated PC and PE bilayers, except that (LA) $_{12}$ decreases the temperature and enthalpy of the L_{β}/L_{α} phase transition of

the host PC bilayers to a greater extent than P₂₄ (65-67). This indicates that the thermodynamics of the interactions of transmembrane α -helices with lipid bilayers are affected by factors such as the polarity and topology of the helical surface of the hydrophobic core of the peptide, which are dependent on the primary sequence of the helix. In order to gain insight into how the transmembrane helices are mixed with phospholipids, ESR spectroscopy had been used to study the effects of two P₂₄ analogues, (LA)₁₂ and acetyl-K₂-L₂₄-K₂-amide (L₂₄), on the molecular organization and dynamics of 1-palmitoyl-2-oleoyl-phosphatidylcholine (POPC) membranes (68,69). At a peptide to POPC ratio between 1/10 and 1/40, ESR spectroscopy detects the presence of a single membrane environment for both L₂₄ and (LA)₁₂, suggesting that these peptides are well dispersed and that POPC is exchanging rapidly between the peptide-associated and peptide-poor domains. These results also indicate that both L₂₄ and (LA)₁₂ exist primarily as a monomer in the L _{α} POPC bilayers even at relatively high peptide concentrations. Finally, various biophysical techniques have been employed to study the interaction of another P₂₄ analogue, acetyl-K₂-A₂₄-K₂-amide (A₂₄), with PC bilayers (70). It was found that A₂₄ exists as dynamic mixtures of α -helices, β -sheets and other conformers and resides mostly in the aqueous phase in peptide-PC mixtures. Therefore, it was suggested that A₂₄ does not have sufficient hydrophobicity to maintain a stable transmembrane association with phospholipid bilayers in the presence of water.

Another extensively studied transmembrane model peptides are the WALP peptides, which consist of a hydrophobic sequence of alternating leucine and alanine residues of variable length flanked by two tryptophans at both ends. These model peptides were incorporated into model membranes composed of one pure lipid or binary lipid mixtures

and the lipid-peptide interactions were studied by analyzing the effects of progressively shortening the hydrophobic length of the model peptides relative to the bilayer thickness on lipid organization. First, the effects of WALP peptides on the thickness of PC bilayers were investigated by ESR and ^2H -NMR spectroscopy (71) and X-ray diffraction (72). ESR and ^2H -NMR spectroscopic studies show that in di-12:0 and di-14:0 PC, the longer WALP peptides cause larger increases in the bilayer thickness than the shorter ones, whereas in di-18:0 PC, the shorter WALP peptides cause larger decreases in the bilayer thickness than the longer ones (71). Thus the incorporation of WALP peptides produces systematic changes in the bilayer thickness dependent on the hydrophobic mismatch between the peptides and the lipid bilayer. In contrast, a recent X-ray diffraction study showed that the incorporation of WALP peptides does not alter the bilayer thickness, regardless of the conditions of the hydrophobic mismatch between the WALP peptides and the PC bilayers (72). These contradictory results raise the question of the reliability of these techniques to measure the effects of these peptides on the thickness of phospholipid bilayers. Second, the effects of WALP peptides on the nonlamellar phase-formation properties of phospholipid bilayers were studied by ^{31}P -NMR (73,74). When the hydrophobic length of WALP peptide is much shorter than the hydrophobic thickness of PC bilayer, the incorporation of WALP peptides can induce the formation of nonlamellar phases in PC systems and the type of nonlamellar phase formed is dependent on the precise extent of hydrophobic mismatch between the peptides and the lipid bilayers. For example, WALP19 (19 is the total number of amino acids) can induce the formation of an isotropic, most likely cubic phase, and an H_{II} phase in the di-18:1_c-(c means *cis* double bond) and di-22:1_cPC bilayers, respectively (73). However, in the di-

elaidoyl (18:1_t)-phosphatidylethanolamine (DEPE) system, which by itself has a tendency to form nonlamellar phases, the incorporation of relatively short WALP peptides was found to lower the L_{α}/H_{II} phase transition temperature of DEPE in a manner independent of the hydrophobic mismatch between the peptides and lipid matrix (74). Third, the possible tilt of WALP peptides in PC bilayers was determined by ^2H -NMR spectroscopy (75). In di-12:0, 14:0, and 18:1_c PC bilayers, WALP19 had a tilt angle of $\sim 4^\circ$ from the membrane normal and experienced rapid reorientation around the membrane normal. Since the orientation of WALP19 only varied slightly in three different lipids, the lipid-peptide hydrophobic mismatch seems not to be the dominant factor causing the tilt. Fourth, the aggregation states of WALP peptides in phospholipid bilayers were studied by various biophysical techniques. The ESR studies show no evidence for the peptide aggregation in the di-14:0 PC bilayer when WALP peptides with different hydrophobic length are incorporated into lipid bilayer, even at a lipid to peptide mole ratio of 1/10 (71). However, FTIR spectroscopy and sucrose density gradient centrifugation experiments strongly support the idea that some peptide aggregation does occur when the WALP peptide is either too short or too long relative to the bilayer thickness (73,76). Finally, the effects of KALP peptides, in which the two pairs of tryptophan residues in WALP are replaced with lysine residues, on the bilayer thickness and on the nonlamellar phase-forming properties of phospholipid bilayers have been studied by ^2H -NMR and ^{31}P -NMR spectroscopy. These studies show that KALP peptides could also alter the bilayer thickness and promote formation of nonlamellar phase in PC bilayers in a manner dependent on the lipid-peptide hydrophobic mismatch (51,52). Moreover, these studies indicate that the hydrophobic length of KALP peptides seems to

be different from that of comparable WALP peptides. For example, KALP23 was found to induce smaller increase in the bilayer thickness of 14:0 PC (0.2Å) than did WALP23 (1.0Å) (51), indicating that the lysine-flanked peptides may have a shorter effective hydrophobic length than the comparable tryptophan-flanked peptides.

It appears from above that the lipid-peptide interactions are affected not only by the hydrophobic mismatch between peptide hydrophobic length and lipid bilayer hydrophobic thickness, but also by the electrostatic and H-bonding interactions between the lipid polar headgroups and the peptide terminal aromatic and charged residues. To further explore the nature and magnitude of the various electrostatic, H-bonding, and hydrophobic interactions occurring between the phospholipid bilayers and the model peptides, I have studied the interactions of three derivatives of P₂₄, specifically, L₂₄ (acetyl-Lys₂-Leu₂₄-Lys₂-amide), L₂₄DAP (acetyl-DAP₂-Leu₂₄-DAP₂-amide, DAP is diaminopropionic acid), and WL₂₂W (acetyl-Lys₂-Trp-Leu₂₂-Trp-Lys₂-amide), with phospholipid bilayers with different headgroups and different hydrocarbon chain length and structures. First, with the peptide L₂₄DAP, the two pairs of capping lysine residues at the ends of L₂₄ are replaced with the lysine analogues DAP, in which three of the four side-chain methylene groups of lysine residues have been removed. This peptide is used to test the effects of lysine snorkeling on protein-lipid interactions. The snorkel model suggests that the long, flexible side chains of lysine or arginine can extend along the transmembrane helix so that the charged amino group can reside in the lipid polar headgroup region while the α -carbon of the amino acid residue remains well below (or possibly above) the membrane/water interface (77,78). Because of the shorter spacer arms between the charged amino group and the α -carbon in DAP, L₂₄DAP is expected to

be less accommodating to the hydrophobic mismatch between the peptides and the lipid bilayers, and any effects of such mismatch on the thermotropic phase behavior of the host lipid bilayers should thus be exaggerated. Second, with the peptide WL₂₂W, the residues Leu-3 and Leu-26 of L₂₄ are replaced by tryptophans. This peptide is used to study the role of interfacially located tryptophan residues in protein-lipid interactions. In this thesis, various biophysical techniques have been applied to study the effects of L₂₄, L₂₄DAP, and WL₂₂W on the thermotropic phase behaviors and the structures and organizations of phospholipids with different polar headgroup and hydrocarbon chain structures. The effects of these peptides on the L_β/L_α phase transitions of zwitterionic PC and PE bilayers are studied in chapter 2 and 3, respectively. Chapter 4 addresses the effects of these peptides on the L_β/L_α phase transitions of anionic PG bilayers. In chapter 5, the effects of the three model peptides on the nonlamellar phase-forming propensity of DEPE are described. Finally, these results are summarized and discussed in chapter 6. I have also contributed to a DSC, FTIR, and ²H-NMR studies on the effect of the incorporation of L₂₄ and (LA)₁₂ on the organization of the hydrocarbon chains in DPPC and DOPC bilayers, a copy of which is included as Appendix-1 of this thesis.

References:

1. Gennis, R.B. (1989) Introduction: the structure and composition of biomembranes, in *Biomembranes: Molecular Structure and Function*, pp1-35, Springer-Verlag, New York.
2. Oparin, A.I. (1957) *The Origin of Life on the Earth*, Academic Press, New York.
3. Jain, M.K. (1972) Energy transduction in biological systems, in *The Biomolecular Lipid Membrane*, pp253-320, Van Nostrand Reinhold Company, New York.
4. Devaux, P.F., and Seigneuret, M. (1985) Specificity of lipid-protein interactions as determined by spectroscopic techniques, *Biochim. Biophys. Acta* 822,63-125.
5. Fisher, K., and Branton, D. (1974) Application of the freeze-fracture technique to natural membranes, in *Methods in Enzymology*, vol 32, pp 35-44, Academic Press, New York.
6. Verkleij, A.J., Zwaal, R.F., Roelofsen, B., Comfurius, P., Kastelijn, D., and van Deenen, L.L. (1973) The asymmetric distribution of phospholipids in the human red cell membrane, *Biochim. Biophys. Acta* 323,178-193.
7. Begenisich, T. (1989) The role of membrane potentials and currents in neuronal cells, *Curr.Opin.Cell.Biol.* 1,765-770.
8. Singer, S.J., and Nicholson, G.L. (1972) The fluid-mosaic model of the structure of the cell membranes, *Science* 175, 720-731.
9. Simons, K., and Ikonen, E. (1997) Functional rafts in cell membranes, *Nature* 387, 569-572.
10. Edidin, M. (2003) The state of lipid rafts: from model membranes to cells, *Annu. Rev. Biophys. Biomol.* 32, 257-283.

11. Munro, S. (2003) Lipid rafts: elusive or illusive, *Cell* 115,377-388
12. McElhaney, R.N. (2003) Cholesterol-phospholipid interactions, the lipid-ordered phase and lipid rafts in model and biological membranes, *Curr. Opin. Colloid. Intergace. Sci. (in press)*.
13. Daum, G. (1985) Lipids of mitochondria, *Biochim. Biophys. Acta* 822,1-42.
14. Raetz, C.R.H., and Dowhan, W. (1990) Biosynthesis and function of phospholipids in *Escherichia coli*, *J.Biol.Chem.*265, 1235-1238.
15. Wiener, M.C., and White, S.H. (1992) Structure of a fluid dioleoylphosphatidylcholine bilayer determined by joint refinement of X-ray and neutron diffraction data. III. Complete structure, *Biophys. J.* 61, 437-447.
16. van Deenen, L.L.M., and de Gier, J. (1974) Lipids of the red cell membrane, in *The Red Blood Cell* (D.Surgenor,Ed.), pp147-213, Academic Press, New York.
17. Gounaris, K., and Barber, J. (1983) Monogalactosyldiacylglycerol:the most abundant polar lipids in nature, *TIBS.*8, 378-381.
18. Evans, W.H., and Hardison, W.G.M. (1985) Phospholipid, cholesterol, polypeptide and glycoprotein composition of hepatic endosome subfractions, *Biochem.J.* 232, 33-36
19. Jones, M.R., Faye, P.K., Roszak, A.W.R., Isaacs, N.W., and Cogdell, J. (2002) Protein-lipid interactions in the purple bacterial reaction center, *Biochim. Biophys. Acta* 1565,206-214.
20. Lee, A.G. (1998) How lipids interact with an intrinsic membrane protein: the case of the calcium pump, *Biochim. Biophys. Acta* 1376,381-390.

21. Williamson, I.M., Alvis, S.J., East, J.M., and Lee, A.G. (2003) The potassium channel KcsA and its interaction with the lipid bilayer, *Cell. Mol. Life.Sci.* 60, 1581-1590.
22. McElhaney, R.N. (1982) The use of differential scanning calorimetry and differential thermal analysis in studies of model and biological membranes, *Chem. Phys. Lipids* 30, 229-259.
23. Lewis, R.N.A.H., and R.N. McElhaney. (1996) FTIR spectroscopy in the study of hydrated lipids and lipid bilayer membranes, in *Infrared Spectroscopy of Biomolecules*, (H.H. Mantsch and D. Chapman, Eds.), pp. 159-202, John Wiley & Sons, New York.
24. Torii, H., and Tasumi, M. (1996) Theoretical analysis of the amide I infrared bands of globular proteins, in *Infrared Spectroscopy of Biomolecules*, (H.H. Mantsch and D. Chapman, Eds.), pp. 159-202, John Wiley & Sons, New York.
25. Cullis, P.R., de Kruijff, B., Hope, M.J., Verkleij, A.J., Nayar, R., Farren, S.B., Tilcock, C., Madden, T.D., and Bally, M.B. (1983) Structural properties of lipids and their functional roles in biological membranes, in *Membrane Fluidity in Biology* (Aloia, R.C., Ed.), vol 1, pp39-81, Academic Press, New York.
26. Seddon, J.M. (1990) Structure of the inverted hexagonal phase, and non-lamellar phase transitions of lipids, *Biochim. Biophys. Acta* 1031,1-69.
27. Gerke, V., and Moss, S.E. (1997) Annexins and membrane dynamics, *Biochim. Biophys. Acta* 1357,129-154.
28. http://blanco.biomol.uci.edu/Membrane_Proteins_xtal.html.

29. Koebnik, R., Locher, K.P., and Van Gelder, P. (2000) Structure and function of bacterial outer membrane proteins: barrels in a nutshell, *Mol. Microbiol.* 37,239-253.
30. Subramaniam, S. (1999) The structure of bacteriorhodopsin: an emerging consensus, *Curr. Opin. Struc. Biol.* 9, 462-468.
31. Silvius, J.R., and McElhaney, R.N. (1980) Membrane lipid physical state and modulation of the (Na⁺Mg²⁺)-ATPase activity in *Acholeplasma laidlawii* B, *Proc. Natl. Acad. Sci. U.S.A.* 77,1255-1259.
32. Silvius, J.R., and McElhaney, R.N. (1982) Membrane lipid fluidity and physical state and the activity of the Na⁺, Mg²⁺-ATPase of *Acholeplasma laidlawii* B, *Biophys. J.* 37, 36-38.
33. Chong, P.L., Fortes, P.A., and Jameson, D.M. (1985) Mechanisms of inhibition of (Na⁺,K⁺)-ATPase by hydrostatic pressure studied with fluorescent probes, *J. Biol. Chem.* 260, 14484-14490.
34. Mouritsen, O.G., and Bloom, M. (1984) Mattress model of lipid-protein interactions in membranes, *Biophys. J.* 46, 141-153.
35. Bretscher, M.S., and Munro, S. (1993) Cholesterol and the Golgi apparatus, *Science* 261,1280-1281.
36. Johannsson, A., Keightley, C.A., Smith, G.A., Richards, C.D., Hesketh, T.R., and Metcalfe, J.C. (1981) The effect of bilayer thickness and *n*-alkanes on the activity of the (Ca²⁺+Mg²⁺)-dependent ATPase of sarcoplasmic reticulum, *J. Biol. Chem.* 256, 1643-1650.
37. Johannsson, A., Smith, G.A., and Metcalfe, J.C. (1981) The effect of bilayer thickness on the activity of (Na⁺+K⁺)-ATPase, *Biochim. Biophys. Acta* 641,416-421.

38. George, R., Lewis, R.N.A.H., Mahajan, S., and McElhaney, R.N. (1989) Studies on the purified, lipid-reconstituted (Na⁺+Mg²⁺)-ATPase from *Acholeplasma laidlawii* B membranes: Dependence of enzyme activity on lipid headgroup and hydrocarbon chain structure, *J. Biol. Chem.* 264, 11598-11604.
39. Bevers, E.M., Snoek, G.T., Op Den Kamp, J.A., and van Deenen, L.L. (1977) Phospholipid requirement of the membrane-bound Mg²⁺-dependent adenosine-triphosphatase in *Acholeplasma laidlawii*, *Biochim. Biophys. Acta* 467,346-356.
40. Valiyaveetil, F.I., Zhou, Y., and MacKinnon, R. (2002) Lipids in the structure, folding, and function of the KcsA K⁺ channel, *Biochemistry* 41,10771-10777.
41. Brown, M.F. (1997) Influence of nonlamellar-forming lipids on rhodopsin, in *Lipid Polymorphism and Membrane Properties* (Epanand, R.M), pp285-356, Academic Press, San Diego, CA.
42. Mosior, M., Golini, E.S., and Epanand, R.M. (1996) Chemical specificity and physical properties of the lipid bilayer in the regulation of protein kinase C by anionic phospholipids: evidence for the lack of a specific binding site for phosphatidylserine, *Proc. Natl. Acad. Sci. USA*, 93,1907-1912.
43. Burger, K., Gimpl, G., and Fahrenholz, F. (2000) Regulation of receptor function by cholesterol, *Cell.Mol. Life. Sci.* 57, 1577-1592.
44. Schubert, D., and Boss, K. (1982) Band 3 protein-cholesterol interactions in erythrocyte membranes. Possible role in anion transport and dependency on membrane phospholipid, *FEBS Letters.* 150, 4-8.
45. Belrhali, H., Nollert, P., Royant, A., Menzel, C., Rosenbusch, J.P., Landau, E.M., and Pebay-Peyroula, E. (1999) Protein, lipid and water organization in bacteriorhodopsin

- crystals: a molecular view of the purple membrane at 1.9 Å resolution, *Structure* 7, 909-917.
46. Tsukihara, T., Aoyama, H., Yamashita, E., Tomizaki, T., Yamaguchi, H., Shinzawa-Itoh, K., Nakashima, R., Yaono, R., and Yoshikawa, S. (1996) The whole structure of the 13-subunit oxidized cytochrome c oxidase at 2.8 Å, *Science* 272,1136-1144.
47. Jormakka, M., Tornroth, S., Byrne, B., and Iwata, S. (2002) Molecular basis of proton motive force generation: structure of formate dehydrogenase-N, *Science* 295,1863-1868.
48. Killian, J.A., and von Heijne, G. (2000) How proteins adapt to a membrane–water interface, *TIBS* 25,429-434.
49. Stopar, D., Spruijt, R.B., Wolfs, C.J.A.M., and Hemminga, M.A. (2003) Protein-lipid interactions of bacteriophage M13 major coat protein, *Biochim. Biophys. Acta* 1611,5-15.
50. Yau, W-M., Wimley, W.C., Gawrisch, K., and White, S.H. (1998) The preference of tryptophan for membrane interfaces, *Biochemistry* 37, 14713-14718.
51. de Planque, M.R.R., Kruijtz, J.A.W., Liskamp, R.M.J., Marsh, D., Greathouse, D.V., Koeppe II, R.E., de Kruijff, B., and Killian. J.A. (1999) Different membrane anchoring positions of tryptophan and lysine in synthetic transmembrane α -helical peptides, *J. Biol. Chem.* 274, 20839–20846.
52. Strandberg, E., Morein, S., Rijkers, D.T.S., Liskamp, R.M.J., Van der Wel, P.C.A., and Killian, J.A. (2002) Lipid dependence of membrane anchoring properties and snorkeling behavior of aromatic and charged residues in transmembrane peptides, *Biochemistry* 41, 7190–7198.

53. de Planque, M.M.R., Bonev, B.B., Demmers, J.A.A., Greathouse, D.V., Koeppe, II, R.E., Separovic, F., Watts, A., and Killian, J.A. (2003) Interfacial anchor properties of tryptophan residues in transmembrane peptides can dominate over hydrophobic matching effects in peptide-lipid interactions, *Biochemistry* 42, 5341–5348.
54. Gennis, R.B. (1989) Membrane dynamics and protein-lipid interactions, in *Biomembranes: Molecular Structure and Function*, pp 166-198, Springer-Verlag, New York.
55. Selinsky, B.S. (1992) Protein-lipid interactions and membrane function, in *The Structure of Biological Membranes*(Yeagle, P), pp 603-651,CRC Press, Boca Raton, FL.
56. Marsh, D., and Horváth, L.I. (1998) Structure, dynamics and composition of the lipid-protein interface. Perspectives from spin-labelling, *Biochim. Biophys. Acta* 1376, 267-296.
57. Davis, J.H., Clare, D.M., Hodges, R.S., and Bloom, M. (1983) Interaction of a synthetic amphiphilic polypeptide and lipids in a bilayer structure, *Biochemistry* 22, 5298-5305.
58. Zhang, Y.-P., Lewis, R.N.A.H., Hodges, R.S., and McElhaney, R.N. (1992) Interaction of a peptide model of a hydrophobic transmembrane α -helical segment of a membrane protein with phosphatidylcholine bilayers: differential scanning calorimetric and FTIR spectroscopic studies, *Biochemistry* 31, 11579-11588.
59. Ren, J., Lew, S., Wang, Z., and London, E. (1997) Transmembrane orientation of hydrophobic α -helices is regulated both by the relationship of helix length to bilayer thickness and by the cholesterol concentration, *Biochemistry* 36, 10213-10220.

60. Zhang, Y.-P., Lewis, R.N.A.H., Hodges, R.S., and McElhaney, R.N. (1992) FTIR spectroscopic studies of the conformation and amide hydrogen exchange of a peptide model of the hydrophobic transmembrane α -helices of membrane proteins, *Biochemistry* 31, 11572-11578.
61. Axelsen, P.H., Kaufman, P.H., McElhaney, R.N., and Lewis, R.N.A.H. (1995) The infrared dichroism of transmembrane helical polypeptides, *Biophys. J.* 69, 2770-2781.
62. Huschilt, J.C., Millman, B.M., and Davis, J.H. (1989) Orientation of alpha-helical peptides in a lipid bilayer, *Biochim. Biophys. Acta* 979, 139-141.
63. Bolen, E.J., and Holloway, P.W. (1990) Quenching of tryptophan fluorescence by brominated phospholipid, *Biochemistry* 29, 9638-9643.
64. Zhang, Y.-P., Lewis, R.N.A.H., Hodges, R.S., and McElhaney, R.N. (1995) Interaction of a peptide model of a hydrophobic transmembrane α -helical segment of a membrane protein with phosphatidylethanolamine bilayers: differential scanning calorimetric and FTIR spectroscopic studies, *Biophys. J.* 68, 847-857.
65. Zhang, Y.-P., Lewis, R.N.A.H., Henry, Hodges, R.S., and McElhaney, R.N. (1995) Peptide models of helical hydrophobic transmembrane segments of membrane proteins. II. DSC and FTIR spectroscopic studies of the interaction of Ac-K₂-(LA)₁₂-K₂-amide with phosphatidylcholine bilayers, *Biochemistry* 34, 2362-2371
66. Zhang, Y.-P., Lewis, R.N.A.H., Henry, G.D., Sykes, B.D., Hodges, R.S., and McElhaney, R.N. (1995) Peptide models of helical hydrophobic transmembrane segments of membrane proteins. I. Studies of the conformation, intrabilayer orientation and amide hydrogen exchangeability of Ac-K₂-(LA)₁₂-K₂ amide, *Biochemistry* 34, 2348-2361.

67. Zhang, Y.-P., Lewis, R.N.A.H., Hodges, R.S., and McElhaney, R.N. (2001) Peptide models of the helical hydrophobic transmembrane segments of membrane proteins: Interactions of acetyl-K₂-(LA)₁₂-K₂-amide with phosphatidylethanolamine bilayer membranes, *Biochemistry* 40,474-482.
68. Subczynski, W.K., Lewis, R.N.A.H., McElhaney, R.N., Hodges, R.S., Hyde, J.S., and Kusumi, A. (1998) Molecular organization and dynamics of 1-palmitoyl-2-oleoyl-phosphatidylcholine bilayers containing a trans-membrane α -helical peptide, *Biochemistry* 37, 3156-3164.
69. Subczynski, W.K., McElhaney, R.N., Hyde, J.S., and Kusumi, A. (2003) Molecular organization and dynamics of 1-palmitoyl-2-oleoyl phosphatidylcholine bilayer membranes containing a transmembrane α -helical peptide with hydrophobic surface roughness, *Biochemistry* 42, 3939-3948.
70. Lewis, R.N.A.H., Zhang, Y.-P., Hodges, R.S., Subczynski, W.K., Kusumi, A., Flach, C.R., Mendelsohn, R., and McElhaney, R.N. (2001) A polyalanine-based peptide cannot form a stable transmembrane α -helix in fully hydrated phospholipid bilayers, *Biochemistry* 40, 12103-12111.
71. de Planque, M.R.R., Greathouse, D.V., Koeppe, II, R.E., Schäfer, H., Marsh, D., and Killian, J.A. (1998) Influence of lipid/peptide hydrophobic mismatch on the thickness of diacylphosphatidylcholine bilayers. A ²H-NMR and ESR study using designed transmembrane α -helical peptides and gramicidin A, *Biochemistry* 37, 9333–9345.
72. Weiss, T.M., van der Wel, P.C.A., Killian, J.A., Koeppe, II, R.E., and Huang, H.W. (2003) Hydrophobic Mismatch between Helices and Lipid Bilayers, *Biophys. J.* 84, 379-385.

73. Killian, J.A., Salemink, I., de Planque, M.R.R., Lindblom, G., Koeppe II, R.E., and Greathouse, D.V. (1996) Induction of nonbilayer structures in diacylphosphatidylcholine model membranes by transmembrane α -helical peptides: importance of hydrophobic mismatch and proposed role of tryptophans, *Biochemistry* 35, 1037–1045.
74. van der Wel, P.C.A., Pott, T., Morein, S., Greathouse, D.V., Koeppe II, R.E., and Killian, J.A. (2000) Tryptophan-anchored transmembrane peptides promote formation of nonlamellar phases in phosphatidylethanolamine model membranes in a mismatch-dependent manner, *Biochemistry* 39, 3124-3133.
75. van der Wel, P.C.A., Strandberg, E., Killian, J.A., and Koeppe, II, R.E. (2002) Geometry and intrinsic tilt of a tryptophan-anchored transmembrane α -helix determined by ^2H -NMR, *Biophys. J.* 83, 1479-1488.
76. de Planque, M.R.R., Goormaghtigh, E., Greathouse, D.V., Koeppe II, R.E., Kruijtzter, J.A.W., Liskamp, R.M.J., de Kruijff, B., and Killian, J.A. (2001) Sensitivity of single membrane-spanning α -helical peptides to hydrophobic mismatch with a lipid bilayer: effects on backbone structure, orientation, and extent of membrane incorporation, *Biochemistry* 40, 5000–5010.
77. Segrest, J.P., De Loof, H., Dohlman, J.G., Brouillette, C.G., and Anantharamaiah, G.M. (1990) Amphipathic helix motif: classes and properties, *Proteins: Struct. Funct. Genet.* 8, 103-117.
78. Monne, M., Nilsson, I., Johansson, M., Elmhed, N., and van Heijne, G. (1998) Positively and negatively charged residues have different effects on the position in the membrane of a model transmembrane helix, *J. Mol. Biol.* 284, 1177-1183.

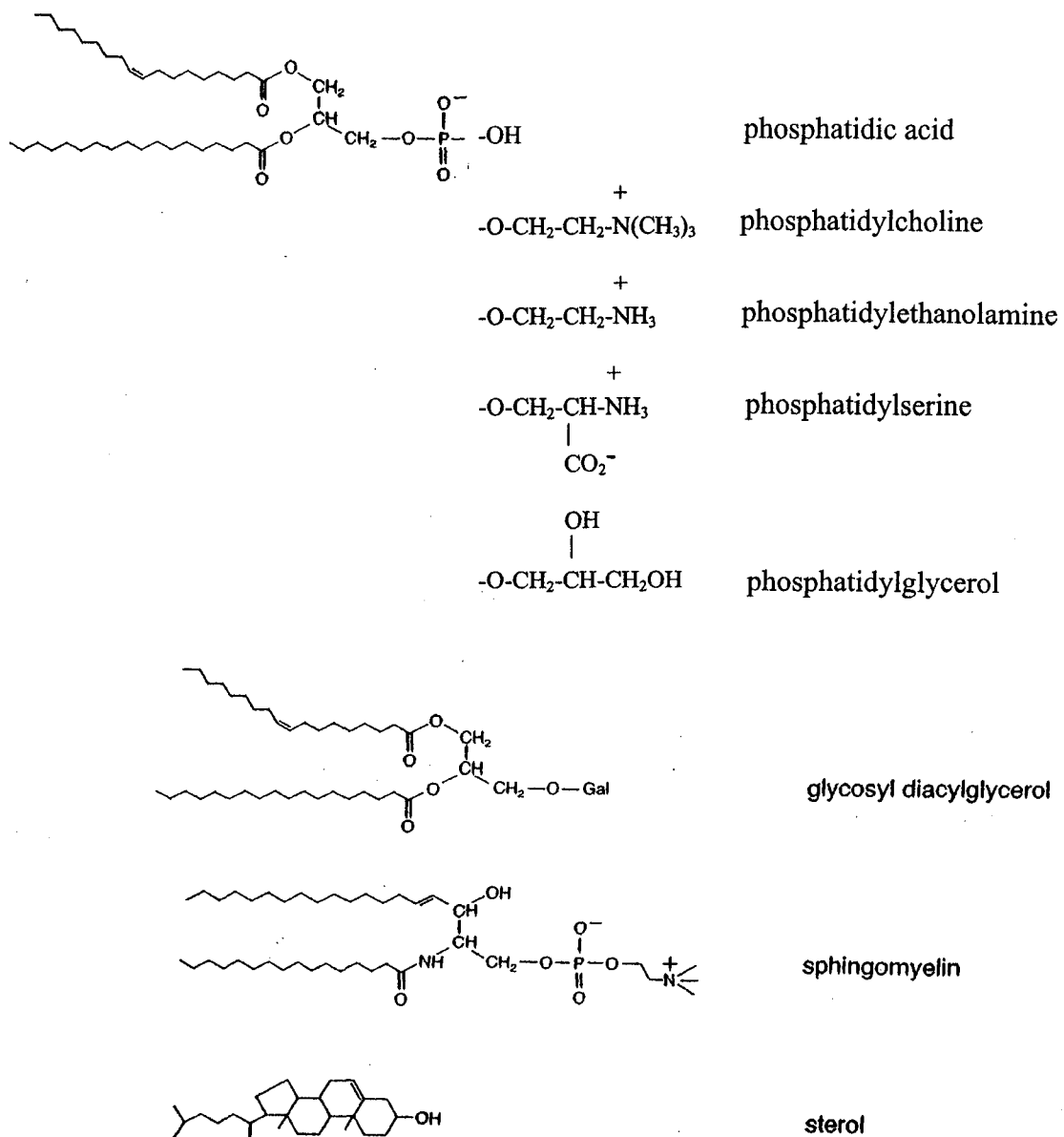


FIGURE 1. Representative structures for selected membrane lipids.

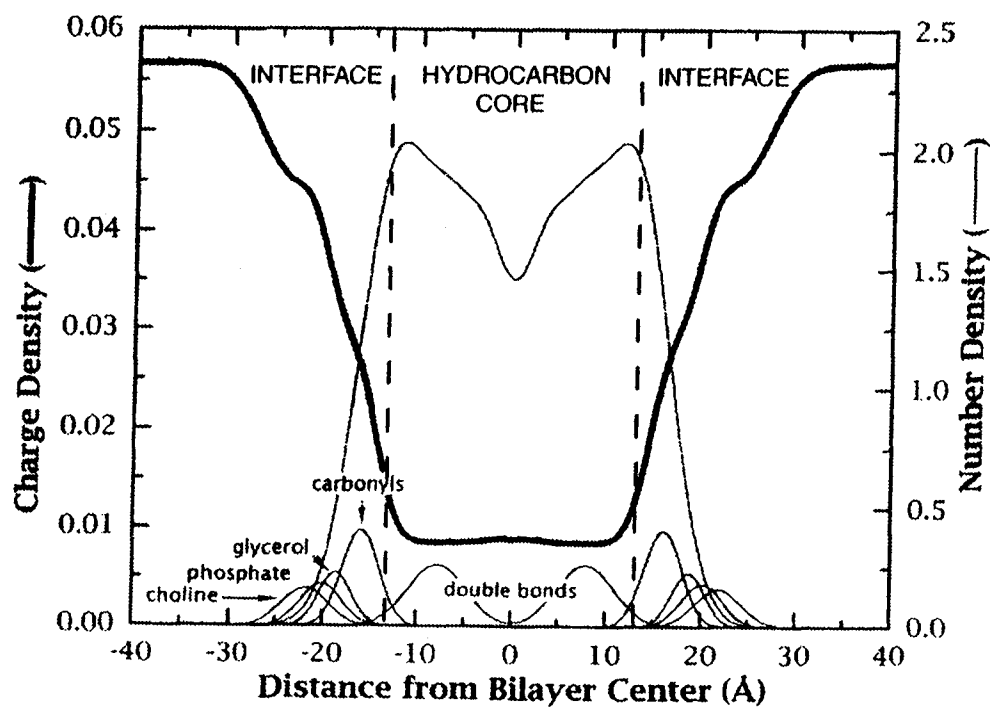


FIGURE 2. The time-averaged distributions of the principle structural groups of dioleoylphosphatidylcholine, together with the resulting polarity profile. Adapted from ref. 15.

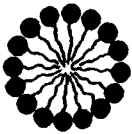

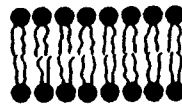

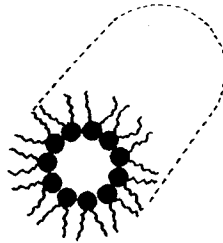

LIPID	PHASE	MOLECULAR SHAPE
Lysophospholipids Detergents	 Micellar	 Inverted Cone
Phosphatidylcholine Sphingomyelin Phosphatidylserine Phosphatidylinositol Phosphatidylglycerol Phosphatidic Acid Cardiolipin Digalactosyldiglyceride	 Bilayer	 Cylindrical
Phosphatidylethanolamine (Unsaturated) Cardiolipin - Ca ²⁺ Phosphatidic Acid - Ca ²⁺ (pH < 6.0) Phosphatidic Acid (pH < 3.0) Phosphatidylserine (pH < 4.0) Monogalactosyldiglyceride	 Hexagonal (H _{II})	 Cone

FIGURE 3. Polymorphic phases and molecular shapes for some membrane lipids.

Adapted from ref. 25.

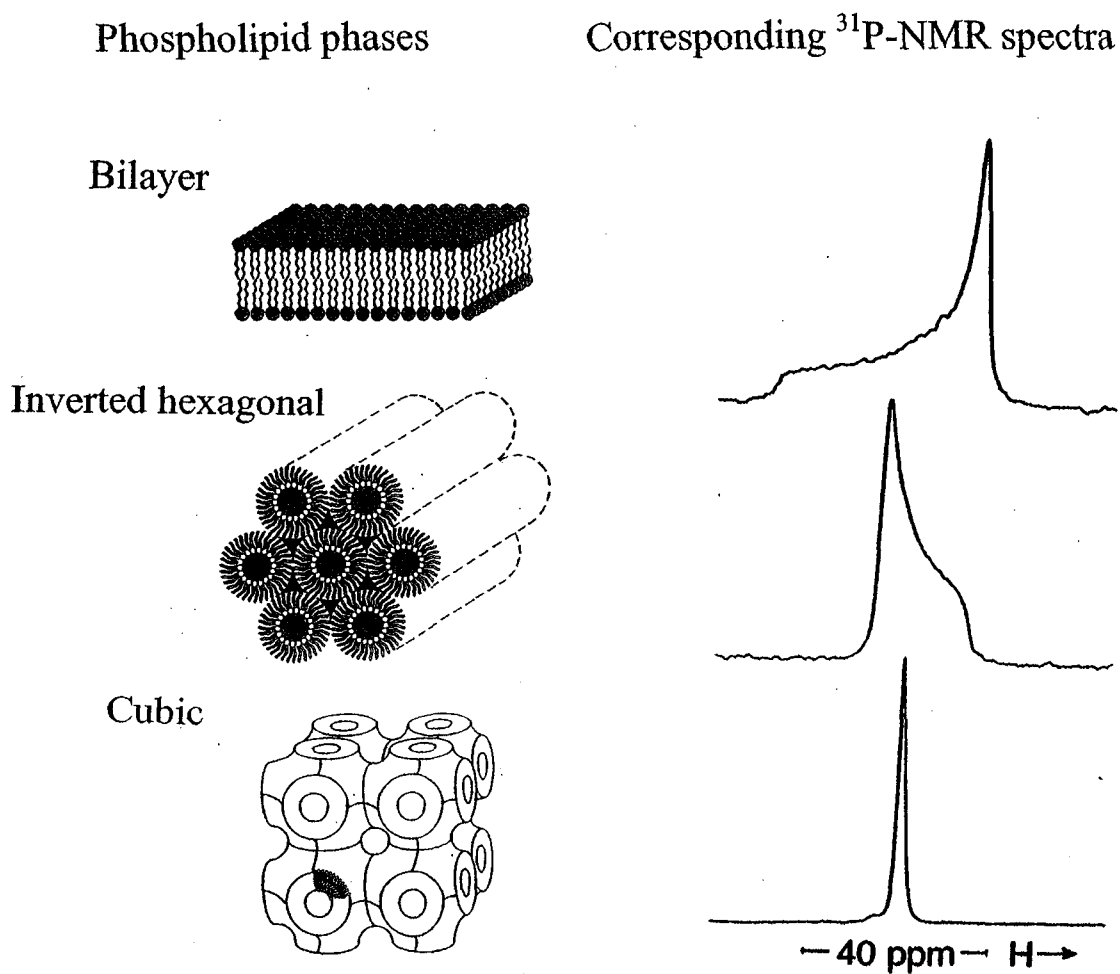


FIGURE 4. ^{31}P -NMR characteristics of phospholipids in various phases. Adapted from ref. 25.

CHAPTER II. Effect of Variations in the Structure of a Polyleucine-Based α -Helical Transmembrane Peptide on Its Interaction with Phosphatidylcholine Bilayers

Introduction

The mutual interactions of lipids and proteins are fundamentally important to both the structure and the function of all biological membranes (1,2). In particular, the chemical composition and physical properties of the host lipid bilayer can markedly influence the activity and thermal stability of a large number of integral membrane proteins in both model and biological membrane systems (1-5). For this reason, there have been many studies of the interactions of membrane proteins with their host lipid bilayers, in both biological and reconstituted model membrane systems, employing a wide range of different physical techniques (6-10). However, our understanding of the physical principles underlying lipid-protein interactions remains incomplete and the actual molecular mechanisms whereby associated lipids actually alter the activity, and presumably also the structure and dynamics, of integral membrane proteins are largely unknown. This situation is due in part to the fact that most transmembrane proteins are relatively large, multidomain macromolecules of complex and often unknown three-dimensional structure and topology that can interact with lipid bilayers in complex,

A version of this chapter has been published. Liu, F., Lewis, R.N.A.H., Hodges, R.S., and McElhaney, R.N. (2002) *Biochemistry* 41, 9197-9207.

multifaceted ways (1-10). To overcome this problem, a number of workers have designed and synthesized peptide models of specific regions of natural membrane proteins and have studied their interactions with model lipid membranes of defined composition (11, 12). Physical studies of such relatively tractable model membrane systems have already significantly advanced our understanding of the molecular basis of lipid-protein interactions.

The synthetic peptide acetyl-K₂-G-L₂₄-K₂- A-amide (P₂₄)¹ and its analogues have been successfully utilized as a model of the hydrophobic transmembrane α -helical segments of integral membrane proteins (12, 13). These peptides contain a long sequence of hydrophobic leucine residues capped at both the N- and C-termini with two positively charged, relatively polar lysine residues. Moreover, the normally positively charged N-terminus and the negatively charged C-terminus have both been blocked to provide a symmetrical tetracationic peptide that will more faithfully mimic the transbilayer region of natural membrane proteins. The central polyleucine region of these peptides was designed to form a maximally stable α -helix, particularly in the hydrophobic environment of the lipid bilayer core, while the dilysine caps were designed to anchor the ends of these peptides to the polar surface of the lipid bilayer and to inhibit the lateral aggregation of these peptides. In fact, CD (13) and FTIR (14-16) spectroscopic studies of P₂₄ have shown that it adopts a very stable α -helical conformation both in solution and in lipid bilayers, and X-ray diffraction (17), fluorescence quenching (18), and FTIR spectroscopic (14 - 16) studies have confirmed that P₂₄ and its analogues assume a transbilayer orientation with the N- and C-termini exposed to the aqueous environment and the hydrophobic polyleucine core embedded in the hydrocarbon core of the lipid

bilayer when reconstituted with various PCs. DSC (13, 15, 19-21) and ^2H NMR spectroscopy (13, 19, 20) studies have shown that P_{24} broadens the gel/liquid-crystalline phase transition and reduces its enthalpy. The phase transition temperature is shifted either upward or downward, depending on the degree of mismatch between the hydrophobic length of the peptide and the hydrophobic thickness of PC lipid bilayers (15), but this is not observed in PE bilayers, where P_{24} substantially decreases the phase transition temperature in a hydrocarbon chain length-independent manner (16). As well, small distortions of the α -helical conformation of P_{24} are also observed in response to peptide-lipid hydrophobic mismatch (15). ^2H NMR (22) and ESR (23) spectroscopic studies have shown that the rotational diffusion of P_{24} about its long axis perpendicular to the membrane plane is rapid in the liquid-crystalline state of the bilayer and that the closely related peptide L_{24} exists at least primarily as a monomer in liquid-crystalline POPC bilayers, even at relatively high peptide concentrations.

A similarly designed peptide, $(\text{LA})_{12}$, in which the polyleucine core of L_{24} is replaced by alternating leucine and alanine residues, has also been investigated to examine whether the replacement of one-half of the leucine residues by smaller and less hydrophobic alanine residues would influence the stability of the helical form of the peptide and if the surface topology of a transmembrane peptide would alter its effects on lipid bilayers. The application of a variety of physical techniques has revealed that the behavior of $(\text{LA})_{12}$ in solution and in lipid micelles or bilayers is generally similar to that of P_{24} (24-26). However, $(\text{LA})_{12}$ perturbs the gel/liquid-crystalline phase transition of PC and PE bilayers to a greater extent than does P_{24} at comparable concentrations, as inferred from the greater decrease of the temperature and enthalpy of the gel/liquid-crystalline

phase transition, possibly due partly to its rougher surface topology. However, the influence of the hydrophobic mismatch between the peptide and the host PC bilayer on the shift in the phase transition temperature is less pronounced for (LA)₁₂ than that for L₂₄, perhaps due in part to the greater conformational plasticity of (LA)₁₂ in response to alterations of the bilayer thickness (25, 26). Finally, we have recently shown that the related polyalanine-based peptide A₂₄ is insufficiently hydrophobic to assume an α -helical transmembrane orientation in hydrated PC bilayers (27).

In this study, we investigate the effects of the α -helical transmembrane peptide L₂₄ and the structurally related peptides L₂₄-DAP and W-L₂₂W on the thermotropic phase behavior of four odd-chain PC bilayers of differing hydrocarbon chain lengths. These structural derivatives of L₂₄ were used to evaluate several hypotheses related to the effects of peptide-lipid hydrophobic mismatch on the thermotropic phase behavior of phospholipid model membranes. First, with the peptide L₂₄-DAP, the two pairs of capping lysine residues at the terminus of L₂₄ have been replaced with the lysine analogues DAP, in which three of the four side-chain methylene groups have been removed. This peptide was used to test the so-called snorkel model first suggested by Segrest *et al.* (28) to explain the behavior of positively charged residues in the amphipathic helices present at the surfaces of blood lipoproteins and later extended to transmembrane α -helices by von Heijne *et al.* (29). According to the transmembrane peptide version of the snorkel model, the long, flexible hydrophobic side chains of lysine or arginine can extend along the transmembrane helix so that the terminal charged moiety can reside in the lipid polar headgroup region while the α -carbon of the amino acid residue remains well below (or possibly above) the membrane-water interface, even when

the hydrophobic length of the peptide is considerably different from that of the host lipid bilayer. Because of the shorter spacer arms between the charged group and the α -carbon of DAP, the peptide L₂₄-DAP is expected to be less accommodating to hydrophobic mismatch and any effects of such mismatch on the thermotropic phase behavior of its host lipid bilayer should be exaggerated.

Second, to investigate the importance of interfacially located tryptophan residues with respect to the effects of transmembrane peptides on their host lipid bilayer, we have also examined the effect of the peptide W-L₂₂-W on the thermotropic phase behavior of PC model membranes. W-L₂₂-W is an L₂₄ derivative in which the residues Leu-3 and Leu-26 are replaced with tryptophans. The preference of tryptophan and tyrosine residues for the polar-apolar interfaces of the membrane lipid bilayer is found to be one of the common features of natural membrane proteins (30-32).

Materials and methods

The phospholipids used in this study were obtained from Avanti Polar Lipids Inc. (Alabaster, AL) and were used without further purification. Commercially supplied solvents of at least analytical grade quality were redistilled prior to use. Peptides were synthesized and purified as TFA salts using previously published solid-phase synthesis and reversed phase high-performance liquid chromatographic procedures (24).

Samples were prepared for DSC as follows. Lipid and peptide were co-dissolved in methanol to attain the desired lipid-to-peptide ratio and the solvent was removed with a stream of nitrogen, leaving a thin film on the sides of a clean glass test tube. This film was subsequently dried *in vacuo* for several hours to ensure removal of the last traces of solvent. Samples containing 0.5-0.8 mg of lipid were then hydrated by vigorous

vortexing with a buffer (50 mM Tris, 150 mM NaCl, 1mM NaN₃, pH 7.4) at temperatures some 10-15°C above the gel/liquid-crystalline phase transition temperature of the lipid. DSC thermograms were obtained from 0.5 ml samples with a high sensitivity Microcal VP-DSC instrument (Microcal Inc., Northampton MA), operating at heating and cooling rates of 10° C per hour. The data were analyzed and plotted with the Origin software package (OriginLab Corporation, Northampton, MA).

Peptide samples to be used in FTIR spectroscopic experiments were converted to the hydrochloride salt by two cycles of lyophilization from 10 mM hydrochloric acid. This procedure was necessary because the trifluoroacetate ion gives rise to a strong absorption band (~1670 cm⁻¹) which partially overlaps the amide I absorption band of the peptide (15). Typically, samples were prepared by co-dissolving lipid and peptide in methanol at a lipid:peptide ratios near 30:1 (mol:mol). After removal of the solvent and drying of the film (see above), samples containing 2-3 mg of lipid were hydrated by vigorous mixing with 75 µl of a D₂O-based buffer (50 mM Tris, 150 mM NaCl, 1mM NaN₃, pH 7.4). The paste obtained was then squeezed between the CaF₂ windows of a heatable, demountable liquid cell (NSG Precision Cells, Farmingdale, NY) equipped with a 25 µm teflon spacer. Once mounted in the sample holder of the spectrometer, the sample temperature could be varied between 20° C and 90° C by an external, computer-controlled water bath. Infrared spectra were acquired as a function of temperature with a Digilab FTS-40 Fourier-transform spectrometer (Bio-Rad, Digilab Division, Cambridge, MA) using data acquisition parameters similar to those described by Mantsch *et al.* (33). The experiment involved a sequential series of 2° C temperature ramps with a 20 minute inter-ramp delay for thermal equilibration, and was equivalent to a scanning rate of 4° C per hour. Spectra

were analyzed with software supplied by the instrument manufacturers and other programs obtained from the National Research Council of Canada.

Results

In order to investigate the effects of hydrophobic mismatch between the three peptides studied here and the host lipid bilayer, we utilized four odd-chain linear saturated PCs ranging in chain length from 13 to 19 carbon atoms in the present study. The four PCs utilized, and their hydrophobic thicknesses in both the gel and liquid-crystallites states, are shown in Table 1. These values of bilayer hydrophobic thicknesses can be compared with the effective hydrophobic length of the polyleucine sequence of L₂₄, which we calculate to be 30.6 Å, assuming that this peptide adopts an ideal α -helical conformation when incorporated into phospholipid bilayers. Note that the effective hydrophobic length of L₂₄ of 30.6 Å is defined here as the average length of the polyleucine α -helix as measured at any point on its surface in a direction parallel to the helical axis, and is smaller than the 36.0 Å end-to-end distance of a stretch of 24 leucine residues (see 15). Given this value, note that the effective hydrophobic length of L₂₄ and its analogs approximately matches the hydrophobic thickness of 13:0 PC bilayers in the gel state, but is progressively shorter than the hydrophobic thickness of gel-state bilayers composed of the longer chain PCs studied here. Similarly, peptide effective length will approximately match the hydrophobic thickness of 19:0 PC bilayers in the liquid-crystalline state but will progressively exceed the hydrophobic thicknesses of the shorter chain liquid-crystalline PC bilayers. Finally, note that the mean hydrophobic thickness of 15:0 PC bilayers is very close to the calculated effective hydrophobic length of L₂₄ and

its analogs. Thus a mismatch between peptide hydrophobic length and mean bilayer hydrophobic thickness will occur with both the shorter and longer chain PCs studied here.

We stress that the pattern of hydrophobic mismatch described above strictly applies only if the conformation of L₂₄ and its analogs are not altered by changes in host bilayer thickness and conversely that the presence of these peptides does not significantly alter the conformation of the phospholipid hydrocarbon chains of the host PC bilayer. However, our previous DSC and FTIR spectroscopic studies of P₂₄ (15, 21), and the present studies of L₂₄ (see below), suggest that even these strongly α -helical poly-leucine-based peptides can alter the pitch of their helices in response to variations in host bilayer thicknesses, at least in gel-state bilayers. Conversely, the hydrocarbon chains of PC and PE bilayers can also change their degree of conformational order, and thus their effective hydrophobic thicknesses, to accommodate to the presence of these model peptides (15, 21). Moreover, this previous work and our recent ESR (23) and ²H-NMR (34) studies indicate that these peptides intrinsically disorder gel and order liquid-crystalline PC bilayers, even when hydrophobic mismatch effects are taken into consideration. Also, when the hydrophobic length of the peptide significantly exceeds that of the hydrophobic thickness of the liquid-crystalline host bilayer, peptide tilt may occur (see 11, 12). Thus, the actual degree of hydrophobic mismatch between L₂₄ and its analogs and the host PC bilayers studied here may be less than that indicated by the data presented in Table 1, which is for PC bilayers in the absence of peptide.

Thermotropic Phase Behavior of Phosphatidylcholine Bilayers in the Absence of Peptide.

As illustrated in Figure 1, in the absence of peptide the four odd-chain saturated PCs studied here by DSC exhibit a lower temperature, lower enthalpy, less cooperative

pretransition and a higher temperature, higher enthalpy, more cooperative main transition upon heating. The pretransition arises from the conversion of the lamellar gel (L_{β}') phase to the lamellar rippled gel (P_{β}') phase and the main phase transition from the conversion of the P_{β}' to the lamellar liquid-crystalline (L_{α}) phase. Both the pretransition and main phase transition increase in temperature with increases in the length of the PC hydrocarbon chains. However, the pretransition exhibits a steeper dependence on fatty acyl chain length than does the main transition, so that the temperature interval between these two phase transitions decreases as hydrocarbon chain length increases. The 13:0 PC (and 12:0 PC) are unique in the homologous series of linear saturated PCs in exhibiting a high temperature shoulder on the main phase transition endotherm. Although the physical basis of this unusual behavior is not fully understood, both thermal events are known to involve phospholipid hydrocarbon chain melting (35, 36) and will thus be considered as P_{β}'/L_{α} phase transitions in the analysis presented below. The reader is referred to Lewis *et al.* (36) and references cited therein for a more thorough discussion of the thermotropic phase behavior of the entire homologous series of linear saturated PCs.

The Effect of Peptide Incorporation on the Pretransition

The effect of the incorporation of L_{24} and its analogs on the pretransition of 13:0 PC could not be determined by DSC as the pretransition temperature of -1°C overlaps with the ice-melting endotherm centered near 0°C . However, the incorporation of increasing quantities of peptide into the longer chain PC bilayers lowers the temperature, enthalpy and cooperativity of the pretransition in each case, abolishing it entirely at a peptide incorporation levels above 6.7 mol % (see Figure 1). These results suggest that the presence of L_{24} reduces and eventually abolishes hydrocarbon chain tilt in these gel-phase

bilayers, causing the progressive replacement of the L_{β}' and P_{β}' phases with a disordered L_{β} -like phase (15, 25). Interestingly, the incorporation of peptide is more effective in this regard in the shorter chain PC bilayers where the hydrophobic mismatch between peptide hydrophobic length and bilayer hydrophobic thickness in the gel phase is minimal. Essentially identical results were found for the L_{24} analogs L_{24} -DAP and W- L_{22} -W.

The Effect of Peptide Incorporation on the Main Transition

The effect of the incorporation of L_{24} on the main phase transition of the four PCs studied here is also illustrated in Figure 1. In all cases the incorporation of increasing quantities of peptide produces a two-component DSC endotherm (in the case of 13:0 PC, a three-component endotherm, see Figure 2), as well as a progressive decrease in the enthalpy and cooperativity of the overall gel to liquid-crystalline phase transition of the host PC bilayer. The relative contribution of the sharp component of the DSC endotherm, which initially possesses a phase transition temperature, enthalpy and cooperativity relatively similar to that of the PC alone, decreases in magnitude as the proportion of L_{24} increases, and this component vanishes entirely at an L_{24} content of 6.7 mol %. In contrast, the relative contribution of the broad component increases as the peptide concentration increases and it is the only component which persists at the highest peptide concentration tested. Using the rationale provided in our previous DSC studies of the interaction of P_{24} and related peptides with lipid bilayers (15, 21, 25, 26), we assign the sharp component of our DSC endotherms to the hydrocarbon chain-melting phase transition of peptide-poor PC domains and the broad component to the melting of peptide-rich PC domains. Moreover, we ascribe the small decrease in the temperature and cooperativity of the sharp component of the DSC endotherms, to domain boundary

effects arising from the decreasing size of the peptide-poor PC domains, which of course also explains their progressively smaller enthalpy as peptide concentration increases. Note that these characteristic effects of L₂₄ and its analogs on the sharp component are noted in all the PCs studied and are hydrocarbon chain length independent.

In contrast to the PC hydrocarbon chain-length-independent effects of L₂₄ incorporation on the temperature, enthalpy and cooperativity of the sharp component of the DSC endotherm, the effects of peptide incorporation on the thermodynamic parameters of the broad component depend on the hydrocarbon chain length and thus on the thickness of the host PC bilayer. For example, as illustrated in Figure 3, the phase transition temperature of the broad component of the DSC endotherm occurs at a higher temperature than that of the sharp component in 13:0 PC bilayer, at the same temperature in 15:0 PC bilayers, but at lower temperatures in 17:0 and 19:0 PC bilayers, although in all cases the phase transition temperatures of both components decrease with increasing peptide concentration. This result is predicted by hydrophobic mismatch theory, since the effective hydrophobic length of L₂₄ is greater, matches, and is less than the mean hydrophobic thickness of 13:0 PC, 15:0 PC and 17:0 or 19:0 PC bilayers, respectively (37-39).

A comparison of the effects of a mismatch between peptide hydrophobic length and PC bilayer hydrophobic thickness on the magnitude of the shift of the phase transition temperature of the broad component of the phospholipid phase transition is presented in Figure 4. Although the characteristic hydrophobic mismatch-dependent shift in phase transition temperature discussed above for L₂₄ is also observed for the two L₂₄ analogs, the magnitude of this shift is considerably attenuated for W-L₂₂-W and especially for L₂₄

DAP. This result suggests that these two peptides are better able to accommodate alterations in the hydrophobic thickness of the host PC bilayer than can L₂₄ itself. We note here, however, that the snorkel hypothesis would predict that the hydrophobic mismatch effect on the phase transition temperature of the host lipid bilayer would be greater for L₂₄ DAP than for L₂₄ itself, in contrast to the results presented above.

A hydrocarbon chain length-dependent effect was also noted for the dependence of the overall phase transition enthalpy on L₂₄ concentration (see Figure 5). Although in all cases the overall phase transition enthalpy decreases with increasing peptide concentration, the rate of decrease in enthalpy is greatest for the shortest chain PC and decreases as the hydrocarbon chain length increases. Thus both the absolute and relative decreases in overall transition enthalpy are largest for 13:0 PC and smallest for 19:0 PC bilayers. However, the progressive but nonlinear decrease in the transition enthalpy of the sharp component, and the corresponding increase in the transition enthalpy of the broad component, are more or less comparable in each peptide-PC mixture examined. Note that an appreciable phase transition enthalpy remains even at relatively high peptide concentrations where the sharp transition due to the melting of peptide-poor PC domains has completely disappeared. This result indicates that the presence of even high concentrations of L₂₄ modestly reduces the magnitude of the cooperative gel to liquid-crystalline phase transition of the host lipid bilayers but certainly does not abolish it entirely, as also indicated by the FTIR spectroscopic results to be presented below. The same relationship between phase transition enthalpy and peptide concentration observed for L₂₄ was also observed for the L₂₄ analogs DAP-L₂₄ and W-L₂₂-W.

The effect of L₂₄ concentration on the cooperativity of the broad component of the gel/liquid-crystalline phase transition is also dependent on the hydrocarbon chain length of the host PC bilayer, as illustrated in Figure 6. Although in all cases the width of the phase transition increases with increases in the concentration of the peptide, this decrease in cooperativity is greatest for the shorter hydrocarbon chain length PC bilayers, where the peptide hydrophobic length and the hydrophobic thickness of the gel-state bilayer are most closely matched. The possible molecular basis for this effect will be discussed later.

The effect of increasing concentrations of each of the three peptides studied here on the cooperativity of the broad phase transition of 17:0 PC bilayers is presented in Figure 7. Although the cooperativity of this chain-melting phase transition, as measured by the $\Delta T_{1/2}$ parameter, increases more or less linearly in each case, this effect is greatest for L₂₄, intermediate for W-L₂₂-W, and smallest for L₂₄DAP. The possible molecular basis for this effect will also be discussed later.

Fourier Transform Infrared Spectroscopy Studies of Peptide-Containing PC Bilayers

In these studies, infrared spectra of mixtures of the peptide with each of the four PCs studied were recorded as a function of temperature and as a function of the mole fraction of the peptide. The use of FTIR spectroscopy permits a noninvasive monitoring of both the structural organization of the lipid bilayer and the conformation of the incorporated peptide. Thus the gel/liquid-crystalline phase transitions of the lipid bilayer and changes in the degree of rotational isomeric disorder of the lipid hydrocarbon chains can be conveniently monitored by changes in the frequency of the CH₂ symmetric stretching band near 2850 cm⁻¹, changes in solid-state hydrocarbon chain packing by changes in the CH₂ scissoring band near 1468 cm⁻¹, changes in the hydration and/or polarity of the

polar/apolar interfacial region of the lipid bilayer by changes in the contours of the ester carbonyl stretching bands nears 1735 cm^{-1} , and changes in peptide secondary structure can be monitored by changes in the conformationally sensitive amide I band near 1650 cm^{-1} (40). We find that the incorporation of these peptides into the lipid bilayer does not result in discernible changes in the hydration or the polarity of the polar/apolar interfacial regions of the lipid bilayer but severely inhibits the formation of lipid subgel phases, with the result that, at low temperature, the gel-phase frequencies of the CH_2 scissoring band near 1468 cm^{-1} are always typical of rotationally disordered hydrocarbon chains. Thus the only spectroscopic parameters we examined in detail were the amide I band of the peptide and the CH_2 symmetric stretching bands of the phospholipid hydrocarbon chains.

Illustrated in Figure 8 are the temperature-dependent changes in the frequencies of the peptide amide I absorption band and the CH_2 symmetric stretching band of the lipid hydrocarbon chains exhibited by mixtures of L_{24} (3.3 mol%) and each of the four PC studied here. The DSC heating endotherms of each sample are also shown to facilitate a comparison of the calorimetric and FTIR spectroscopic results. In all cases the DSC endotherms are accompanied by an increase in the CH_2 symmetric stretching frequency, indicating that both the sharp and broad components of the DSC endotherms are associated with lipid hydrocarbon chain-melting events (see ref. 40). Moreover, the lipid phase transition is accompanied by a decrease in the frequency of the L_{24} amide I band and the magnitude of this frequency change tends to increase with increases in the hydrocarbon chain length of the host PC bilayer. This result is entirely attributable to the fact that amide I band frequencies observed in gel phase bilayers increase with increases in hydrocarbon chain length, whereas the amide I band frequency in the liquid-crystalline

state is essentially independent of bilayer thickness (see Figure 8). Qualitatively similar results were obtained when the peptides L₂₄-DAP and W-L₂₂-W were incorporated into these PC bilayers (data not shown). The pattern of hydrocarbon chain length dependent changes in amide I frequency shifts at the gel/liquid-crystalline phase transition of these lipid/peptide mixtures is similar to that observed when the peptide P₂₄ was incorporated into PC and PE bilayers (15, 21) and has previously been ascribed to small conformational distortions of the peptide helix (41).

The data presented in Figure 9 illustrate the relative magnitudes of the amide I frequency changes exhibited by the peptides L₂₄, L₂₄-DAP and W-L₂₂-W at the gel/liquid-crystalline phase transition of 19:0 PC. As noted above, the behavior of each of these peptides is qualitatively similar in that the main phase transition of the host lipid bilayer is accompanied by a decrease in amide I frequency. The magnitude of this frequency shift ($\sim 3 \text{ cm}^{-1}$) is similar for all three peptides, suggesting that the peptides L₂₄, L₂₄-DAP and W-L₂₂-W are all comparably responsive to alterations in the thickness of the host PC bilayer. However, a close inspection of the contours of the amide I bands of these peptides indicates that these shifts in overall band frequency are actually caused by changes in the relative intensities of the underlying band components (see Figure 10). Specifically, when incorporated into bilayers composed of the longer chain PCs, the amide I absorption bands of all three peptides consist primarily of two components centered near 1653 cm^{-1} and $1658\text{-}1660 \text{ cm}^{-1}$ when the lipids are in the gel state (see Figure 10). Moreover, the lower frequency component exhibited by the peptides L₂₄ and L₂₄-DAP is relatively more prominent whereas with peptide W-L₂₂-W, the higher frequency component is the more prominent (see Figure 10). We also find that both the

intensity and center of gravity of the higher frequency component increase slightly as the thickness of the host bilayer increases in the gel state. However, at temperatures above the lipid gel/liquid-crystalline phase transition, the intensity of the higher frequency component exhibited by all three peptides decreases relative to that the lower-frequency component, and as a result, the overall frequency of the amide I band maximum decreases. Further examination using difference spectra analysis indicates that with all three peptides, the relative decline in the intensity of the higher frequency component near $1658\text{-}1660\text{ cm}^{-1}$ is accompanied by an overall increase in the intensity of broader components centered near $1645\text{-}1649\text{ cm}^{-1}$ (analyses not shown). The possible molecular basis of those spectroscopic observations will be discussed below.

Discussion

A comparison of the thermotropic phase behavior of PC vesicles containing L₂₄ (this study) with those containing the closely related P₂₄ (15) reveals that, in general, these peptides have very similar effects on the organization of their host PC bilayers. With both peptides, DSC thermograms observed at low peptide concentrations can be resolved into two components which are probably attributable to the melting of peptide-poor (sharp component) and peptide-rich (broad component) lipid domains. Moreover, the effects of these peptides on the temperature, enthalpy and overall cooperativity of the lipid hydrocarbon chain-melting phase transition, the sensitivity of these parameters to the variations in lipid hydrocarbon chain length, the apparent stoichiometry of the peptide/PC interactions, and the magnitude of the hydrophobic mismatch effects observed with these two peptides are essentially the same, within experimental error. Finally, both peptides also exhibit similar patterns of lipid phase-state dependent and lipid hydrocarbon chain-

length dependent changes in amide I band frequency when incorporated into PC bilayers. These results provide strong evidence that the spacer amino acid residues Gly-3 and Ala-30 of P₂₄ have no significant effect on its interaction with PC bilayers. We therefore conclude that the results of previous extensive studies of P₂₄-phospholipid interactions can be applied with reasonable confidence to the compositionally similar, second generation peptide L₂₄.

Previous FTIR spectroscopic studies have shown that the gel/liquid-crystalline phase transitions of P₂₄/phospholipid mixtures are accompanied by small phase state-dependent amide I frequency shifts (15, 16). Similar studies of (LA)₁₂/phospholipid mixtures revealed a more complex phase state-dependent behavior in which the main amide I band of (LA)₁₂ appears to be a single component ($\sim 1654\text{ cm}^{-1}$) in the liquid-crystalline state, and a partially resolved summation of two components ($\sim 1665\text{ cm}^{-1}$ and 1655 cm^{-1}) when the peptide is dispersed in the gel phases of PE and longer chain PC bilayers (25, 26). Here, we have also revealed a pattern of phase state-dependent amide I frequency shifts which appear to be of comparable magnitude to those observed in previous studies of P₂₄/phospholipid interactions. However, we also find that when dispersed in the gel phases of the longer chain PCs, the main amide I bands exhibited by L₂₄, L₂₄-DAP and by W-L₂₂-W each contains components centered near $1657\text{-}1659\text{ cm}^{-1}$ and near $1653\text{-}1654\text{ cm}^{-1}$ and, as previously observed in our studies of (LA)₁₂, the intensity of the higher-frequency component decreases when the host lipid bilayer converts to the liquid-crystalline state. We also find that the decrease in intensity of the higher frequency components of the amide I band is accompanied by an increase in the intensity of broader, less defined components centered between $1645\text{-}1649\text{ cm}^{-1}$. Interestingly, a

reexamination of our FTIR spectroscopic data on the interactions of peptides P₂₄ and (LA)₁₂ with phospholipid bilayers indicates that a similar process was also occurring in those systems, albeit of different magnitude. It is therefore possible that the phase state-dependent amide I frequency shifts reported here and in our previous studies of P₂₄ (15,16) and (LA)₁₂ (25,26) may actually be manifestations of the same physical phenomenon.

In considering the possible physical basis of these FTIR spectroscopic results, we note that the amide I frequencies observed are all in a range consistent with the predominance of α -helical structures and it is therefore unlikely that our experimental observations are the result of conformational interconversions between α -helical and non- α -helical forms of these peptides. This conclusion is consistent with those made in our previous studies, wherein we suggested that the observed frequency shifts were the result of small alterations in the pitch of the peptide α -helix in response to changes in lipid bilayer thickness (see 41). We also note that amide I frequencies near 1655 cm⁻¹ are typical of α -helices with fully protonated peptide amide bonds, whereas amide I frequencies near 1645-1650 cm⁻¹ are usually observed when those bonds are fully deuterium exchanged (42 - 44). Moreover, the major amide I component near 1653 cm⁻¹ is relatively insensitive to changes in lipid phase state and/or lipid bilayer thickness. This observation suggests that most of the amide bonds of these peptides are protected from H-D exchange and are not involved in the structural changes induced by the changes in the phase state or thickness of the host lipid bilayer. Given these observations, the fact that interconversion between amide I components absorbing near 1658-1665 cm⁻¹ and a deuterium-exchanged population near 1645-1649 cm⁻¹ seems to constitute the basis of the

frequency shifts reported here and in our previous studies (15, 16, 25, 26), and the fact that the deuterium-exchanged populations of amide bonds are probably localized near the N- and C-terminii of these peptides (45, 46), we suggest that the conformational changes which give rise to the higher frequency components observed when these peptides are incorporated into the gel phases of PE and longer chain PC bilayers occur predominantly in the terminal, deuterium-exchanged portions of the peptide α -helix. That the phase state- and bilayer thickness-induced distortions of the α -helical structures of these peptides may actually be limited to their terminal regions is consistent with the inherent stability of their polyleucine cores and with the fraying of the ends of protein and peptide helices. The fact that the higher frequency component predominates in thicker gel state bilayers, where the thickness of the PC bilayer exceeds the length of the incorporated peptide, is consistent with a stretching of the α -helix to minimize mismatch with host lipid bilayer. Similarly, the fact that the lower frequency component predominates in thinner gel or liquid-crystalline bilayers is consistent with both a reduced stabilization of α -helical structure due to the projection of the peptide terminae beyond the conformationally stabilizing bilayer surface and to the greater exposure of the ends of these α -helices to the aqueous phase. However, it will be necessary to conform these suggestions experimentally, perhaps by using transmembrane peptides with specifically labeled amino acid residues near to the chain terminae.

It is interesting to compare the observed effects of the incorporation of L₂₄ and L₂₄-DAP on the relative thermal stabilities of the gel and liquid-crystalline states of PC bilayers of different hydrocarbon chain lengths with the effects predicted by the snorkel model (28, 29). According to this model, the four methylene groups separating the

terminal amino groups of the side chains of the two Lys residues from the α -carbon atoms should provide considerable flexibility to these residues, allowing L_{24} to better accommodate to any mismatch between the length of the incorporated peptide and the thickness of the host PC bilayer. In contrast, the truncated side chains of the two DAP residues at the ends of L_{24} -DAP should markedly reduce their flexibility and thus their ability to adjust to such mismatches. If one also assumes that the terminal amino groups of the Lys or DAP residues prefer to be located at the level of the polar and negatively charged phosphate group of the PC molecules, where favorable electrostatic and hydrogen bonding interactions are maximized, and neglecting other effects of this structural modification (see below), the following predictions can be made. In the relatively thin gel-state bilayers state formed by 13:0 PC, the two Lys or DAP residues at each end of L_{24} and L_{24} -DAP, respectively, should be located at approximately the same level as the PC headgroups. In this case, these residues should interact with the PC phosphate group in a fairly strong and similar manner, since a snorkeling of the Lys and DAP residue side chains is not required in this case. In contrast, in the relatively very thin liquid-crystalline bilayers formed by 13:0 PC, the two terminal Lys or DAP residues of L_{24} and L_{24} -DAP will be located about 3.5 and 10 Å above the level of the PC polar headgroups, thus projecting into the aqueous phase. Thus, in this case, one predicts that the snorkeling of the Lys but not the DAP residues should permit L_{24} but not L_{24} -DAP to interact more favorably with the PC phosphate groups, differentially stabilizing the liquid-crystalline phase and resulting in a more pronounced decrease in the phase transition temperature in 13:0-PC bilayers containing L_{24} than L_{24} -DAP. Moreover, this result should also be the case even if these peptides tilt to minimize the mismatch

between peptide length and bilayer thickness, since snorkeling of the Lys side chains of L₂₄ should reduce the degree of peptide tilting required, which is energetically costly as it produces disorder in the host phospholipid bilayer (47, 48). In contrast, in the relatively much thicker gel state bilayers formed by 17:0-PC, the terminal amino groups of the Lys and DAP residues of L₂₄ and L₂₄-DAP, respectively, are located about 5.7 and 7.3 Å below the level of the PC polar headgroups, while in the liquid-crystalline state, terminal amino groups are again located at the same level in the bilayer as the lipid phosphate groups. Thus, in this case, snorkeling of the Lys side chains of L₂₄ toward the bilayer surface in the gel-state 17:0-PC system should differentially stabilize this state, resulting in a higher phase transition temperature in L₂₄ – as compared to L₂₄-DAP-containing 17:0-PC dispersions. Interestingly, in 15:0-PC bilayers, where the terminal amino groups of the Lys and DAP residues are located below the level of the PC polar headgroups in the relatively thicker gel-state bilayers but above the level of the lipid phosphate groups in the thinner liquid-crystalline bilayers by roughly comparable distances, one predicts that snorkeling of the Lys side chains of L₂₄ would stabilize both the gel and liquid-crystalline phases of 15:0 PC bilayers, thus producing no net shift in the lipid phase transition temperature as compared to L₂₄-DAP, a result which is in fact observed experimentally (see Figure 4). However, according to the snorkel hypothesis, the major effect of the increased ability of L₂₄ as compared to L₂₄-DAP to accommodate to differences between peptide length and phospholipid bilayer thickness should be that the magnitude of the phase transition temperature shifts as a function of host bilayer thickness should be smaller in the former as compared to the latter peptide. However, the experimental result (see Figure 4) is in fact the opposite of that predicted, suggesting that

the snorkeling of the Lys sidechain, if it occurs, is not the primary factor in producing the experimentally observed effects of these two peptides on the thermotropic phase behaviour of homologous series of PC bilayers examined here. Instead, this result suggests that another effect of the DAP-for-Lys substitution at the peptide terminae must have a greater effect on peptide-phospholipid polar head group interactions.

We note that the truncation of the Lys sidechain should not only inhibit its ability to alter its depth in the PC bilayer, it should also weaken the strength of the attractive electrostatic and hydrogen-bonding interactions between the positively charged amino group of the peptide and the negatively charged phosphate group of the phospholipid molecule by increasing the distance between these moieties in the lipid bilayer, even if these two groups reside in the same plane. This is because the longer side chain of the Lys residue results in its terminal amino group projecting beyond the cylindrical surface formed by the polyLeu core of the peptide, permitting interaction with adjacent PC molecules, whereas this is not the case with the much shorter DAP residues. Due to the stronger attractive peptide-phospholipid polar headgroup interactions in PC bilayers generally, one would predict that PC bilayers, in either the L_{α} or L_{β} state, would be differentially stabilized by L_{24} relative to L_{24} -DAP even in the absence of hydrophobic mismatch. Thus in this case one predicts that L_{24} preferentially stabilizes the gel phase in 13:0-PC bilayers and the liquid-crystalline state in 17:0 PC bilayers, thus producing a steeper dependence of the phase transition temperature on PC hydrocarbon chain length in L_{24} as compared to L_{24} -DAP-containing systems. In fact, this is what is observed experimentally (see Figure 4), suggesting that the length *per se*, rather than the flexibility, of the side chains of the positively charged terminal amino acid residues may be of more

importance for the interactions of these peptides with the polar headgroups of the phospholipid molecules of the host bilayer. Moreover, we would predict that this latter effect would be even more prominent in anionic as compared to zwitterionic phospholipid bilayers, a hypothesis currently being tested. We note here, however, that in all other respects L₂₄ and L₂₄-DAP behave essentially identically when incorporated in PC bilayers of varying thickness. Thus the substitution of DAP for Lys residues has only minor effects on the overall organization of the host PC bilayer.

A comparison of the observed and predicted effects of the incorporation of L₂₄ and WL₂₂W on the relative thermal stabilities of the gel and liquid-crystalline states of bilayers composed of PCs with different hydrocarbon chains can also be made. As discussed earlier, aromatic residues in general, and Trp and Tyr residues in particular, tend to occur near the ends of the α -helical transmembrane segments of membrane proteins, being located in the so-called flanking regions between the hydrophobic central region and the charged amino acids which often terminate the α -helical segment (30-32). These aromatic residues are thus located in the region of glycerol backbone of the phospholipid molecules composing the host bilayer, between the polar headgroup and the nonpolar hydrocarbon chains (30 - 32). It has been suggested that Trp and Tyr residues are particularly well suited to reside in this region of intermediate polarity of the phospholipid bilayer, most likely because their rigidity and flat shape limit access to the hydrocarbon core and the pi electronic structure and aromaticity favor residing in an electrostatically complex interfacial environment (49 - 51).

If we assume that Trp residues are better suited to localization near the glycerol backbone region of the phospholipid molecules than are Leu residues, we can then

predict what the relative effect of L₂₄ and WL₂₂W would be on the gel/liquid-crystalline phase transition temperature of PC bilayers of different thicknesses, using the rationale presented above for the comparison of L₂₄ and L₂₄-DAP. In particular, we predict that mixtures of WL₂₂W and PC bilayers where the length of the peptide and the thickness of the host phospholipid bilayer are well matched should be differentially stabilized relative to the same system containing comparable amounts of L₂₄. Thus WL₂₂W should differentially stabilize the gel phase of bilayers composed of 13:0-PC and the liquid-crystalline phase of bilayers composed of 17:0-PC, as mismatch between the location of the Trp residues of the peptide and the glycerol backbone regions of the host lipid bilayer are minimized in these systems. As well, in thinner PC bilayers, the possible exposure of the more polar and positively charged Trp residues to the phospholipid polar headgroups and to the aqueous phase is probably less energetically costly than is the exposure of the uncharged and hydrophobic Leu residues, and vice versa. These two effects should produce a greater dependence of the peptide-induced shifts in the gel/liquid-crystalline phase transition on the hydrocarbon chain length of the PC molecules for WL₂₂W than for L₂₄. However, the opposite result is observed experimentally (see Figure 4). Again, we conclude that effects of the Trp for Leu substitution, other than the relative affinities of these amino acid residues for the glycerol backbone region of the PC molecule, must have a greater influence on peptide-lipid interactions in these systems.

In closing, we wish to emphasize that our results should not be interpreted as indicating that the possible snorkeling of the Lys side chains, and the affinity of Trp residues for the polar/nonpolar region of the host phospholipid bilayer, are not important for the structure and function of natural transmembrane peptides or for the

accommodation of such proteins to environmentally induced variations in the thickness of the host lipid bilayer. In this regard we note that the focus of the present study is on the perturbation of the thermotropic phase behaviour of bilayers composed of PCs of different hydrocarbon chains length, which can in principle be affected by a variety of physical properties of the peptide analogs examined here. Moreover, the strong affinity of the polyleucine core of L₂₄ and its analogs for the hydrophobic core of the host lipid bilayer may have partially obscured the effects of amino acid substitutions near the peptide terminus. Certainly the work of Killian *et al.* (52 – 54) on Leu-Ala-based transmembrane peptides has demonstrated differential effects on Lys- and Trp-capped peptides on phospholipid thermotropic phase behaviour and organization. Nevertheless, it is noteworthy that the incorporation of L₂₄, L₂₄-DAP and WL₂₂W have such generally similar effects on the thermotropic phase behavior of these PC bilayers.

References

1. Gennis, R.B. (1989) Membrane dynamics and protein-lipid interactions, in *Biomembranes: Molecular Structure and Function*, Springer-Verlag, pp 166-198, New York.
2. Yeagle, P. (1992) *The Structure of Biological Membranes*, CRC Press, Boca Raton, FL.
3. Sandermann, H. (1978) Regulation of membrane enzymes by lipids, *Biochim. Biophys. Acta* 515, 209-237.
4. McElhaney, R.N. (1982) Effects of membrane lipids on transport and enzymic activities, in *Current Topics in Membranes and Transport* (Razin, S., and Rottem, S., Eds.), Vol. 17, pp 317-380, Academic Press, New York.
5. McElhaney, R.N. (1985) Membrane lipid fluidity, phase state and membrane function in prokaryotic microorganisms, in *Membrane Fluidity in Biology* (Alora, R.A., and Boggs, J.M., Eds.), Vol. 4, pp 147-208, Academic Press, New York.
6. McElhaney, R.N. (1986) Differential scanning calorimetric studies of lipid-protein interactions in model membrane systems, *Biochim. Biophys Acta* 864, 361-421.
7. Watts, A., and De Pont, J.J.H.H.M. (Eds.) (1985) *Progress in Lipid-Protein Interactions*, Vol. 1, Elsevier, Amsterdam.
8. Watts, A., and De Pont, J.J.H.H.M. (Eds.) (1986) *Progress in Lipid-Protein Interactions*, Vol. 2, Elsevier, Amsterdam.
9. Marsh, D., and Horváth, L.I. (1998) Structure, dynamics and composition of the lipid-protein interface. Perspectives from spin-labelling, *Biochim. Biophys. Acta* 1376, 267-296.

10. Watts, A. (1998) Solid-state NMR approaches for studying the interaction of peptides and proteins with membranes, *Biochim. Biophys Acta* 1376, 297-318.
11. White, S.H., and Wimley, W.C. (1998) Hydrophobic interactions of peptides with membrane interfaces, *Biochim. Biophys. Acta* 1376, 339-352.
12. Killian, J.A. (1998) Hydrophobic mismatch between proteins and lipids in membranes, *Biochim. Biophys. Acta* 1376, 401-416.
13. Davis, J.M., Clare, J.M., Hodges, R.S., and Bloom, M. (1983) Interaction of a synthetic amphiphilic polypeptide and lipids in a bilayer structure, *Biochemistry* 22, 5298-5305.
14. Zhang, Y.-P., Lewis, R.N.A.H., Hodges, R.S., and McElhaney, R.N. (1992) FTIR spectroscopic studies of the conformation and amide hydrogen exchange of a peptide model of the hydrophobic transmembrane α -helices of membrane proteins, *Biochemistry* 31, 11572-11578.
15. Zhang, Y.-P., Lewis, R.N.A.H., Hodges, R.S., and McElhaney, R.N. (1992) Interaction of a peptide model of a hydrophobic transmembrane α -helical segment of a membrane protein with phosphatidylcholine bilayers: differential scanning calorimetric and FTIR spectroscopic studies, *Biochemistry* 31, 11579-11588.
16. Axelsen, P.H., Kaufman, P.H., McElhaney, R.N., and Lewis, R.N.A.H. (1995) The infrared dichroism of transmembrane helical polypeptides, *Biophys. J.* 69, 2770-2781.
17. Huschilt, J.C., Millman, B.M., and Davis, J.H. (1989) Orientation of alpha-helical peptides in a lipid bilayer, *Biochim Biophys. Acta* 979, 139-141. *Biochim Biophys. Acta* 979, 139-141.

18. Bolen, E.J., and Holloway, P.W. (1990) Quenching of tryptophan fluorescence by brominated phospholipid, *Biochemistry* 29, 9638-9643.
19. Huschilt, J.C., Hodges, R.S., and Davis, J.H. (1985) Phase equilibria in an amphiphilic peptide-phospholipid model membrane by deuterium nuclear magnetic resonance difference spectroscopy, *Biochemistry* 24, 1377-1386.
20. Morrow, M.R., Huschilt, J.C., and Davis, J.H. (1985) Simultaneous modeling of phase and calorimetric behavior in an amphiphilic peptide/phospholipid model membrane, *Biochemistry* 24, 5396-5406.
21. Zhang, Y.-P., Lewis, R.N.A.H., Hodges, R.S., and McElhaney, R.N. (1995) Interaction of a peptide model of a hydrophobic transmembrane α -helical segment of a membrane protein with phosphatidylethanolamine bilayers: differential scanning calorimetric and FTIR spectroscopic studies, *Biophys. J.* 68, 847-857.
22. Pauls, K.P., MacKay, A.L., Soderman, O., Bloom, M., Taneja, A.K., and Hodges, R.S. (1985) Dynamic properties of the backbone of an integral membrane polypeptide measured by ^2H -NMR, *Euro. Biophys. J.* 12, 1-11.
23. Subczynski, W.K., Lewis, R.N.A.H., McElhaney, R.N., Hodges, R.S., Hyde, J.S., and Kusumi, A. (1998) Molecular organization and dynamics of 1-palmitoyl-2-oleoyl-phosphatidylcholine bilayers containing a transmembrane α -helical peptide, *Biochemistry* 37, 3156-3164.
24. Zhang, Y.-P., Lewis, R.N.A.H., Henry, G.D., Sykes, B.D., Hodges, R.S., and McElhaney, R.N. (1995) Peptide models of helical hydrophobic transmembrane segments of membrane proteins. I. Studies of the conformation, intrabilayer

- orientation and amide hydrogen exchangeability of Ac-K₂-(LA)₁₂-K₂ amide, *Biochemistry* 34, 2348-2361.
25. Zhang, Y.-P., Lewis, R.N.A.H., Hodges, R.S., and McElhaney, R.N. (1995) Peptide models of helical hydrophobic transmembrane segments of membrane proteins. II. DSC and FTIR spectroscopic studies of the interaction of Ac-K₂-(LA)₁₂-K₂-amide with phosphatidylcholine bilayers, *Biochemistry* 34, 2362-2371.
26. Zhang, Y.-P., Lewis, R.N.A.H., Hodges, R.S., and McElhaney, R.N. (2001) Peptide models of the helical hydrophobic transmembrane segments of membrane proteins: Interactions of acetyl-K₂-(LA)₁₂-K₂-amide with phosphatidyl-ethanolamine bilayer membranes, *Biochemistry* 40, 474-482.
27. Lewis, R.N.A.H., Zhang, Y.-P., Hodges, R.S., Subczynski, W.K., Kusumi, A., Flach, C.R., Mendelsohn, R., and McElhaney, R.N. (2001) A polyalanine-based peptide cannot form a stable transmembrane α -helix in fully hydrated phospholipid bilayers, *Biochemistry* 40, 12103-12111.
28. Segrest, J.P., De Loof, H., Dohlman, J.G., Brouillette, C.G., and Anantharamaiah, G.M. (1990) Amphipathic helix motif: classes and properties, *Proteins: Struct., Funct. Genet.* 8, 103-117.
29. Monne, M., Nilsson, I., Johansson, M., Elmhed, N., and van Heijne, G. (1998) Positively and negatively charged residues have different effects on the position in the membrane of a model transmembrane helix, *J. Mol. Biol.* 284, 1177-1183.
30. Von Heijne, G. (1999) Recent advances in the understanding of membrane protein assembly and structure, *Quart. Rev. Biophys.* 32, 285-307.

31. Popot, J.-L., and Engelman, D.M. (2000) Helical membrane protein folding, stability, and evolution, *Annu. Rev. Biochem.* 69, 881-992.
32. Jayasinghe, S., Hristova, K., and White, S.H. (2001) MPtopo: A database of membrane protein topology, *Protein Sci.* 10, 455-458.
33. Mantsch, H.H., Madec, C., Lewis, R.N.A.H., and McElhaney, R.N. (1985) The thermotropic phase behaviour of model membranes composed of phosphatidylcholines containing isobranched fatty acids. II. Infrared and ³¹P-NMR spectroscopic studies, *Biochemistry* 24, 2440-2446.
34. Pare, C., Lafleur, M., Liu, F., Lewis, R.N.A.H., and McElhaney, R.N. (2001) Differential scanning calorimetry and ²H-nuclear magnetic resonance and Fourier transform infrared spectroscopic studies of the effects of transmembrane α -helical peptides on the organization of phosphatidylcholine bilayers, *Biochim. Biophys. Acta* 1511, 60-73.
35. Morrow, M.R., Huschilt, J.C., and Davis, J.H. (1985) Simultaneous modeling of phase and calorimetric behavior in an amphiphilic peptide/phospholipid model membrane, *Biochemistry* 24, 5396-5406.
36. Lewis, R.N.A.H., Mak, N., and McElhaney, R.N. (1987) A differential scanning calorimetric study of the thermotropic phase behavior of model membranes composed of phosphatidylcholines containing linear saturated fatty acyl chains, *Biochemistry* 26, 6118-6126.
37. Owicki, J.C., and McConnell, H.M. (1979) Theory of protein-lipid and protein-protein interactions in bilayer membranes, *Proc. Natl. Acad. Sci. U.S.A.* 76, 4750-4754.

38. Mouritsen, O.G., and Bloom, M. (1984) Mattress model of lipid-protein interactions in membranes, *Biophys. J.* *46*, 141-153.
39. Riegler, J., and Muhwald, H. (1986) Elastic interactions of photosynth ETIC reaction center proteins affecting phase transitions and protein distributions, *Biophys. J.* *49*, 1111-1118.
40. Lewis, R.N.A.H., and McElhaney, R.N. (1996) FTIR spectroscopy in the study of hydrated lipids and lipid bilayer membranes, in *Infrared Spectroscopy of Biomolecules*, (Mantsch, H.H., and Chapman, D., Eds.) pp 159-202, John Wiley and Sons, New York.
41. Chirgadze, Y.N., Brazhnikov, E.V., Nevskaya, N.A. (1976) Intramolecular distortion of the alpha-helical structure of polypeptides, *J. Mol. Biol.* *102*, 781-792.
42. Chirgadze, Y.N., and Brazhnikov, E.V. (1974) Intensities and other spectral parameters of infrared amide bands of polypeptides in the alpha-helical form, *Biopolymers* *13*, 1701-1712.
43. Rabolt, J.F., Moore, W.H., and Krimm, S. (1977) Vibrational analysis of peptides, polypeptides, and proteins. 3. alpha-Poly (L-alanine), *Macromolecules* *10*, 1065-1074.
44. Dwivedi, A.M. and Krimm, S. (1984) Vibrational analysis of peptides, polypeptides, and proteins. XVIII. Conformational sensitivity of the alpha-helix spectrum: alpha I- and alpha II-poly (L-alanine), *Biopolymers* *23*, 923-943.
45. Nakanishi, M., Tsuobi, M., Ikegami, A., and Kanehisa, M. (1972) Fluctuation of an alpha-helix structure. Difference between the central and terminal portions, *J. Mol. Biol.* *64*, 363-378.

46. Dempsey, C.E. (1988) pH Dependence of hydrogen exchange from backbone peptide amides of melittin in methanol, *Biochemistry* 27, 6893-6901
47. Li, L. (2000) Relating helix tilt in a bilayer to lipid disorder: a mean-field theory, *Biophys. Chem.* 86, 79-83.
48. Harzer, U., and Bechinger, B. (2000) Alignment of lysine-anchored membrane peptides under conditions of hydrophobic mismatch: a CD, 15N and 31P solid-state NMR spectroscopy investigation *Biochemistry* 39, 13106-13114
49. Yau, W.M., Wimley, W.C., Gawrisch, K., and White, S.H. (1998) The preference of tryptophan for membrane interfaces, *Biochemistry* 37, 14713-14718.
50. Persson, S., Killian, J.A., and Lindblom, G. (1998) Molecular ordering of interfacially localized tryptophan analogs in ester- and ether-lipid bilayers studied by 2H-NMR, *Biophys. J.* 75, 1365-1371.
51. White, S.H., and Wimley, W.C. (1999) Membrane protein folding and stability: physical principles, *Ann. Rev. Biophys. Biomol. Struct.* 28, 319-365.
52. Killian, J.A., Salemink, I., de Planque, M.R.R., Lindblom, G., Koeppe, R.E., and Greathouse, D.V. (1996) Induction of nonbilayer structures in diacylphosphatidylcholine model membranes by transmembrane alpha-helical peptides: importance of hydrophobic mismatch and proposed role of tryptophans, *Biochemistry* 35, 1037-1045.
53. de Planque, M.R.R., Greathouse, D.V., Koeppe, R.E., Schafer, H., Marsh, D., and Killian, J.A. (1998) Influence of lipid/peptide hydrophobic mismatch on the thickness of diacylphosphatidylcholine bilayers. A ²H NMR and ESR study using designed transmembrane α -helical peptides and gramicidin A, *Biochemistry* 37, 9333-9345.

54. de Planque, M.R.R., Kruijtzter, J.A.W., Liskamp, R.M.J., Marsh, D., Greathouse, D.V., Koeppe, R.E., de Kruijff, B., and Killian, J.A. (1999) Different membrane anchoring positions of tryptophan and lysine in synthetic transmembrane α -helical peptides, *J. Biol. Chem.* 274, 20839-20846.

Table I: Hydrophobic Thickness of the Bilayers Formed by Various Phosphatidylcholines

PC	hydrophobic thickness (Å) ^a		
	gel phase	liquid-crystalline phase	mean ^b
13:0	31.5	21.0	26.3
15:0	36.8	24.5	30.7
17:0	42.0	28	35
19:0	47.2	31.5	39.4

^a Hydrophobic thickness were calculated as Zhang (15).

^b The mean of the hydrophobic thickness of the gel and liquid-crystalline phase.

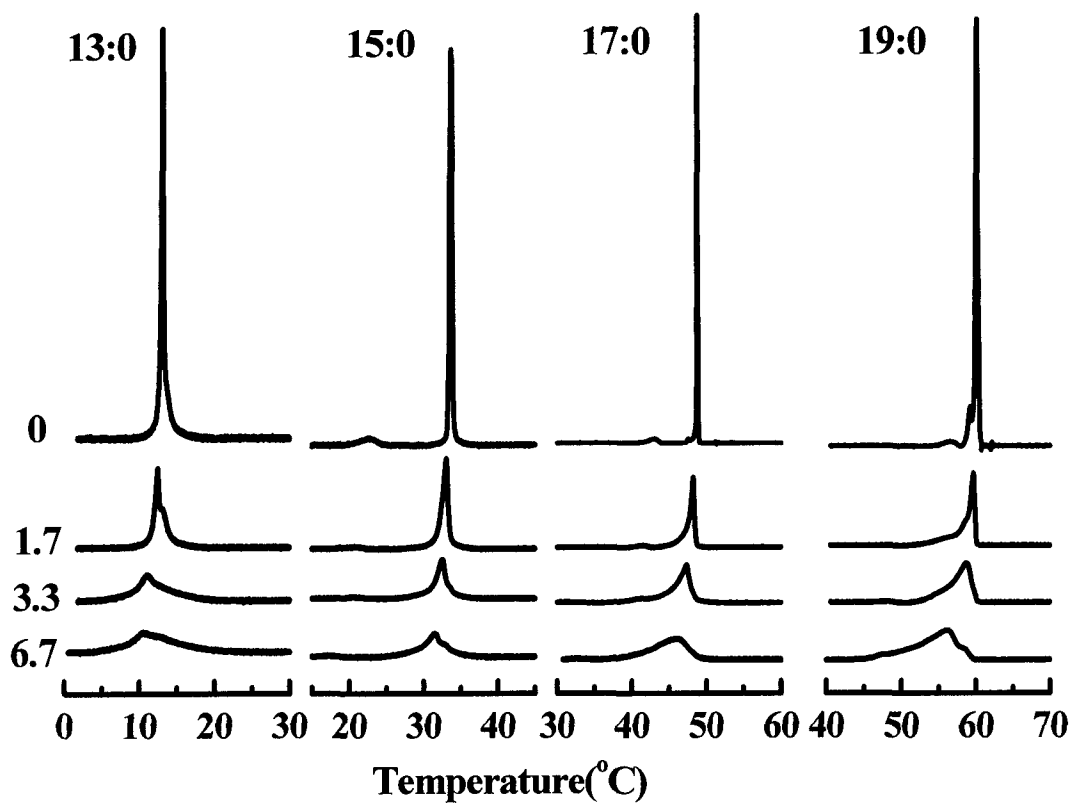


FIGURE 1. Effect of L₂₄ on the DSC heating thermograms of a series of *n*-saturated diacyl-PCs varying in hydrocarbon chain length. The mole percent of peptide present in each sample is indicated in the column of numbers printed on the left side of the figure.

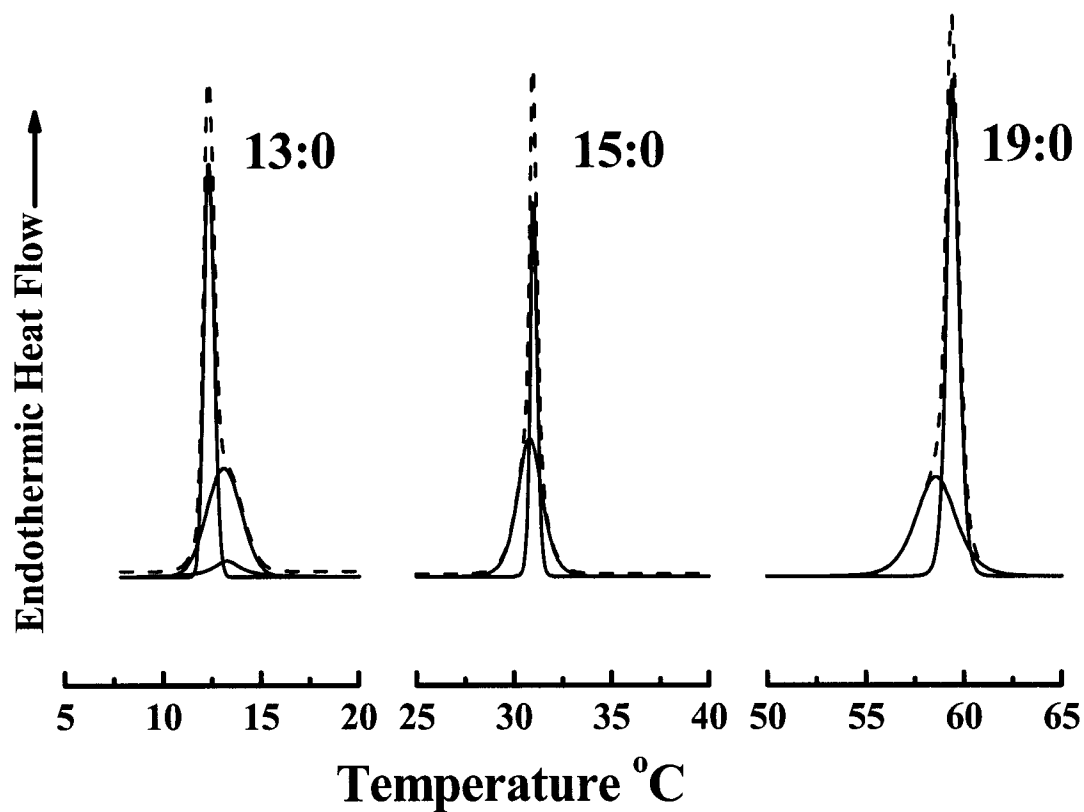


FIGURE 2. Illustration of the results of the curve-fitting procedure used to resolve the components of the DSC heating thermograms exhibited by mixtures of L_{24} with PC bilayers. The examples shown are $L_{24}/13:0PC$ (left panel); $L_{24}/15:0PC$ (middle panel); $L_{24}/19:0PC$ (right panel). In all cases the samples contained 3.3 mol % of L_{24} .

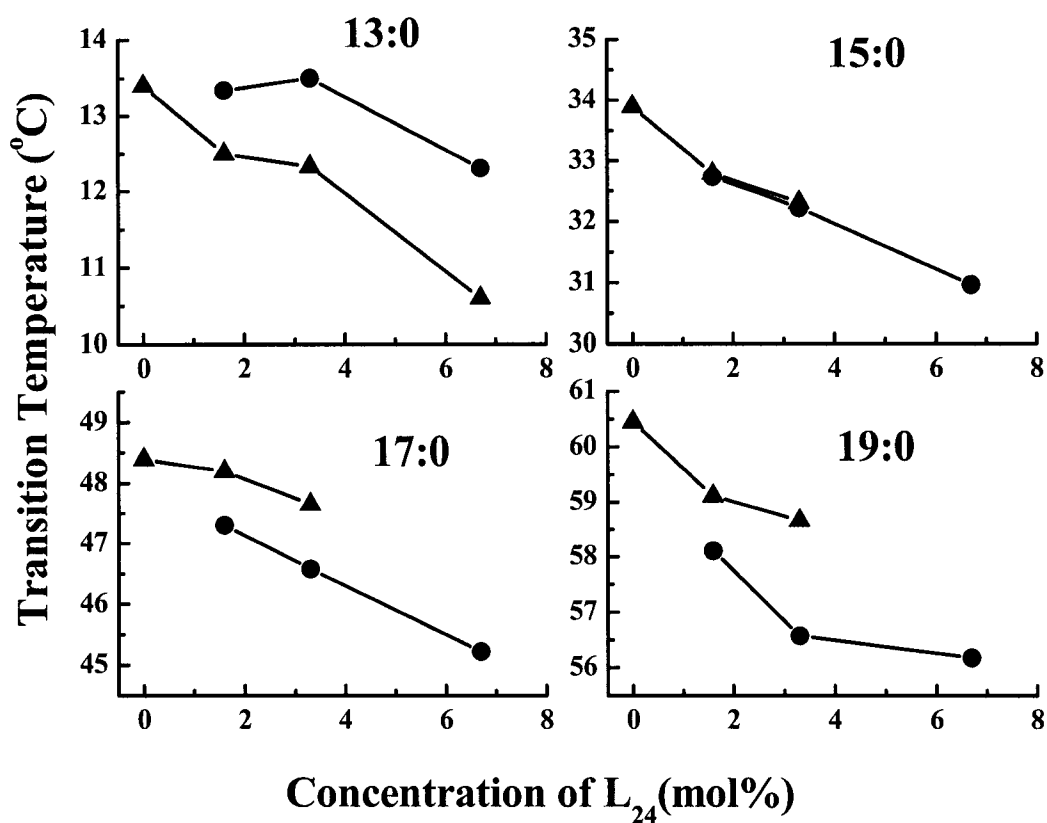


FIGURE 3. Effect of L₂₄ concentration on the peak temperature of the two components of the DSC thermograms exhibited by the mixtures of L₂₄ and the *n*-saturated diacyl-PCs studied. The symbols (▲) and (●) represent the sharp and broad components of the DSC endotherms, respectively.

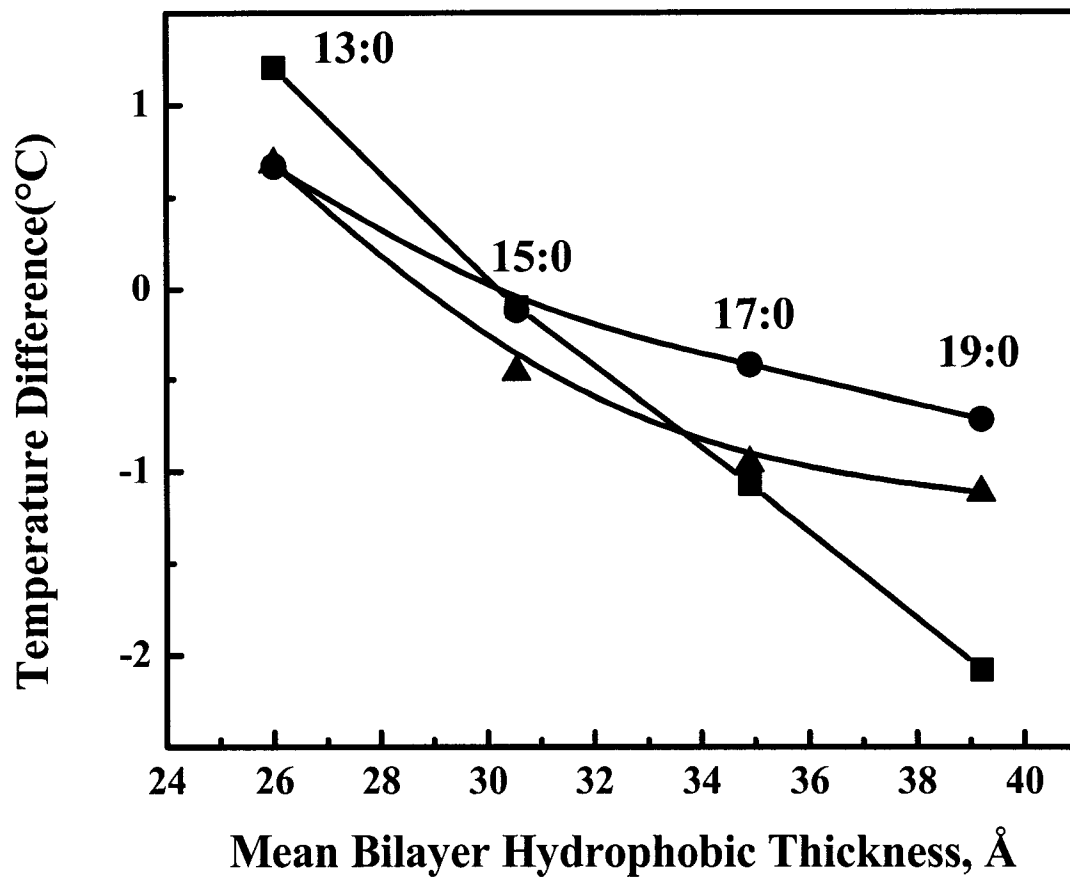


FIGURE 4. Plot of the differences of the transition temperatures of the peptide-associated and the bulk lipids versus the mean hydrophobic thickness of the lipid bilayer at a peptide concentration of 3.3 mol %. The symbols (■), (●) and (▲) represent the peptides L₂₄, L₂₄DAP, and W-L₂₂-W, respectively.

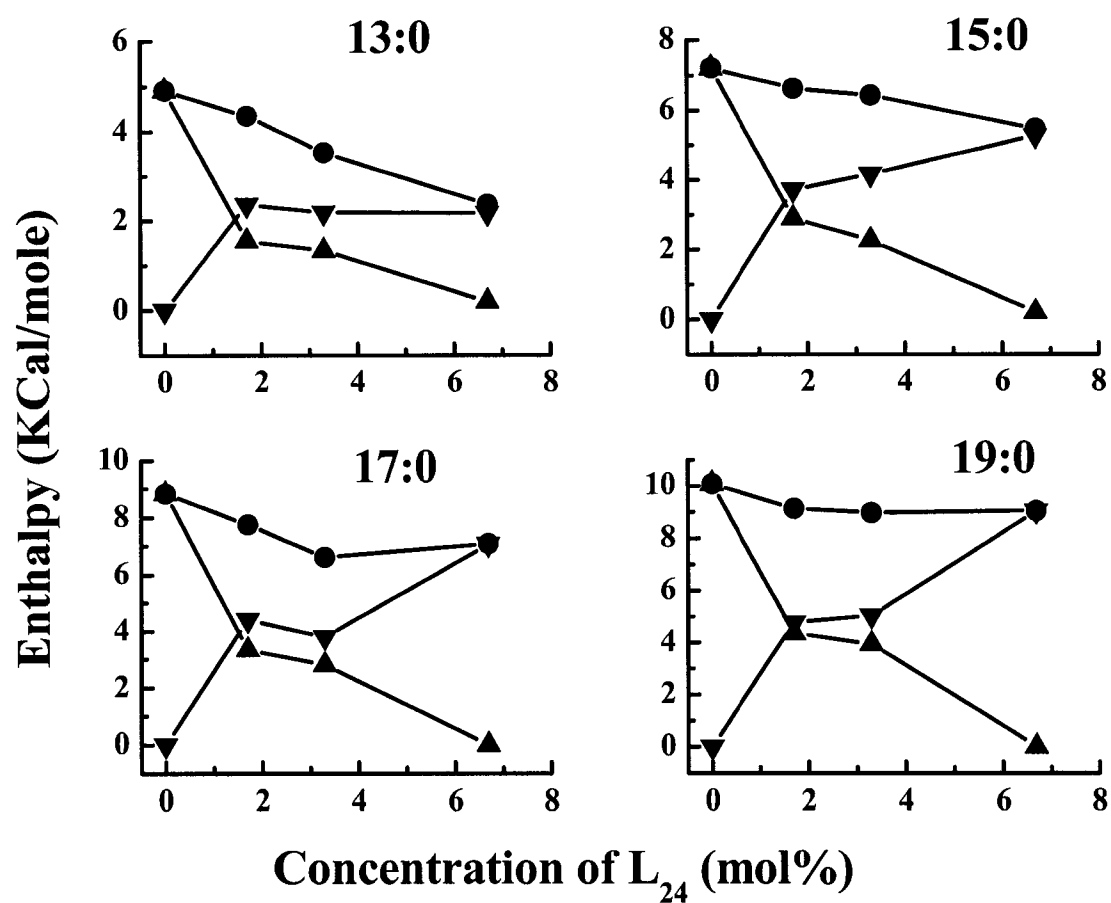


FIGURE 5. Effect of L₂₄ concentration on the transition enthalpies of the two components of the DSC thermograms exhibited by mixtures of peptides and *n*-saturated diacyl PCs. The symbols (●), (▲), and (▼) represent the total enthalpy and the enthalpy of the sharp and broad components of the DSC endotherms, respectively.

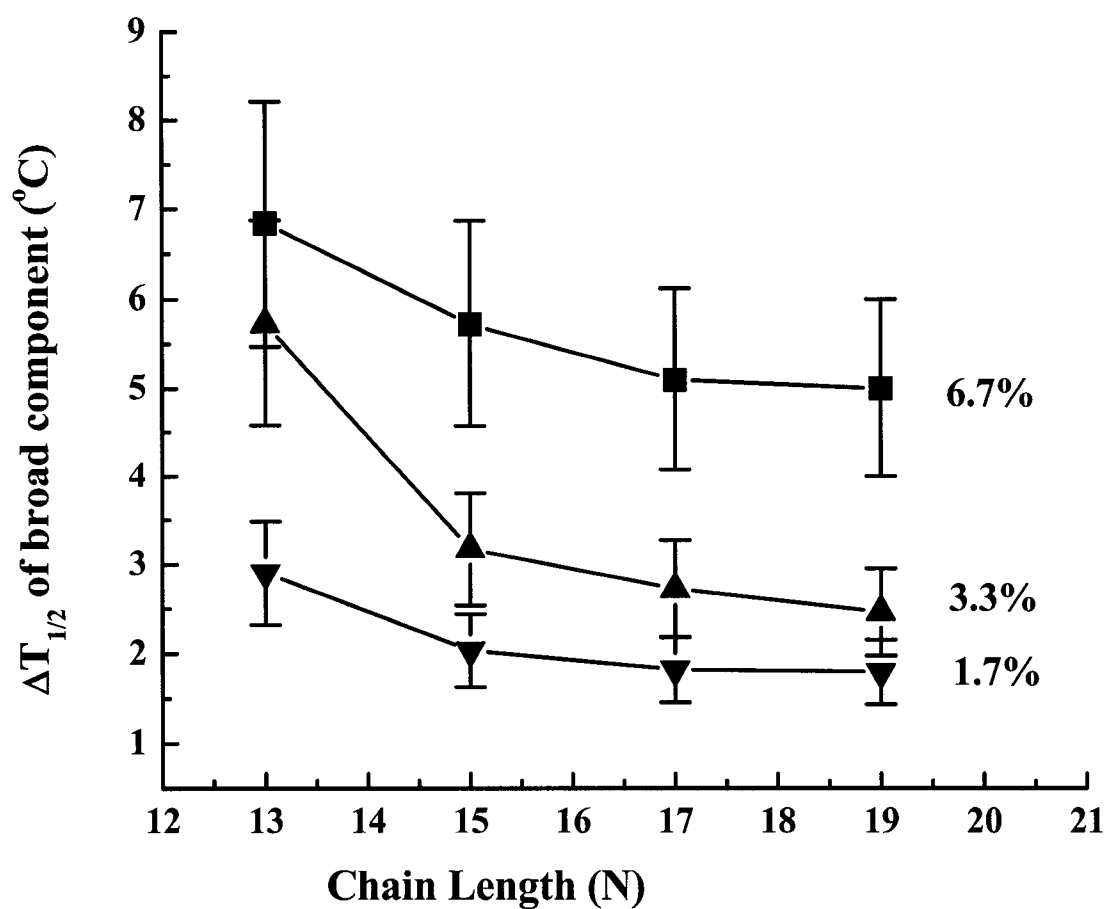


FIGURE 6. Effect of L_{24} concentration on the cooperativity ($\Delta T_{1/2}$) of the broad component of the DSC thermograms of the various PCs studied. The symbols (∇), (\blacktriangle), and (\blacksquare) represent peptide concentrations of 1.7, 3.3 and 6.7 mol %, respectively.

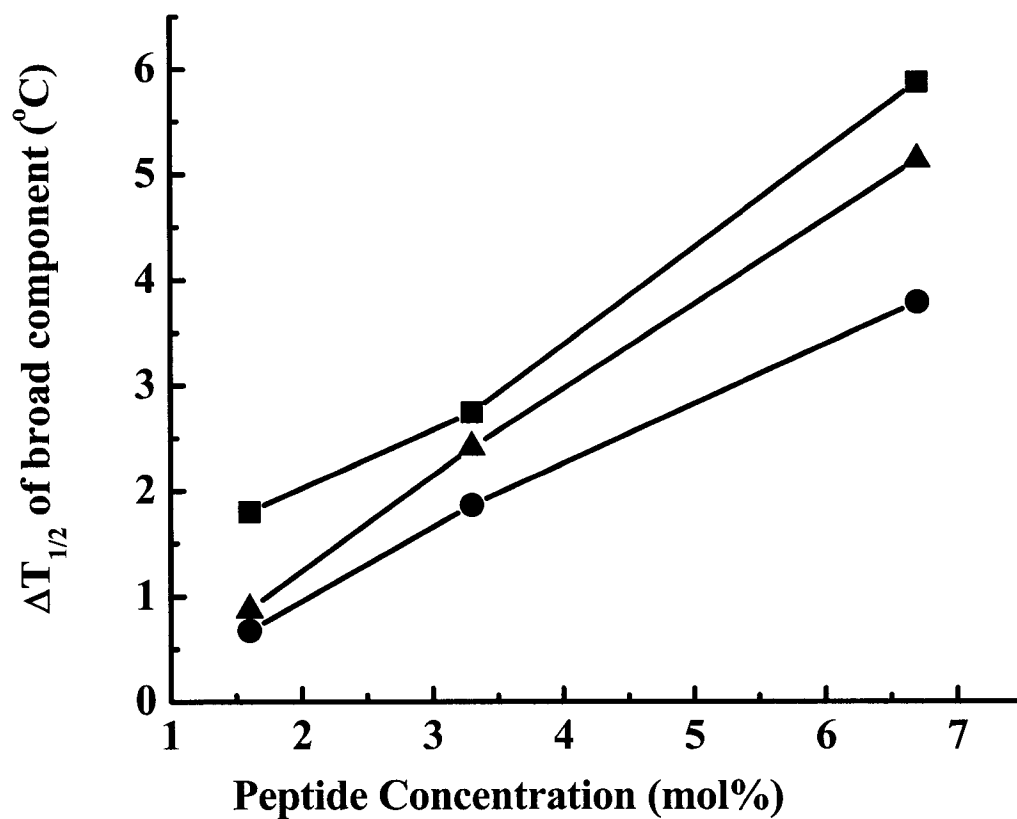


FIGURE 7. Comparison of the effects of variations in the concentration of L₂₄ (■), L₂₄DAP (●), and W-L₂₂-W (▲) on the cooperativity ($\Delta T_{1/2}$) of the broad component of the DSC thermograms in the mixtures of peptide and 17:0 PC.

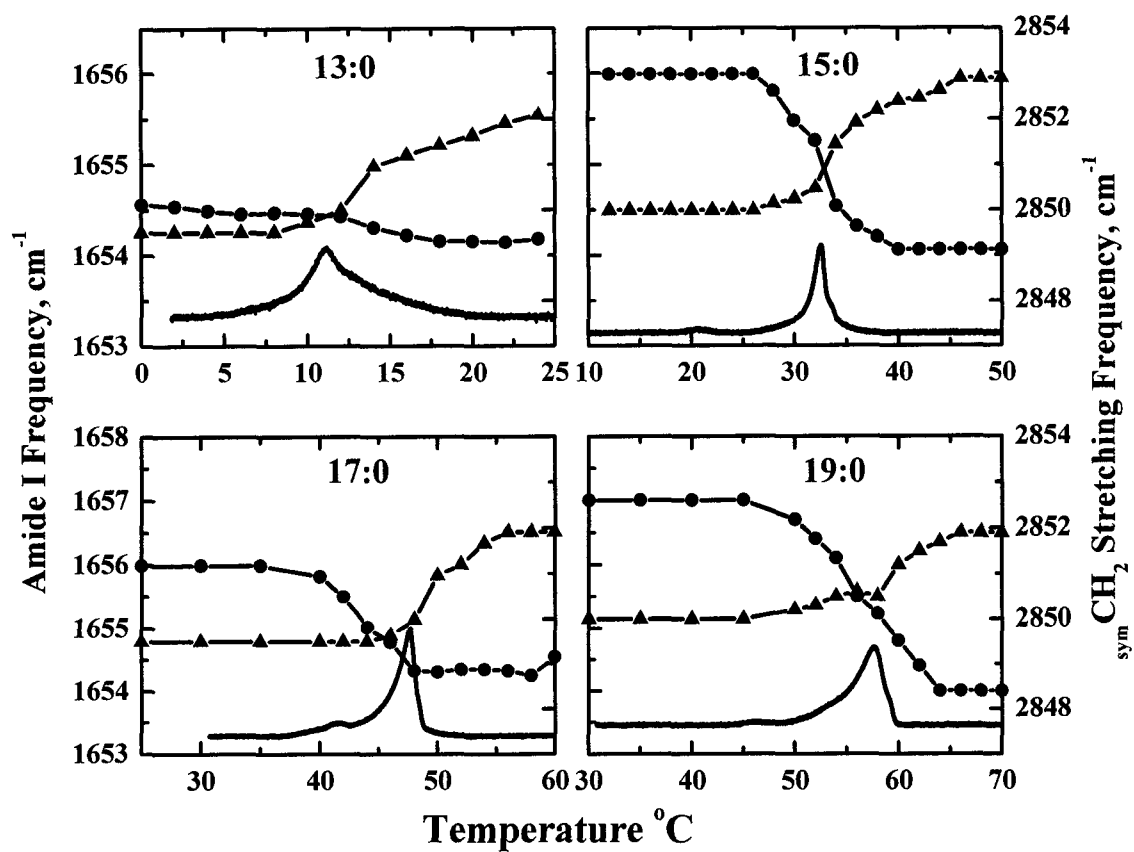


FIGURE 8. Combined plots of CH₂ symmetric stretch (▲), peptide amide I band (●), and DSC thermograms as a function of temperature for systems of L₂₄/13:0, 15:0, 17:0, and 19:0 PC. The peptide concentration is 3.3 mol %.

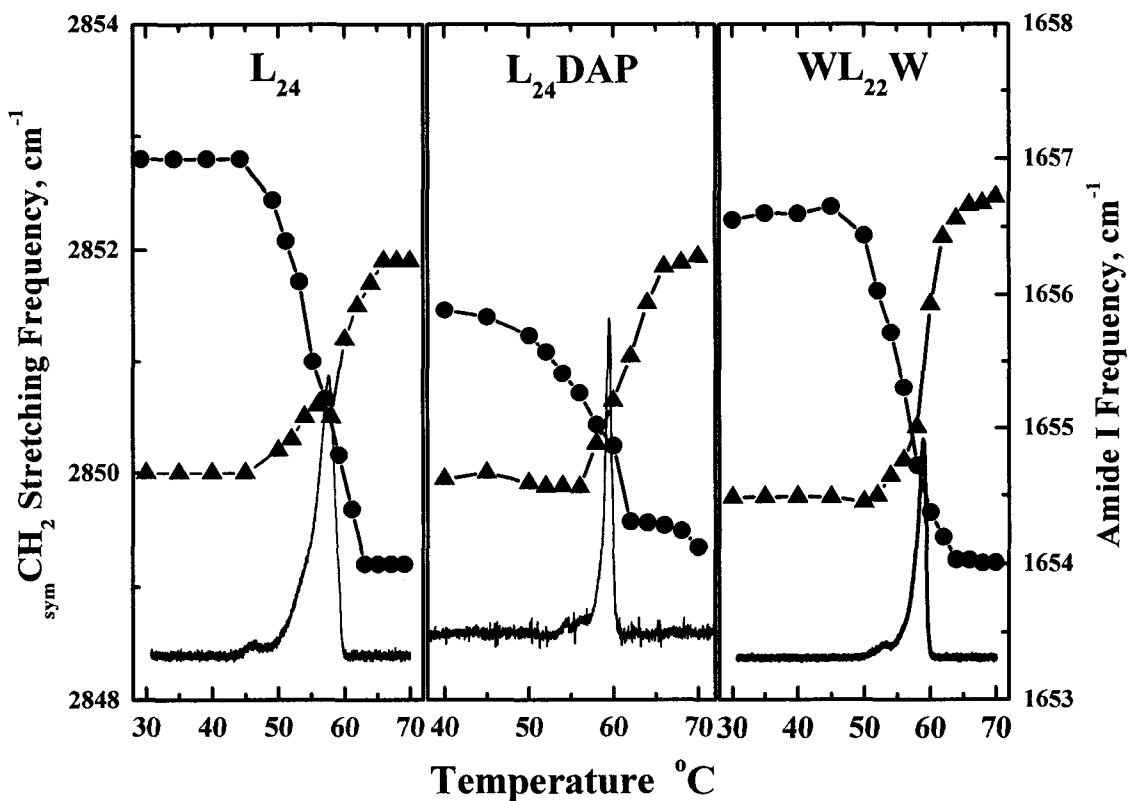


FIGURE 9. Combined plots of CH_2 symmetric stretch (\blacktriangle), peptide amide I band (\bullet), and calorimetric thermograms as a function of temperature for systems of L_{24} , $L_{24}DAP$, $W-L_{22}-W$ and 19:0 PC. The peptide concentration is 3.3 mol %. Left panel, $L_{24}/19:0$ PC, middle panel, $L_{24}DAP/19:0$ PC and right panel, $W-L_{22}-W/19:0$ PC.

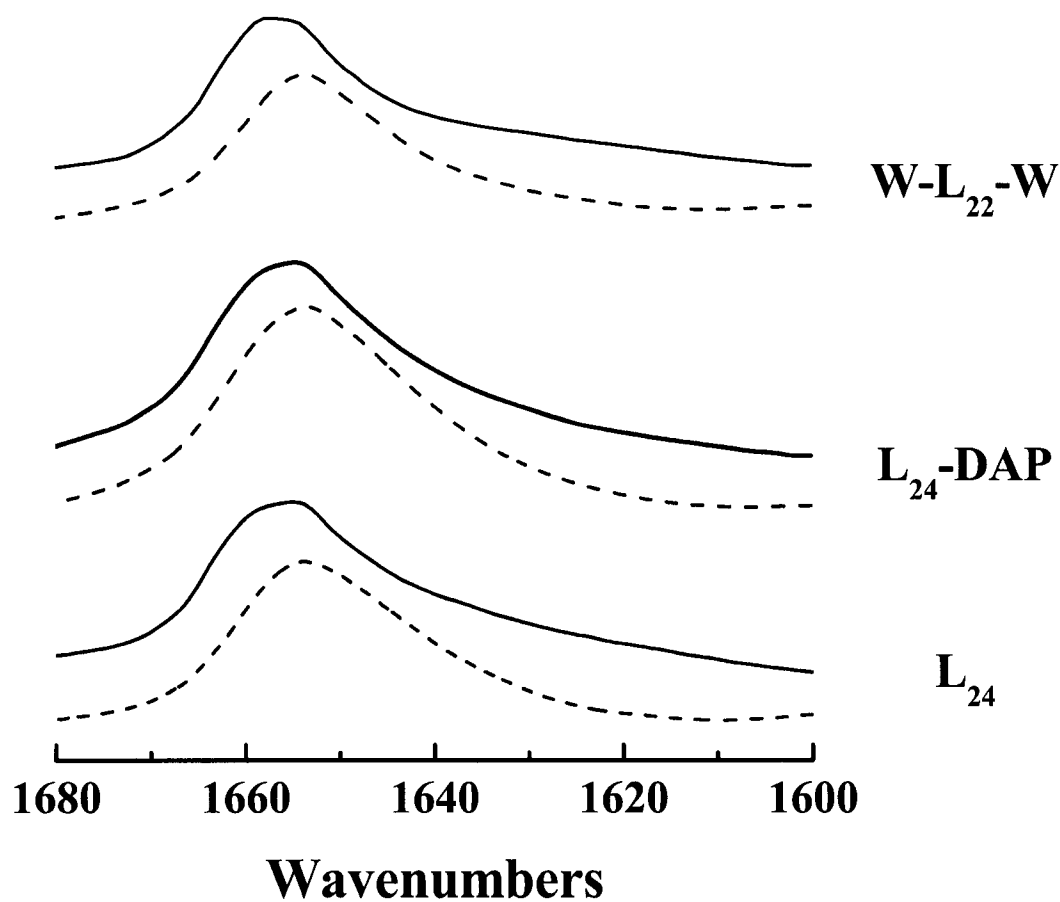


FIGURE 10. Amide I band contours exhibited by the peptides L₂₄, L₂₄-DAP and W-L₂₂-W incorporated into 19:0 PC bilayers. Absorbance spectra are shown for the peptides indicated at temperatures below (solid line) and above (dashed line) the gel/liquid-crystalline phase transition temperatures of the lipid/peptide mixtures. The peptide concentration is 3.3 mol %.

CHAPTER III. Effect of Variations in the Structure of a Polyleucine-Based α -Helical Transmembrane Peptide on Its Interaction with Phosphatidylglycerol Bilayers

Introduction

Despite the fact that about one third of all proteins are integral membrane proteins, relatively little is known about the detailed structures of membrane proteins (1). To date, only 76 unique membrane protein structures have been reported (2), compared with the huge number (over 14000) of soluble proteins in the Protein Data Bank. Most of these integral membrane proteins are composed of tightly packed bundles of transmembrane α -helices that contain about 20 hydrophobic amino acid residues. Statistical analysis shows that the hydrophobic core of these transmembrane α -helices are normally flanked by aromatic residues like tryptophan or tyrosine and that positively-charged lysine or arginine residues are found adjacent to these aromatic residues (3). In addition, the orientation of transmembrane proteins obeys the positive-inside rule, that is, the hydrophilic loops rich in positive charges are predominantly located in the cytoplasm. Moreover, although the majority of the phospholipids in cell membranes are zwitterionic or uncharged, phospholipids possessing a negative charge are also present (4). Phosphatidylserine is usually the major anionic lipid found in the inner surface of the eukaryotic cell membranes, whereas phosphatidylglycerol is the predominant anionic lipid found in prokaryotic membranes (5,6). Thus, elucidating the nature of the

A version of this chapter has been published. Liu, F., Lewis, R.N.A.H., Hodges, R.S., and McElhaney, R.N. (2004) *Biochemistry* 43, 3679-3687

interactions between integral transmembrane proteins and anionic phospholipids is important for an understanding of the structure and function of membrane proteins. Indeed, many studies have shown that some membrane-associated enzymes and transporters have a requirement for specific anionic phospholipids (7-10). For example, in *Escherichia coli* anionic lipids are necessary for the translocation activity of SecA and for the efficient integration of the leader peptidase (9,10). In addition, our previous studies have shown that the Na⁺-Mg²⁺-ATPase of *Acholeplasma laidlawii* requires the presence of an optimal amount of anionic phospholipid for maximal activity, while high levels of anionic phospholipid inhibit activity and may even irreversibly denature the protein (8).

Because most transmembrane proteins are relatively large, multidomain macromolecules of complex and often unknown three-dimensional structure and topology that can interact with lipid bilayers in complex, multifaceted ways (11-13), our understanding of the physical principles underlying lipid-protein interactions remains incomplete and the actual molecular mechanisms whereby associated lipids could alter the activity, and presumably also the structure and dynamics, of integral membrane proteins are largely unknown. To overcome this problem, a number of workers have designed and synthesized peptide models of specific regions of natural membrane proteins and have studied their interactions with model membranes of defined lipid composition (14). The synthetic peptide acetyl-K₂-G-L₂₄-K₂-A-amide (P₂₄)¹ and its analogues have been successfully utilized as a model of the hydrophobic transmembrane α -helical segments of integral membrane proteins (14,15). These peptides contain a long sequence of hydrophobic leucine residues capped at both the N- and C-termini with two

positively charged, relatively polar lysine residues. Moreover, the normally positively charged N-terminus and the negatively charged C-terminus are blocked to provide a symmetrical tetracationic peptide that will more faithfully mimic the transbilayer region of natural membrane proteins. The central polyleucine region of these peptides was designed to form a maximally stable α -helix, particularly in the hydrophobic environment of the lipid bilayer core, while the dilysine caps were designed to anchor the ends of these peptides to the polar surface of the lipid bilayer and to inhibit the lateral aggregation of these peptides. In fact, CD (14) and FTIR (16-18) spectroscopic studies of P₂₄ have shown that it adopts a very stable α -helical conformation both in solution and in lipid bilayers, and X-ray diffraction (19), fluorescence quenching (20) and FTIR spectroscopic (16-18) studies have confirmed that P₂₄ and its analogues assume a transbilayer orientation with the N- and C-termini exposed to the aqueous environment and the hydrophobic polyleucine core embedded in the hydrocarbon core of the lipid bilayer when reconstituted with various PCs. DSC (21-23) and ²H NMR spectroscopy (21,22) studies have shown that P₂₄ broadens the L _{β} /L _{α} phase transition of the host phospholipid bilayer and reduces its enthalpy. The T_m is shifted either upward or downward, depending on the degree of mismatch between the hydrophobic length of the peptide and the hydrophobic thickness of PC lipid bilayers (17), but this shift is not observed in PE bilayers, where P₂₄ substantially decreases the T_m in a hydrocarbon chain length-independent manner (23). As well, small distortions of the α -helical conformation of P₂₄ are also observed in response to peptide-lipid hydrophobic mismatch (17). ²H NMR (24) and ESR (25,26) spectroscopic studies have shown that the rotational diffusion of P₂₄ about its long axis perpendicular to the membrane plane is rapid in the L _{α}

state of the bilayer and that the closely related peptides L_{24} and $(LA)_{12}$ exist at least primarily as monomers in L_{α} POPC bilayers, even at relatively high peptide concentrations.

We have previously used three analogues of P_{24} , Ac-K₂-L₂₄-K₂-amide (L_{24}), Ac-DAP₂-L₂₄-DAP₂-amide (L_{24} DAP, DAP is diaminopropionic acid), and Ac-K₂-W-L₂₂-W-K₂-amide ($WL_{22}W$) to study the roles of tryptophan and lysine residues in membrane-protein interactions in zwitterionic PC bilayers (27,28). First, with the peptide L_{24} DAP, the two pairs of capping lysine residues at the N- and C- termini of L_{24} have been replaced with the lysine analogues DAP, in which three of the four side-chain methylene groups have been removed. This peptide was used to test the so-called snorkel model first suggested by Segrest *et al.* (29) to explain the behavior of positively charged residues in the amphipathic helices present at the surfaces of blood lipoproteins and later extended to transmembrane α -helices by von Heijne *et al.* (30). According to the transmembrane peptide version of the snorkel model, the long, flexible hydrophobic side chains of lysine or arginine residues could extend along the transmembrane helix so that the terminal charged moiety can reside in the lipid polar headgroup region while the α -carbon of the amino acid residue remains well below (or possibly above) the membrane-water interface, even when the hydrophobic length of the peptide is considerably different from that of the host lipid bilayer. Because of the shorter spacer arms between the charged amino group and the α -carbon in DAP, L_{24} DAP is expected to be less accommodating to the hydrophobic mismatch between the peptides and the lipids, and any effects of such mismatch on the thermotropic phase behavior of the host lipid bilayer should thus be exaggerated. Second, with the peptide $WL_{22}W$, the residues Leu-3 and Leu-26 of L_{24} are

replaced with tryptophans. The preference of aromatic tryptophan or tyrosine residues for the membrane polar/apolar interface has been found to be one of the common features of natural membrane proteins (31). Recent studies with WALP peptides (model peptides with only tryptophan as its terminal anchor) have suggested that the interfacial anchoring properties of tryptophan residues in transmembrane peptides can dominate over hydrophobic match effects in the peptide-lipid interactions since the tryptophan indole ring was consistently found to be located near the lipid carbonyl region, regardless of the condition of hydrophobic mismatch between the peptide and the lipid (32). Since tryptophan residues have been proposed to anchor the ends of α -helical transmembrane peptides to the polar/apolar interface of the lipid bilayer, we would also expect that WL₂₂W would be less accommodating to hydrophobic mismatch between the peptides and host lipid bilayer than would L₂₄.

To further clarify the role of interfacially localized tryptophan and lysine residues in lipid-protein interactions, we have used DSC and FTIR spectroscopy to study the interactions of L₂₄, L₂₄DAP and WL₂₂W with a series of anionic PGs with different hydrocarbon chain lengths and have compared these results with those obtained previously for a homologous series of zwitterionic PCs (28). Our results demonstrate that the negative charge of the host lipid bilayer has modest but potentially important effects on the electrostatic and hydrogen-bonding interactions between the polar residues at the termini of these peptides and the polar headgroups of the phospholipid. Our results also indicate that the interfacially localized tryptophan residues may play a significant role in the interactions of model peptides with anionic phospholipids, due to its π -electronic structure and/or its strong hydrogen-bonding forming ability.

Materials and methods

The phospholipids used in this study were obtained from Avanti Polar Lipids Inc. (Alabaster, AL) and were used without further purification. Commercially supplied solvents of at least analytical grade quality were redistilled prior to use. Peptides were synthesized and purified as TFA salts using previously published solid-phase synthesis and reversed phase high-performance liquid chromatographic procedures (33).

Samples were prepared for DSC as follows. Lipid and peptide were co-dissolved in methanol to attain the desired lipid-to-peptide ratio and the solvent was removed with a stream of nitrogen, leaving a thin film on the sides of a clean glass test tube. This film was subsequently dried *in vacuo* overnight to ensure removal of the last traces of solvent. Samples containing 0.5-0.8 mg of lipid were then hydrated by vigorous vortexing with a buffer (50 mM Tris, 150 mM NaCl, 1mM NaN₃, pH 7.4) at temperatures some 10-15°C above the gel/liquid-crystalline phase transition temperature of the lipid. DSC thermograms were obtained from 0.5 ml samples with a high-sensitivity Microcal VP-DSC instrument (Microcal Inc., Northampton, MA), operating at heating and cooling rates of 10° C per hour. The data were analyzed and plotted with the Origin software package (OriginLab Corporation, Northampton, MA).

Peptide samples to be used in FTIR spectroscopic experiments were converted to the hydrochloride salt by two cycles of lyophilization from 10 mM hydrochloric acid. This procedure was necessary because the trifluoroacetate ion gives rise to a strong absorption band ($\sim 1670\text{ cm}^{-1}$) which partially overlaps the amide I absorption band of the peptide (17). Typically, samples were prepared by co-dissolving lipid and peptide in methanol at a lipid to peptide ratios near 30:1 (mol:mol). After removal of the solvent and drying of

the film (see above), samples containing 2-3 mg of lipid were hydrated by vigorous mixing with 75 μ l of a D₂O-based buffer (50 mM Tris, 150 mM NaCl, 1mM NaN₃, pD 7.4). The dispersion obtained was then squeezed between the CaF₂ windows of a heatable, demountable liquid cell (NSG Precision Cells, Farmingdale, NY) equipped with a 25 μ m teflon spacer. Once mounted in the sample holder of the spectrometer, the sample temperature could be varied between 0° C and 90° C by an external, computer-controlled water bath. Infrared spectra were acquired as a function of temperature with a Digilab FTS-40 Fourier transform spectrometer (Bio-Rad, Digilab Division, Cambridge, MA) using data acquisition parameters similar to those described by Mantsch *et al.* (34). The experiment involved a sequential series of 2° C temperature ramps with a 20 minute inter-ramp delay for thermal equilibration, and was equivalent to a scanning rate of 4° C per hour. Spectra were analyzed with software supplied by the instrument manufacturers and other programs obtained from the National Research Council of Canada.

Results

Thermotropic Phase Behavior of PG Bilayers in the Absence of Peptides. As illustrated in Figure 1, in the absence of peptides, the DSC thermograms of the four *n*-saturated diacyl PGs studied exhibit two structurally distinct thermotropic phase transitions. The higher temperature main phase transition is highly energetic and more cooperative. It is also freely reversible, as shown by the absence of significant cooling hysteresis (data not presented). In addition, the temperature of the main phase transitions of these PGs increases smoothly but nonlinearly, and the Δ Hs increase linearly, with an increase in hydrocarbon chain length. All these thermodynamic properties are comparable to those

reported previously by aqueous dispersions of various n -saturated PGs (35) and are also similar to those of the rippled gel to liquid-crystalline ($P_{\beta'}/L_{\alpha}$) phase transitions of comparable n -saturated PCs (17,28).

The lower temperature transition is less cooperative and much less energetic and exhibits a modest cooling hysteresis (Figure 1). The midpoint temperature of this transition also increases with an increase in hydrocarbon chain length. However, the lower temperature transition exhibits a steeper dependence on hydrocarbon chain length so that the interval between it and the main phase transition decreases with increases in the hydrocarbon chain length. These properties are similar to those of the well-defined pretransitions of the n -saturated 1,2-dicacyl PCs. We therefore suggest that the lower temperature transitions of PGs are $L_{\beta'}/P_{\beta'}$ phase transitions, similar to those exhibited by the corresponding diacyl PCs. This suggestion should be regarded as tentative, however, until further structural studies such as X-ray diffraction are performed.

The Effect of Peptide Incorporation on the Pretransition. The incorporation of increasing quantities of L_{24} into n -saturated dicacyl PG bilayers slightly lowers the T_m and significantly lowers the ΔH and cooperativity of the pretransition in all cases. In addition, the pretransition is completely abolished at the highest peptide concentration examined (6.7 mol %) (see Figure 1). It is interesting that the incorporation of peptide is as effective in this regard in the shorter chain PGs as in longer chain PGs. In contrast, the incorporation of P_{24} and L_{24} is more effective in abolishing the pretransition in shorter chain PC bilayers (17,28). Essentially identical results have been observed for the L_{24} analogs $L_{24}DAP$ and $WL_{22}W$ (data not presented). These findings suggest that the presence of these model peptides may abolish hydrocarbon chain tilt in gel-phase PG

bilayers, causing the progressive replacement of the L_{β}' and P_{β}' phases with a disordered L_{β} -like phase with untilted hydrocarbon chains, as observed previously in PC bilayers (17,28, 36).

The Effect of Peptide Incorporation on the Main Transition. The effects of the incorporation of L_{24} on the main phase transitions of the four PGs studied here are also illustrated in Figure 1. In all cases the incorporation of increasing quantities of peptide produces a two-component DSC endotherm (see Figure 2), as well as a progressive decrease in the ΔH and cooperativity of the overall L_{β}/L_{α} phase transition of the host PG bilayer. The relative contribution of the sharp component of the DSC endotherm, which initially possesses a T_m , ΔH and cooperativity similar to that of the PG alone, decreases in magnitude as the proportion of L_{24} increases. In contrast, the relative contribution of the broad component increases as the peptide concentration increases and it is the predominant component present at the highest peptide concentration tested. Using the rationale provided in our previous DSC studies of the interaction of P_{24} and related peptides with lipid bilayers (17,28,36), we assign the sharp and broad component of our DSC endotherms to the L_{β}/L_{α} phase transitions of peptide-poor and peptide-rich PG domains, respectively. We also observe a small decrease in the temperature and cooperativity of the sharp component of the DSC endotherms. This is ascribed to domain boundary effects arising from the decreasing size of the peptide-poor PG domains, which also explains their progressively smaller ΔH as peptide concentration increases. Note that these characteristic effects of L_{24} and its analogs on the sharp component of the DSC endotherms are noted in all the PGs studied and are hydrocarbon chain length and peptide structure independent.

The effects of peptide incorporation on the thermodynamic parameters of the peptide-rich PG domain, however, do depend on the hydrocarbon chain length and thus on the thickness of the host PG bilayer. For example, as shown in Figure 3, the T_m of the broad component of the DSC endotherm occurs at the same temperature as that of the sharp component in 14:0 PG bilayers, but at progressively lower temperatures in 15:0, 16:0 and 18:0 PG bilayers. If the same trend continues, the T_m of the broad component of the DSC endotherm would occur at higher temperature than that of the sharp component in 13:0 or shorter chain PG bilayers, as observed previously in PC bilayers (17,28). Furthermore, in all cases the T_m s of both components decrease with increasing peptide concentration. It is interesting that the phase transition temperatures of the broad and sharp components are almost equal in 14:0 PG but in 15:0 PC bilayers (17,28). This difference in behavior is likely due to the greater depression of the T_m in PG bilayers compared to PC bilayers produced by the incorporation of comparable amounts of these peptides.

The effects of the lipid hydrocarbon chain length on the shift of the T_m of the broad component relative to that of the sharp component (ΔT) in PG bilayers are presented in Figure 4. With all three model peptides examined, the ΔT of the PG/peptide mixtures becomes larger and more negative with the increase in lipid hydrophobic chain length, which is similar to that reported previously in PC/peptide mixtures with chain lengths of 15 carbons or more (28). In addition, we observe that all three model peptides reduce the ΔT of PG bilayers to a greater extent than that of PC bilayers of comparable hydrocarbon chain length. Moreover, in all four PGs examined, WL₂₂W reduces the ΔT to a greater extent than L₂₄, and L₂₄ reduces the ΔT to a larger extent than L₂₄DAP. In PC bilayers, these model peptides also affect the ΔT in a manner dependent on the hydrophobic

mismatch between the model peptides and the lipid hydrophobic thickness, but exhibit a different dependence on the structure of these peptides. The differential effects of these peptides on the ΔT of PG and PC bilayers suggest that the thermotropic phase behavior of peptide/lipid mixtures is influenced by other forces besides those arising from hydrophobic mismatch between the model peptides and the host phospholipid bilayers. A possible molecular mechanism for rationalizing these results will be presented later.

The effect of peptide incorporation on the ΔH s of the four PG bilayers studied here is shown in Figure 5. In all cases the overall ΔH decreases by about 3 kcal/mole with an increase in peptide concentration. However, the ΔH of the broad component of the DSC endotherm initially increases with increasing peptide concentration before leveling off, while the ΔH of the sharp component decreases rapidly but does not become zero even at the highest peptide concentration tested. In contrast, in comparable PC bilayers, the overall ΔH decreases by only about 2 kcal/mole at the highest peptide concentration (Figure 6). Moreover, the ΔH of the broad component decreases at higher peptide concentration after an initial increase, and the ΔH of the sharp component approaches zero at the highest peptide concentration in PC bilayers. Thus the lower ΔH of the PG as compared to the PC bilayers at higher peptide concentrations is due to the much lower enthalpy of the broad component of the former system. The fact that the ΔH of the sharp component goes to zero at high peptide concentrations in PC but not in PG bilayers suggests that these peptides are not as well dispersed in the latter mixture. However, the fact that the overall ΔH is nevertheless decreased to a greater extent indicates that these peptides disrupt gel-state organization to a considerably larger degree in PG as compared to PC bilayers.

To further explore the physical principles underlying PG-peptide interactions, we have examined the effect of salt concentration on the thermotropic phase behavior of 16:0 PG alone and of L₂₄/16:0 PG mixture containing 3.3 mol% peptide (Figure 7). With an increase of NaCl concentration, there is a gradual increase in the T_m of the main phase transition of the 16:0 PG from 40.1 °C at 0 mM NaCl to 42.1 °C at 900 mM (data not shown). A similar increase is observed in the temperature of the sharp component of the main phase transitions of the L₂₄/16:0 PG mixture, from 39.9 °C at 0 mM NaCl to 41.8 °C at 900 mM NaCl, while a smaller increase was observed in the temperature of the broad component of the main phase transitions of the L₂₄/16:0 PG mixture, from 38.9 °C at 0 mM NaCl to 40.2 °C at 900 mM NaCl. This suggests that the electrical repulsion between the negatively-charged phosphate groups in the peptide-enriched domains in PG bilayers is weakened by the presence of these cationic peptides. Moreover, with the increase of the salt concentration, a much larger increase was observed for the temperature of the pretransition of the L₂₄/16:0 PG mixture, from 32.2 °C at 0 mM NaCl to 39.6 °C at 900 mM NaCl, which leads to the overlapping of the pretransition and the main phase transition at 900 mM NaCl. However, the small effects of increases in salt concentration on the T_m, ΔH and cooperativity of the main phase transition of the L₂₄/16:0 PG mixture suggest that forces other than electrostatic ones play a significant role in the interactions of these model transmembrane peptides with anionic phospholipid bilayers.

Fourier Transform Infrared Spectroscopic Studies of Peptide-containing PG bilayers. In these studies, infrared spectra of mixtures of these peptides with each of the four PGs studied were recorded as a function of temperature and as a function of the mole fraction

of the peptide. The use of FTIR spectroscopy permits a nonperturbing monitoring of both the structural organization of the lipid bilayer and the conformation of the incorporated peptide. Thus the changes in the degree of rotational isomeric disorder of the lipid hydrocarbon chains accompanying the L_{β}/L_{α} phase transitions of the lipid bilayer can be conveniently monitored by changes in the frequency of the CH_2 symmetric stretching band near 2850 cm^{-1} , changes in gel-state hydrocarbon chain packing by changes in the CH_2 scissoring band near 1468 cm^{-1} , changes in the hydration and/or polarity of the phosphate polar headgroup of the lipid bilayer by changes in the frequency of the O-P-O asymmetrical stretching bands near 1215 cm^{-1} , and changes in peptide secondary structure can be monitored by changes in the conformationally sensitive amide I band near 1650 cm^{-1} (37).

Illustrated in Figure 8 are the FTIR spectra of $L_{24}/16:0$ PG (3.3 mole% peptide) mixture in the L_{β} (top) and L_{α} (bottom) phases. L_{24} exhibits a sharp band at about 1654 cm^{-1} , indicating that this peptide adopts a predominantly α -helical structure in both phases. A similar sharp amide I band was observed for all three model peptides in all four PGs examined. These results indicate that the potentially stronger electrostatic and hydrogen-bonding interactions between the model peptides and the polar headgroups of anionic PG bilayers do not change the peptide conformation dramatically relative to comparable zwitterionic PC-peptide mixtures. In addition, in the L_{α} phase, the PG broad C=O stretching bands centered near 1738 cm^{-1} contain subcomponents centered near 1741 cm^{-1} and 1726 cm^{-1} . Upon cooling, an increase in the intensity of higher frequency component relative to that of the lower frequency component is observed. Since these two components have been attributed to a differential infrared absorption by free and

hydrogen-bonded ester carbonyl groups, respectively (34,38,39), this observation indicates a loss of water from this region of the bilayer upon entering the L_{β} state.

Illustrated in Figure 9 are the temperature-dependent changes in the frequencies of the peptide amide I absorption band and the CH_2 symmetric stretching band of the lipid hydrocarbon chains exhibited by a mixture of L_{24} and 16:0 PG (3.3 mole% peptide). The DSC heating endotherm of this sample is also shown to facilitate a comparison of the calorimetric and FTIR spectroscopic results. The heating endothermic transitions reported by DSC are accompanied by an increase in the CH_2 symmetric stretching frequency, indicating that both the sharp and broad components of the DSC endotherms are associated with lipid hydrocarbon chain-melting events (17). Moreover, the lipid phase transition is accompanied by a small decrease in the frequency of the L_{24} amide I band. This frequency change is both reproducible and reversible, suggesting that the conformation of the model peptide is slightly altered by the lipid phase transition. Qualitatively similar results were obtained when the peptides $L_{24}\text{DAP}$ and WL_{22}W were incorporated into all four PG bilayers examined here (data not shown). The pattern of the amide I frequency shifts of the model peptide at the gel/liquid-crystalline phase transition of PG bilayers is very similar to that observed when these peptides are incorporated into PC bilayers (17,28) and thus is also ascribed to small conformational distortions of the peptide helix induced by changes in phospholipid bilayer hydrophobic thickness.

In order to study the effects of peptide incorporation on the PG polar headgroups in both the L_{β} and L_{α} phases, FTIR spectra in the O-P-O asymmetrical stretching region of PG bilayers with and without peptides were obtained at various temperatures. The FTIR spectra of the O-P-O asymmetrical stretching absorption bands of pure 16:0 PG are

illustrated in Figure 10a. The strong, relatively broad absorption band centered at 1205 cm^{-1} is the O-P-O asymmetric stretching band and the series of weaker, overlapping band at 1200, 1222, 1244, 1266, and 1288 cm^{-1} are the CH_2 wagging band progression arising from the gel-state all-*trans* hydrocarbon chains. With an increase in temperature, the intensity of the CH_2 wagging bands decreases significantly and almost disappears completely upon the gel to liquid-crystalline phase transition which occurs around 40°C. Moreover, above the lipid phase transition, the O-P-O absorption band remains broad but its maximum frequency shifts to about 1218 cm^{-1} . Similar results were observed for the other three PGs examined here (data not presented). These observations suggest that in the gel phase, the PG phosphate polar headgroups reside in more polar environment, or are involved in stronger hydrogen-bonding interactions than in the liquid-crystalline phase.

Because of the overlapping of the strong CH_2 wagging band and the O-P-O absorption bands in the gel phase, we will only discuss the effects of the incorporation of model peptides on the O-P-O absorption bands in the L_α phase. Illustrated in Figure 10B are the FTIR spectra of the O-P-O absorption bands of 16:0 PG alone and the mixtures of 16:0 PG with L_{24} , $L_{24}\text{DAP}$ or WL_{22}W , respectively, in the L_α phase. The O-P-O absorption bands of the mixtures of 16:0 PG with either L_{24} or $L_{24}\text{DAP}$ exhibit two components, with one component centered near 1215 cm^{-1} , which is similar to the O-P-O spectra of 16:0 PG alone, and the other centered at a lower frequency of about 1208 cm^{-1} . These observations suggest that some of the phosphate polar headgroups of the PG bilayer reside in more polar environments than others in the presence of these peptides. The lower-frequency population of phospholipids are likely peptide-associated molecules that

form more extensive electrostatic and hydrogen-bonding interactions with L₂₄ or L₂₄DAP. In contrast, the O-P-O absorption bands exhibited by the mixture of 16:0 PG and WL₂₂W exhibit a one-component spectra centered around 1215 cm⁻¹, which is very similar to that of the pure 16:0 PG. Similar results were obtained with the other PGs studied (data not presented), suggesting that these differences between WL₂₂W and L₂₄ or L₂₄DAP are independent of the mismatch between peptide hydrophobic length and lipid hydrophobic thickness. The possible molecular basis for this difference in behaviors between WL₂₂W and L₂₄ or L₂₄DAP will be discussed later.

Discussion

In this study we have shown that model peptides that mimic the hydrophobic transmembrane α -helical segments of integral membrane proteins have somewhat different interactions with anionic PG bilayers than with zwitterionic PC bilayers. In particular, all the three model peptides reduce the phase transition temperatures and enthalpies of the PG bilayers to a greater extent than PC bilayers. These results indicate that the nature and strength of the interactions between the somewhat polar and charged amino acid residues at the ends of these model peptides and the polar headgroups of anionic PG and zwitterionic PC bilayers are different.

It is instructive to compare the effects of L₂₄ and the closely related peptide P₂₄ on the T_m and ΔH of the main phase transitions of zwitterionic PC (17, 28) and PE (23, unpublished data) bilayers with that of anionic PG bilayers (this study) of comparable hydrocarbon chain length. As mentioned previously, L₂₄ and P₂₄ decrease the T_m and ΔH of the main phase transitions of PE bilayers to a greater extent than that of PC bilayers and the characteristic effects of these peptides on PE bilayers are not as strongly

dependent on the bilayer thickness as with PC bilayers. We suggested earlier that the differing effects of peptide incorporation of PE and PC bilayers were due primarily to the stronger lipid polar headgroup interactions in the former system. More specifically, we postulated that the larger effect of transmembrane peptide incorporation on gel state PE bilayer results from a relatively greater disruption of the intrinsically stronger attractive electrostatic and hydrogen-bonding interactions at the PE bilayer surface as compared to PC bilayers, and that this disruption of attractive interactions between adjacent polar headgroups is sufficiently large to attenuate the effects of hydrophobic mismatch between the peptide and the host lipid bilayer. In the case of anionic PG bilayers, L_{24} incorporation produces a hydrophobic mismatch-dependent decrease in the T_m and ΔH which is less than that observed in PE bilayers but greater than that found in PC bilayers of comparable hydrocarbon chain length. This result is surprising in one sense, in that the binding of water soluble-cationic peptides or proteins to anionic phospholipid bilayers usually produces an increase in T_m and ΔH due to a partial alleviation of the electrostatic repulsion arising from adjacent anionic polar headgroups at the surface of the bilayers, thus stabilizing the gel state (40, 41). The fact that the incorporation of these cationic transmembrane peptides instead actually reduces T_m s of these anionic PG bilayers suggests that their disruption of the attractive hydrogen-bonding network present in gel-state PG bilayers is the dominant effect here. This conclusion is supported by our finding that the thermotropic phase behavior of $L_{24}/16:0$ PG bilayers is only weakly dependent on variations in salt concentration, which indicates that electrostatic effects are not of primary importance here. It is interesting to note that the overall effects of L_{24} and P_{24} incorporation are more similar in zwitterionic PC and anionic PG bilayers than in

zwitterionic PE bilayers. This suggests that the strength of the electrostatic and hydrogen-bonding interactions between adjacent polar headgroups, rather than polar headgroup charge *per se*, is the primary determinant of the effect of the incorporation of these transmembrane peptides on the thermotropic phase behavior of the host phospholipid bilayer.

One purpose of this paper is to study the potential role of snorkel effect in lipid-peptide interactions by studying the interactions of these model peptides with anionic PG and zwitterionic PC bilayers. The transmembrane version of the snorkel model suggests that the long side chain of Lys can reach up along the transmembrane helix to allow the terminal charged amino group to reside in the lipid polar headgroup region while the α -carbon of the residue is positioned well below the membrane-water interface. Because of the shorter spacer arms between the charged group and the α -carbon of DAP, the peptide L₂₄DAP is expected to be less accommodating to the hydrophobic mismatch between model peptides and lipid bilayers, and any effects of such mismatch on the thermotropic phase behavior of its host lipid bilayer should be exaggerated. In contrast to this prediction, our previous study actually showed that replacing the terminal Lys residues of L₂₄ by DAP attenuates the hydrophobic mismatch effects of the peptide on the thermotropic phase behavior of the host zwitterionic PC bilayer (28). This attenuated hydrophobic mismatch effect was rationalized by postulating that the DAP residues are too short to engage in significant electrostatic interactions with the polar headgroups of the host phospholipid bilayer. Therefore, we expect that a differential hydrophobic mismatch effect of L₂₄DAP relative to that of L₂₄ will also be observed in PG bilayers, and may be more prominent there because of the potentially stronger electrostatic

attractive interactions between these cationic model peptides and the polar headgroups of the anionic phospholipid. Indeed, our results show that the dependence of the ΔT of PG bilayers on hydrophobic mismatch is less for L₂₄DAP than for L₂₄, as predicted. However, the magnitude of the variation of ΔT with changes in hydrocarbon chain length produced by L₂₄ DAP incorporation relative to that by L₂₄ is only slightly greater in PG than in PC bilayers, suggesting that the magnitude of the attractive electrostatic interactions between the positively charged lysine or DAP residues at the peptide terminae and the negatively charged phosphate groups of PG and PC bilayers are not greatly different.

A comparison of the effects of the incorporation of L₂₄ and WL₂₂W on various PG bilayers reveals that the latter peptide produces a slightly greater decrease in the T_m of the broad component of the DSC endotherm than does the former. However, the variations of the difference in temperature between the sharp and broad component with variations in PG hydrocarbon chain length are identical within experimental error for both peptides. Thus, although the presence of tryptophan residues at the ends of the polyleucine core of WL₂₂W perturbs the organization of gel-state PG bilayers slightly, they do not seem to alter the magnitude of the hydrophobic mismatch response between WL₂₂W and the host lipid bilayers, as might be predicted if the tryptophan residues interact strongly with the glycerol backbone region of the PG molecules. A possible reason for these findings will be offered below.

Our current studies also show that L₂₄ and L₂₄DAP lower the frequencies of the O-P-O asymmetrical stretching absorption bands of the peptide-associated PGs in the liquid-crystalline phase. Our previous studies have shown that the frequency of the O-P-O

asymmetric stretching absorption bands of PGs (1205 cm^{-1} in the L_{β} phase and 1215 cm^{-1} in the L_{α} phase) are significantly lower than observed with other phospholipids ($1220\text{--}1230\text{ cm}^{-1}$) (42), suggesting that the phosphate moieties of the PG molecules are involved in stronger hydrogen-bonding interactions than are other phospholipids. However, our previous studies have shown that the incorporation of model peptides into PC bilayers does not cause any discernible changes in the frequency of the O-P-O asymmetrical stretching absorption bands of the peptide-associated PCs (unpublished data). Taken together, these results suggest that the incorporation of the model peptides L_{24} or $L_{24}\text{DAP}$ increase the polarity of the microenvironment of the phosphate group in PG bilayers in the L_{α} state while having no discernible effect in PC bilayers. Thus, it is possible that the amino groups at both ends of these model peptides are engaged in stronger hydrogen-bonding interactions with the glycerol hydroxyl groups and the phosphate moieties in PG bilayers, or that the model peptides form stronger electrostatic attractions with the negatively charged phosphate moieties in PG than in PC bilayers. The results of our DSC studies, which show only a weak dependence of the thermotropic phase behavior of L_{24}/PG mixtures on salt concentration, would favor the first possibility.

It is interesting to note that the model peptide WL_{22}W , in contrast to L_{24} and $L_{24}\text{DAP}$, does not induce any discernible changes in the O-P-O asymmetric stretching absorption bands of PG bilayers in the L_{α} phase. A possible explanation for the attenuation of the interaction between the lysine residues and the PG phosphate groups is that the tryptophan residues may engage in cation- π interactions with the positively charged side chains of the lysine residues at the N- and C- termini of WL_{22}W . The cation- π interaction is a noncovalent force between a positive charge and the quadrupole moment of an

aromatic structure (43). Considerable evidence suggests that cation- π interactions are important in many proteins that bind cationic substrates (44-46). Previous studies of the interactions of four tryptophan analogues with PC bilayers suggested that the preference of tryptophan for the membrane interface is dominated by its π -electronic structure and associated quadrupolar moment (aromaticity) that favor residing in the electrostatically complex interfacial environment (47). In the PG/WL₂₂W mixtures, if the positively-charged amino groups of the lysine residues might form cation- π interactions with the adjacent tryptophan residues, we would expect that these lysine residues would be less likely to form electrostatic attractions with the anionic phosphate group of the PG bilayer. As a result, the model peptide WL₂₂W will have a much smaller effect on the frequency of the O-P-O asymmetrical stretching absorption bands of the peptide-associated PGs in the L _{α} phase than would L₂₄ and L₂₄DAP, as shown by our FTIR results.

In conclusion, the present study and our previous work highlight the importance of the electrostatic and hydrogen-bonding interactions between the amino acid residues at the ends of α -helical transmembrane peptides and the polar headgroups of the phospholipids in lipid bilayer membranes. These studies also suggest that specific residues, such as the aromatic tryptophan residues, may modulate such interactions between model peptides and lipid polar headgroups. We hope that further structural and computer modeling investigations will help to further elucidate the molecular basis for these observations.

References

1. Kleinschmidt, J.H. (2003) Membrane proteins—introduction, *Cell.Mol.Life.Sci.* 60, 1527-1528.
2. http://blanco.biomol.uci.edu/Membrane_Proteins_xtal.html.
3. Killian, J.A., and von Heijne, G. (2000) How proteins adapt to a membrane–water interface, *TIBS* 25,429-434.
4. Sandermann, H. (1978) Regulation of membrane enzymes by lipids, *Biochim. Biophys. Acta* 515, 209-237.
5. McElhaney, R.N. (1982) Effects of membrane lipids on transport and enzymic activities, in *Current Topics in Membranes and Transport* (Razin, S., and Rottem, S., Eds.), Vol. 17, pp 317-380, Academic Press, New York.
6. McElhaney, R.N. (1985) Membrane lipid fluidity, phase state and membrane function in prokaryotic microorganisms, in *Membrane Fluidity in Biology* (Alora, R.A., and Boggs, J.M., Eds.), Vol. 4, pp 147-208, Academic Press, New York.
7. McElhaney, R.N.(1984) The structure and function of the *Acholeplasma laidlawii* plasma membrane. *Biochim. Biophys Acta* 779, 1-42.
8. George, R., Lewis, R.N.A.H., Mahajan, S., and McElhaney, R.N. (1989) Studies on the purified, lipid-reconstituted (Na⁺+Mg²⁺)-ATPase from *Acholeplasma laidlawii* B membranes: dependence of enzyme activity on lipid headgroup and hydrocarbon chain structure, *J. Biol. Chem.* 264, 11598-11604.
9. Matsumoto, K. (2001) Dispensable nature of phosphatidylglycerol in *Escherichia coli*: dual roles of anionic phospholipids, *Mol Microbiol.* 39,1427-33.

10. van Klompenburg, W., Ridder, A.N., van Raalte, A.L., Killian, J.A., von Heijne, G., and de Kruijff, B. (1997) In vitro membrane integration of leader peptidase depends on the Sec machinery and anionic phospholipids and can occur post-translationally, *FEBS Lett.* 413, 109-14.
11. Gennis, R.B. (1989) Membrane dynamics and protein-lipid interactions, in *Biomembranes: Molecular Structure and Function*, Springer-Verlag, pp 166-198, New York.
12. Selinsky, B.S. (1992) Protein-lipid interactions and membrane function, in *The Structure of Biological Membranes*(Yeagle, P), pp 603-651,CRC Press, Boca Raton, FL
13. Marsh, D., and Horváth, L.I. (1998) Structure, dynamics and composition of the lipid-protein interface. Perspectives from spin-labelling, *Biochim. Biophys. Acta* 1376, 267-296.
14. Davis, J.H., Clare, D.M., Hodges, R.S., and Bloom, M. (1983) Interaction of a synthetic amphiphilic polypeptide and lipids in a bilayer structure, *Biochemistry* 22, 5298-5305.
15. de Planque, M.R.R., and Killian, J.A. (2003) Protein-lipid interactions studied with designed transmembrane peptides: role of hydrophobic matching and interfacial anchoring, *Mol.Mem.Biol.* 20, 271-284.
16. Zhang, Y.-P., Lewis, R.N.A.H., Hodges, R.S., and McElhaney, R.N. (1992) FTIR spectroscopic studies of the conformation and amide hydrogen exchange of a peptide model of the hydrophobic transmembrane α -helices of membrane proteins, *Biochemistry* 31, 11572-11578.

17. Zhang, Y.-P., Lewis, R.N.A.H., Hodges, R.S., and McElhaney, R.N. (1992) Interaction of a peptide model of a hydrophobic transmembrane α -helical segment of a membrane protein with phosphatidylcholine bilayers: differential scanning calorimetric and FTIR spectroscopic studies, *Biochemistry* 31, 11579-11588.
18. Axelsen, P.H., Kaufman, P.H., McElhaney, R.N., and Lewis, R.N.A.H. (1995) The infrared dichroism of transmembrane helical polypeptides, *Biophys. J.* 69, 2770-2781.
19. Huschilt, J.C., Millman, B.M., and Davis, J.H. (1989) Orientation of alpha-helical peptides in a lipid bilayer, *Biochim Biophys. Acta* 979, 139-141.
20. Bolen, E.J., and Holloway, P.W. (1990) Quenching of tryptophan fluorescence by brominated phospholipid, *Biochemistry* 29, 9638-9643.
21. Huschilt, J.C., Hodges, R.S., and Davis, J.H. (1985) Phase equilibria in an amphiphilic peptide-phospholipid model membrane by deuterium nuclear magnetic resonance difference spectroscopy, *Biochemistry* 24, 1377-1386.
22. Morrow, M.R., Huschilt, J.C., and Davis, J.H. (1985) Simultaneous modeling of phase and calorimetric behavior in an amphiphilic peptide/phospholipid model membrane, *Biochemistry* 24, 5396-5406.
23. Zhang, Y.-P., Lewis, R.N.A.H., Hodges, R.S., and McElhaney, R.N. (1995) Interaction of a peptide model of a hydrophobic transmembrane α -helical segment of a membrane protein with phosphatidylethanolamine bilayers: differential scanning calorimetric and FTIR spectroscopic studies, *Biophys. J.* 68, 847-857.
24. Pauls, K.P., MacKay, A.L., Soderman, O., Bloom, M., Taneja, A.K., and Hodges, R.S. (1985) Dynamic properties of the backbone of an integral membrane polypeptide measured by ^2H -NMR, *Euro. Biophys. J.* 12, 1-11.

25. Subczynski, W.K., Lewis, R.N.A.H., McElhaney, R.N., Hodges, R.S., Hyde, J.S., and Kusumi, A. (1998) Molecular organization and dynamics of 1-palmitoyl-2-oleoyl-phosphatidylcholine bilayers containing a transmembrane α -helical peptide, *Biochemistry* 37, 3156-3164.
26. Subczynski, W.K., Pasenkiewicz-Gierula, McElhaney, R.N, Hyde, J.S., and Kusumi, A. (2003) Molecular organization and dynamics of 1-palmitoyl-2-oleoyl phosphatidylcholine bilayer membranes containing a transmembrane α -helical peptide with hydrophobic surface roughness, *Biochemistry* 42, 3939-3948.
27. Liu, F., Lewis, R.N.A.H., Hodges, R.S., and McElhaney, R.N. (2001) A differential scanning calorimetric and ^{31}P -NMR spectroscopic study of the effect of transmembrane α -helical peptides on the lamellar/reversed hexagonal phase transition of phosphatidylethanolamine model membranes, *Biochemistry* 40, 760-768.
28. Liu, F., Lewis, R.N.A.H., Hodges, R.S., and McElhaney, R.N. (2002). Effect of variations in the structure of a polyleucine-based α -helical transmembrane peptide on its interaction with phosphatidylcholine bilayers, *Biochemistry* 41, 9197-9207.
29. Segrest, J.P., De Loof, H., Dohlman, J.G., Brouillette, C.G., and Anantharamaiah, G.M. (1990) Amphipathic helix motif: classes and properties, *Proteins: Struct. Funct. Genet.* 8, 103-117.
30. Monne, M., Nilsson, I., Johansson, M., Elmhed, N., and van Heijne, G. (1998) Positively and negatively charged residues have different effects on the position in the membrane of a model transmembrane helix, *J. Mol. Biol.* 284, 1177-1183.
31. von Heijne, G. (1994) Membrane proteins: from sequence to structure, *Annu.Rev.Biophys.Biomol.Struct.* 23, 167-192.

32. de Planque, M.R.R., Bonev, B.B., Demmers, J.A.A., Greathouse, D.V., Koeppe II, R.E., Separovic, F., Watts, A., and Killian, J.A. (2003) Interfacial anchor properties of tryptophan residues in transmembrane peptides can dominate over hydrophobic Matching effects in peptide-lipid interactions, *Biochemistry*. 42, 5341-5348.
33. Zhang, Y.-P., Lewis, R.N.A.H., Henry, G.D., Sykes, B.D., Hodges, R.S., and McElhaney, R.N. (1995) Peptide models of helical hydrophobic transmembrane segments of membrane proteins. I. Studies of the conformation, intrabilayer orientation and amide hydrogen exchangeability of Ac-K₂-(LA)₁₂-K₂ amide, *Biochemistry*. 34, 2348-2361.
34. Mantsch, H.H., Madec, C., Lewis, R.N.A.H., and McElhaney, R.N. (1985) The thermotropic phase behaviour of model membranes composed of phosphatidylcholines containing isobranched fatty acids. II. Infrared and ³¹P-NMR spectroscopic studies, *Biochemistry* 24: 2440-2446.
35. Zhang, Y.-P., Lewis, R.N.A.H., and McElhaney, R.N. (1997) Calorimetric and spectroscopic studies of the thermotropic phase behavior of the *n*-saturated 1,2-diacyl-phosphatidylglycerols, *Biophys. J.* 72, 779-793.
36. Zhang, Y.-P., Lewis, R.N.A.H., Henry, Hodges, R.S., and McElhaney, R.N. (1995) Peptide models of helical hydrophobic transmembrane segments of membrane proteins. II. DSC and FTIR spectroscopic studies of the interaction of Ac-K₂-(LA)₁₂-K₂-amide with phosphatidylcholine bilayers, *Biochemistry*. 34, 2362-2371.
37. Lewis, R. N. A. H., and McElhaney, R. N. (1996) FTIR spectroscopy in the study of hydrated lipids and lipid bilayer membranes, in *Infrared Spectroscopy of Biomolecules*

- (Mantsch, H. H., and Chapman, D., Eds.) pp 159-202, John Wiley and Sons, New York
38. Blume, A., Hubner, W., and Messner, G. (1988) Fourier transform infrared spectroscopy of $^{13}\text{C}=\text{O}$ -labeled phospholipids hydrogen bonding to carbonyl groups, *Biochemistry*. 27, 8239-8249.
39. Lewis, R.N.A.H., McElhaney, R.N., Pohle, W., and Mantsch, H.H. (1994) The components of the carbonyl stretching band in the infrared spectra of hydrated 1,2-diacylglycerolipid bilayers: a reevaluation, *Biophys. J.* 67, 2367-2375.
40. McElhaney, R.N. (1986) Differential scanning calorimetric studies of lipid-protein interactions in model membrane systems, *Biochim. Biophys Acta* 864, 361-421.
41. Lewis, R.N.A.H. and McElhaney, R.N. (1992) The mesomorphic phase behavior of lipids bilayers, in "*The Structure of Biological Membranes*" (P.L. Yeagle, ed.) pp. 73-155, CRC Press, Boca Raton, Florida, 1992.
42. Lewis, R.N.A.H., Pohle, W., and McElhaney, R.N. (1997) The interfacial structure of phospholipid bilayers: Differential scanning calorimetry and Fourier transform infrared spectroscopic studies of 1,2-dipalmitoyl-*sn*-glycero-3-phosphorylcholine and its dialkyl and acyl-alkyl analogs. *Biophys. J.* 70, 2736-2746 .
43. Dougherty, D.A. (1996) Cation- π interactions in chemistry and biology: a new view of benzene, Phe, Tyr, and Trp, *Science* 271, 163-168.
44. Sussman, J.L., Harel, M., Frolow, F., Oefner, C., Goldman, A., Toker, L., and Silman, I. (1991) Atomic structure of acetylcholinesterase from *Torpedo californica*: a prototypic acetylcholine-binding protein, *Science* 253, 872-879.

45. Unwin, N. (1993) Nicotinic acetylcholine receptor at 9 Å resolution, *J.Mol.Biol.* 229, 1101-1124.
46. Satin, J., Kyle, J.W., Chen, M., Bell, P., Cribbs, L.L., Fozzard, H.A., and Rogart, R.B.(1992) A mutant of TTX-resistant cardiac sodium channels with TTX-sensitive properties, *Science* 256, 1202-1205.
47. Yau, W-M., Wimley, W.C., Gawrisch, K., and White, S.H. (1998) The preference of tryptophan for membrane interfaces, *Biochemistry* 37, 14713-14718.

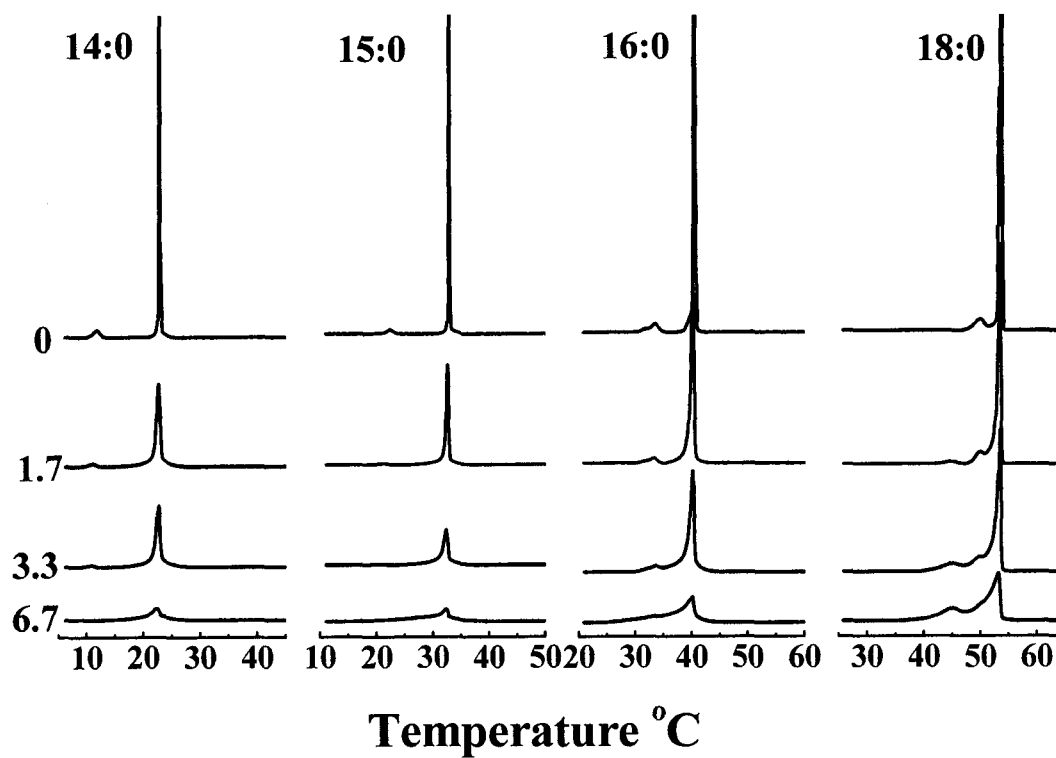


FIGURE 1. Effect of L₂₄ on the DSC thermograms of a series of *n*-saturated diacyl-PGs. Thermograms are shown as a function of the acyl chain length (*N*:0) of the lipids, and the mole percent of peptide present in each sample is indicated in the column of numbers printed on the left side of the figure.

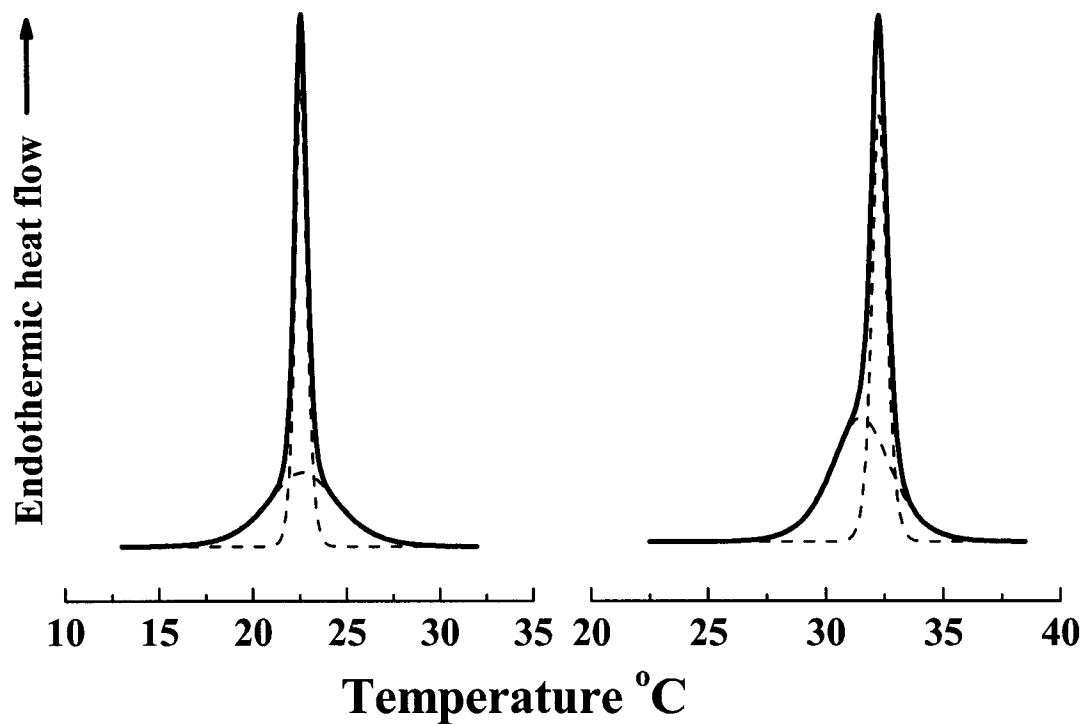


FIGURE 2. Illustration of the curve-fitting procedure used to resolve the components of the DSC heating thermograms. The examples shown are $L_{24}/14:0PG$ (left panel) and $L_{24}/15:0PG$ (right panel). Both samples contained 3.3 mol% L_{24} .

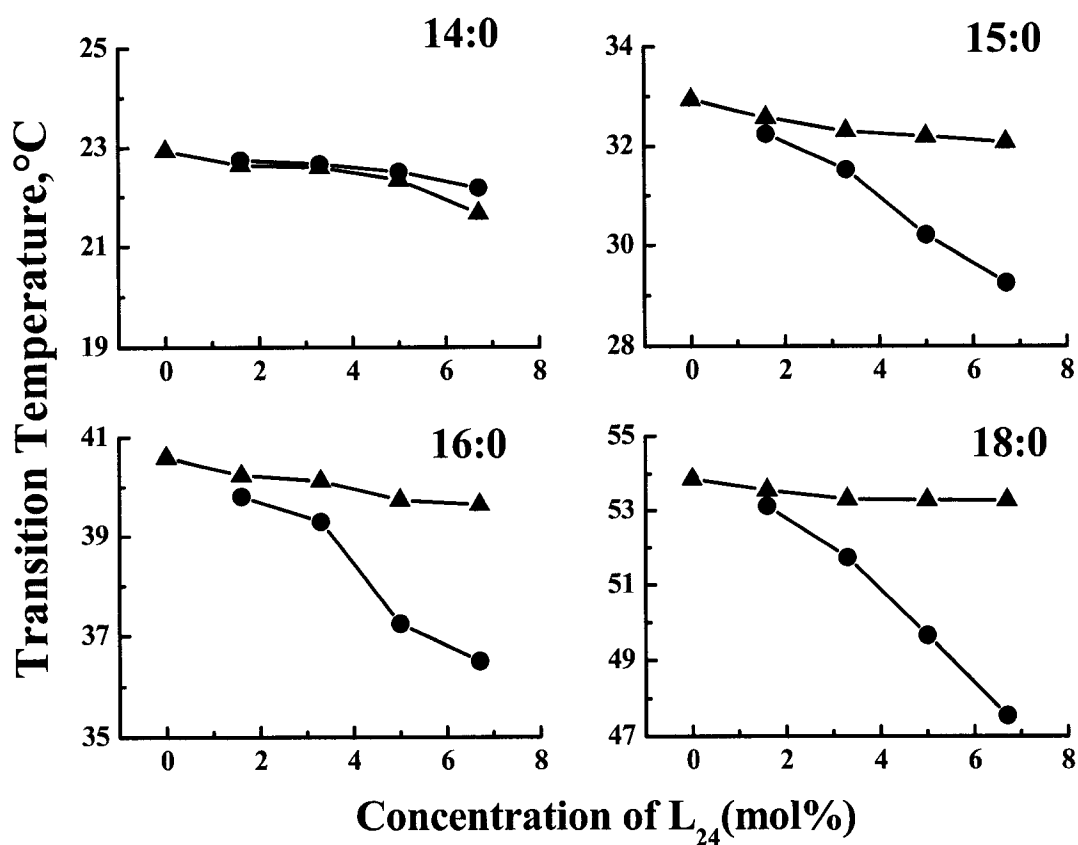


FIGURE 3. Effects of L₂₄ concentration on the peak temperatures of the two components of the DSC thermograms exhibited by the mixtures of L₂₄ and the *n*-saturated diacyl-PGs. The symbols (▲) and (●) represent the sharp and broad components of the DSC endotherms, respectively.

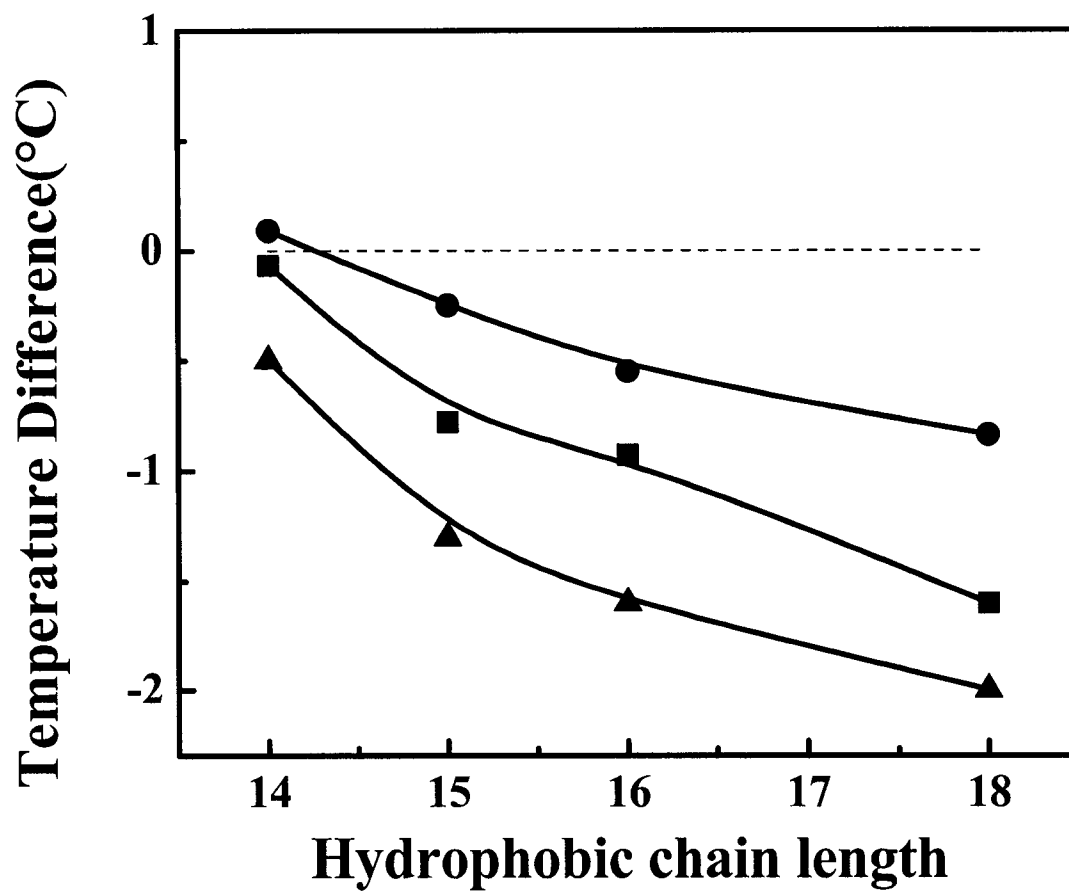


FIGURE 4. Plot of the differences of the transition temperatures of the peptide-associated and the peptide-poor PGs versus the hydrophobic chain length of the lipid bilayer at a peptide concentration of 3.3 mol%. The symbols (▲), (●), and (■) represent peptides WL₂₂W, L₂₄DAP, and L₂₄, respectively.

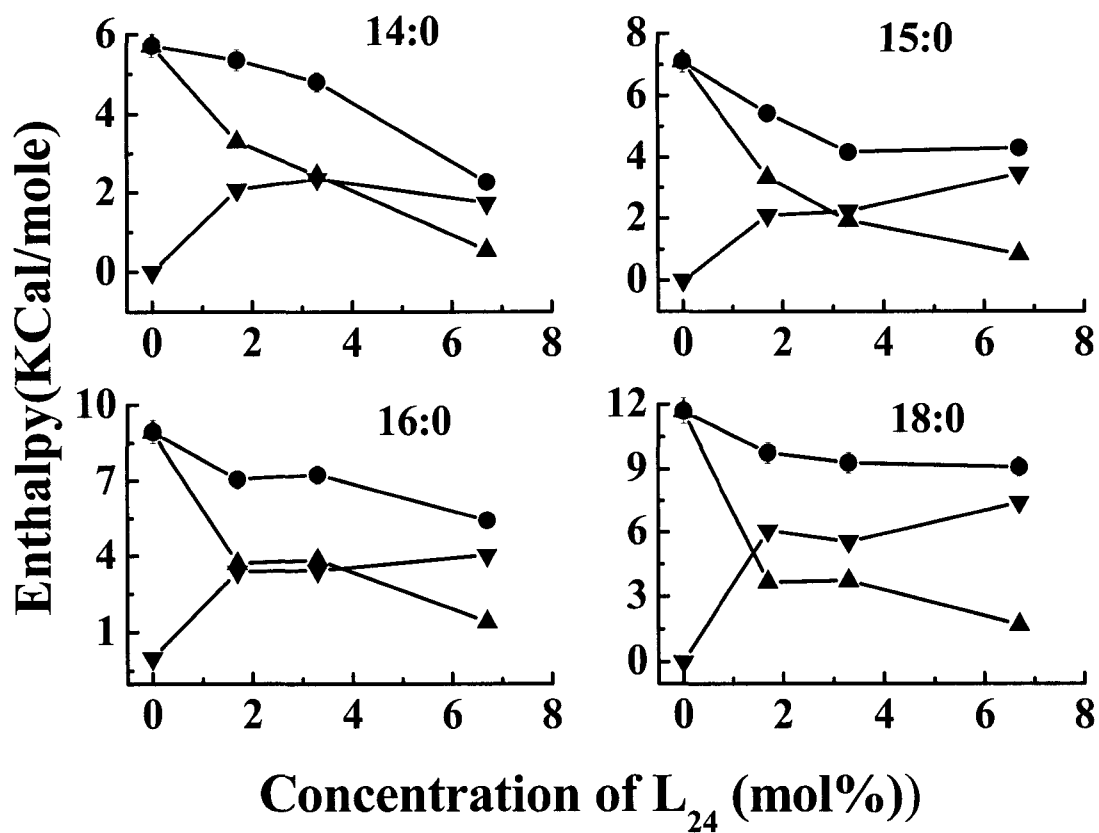


FIGURE 5. Effects of L₂₄ concentration on the transition enthalpies of the two components of the DSC thermograms exhibited by mixtures of L₂₄ and *n*-saturated diacyl-PGs. The symbols (●), (▲), and (▼) represent the total enthalpy and the enthalpy of the sharp and the broad components of DSC endotherms, respectively.

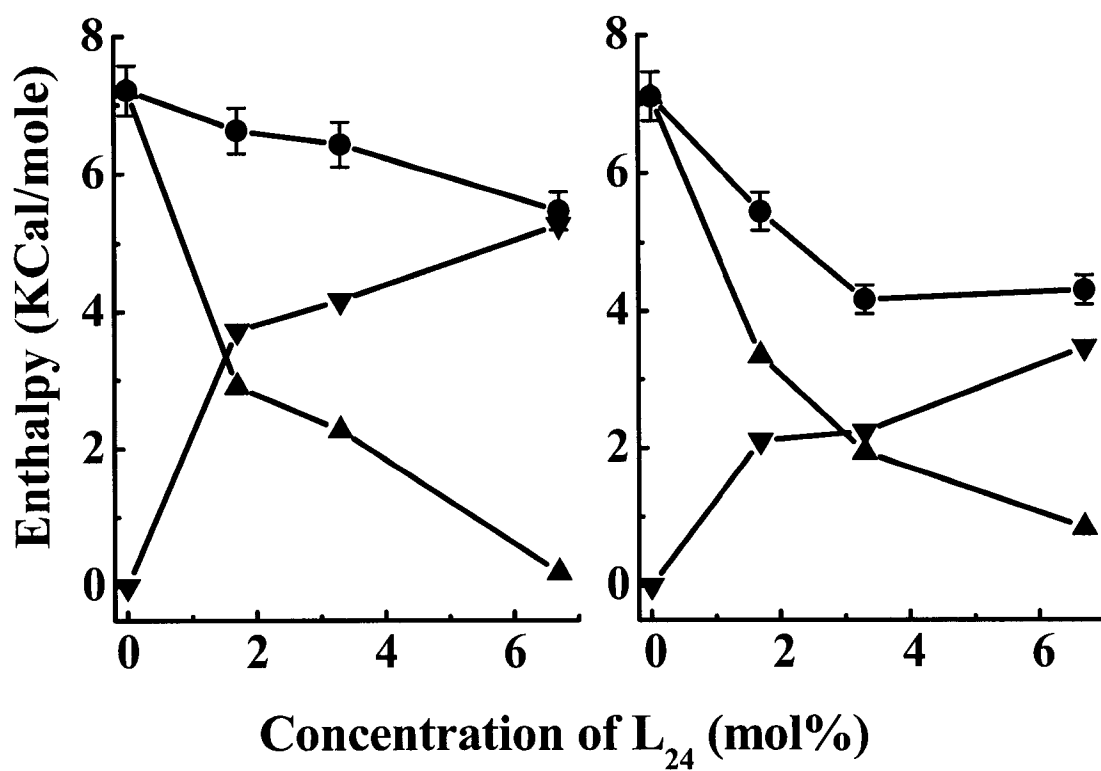


FIGURE 6. Comparison of the effects of L₂₄ concentration on the transition enthalpies of L₂₄/15:0 PG mixture (right panel) with that on the transition enthalpies of L₂₄/15:0 PC mixture (left panel). The symbols (●), (▲), and (▼) represent the total enthalpy and the enthalpy of the sharp and the broad components of DSC endotherms, respectively.

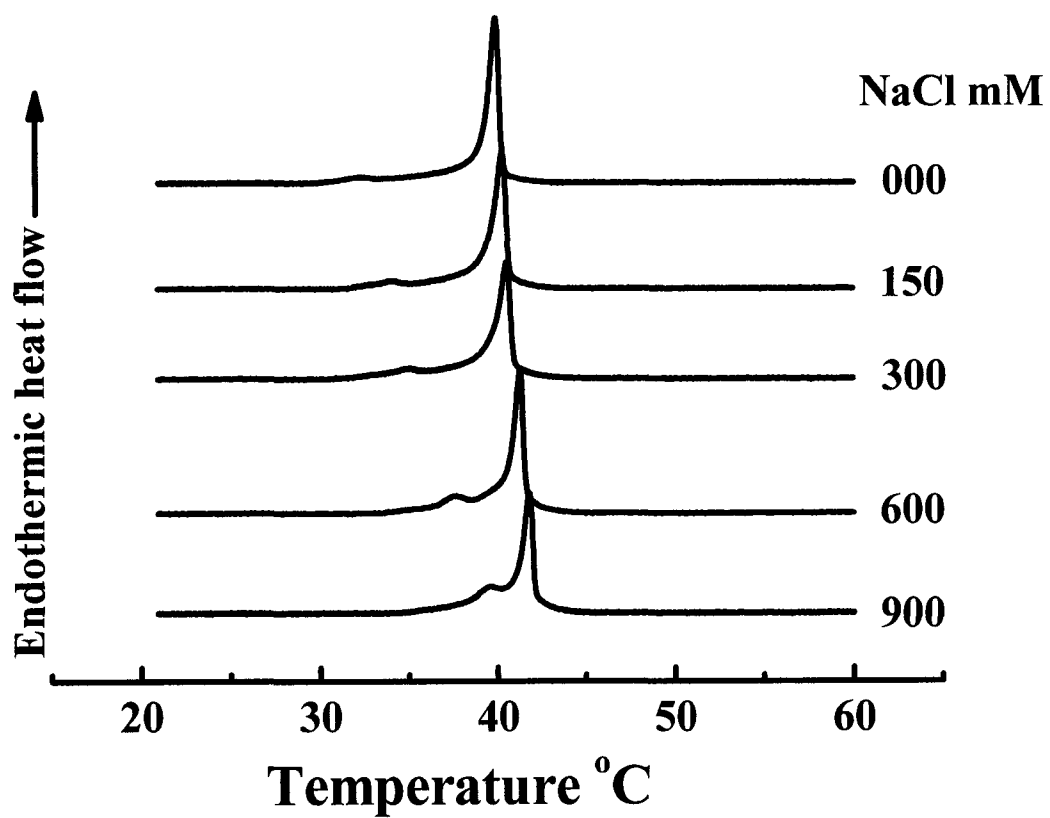


FIGURE 7. Effect of NaCl concentration on the phase behaviors of L₂₄/16:0PG mixtures at a peptide concentration of 3.3 mol%.

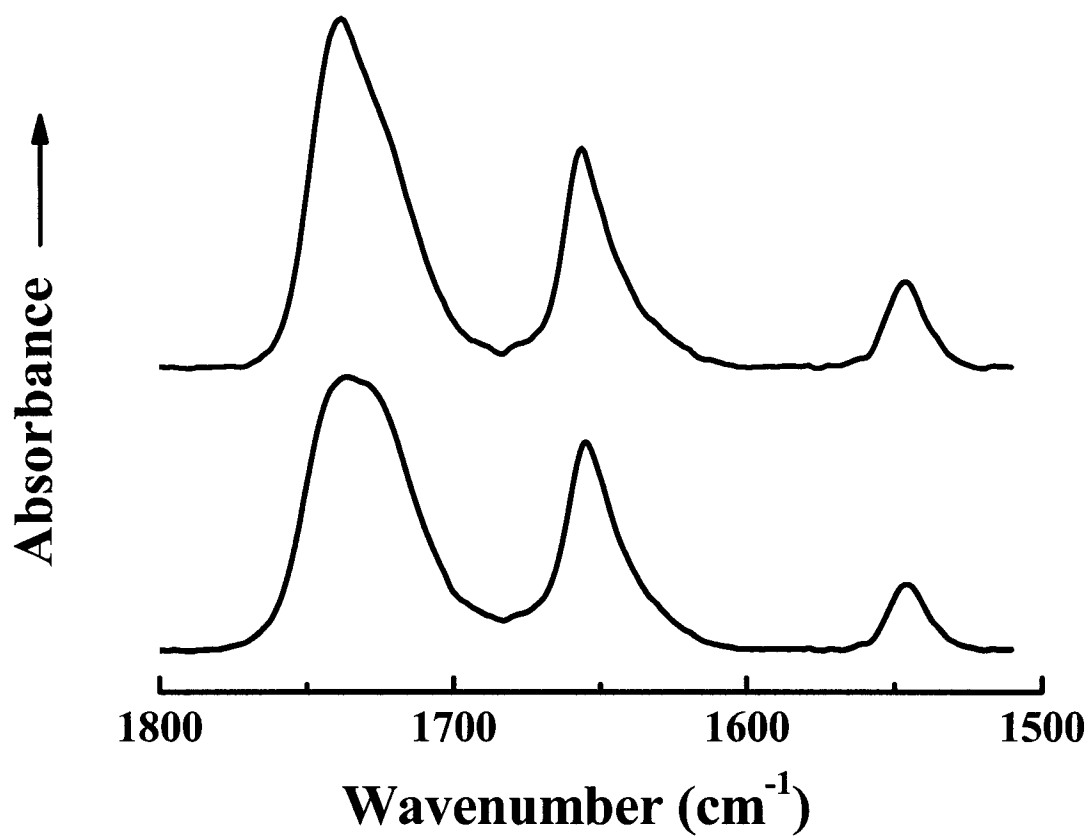


FIGURE 8. FTIR spectra of gel (top) and the liquid-crystalline phase (bottom) formed by a mixture of L₂₄ with 16:0 PG at a peptide concentration of 3.3 mol%.

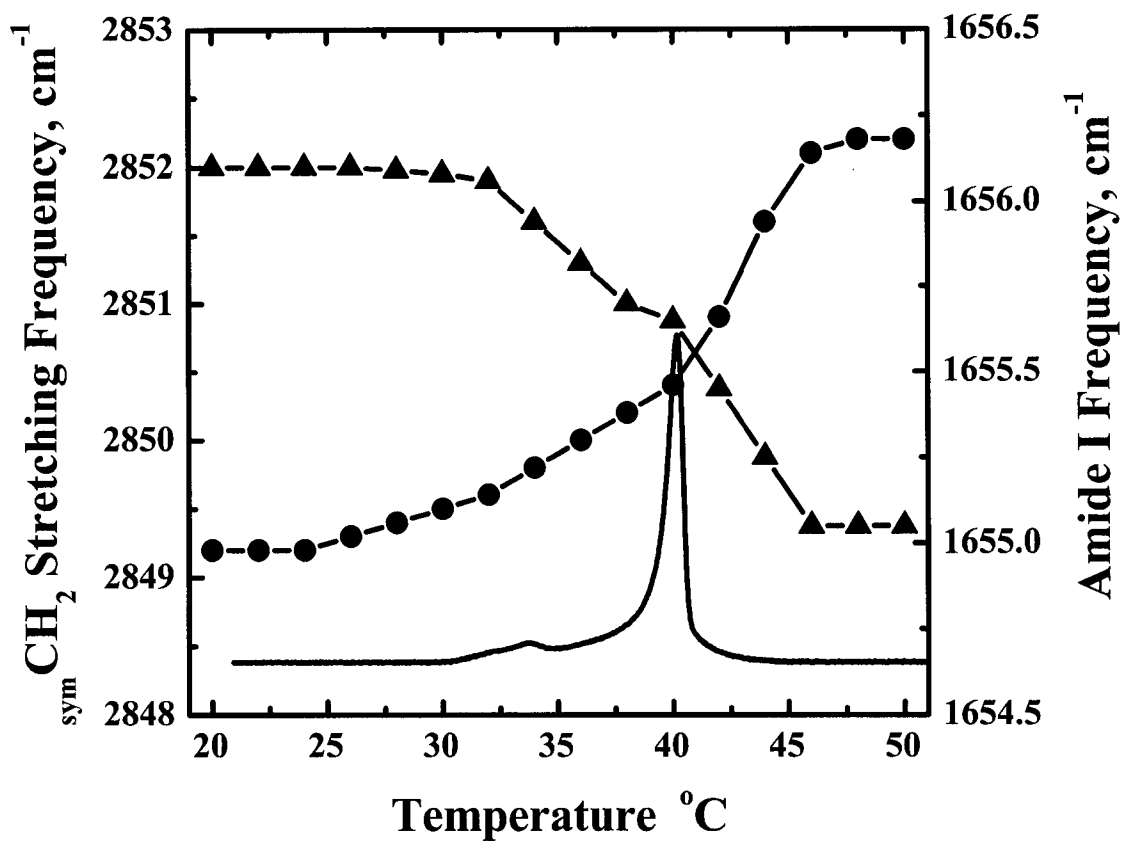


FIGURE 9. Combined plots of CH_2 symmetric stretch (●), peptide amide I band (▲), and calorimetric thermograms as a function of temperature for systems of $\text{L}_{24}/16:0$ PG at a peptide concentration of 3.3 mol%.

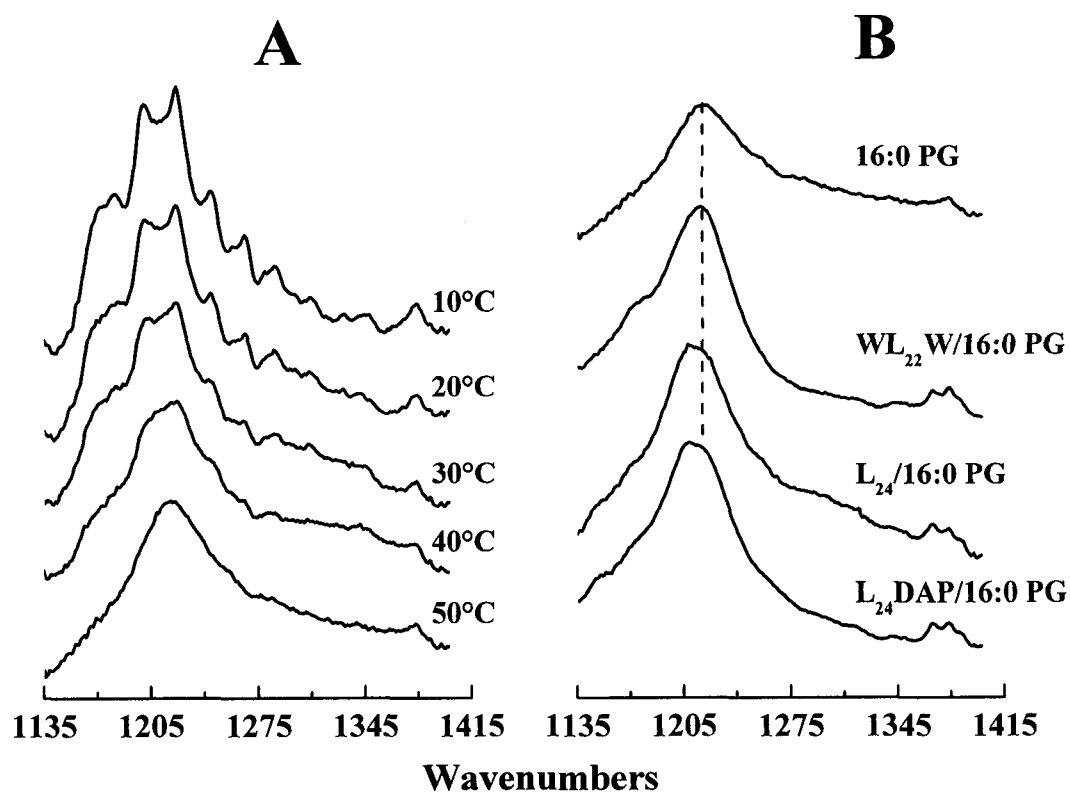


FIGURE 10.

(A). The asymmetrical phosphate stretching regions of infrared spectra of 16:0 PG alone in the gel and the liquid-crystalline phases.

(B) The asymmetrical phosphate stretching regions of infrared spectra of pure 16:0 PG, L₂₄/16:0 PG, L₂₄DAP/16:0 PG and WL₂₂W/16:0 PG at a peptide concentration of 3.3 mol%. The absorbance spectra shown here were acquired in the liquid-crystalline phase of the lipids.

CHAPTER IV. Effect of Variations in the Structure of a Poly-leucine-Based α -Helical Transmembrane Peptide on Its Interaction with Phosphatidylethanolamine Bilayers

Introduction

All biological membranes consist of lipid and protein molecules held together by noncovalent interactions (1). The fundamental structural element of all biological membranes is a lipid bilayer, which also functions as the major permeability barrier. The zwitterionic phospholipids phosphatidylcholine (PC)¹ and PE are the major lipid components in animal cell membranes, and PE is often a major component of bacterial cell membranes as well (2,3). In addition, eukaryotic cell membranes exhibit an asymmetry in lipid distribution across the lipid bilayer. For example, in human erythrocyte membranes, PC and sphingomyelin are mainly found in the outer leaflet, while PE and PS are mainly found in the inner leaflet of the bilayer (4). The basic functions of biological membranes are carried out by membrane proteins that may associate loosely with the membrane surface (peripheral proteins) or traverse the lipid bilayer (integral membrane proteins). Most of the integral membrane proteins are composed of tightly packed bundles of transmembrane α -helical segments that contain about 20 hydrophobic residues (5). Recent studies have shown that PE can assist in the correct folding of integral membrane proteins such as the lactose permease and the

A version of this chapter has been submitted for publication to *Biochemistry* Liu, F., Lewis, R.N.A.H., Hodges, R.S., and McElhaney, R.N. (2004).

high affinity phenylalanine permease of *Escherichia coli* (6, 7). A number of X-ray crystal structures also indicate that integral membrane proteins such as cytochrome c oxidase from *Rhodobacter sphaeroides* (8) and the purple bacterial reaction center from *Thermochromatium tepidum* (9) may contain bound PE or other phospholipids. It was also found that aminophospholipids such as PE in the cytoplasmic leaflet of Golgi, endosome and plasma membranes contribute to the protein-mediated vesicle budding competence of these membrane systems (10).

Although the mutual interactions of lipids and proteins are fundamentally important to both the structure and the function of all biological membranes, our understanding of the physical principles underlying lipid-protein interactions remains incomplete and the actual molecular mechanisms whereby associated lipids could alter the activity, and presumably also the structure and dynamics, of integral membrane proteins are largely unknown. This is due in part to the fact that most transmembrane proteins are relatively large, multidomain macromolecules with complex and often unknown three-dimensional structure and topology. Despite the fact that about one third of all proteins are integral membrane proteins, less than one hundred unique membrane protein structures have been reported to date, compared with the huge number (over 14000) of soluble proteins in the Protein Data Bank (11). Moreover, membrane proteins can interact with lipid bilayers in complex, multifaceted ways (12-14). To overcome this problem, a number of workers have designed and synthesized peptide models of specific regions of natural membrane proteins and have studied their interactions with model membranes of defined lipid composition (15-17).

The synthetic peptide acetyl-K₂-G-L₂₄-K₂-A-amide (P₂₄) and its analogues have been successfully utilized as a model of the hydrophobic transmembrane α -helical segments of integral membrane proteins (15). These peptides contain a long sequence of hydrophobic leucine residues capped at both the N- and C-termini with two positively charged, relatively polar lysine residues. Moreover, the normally positively charged N-terminus and the negatively charged C-terminus are blocked to provide a symmetrical tetracationic peptide that will more faithfully mimic the transbilayer region of natural membrane proteins. The central polyleucine region of these peptides was designed to form a maximally stable α -helix, particularly in the hydrophobic environment of the lipid bilayer core, while the dilysine caps were designed to anchor the ends of these peptides to the polar surface of the lipid bilayer and to inhibit the lateral aggregation of these peptides. In fact, CD (15) and FTIR (18-20) spectroscopic studies of P₂₄ have shown that it adopts a very stable α -helical conformation both in solution and in lipid bilayers, and X-ray diffraction (21), fluorescence quenching (22) and FTIR spectroscopic (18-20) studies have confirmed that P₂₄ and its analogues assume a transbilayer orientation with the N- and C-termini exposed to the aqueous environment and the hydrophobic polyleucine core embedded in the hydrocarbon core of the lipid bilayer when reconstituted with various PCs. DSC (23-25) and ²H NMR spectroscopy (23-24) studies have shown that P₂₄ broadens the gel/liquid-crystalline phase transition of the host phospholipid bilayer and reduces its enthalpy. The phase transition temperatures of PC and PG bilayers are shifted either upward or downward, mainly depending on the degree of mismatch between the peptide hydrophobic length and the lipid hydrophobic thickness (19,26,27). In contrast, the phase transition temperatures of PE bilayers are substantially decreased by the

presence of P₂₄ and a closely related peptide (LA)₁₂ in a manner somewhat independent of the peptide-lipid hydrophobic mismatch (25,28). ²H NMR (29) and ESR (30,31) spectroscopic studies have shown that the rotational diffusion of P₂₄ about its long axis perpendicular to the membrane plane is rapid in the liquid-crystalline state of the bilayer and that the closely related peptides L₂₄ and (LA)₁₂ exist at least primarily as monomers in liquid-crystalline POPC bilayers, even at relatively high peptide concentrations.

Statistical analysis shows that the hydrophobic core of the transmembrane α -helices in many integral membrane proteins are normally flanked by aromatic residues like tryptophan or tyrosine and that the positively-charged lysine or arginine residues are found adjacent to these aromatic residues (32). To study the roles of tryptophan and lysine residues in lipid-protein interactions, we have previously synthesized three analogues of P₂₄, Ac-K₂-L₂₄-K₂-amide (L₂₄), Ac-DAP₂-L₂₄-DAP₂-amide (L₂₄DAP, DAP is diaminopropionic acid), and Ac-K₂-W-L₂₂-W-K₂-amide (WL₂₂W) and studied their interactions with zwitterionic PC and anionic PG bilayers (27,28). First, with the peptide L₂₄DAP, the two pairs of capping lysine residues at the N- and C- termini of L₂₄ have been replaced with the lysine analogues DAP, in which three of the four side-chain methylene groups have been removed. This peptide was used to test the so-called snorkel model first suggested by Segrest *et al.* (33) to explain the behavior of positively charged residues in the amphipathic helices present at the surfaces of blood lipoproteins and later extended to transmembrane α -helices by von Heijne *et al.* (34). According to the transmembrane peptide version of the snorkel model, the long, flexible hydrophobic side chains of lysine or arginine residues could extend along the transmembrane helix so that the terminal charged moiety can reside in the lipid polar headgroup region while the α -

carbon of the amino acid residue remains well below (or possibly above) the membrane-water interface, even when the hydrophobic length of the peptide is considerably different from that of the host lipid bilayer. Because of the shorter spacer arms between the charged group and the α -carbon in DAP, L₂₄-DAP is expected to be less accommodating to the hydrophobic mismatch between the peptides and the lipids, and any effects of such mismatch on the thermotropic phase behavior of the host lipid bilayer should thus be exaggerated. Second, in peptide WL₂₂W, the residues Leu-3 and Leu-26 of L₂₄ are replaced with tryptophans. The preference of aromatic tryptophan or tyrosine residues for the membrane polar/apolar interface has been found to be one of the common features of natural membrane proteins (35). Since tryptophan residues have been proposed to anchor the ends of α -helical transmembrane peptides to the polar/apolar interface of the lipid bilayer, we would also expect that WL₂₂W would be less accommodating to hydrophobic mismatch between the peptides and host lipid bilayer than would L₂₄.

To further clarify the role of interfacially localized tryptophan and lysine residues in lipid-protein interactions, we have used DSC and FTIR spectroscopy to study the interactions of L₂₄, L₂₄DAP and WL₂₂W with a series of zwitterionic PEs with different hydrocarbon chain lengths and have compared these results with those obtained previously for a homologous series of zwitterionic PCs (27) and anionic PGs (28). Our results demonstrate that the snorkeling of the terminal lysine residues at the end of the model peptides is required for optimization of the hydrogen-bonding and/or electrostatic interactions between the lysine residues at the termini of these peptides and the polar headgroups of the PE. Our results also indicate that the presence of interfacially localized

tryptophan residues only slightly affects the interactions of these model peptides with the zwitterionic phospholipids PE and PC (27), although tyryptophan residues strongly modulate such interactions in anionic PG bilayers (28).

Materials and methods

The phospholipids used in this study were obtained from Avanti Polar Lipids Inc. (Alabaster, AL) and were used without further purification. Commercially supplied solvents of at least analytical grade quality were redistilled prior to use. Peptides were synthesized and purified as TFA salts using previously published solid-phase synthesis and reversed phase high-performance liquid chromatographic procedures (36).

Samples were prepared for DSC as follows. Appropriate quantities of peptides and PE were codissolved in methanol to obtain the desired lipid/peptide ratio, and the solvent was removed in a stream of nitrogen at temperatures near 60-70 °C to ensure sample homogeneity. Then the sample was redissolved in chloroform/methanol (1:1) and the solvent was again removed in a stream of nitrogen at temperatures near 60-70 °C. Later the sample was redissolved in benzene and lyophilized overnight to form a white powder. Samples containing 0.5 mg of lipid were then hydrated by vigorous vortexing with water at temperatures some 10-15°C above the gel/liquid-crystalline phase transition temperature of the lipid. DSC thermograms were obtained from 0.5 ml samples with a high sensitivity Microcal VP-DSC instrument (Microcal Inc., Northampton MA), operating at heating and cooling rates of 10° C per hour. The data were analyzed and plotted with the Origin software package (OriginLab Corporation, Northampton, MA).

Peptide samples to be used in FTIR spectroscopic experiments were converted to the hydrochloride salt by two cycles of lyophilization from 10 mM hydrochloric acid. This procedure was necessary because the trifluoroacetate ion gives rise to a strong absorption band ($\sim 1670\text{ cm}^{-1}$) which partially overlaps the amide I absorption band of the peptide (15). Typically, samples were prepared by co-dissolving lipid and peptide in methanol at a lipid to peptide ratio of near 30:1 (mol/mol). After removal of the solvent and drying of the film (see above), samples containing 2-3 mg of lipid were hydrated by vigorous mixing with 75 μl of a D_2O -based buffer (50 mM Tris, 150 mM NaCl, 1mM NaN_3 , pH 7.4). The paste obtained was then squeezed between the CaF_2 windows of a heatable, demountable liquid cell (NSG Precision Cells, Farmingdale, NY) equipped with a 25 μm teflon spacer. Once mounted in the sample holder of the spectrometer, the sample temperature could be varied between 20 $^\circ\text{C}$ and 90 $^\circ\text{C}$ by an external, computer-controlled water bath. Infrared spectra were acquired as a function of temperature with a Digilab FTS-40 Fourier-transform spectrometer (Bio-Rad, Digilab Division, Cambridge, MA) using data acquisition parameters similar to those described by Mantsch *et al.* (36). The experiment involved a sequential series of 2 $^\circ\text{C}$ temperature ramps with a 20 minute inter-ramp delay for thermal equilibration, and was equivalent to a scanning rate of 4 $^\circ\text{C}$ per hour. Spectra were analyzed with software supplied by the instrument manufacturers and other programs obtained from the National Research Council of Canada.

Results

In order to evaluate the DSC and FTIR spectroscopic data presented below, we need to compare the intrinsic hydrophobic length of the model peptides L_{24} , L_{24}DAP , and WL_{22}W with the intrinsic hydrophobic thickness of the various PE bilayers used in this

study (see Table 1). On the basis of measurements of a molecular model of L₂₄ in an ideal α -helical conformation, we estimate that the mean hydrophobic length of L₂₄ (the average length of the leucine sequence measured at any point on the surface of the helix) is about 30.6 Å. Note that the effective hydrophobic length measured in this manner is two helical half-turns shorter at each end of the hydrophobic helical core than the maximum hydrophobic length of this peptide which would be 36.0 Å. Thus the mean hydrophobic length of L₂₄ is intermediate between the mean hydrophobic thickness of 14:0 PE and 16:0 PE bilayers. For the shorter chain 12:0 PE bilayers, L₂₄ hydrophobic length exceeds its hydrophobic thickness in both the gel and the liquid-crystalline phases, while for other three PEs, the hydrophobic length of L₂₄ will be less than that of gel state but more than that of the liquid-crystalline bilayer. The same considerations also apply to L₂₄DAP and WL₂₂W, which are taken to have the same effective hydrophobic length as L₂₄.

We stress here that the pattern of matching of lipid bilayer thickness and peptide hydrophobic length just described applies only if these model peptides adopt an ideal α -helical conformation that is not influenced by lipid bilayer thickness. In fact, our spectroscopic studies show that in PE bilayers these model peptides do adopt a predominantly α -helical conformation which is, however, affected by gel-state PE bilayer thickness (see below). Moreover, the hydrocarbon chains of the PE molecules do change their degree of conformational order, and thus the effective hydrophobic thickness of the PE bilayer, in response to the presence of these model peptides. Thus the actual degree of hydrophobic mismatch between these model peptides and the various PE bilayers, in both the gel and the liquid-crystalline states, may be different than indicated by the intrinsic

effective hydrophobic length of this peptide and the hydrophobic thickness of PE bilayers in the absence of peptide.

Thermotropic Phase Behavior of PE Bilayers in the Absence of Peptides. As illustrated in Figure 1, in the absence of peptides the DSC thermograms of unannealed aqueous dispersions of each of four *n*-saturated diacyl PEs studied here exhibit a single fairly energetic and highly cooperative lamellar gel/lamellar liquid-crystalline phase transition on heating. This transition is freely reversible, as shown by the absence of significant cooling hysteresis (data not shown). In addition, the temperatures of the phase transitions of these PEs increase progressively but nonlinearly, and the transition enthalpy increases linearly, with increases in the hydrocarbon chain length, as expected. For a thorough discussion of the thermotropic phase behavior of the complete homologous series of *n*-saturated diacyl PEs, see (37) and references cited therein.

Thermotropic Phase Behavior of Various PE Bilayers in the Presence of L₂₄. The effects of the incorporation of L₂₄ on the main phase transition of PE bilayers are also illustrated in Figure 1. In all cases the incorporation of increasing quantities of L₂₄ produces an apparently two-component DSC endotherm, consisting of a broad, lower-temperature component and a sharp, higher-temperature component. The relative contribution of the sharp component of the DSC endotherm, which initially possesses a phase transition temperature, enthalpy and cooperatively similar to that of the PE alone, decreases in magnitude as the concentration of L₂₄ increases. In fact, the sharp component of the DSC endotherm is barely detectable at a peptide concentration of 3.3 mol % in 12:0 PE bilayers and a concentration of 6.7 mol % in the three larger-chain PE bilayers studied. In contrast, the relative contribution of the broad component increases as the peptide

concentration increases and it is the only or at least the major component that persists at the highest peptide concentrations tested. Moreover, our FTIR spectroscopic studies of the temperature dependence of the methylene stretching frequency changes indicate that both the sharp and broad components of the DSC endotherms are accompanied by increases in the rotational conformational disorder of the PE hydrocarbon chains (data not shown). Using the rationale provided in our previous DSC studies of the interaction of P₂₄ and related peptides with PC, PE and PG bilayers (15, 21, 25, 26), we thus assign the sharp component of our DSC endotherms to the hydrocarbon chain-melting phase transition of peptide-poor PE domains and the broad component to the melting of peptide-rich PE domains. Note that these characteristic effects of the incorporation of L₂₄ and its analogs on the sharp component of the DSC endotherm are noted in all the PEs studied and are essentially hydrocarbon chain length independent.

The effects of L₂₄ incorporation on the temperatures of the sharp and broad components of the DSC heating endotherms for all four PEs are illustrated in Fig 2. As noted above, the temperature of the sharp component changes little with increases in L₂₄ concentration in each of the four PE bilayers examined. However, in all cases there is a gradual decrease in the temperature of the broad component with increasing peptide concentration, resulting in a gradual increase in ΔT (the shift of the phase transition temperature of the broad component relative to that of the sharp component). Moreover, at all peptide concentrations, the phase transition temperature of the broad component of the DSC endotherm always occurs at lower temperature than that of the sharp component, regardless of PE hydrocarbon chain length. At 6.7 mol % L₂₄ concentration, the ΔT is largest in 12:0 PE and smallest in 18:0 PE bilayers but the variation with hydrocarbon

chain length is small (< 1 °C). Qualitatively similar results were observed when L₂₄ DAP and WL₂₂W are incorporated into PE bilayers.

The effects of the lipid acyl chain length on the ΔT values observed with PE-peptide mixtures containing containing 3.3 mol % L₂₄ are illustrated in Figure 3. With all of the PEs examined, the ΔT values obtained are all negative and only weakly dependent on lipid hydrocarbon chain length, with the absolute ΔT values diminishing only slightly with increasing hydrocarbon chain length (-2.6 °C for 12:0 PE to -2.0 °C for 18:0 PE). As illustrated in Figure 3, these observations contrast sharply from those which occur when L₂₄ is incorporated into PC bilayers. With the latter, the sign and magnitude of ΔT is strongly hydrocarbon chain length dependent in a manner consistent with the sign and degree of the hydrophobic mismatch between peptide hydrophobic length and lipid bilayer hydrophobic thickness. With the shorter chain PC bilayers ($\leq 14:0$ PC), the temperature of the broad component of the DSC endotherm is progressively increased relative to that of the sharp component as hydrocarbon chain length decreases, and vice versa in the longer chain PC bilayers ($\geq 16:0$ PC), whereas the ΔT value is near zero for 15:0 PC bilayers. As noted previously (27), the effective hydrophobic length of P₂₄ (or L₂₄) match the mean thickness of 15:0 PC bilayers. Thus the ΔT value becomes increasing positive in PC bilayers with mean hydrophobic thicknesses which are progressively less than the effective hydrophobic length of the peptide and vice versa. Qualitatively similar results are also obtained when L₂₄ is incorporated into in anionic PG bilayers (28). The possible molecular basis for these results will be discussed later.

The variation in the enthalpy of the overall phase transition as a function of L₂₄ concentration in each of the four PE bilayers studied is shown in Figure 4. As noted

earlier, in all cases the contribution of the sharp component to the total enthalpy change measured decreases steeply with increasing peptide concentration with little dependence on PE hydrocarbon chain length (see Figure 1). However, the variation in the enthalpy of the overall and broad components of the DSC endotherms depend strongly on PE hydrocarbon chain length. With the shorter chain PEs (i.e. 12:0 and 14:0 PE), the transition enthalpies of both components decrease as L_{24} concentration increases. However, in the longer chain PE bilayers, these transition enthalpies first decrease and then increase again as peptide concentration increases, with this effect becoming more pronounced as PE hydrocarbon chain length increases. A similar pattern of behavior was observed in our previous studies of P_{24} /PE systems (25), in which case the apparent increase in the overall phase transition enthalpy, and that of the broad component of the DSC endotherm, was ascribed to the release of heat due to the disaggregation of peptide clusters in the gel states of the longer chain PE bilayers as the gel/liquid-crystalline phase transition is approached on heating. It is noteworthy, however, that similar behavior is not observed when L_{24} is incorporated into PC and PG bilayers (28). With the latter lipids the overall phase transition enthalpy decreases linearly with increasing L_{24} concentration over a similar range of hydrocarbon chain lengths, indicating that significant peptide clustering does not occur in the more loosely packed gel states of these phospholipids.

A closer examination of Figure 1 also shows that the width of the broad component of the DSC endotherms increases modestly with increases in peptide concentration but is almost independent of lipid hydrocarbon chain length. For example, in 12:0 PE bilayers, the width of the broad component (as measured from the starting to completion temperatures) exhibits an increase from 8°C to 10-12°C as peptide concentrations

increases from 1.7 to 6.7 mol %. Similar behavior occurs when the peptide P₂₄ is incorporated into the same PE bilayers (25). However, markedly different behavior occurs when L₂₄ is incorporated into either PC or PG bilayers (26, 27). With either L₂₄-containing PC or L₂₄-containing PG bilayers, the widths of the broad component in the DSC thermograms are always considerably larger at comparable peptide concentrations and decrease markedly with increases in lipid hydrocarbon chain length. The possible basis of these experimental observations will be explored in the Discussion.

Thermotropic Phase Behavior of PE Bilayers in the Presence of Various Peptides. To examine the effect of truncating the lysine side chains of L₂₄ or of replacing the terminal leucines with aromatic tryptophan residues on the peptide-PE interactions, we have also studied the effects of L₂₄DAP and WL₂₂W incorporation on the thermotropic phase behavior of various PE bilayers by high-sensitivity DSC. A comparison of the effects of the incorporation of various amounts of L₂₄, L₂₄DAP, and WL₂₂W on the phase behavior of 16:0 PE bilayers is shown in Figure 5. The patterns of peptide concentration-dependent changes in PE thermotropic phase behavior shown therein are typical of our observations of the interactions of these peptides with all of the other PEs examined. We will therefore present the overall effects of these peptides on the thermotropic phase behavior of 16:0 PE bilayers as a qualitative example of what occurs with all of the PE bilayers studied. As noted earlier, the DSC thermograms exhibited by the L₂₄/16:0 PE mixtures (left panel) are composed of overlapping short and broad components with the former decreasing and the latter increasing with increases in L₂₄ concentration. At the 6.7 mol% peptide, the DSC thermogram exhibited by the L₂₄/16:0 PE mixture is mainly composed of a broad component centered near 57.8 °C with only traces of the sharp component centered near

63.2 °C. The DSC thermogram exhibited by the corresponding WL₂₂W/16:0 PE mixtures (right panel) is also composed of overlapping sharp and broad components, but in this case the sharp component of the DSC endotherm predominates over the broad component, even at the highest peptide concentration tested. In contrast to L₂₄ and WL₂₂W, the incorporation of L₂₄DAP has only a small effect on the gel/liquid-crystalline phase transition of 16:0 PE bilayers and does not appear to induce clearly resolvable sharp and broad components in the DSC endotherm. At 6.7 mol% peptide concentration, the DSC thermogram exhibited by the L₂₄DAP/16:0 PE mixture is only slightly broader than that of the pure 16:0 PE. This marked difference between L₂₄DAP and L₂₄ or WL₂₂W is also observed when these peptides are incorporated into 12:0-, 14:0-, and 18:0- PE bilayers and suggests that the L₂₄DAP is not interacting strongly with the host PE bilayers.

The plot of ΔT versus the hydrocarbon chain length of the PE bilayers for L₂₄, L₂₄DAP and WL₂₂W are shown in Figure 6. Although ΔT remains negative in all of the peptide/PE mixtures studied, the magnitude of the decrease in the temperature of the broad component is largest for L₂₄, moderate for WL₂₄W and smallest for L₂₄DAP, especially in the longer chain PEs. For all the three model peptides, only a very small increase in ΔT is observed in when the hydrocarbon chain length of PE bilayers is increased from 12 to 18 carbons. This is markedly different from the results of the same three model peptides in PC and PG bilayers, in which the ΔT initially decreases significantly with an increase of the lipid hydrocarbon chain length and is strongly positive in very short chain phospholipids. It is also interesting to note that in all four hydrocarbon chain lengths studied, the ΔT values exhibited by L₂₄/PE and WL₂₂W/PE

mixtures are about 1.5°C and 1.0°C lower, respectively, than that the ΔT exhibited by L₂₄DAP/PE mixtures, again indicating weaker interactions between the latter peptide its PE t bilayer hosts.

Illustrated in Figure 7 is a comparison of the peptide concentration-dependent changes in the enthalpy of the thermotropic phase transitions observed when the peptides L₂₄, L₂₄DAP and WL₂₂W are incorporated into the various PE bilayers examined. With the shorter chain lipids 12:0 PE and 14:0 PE, incremental increases in peptide content are accompanied by a progressive decrease in the enthalpy values throughout the peptide concentration range examined. Also, the magnitude of this effect varies with the nature of the peptide and decreases in the order L₂₄>WL₂₂W> L₂₄DAP. With the longer chain PEs, the measured enthalpy values also decrease at low peptide concentrations, in a manner and magnitude comparable to what occurs with the shorter chain lipids. Unlike the shorter chain PE's, however, at higher peptide concentrations a marked increase in enthalpy values is observed. Similar behavior has been observed previously in studies of P₂₄⁻ and (LA)₁₂-containing PE membranes (25, 28) and have been ascribed to additional energy arising from increased dispersal of the peptide at temperatures below the onset of the lipid hydrocarbon phase transition. Here, we also find that the magnitude of this phenomenon is dependent on the nature of the peptide and decreases in the same order described above (i.e. L₂₄>WL₂₂W>> L₂₄DAP). We also note that across the range of PE hydrocarbon chain lengths examined, the effects of L₂₄-DAP on the enthalpy of the lipid phase transition are considerably smaller than observed with peptides L₂₄ and WL₂₂W. These results suggest either that L₂₄DAP is intrinsically less disordering to PE bilayers

than are L₂₄ and WL₂₂W, or that that PE-L₂₄DAP interactions are being minimized by a low miscibility of L₂₄DAP in PE bilayers.

A comparison of the effects of L₂₄, L₂₄DAP, and WL₂₂W on the transition widths of PE bilayers was shown in Figure 8. The transition widths were measured from the starting temperature to the ending temperature of the broad component of the DSC endotherms at 3.3 mol % peptide concentration. For all three model peptides, there is only slight change in the transition widths of the broad component of the peptide/PE mixtures when the acyl chain length of PE bilayers is increased from 12 to 18 carbons. Moreover, in all four PEs examined, the transition widths of the broad component of L₂₄DAP/PE mixtures (about 5.2 °C) is much smaller than that of L₂₄/PE mixtures and WL₂₂W/PE mixtures (about 9.2 and 8.4 °C, respectively). These results again show that the incorporation of L₂₄ or WL₂₂W have much larger effects on the organization of PE bilayers than does the incorporation of L₂₄DAP.

Fourier Transform Infrared Spectroscopic Studies of Peptide-containing PE bilayers. In these studies, infrared spectra of mixtures of the peptide with each of the four PEs studied were recorded as a function of temperature and as a function of the mole fraction of the peptide. The use of FTIR spectroscopy permits a noninvasive monitoring of both the structural organization of the lipid bilayer and the conformation of the incorporated peptide (for a more detailed description of this application of IR spectroscopy, see references 38, 39, 40 and references cited therein). Here, changes in the degree of hydrocarbon chain rotational isomeric disorder coincident with the lipid gel/liquid-crystalline phase transition was monitored by an examination of the methylene symmetric stretching band near 2850 cm⁻¹, and the conformational stability of the embedded peptide

was monitored by an examination of the contours of the amide-I band centered near 1650 cm^{-1} . Our preliminary studies showed that the incorporation of these peptides into PE bilayers had no discernable effect on the ester carbonyl stretching band near 1735 cm^{-1} , nor on the O-P-O asymmetrical stretching bands near 1230 cm^{-1} , suggesting that the peptide incorporation at the levels studied here (~ 3.3 mol%) did not have a major effect on the hydration of either the phosphate polar headgroups or the polar/apolar interfacial regions of these lipid bilayers.

Illustrated in Figure 9 are the amide I and C=O stretching regions of the FTIR spectra exhibited by mixtures of L_{24} with the four PEs examined here. The spectra shown were acquired at temperatures where the host lipids are in their gel (L_{β}) and liquid-crystalline (L_{α}) phases. Under all conditions examined, the amide I absorption band of L_{24} is dominated by sharp absorption components centered near 1655-1657 cm^{-1} and near 1647-1650 cm^{-1} . These absorption bands can be ascribed to the amide I vibrations of unexchanged- and deuterium-exchanged α -helical peptide domains (41, 42) and their prominence is therefore consistent with L_{24} maintaining a predominantly α -helical conformation under all conditions examined. However, Figure 9 also shows that the gel to liquid-crystalline phase transition of the host PE bilayer is accompanied by a small downward shift in the frequency of the absorption maximum of the amide-I band envelope. This frequency shift is minimal (< 2 cm^{-1}) with L_{24} -containing 12:0 PE mixtures but increases with increases in lipid hydrocarbon chain length and approaches values near 5-6 cm^{-1} with 18:0 PE-based mixtures. A similar pattern of behavior has been reported in our studies of mixtures of L_{24} with PC and PG bilayers (26, 27 and in studies of the interaction of the peptides P_{24} and $(LA)_{12}$ with PC and PE bilayers (19, 25, 28, 43).

A comparison of the lipid phase state-induced changes in the amide I band maxima observed with mixtures of peptides L₂₄, L₂₄DAP and WL₂₂W with 16:0 PE is shown in Figure 10. These peptides all exhibit a similar pattern of incremental hydrocarbon chain length-dependent decreases in amide I band maxima which is qualitatively similar to that described for L₂₄ above. However, as is evident from Figure 10, the magnitude of this effect is markedly smaller with the peptide L₂₄DAP, for which the maximal chain length-dependent frequency shifts observed never exceeds 2 cm⁻¹, suggesting that interactions between L₂₄DAP and all of these PE bilayers are weaker than is the case with the other two peptides. Interestingly, our studies of the interactions of these same peptides with PC and PG bilayers (26, 27) also show a similar pattern in which lipid phase state-induced decreases in the amide I band maxima of L₂₄DAP are smaller than occur with L₂₄ and WL₂₂W although in those cases this affect is smaller in magnitude than observed here with PE bilayers. The molecular basis of these experimental observations are explored in the Discussion below.

Discussion

In this study we have shown that interactions of model peptides that mimic the hydrophobic transmembrane α -helical segments of integral membrane proteins with zwitterionic PE bilayers are quite different from their interactions with zwitterionic PC or anionic PG bilayers. Specifically, we demonstrate that all three model peptides reduce the T_ms of PE bilayers to a grater extent than occurs with PC and PG bilayers and that the peptide-induced reduction of the T_ms of these PE bilayers is largely independent of the lipid bilayer thickness. The latter observations contrast sharply from those reported in our previous work, in which magnitude of the peptide-induced reduction in the T_ms of PC and

PG bilayers was shown to be dependent on the thickness of the lipid bilayer (26, 27). Evidently the nature and strength of the interactions of the somewhat polar and charged amino acid residues at the ends of these model peptides with the polar headgroups of zwitterionic PE and anionic PG or zwitterionic PC bilayers are quite different.

In considering the possible molecular basis of our experimental observations, it is instructive to compare the effects of L_{24} and the closely related peptide P_{24} on the T_m s of zwitterionic PE bilayers with that of zwitterionic PC and anionic PG bilayers. Previous studies reveal that L_{24} and P_{24} affect the T_m of PC bilayers in a manner dependent on the hydrophobic mismatch between the peptides and the lipid bilayers, that is, when the mean hydrophobic thickness of the PC bilayer is less than the peptide hydrophobic length, the peptide-associated lipid melts at higher temperatures than does the peptide-poor lipid and *vice versa* (19, 26). Similarly, L_{24} affects the T_m of PG bilayers in a manner dependent on the hydrophobic mismatch between the peptides and the lipid bilayers, albeit the T_m of PG bilayers is reduced to a greater extent than that of PC bilayers. In contrast, this study and our previous study of P_{24} show that the incorporation of these peptides into PE bilayers results in a progressive and more significant reduction in T_m in a manner independent of the hydrocarbon mismatch between the lipids and peptides. In particular, at 3.3 mol % L_{24} concentration, the ΔT remains at about -2°C from 12:0 PE to 18:0 PE. The fact that model peptides have different effects on the phase behaviors of PC, PG, and PE bilayers with comparable chain length indicates that the peptide-lipid interactions are determined by forces other than the hydrophobic mismatch between the peptides and the lipid bilayers. We therefore suggest that these model peptides have different effects on

the electrostatic and H-bonding interactions in the polar headgroup regions of PC, PG, and PE bilayers.

It is well established that the T_{ms} of saturated PCs are comparable to those of saturated PG bilayers, and that they can be some 20-30 °C lower than those of saturated PE bilayers of comparable hydrocarbon chain length (see 44, 45 and references cited therein). Such observations can be rationalized on the basis of stronger electrostatic and H-bonding interactions between the polar headgroups at the surfaces of PE bilayers (see 46, 47, 48 and references cited therein). Under physiologically relevant conditions, PE amino groups are fully protonated and, being positively charged, they are capable of both electrostatic interactions with charged groups and H-bonding interactions with H-bonding acceptor groups. Thus, the intermolecular forces which constitute the basis of the relatively high transition temperatures of PEs are, in effect, a summation of contributions arising from electrostatic attraction between positively charged amino groups and negatively charged phosphate moieties, electrostatic repulsion arising from both amino-amino and phosphate-phosphate contacts, as well as H-bonding interactions between the headgroup amino protons and H-bonding acceptor groups in the headgroup and polar/apolar interfacial regions of the lipid bilayer. With anionic PG bilayers, their relatively low transition temperatures are probably largely attributable to electrostatic repulsion between the negatively-charged headgroup phosphate moieties, though this effect will be partially mitigated by H-bonding interactions between the exchangeable protons of the headgroup glycerol moiety and H-bonding acceptor groups in the headgroup a polar/apolar interfacial regions of the lipid bilayer. Finally, with PC bilayers, there are no H-bonding donor groups on their polar headgroups and as a result

electrostatic attraction between positively charged choline groups and negatively charged phosphate moieties, and electrostatic repulsion arising from both choline-choline and phosphate-phosphate contacts will predominate. However, the steric bulk of the N-methyl groups will markedly reduce the frequency of close contacts interactions between the positively charged choline nitrogen and the negatively charged phosphate groups and as a result the electrostatic attraction component will be markedly attenuated in magnitude. Thus, despite the zwitterionic character of PC polar headgroups, electrostatic repulsion between phosphate moieties at the surfaces of PC bilayers may well have as big an effect on bilayer T_m as occurs with PG bilayers. Largely because of these effects, the forces favoring the gel phase over liquid-crystalline phases are expected to decrease in the order $PE \gg PG \sim PC$, and the incorporation of peptides such as L_{24} into PE, PC and PG bilayers may be expected to affect interactions between lipid headgroups in two main ways. First, the presence of these peptides will reduce the access of adjacent phospholipid molecules to potential hydrogen-bonding partners, thus leading to the disruption of part of the hydrogen-bonding networks of PG and PE bilayers. Second, the positively-charged side-chain amino groups at the N- and C- termini of these peptides will compete with positively charged and H-bonding donor groups on adjacent lipid polar headgroups for electrostatic and/or H-bonding acceptor sites, thereby disrupting the pattern of lipid-lipid interactions at the surface of these bilayers. As noted above, the electrostatic and H-bonding network at the surface of a PE bilayer is quite strong and is largely responsible for the relatively high transition temperature. Consequently, any significant peptide-induced disruption of the surface electrostatic and H-bonding network of a PE bilayer will have a considerably greater effect on its T_m than will to occur with PC and PG

bilayers, where the corresponding surface networks are considerably weaker. Moreover, given the magnitude of the changes in T_m that are likely to occur upon disruption of the electrostatic and H-bonding network at the surface of a PE bilayer, such changes may well mask the additional changes arising from hydrophobic mismatch effects, which are thus expected to be more modest in magnitude.

A major finding of this study is that the replacement of lysine by DAP residues at the ends of the model peptides markedly affects their interactions with zwitterionic PE bilayers. Specifically, our studies show that L_{24} DAP is much less effective than L_{24} at reducing the T_m and enthalpy and broadening the phase transition of PE bilayers and, regardless of the criteria used, L_{24} DAP has much weaker effects on the overall phase behavior of PE bilayers than does L_{24} . These results suggest that the capacity of L_{24} DAP to disrupt lipid-lipid interactions in PE bilayers may be intrinsically weaker than that of L_{24} or that it may be more prone to clustering in PE bilayers than L_{24} , or both. Our experimental observations can be directly attributed to effects arising from the different lengths of the methylene spacers between the α -carbons and side-chain amino groups of DAP (one CH_2 spacer) and lysine (four CH_2 groups). This is because lysine residues have side-chains that are long enough to extend beyond that of the leucine residues which cover the helical surfaces of these peptides. Thus, when lysine-capped peptides such as L_{24} are incorporated into lipid bilayers, their lysine side-chains can extend away from their helical surfaces and the side-chain amino groups can thus compete effectively with positively charged and H-bonding donor groups on adjacent lipids for electrostatic and/or H-bonding acceptor sites. Also, because the spacer arms on their lysine side-chains can extend beyond that of the leucine residues of the peptide, lateral contacts between L_{24}

molecules in lipid bilayers (i.e. clustering) can result in intermolecular contacts between the positively side-chain amino groups at the peptide termini and, in turn, charge repulsion between these side-chain amino groups will reduce the probability of forming peptide clusters in lipid bilayers. The above contrasts sharply from what is likely to occur with peptides such as L₂₄DAP, where the DAP side chains do not extend beyond that of the leucine residues on the peptide surface. When such peptides are incorporated into lipid bilayers, the side chain amino groups cannot compete with positively charged and H-bonding donor groups on adjacent lipids for electrostatic and/or H-bonding acceptor sites as effectively as can those of L₂₄. Moreover, because the DAP side chains are so short, lateral contacts between L₂₄DAP molecules in a lipid bilayer will not result in the type of intermolecular close contacts between the positively side-chain amino groups at the peptide termini which are likely to occur with a lysine-capped peptide like L₂₄. Consequently, the energetic cost of peptide clustering in L₂₄DAP-containing lipid bilayers will be smaller than that of comparable L₂₄-containing lipid bilayers. We therefore suggest that, in general, L₂₄DAP will not be as perturbing of lipid thermotropic phase behavior as L₂₄ because of a combination of its smaller capacity to disrupt the electrostatic and H-bonding network at the lipid bilayer surfaces, and the smaller energetic penalties against its clustering in lipid bilayers. Moreover, the combined effects of these two parameters may be even more critical to the differential effects of L₂₄ and L₂₄DAP on PE bilayers, because the electrostatic and H-bonding networks at the surfaces of PE bilayers are quite strong and are thus more likely to favor PE-PE interactions over PE-peptide interactions, unless peptide inclusion induces a significant disruption of this network. Thus L₂₄DAP should be inherently less perturbing of PE bilayers than L₂₄.

Moreover, because of the smaller energetic penalties against clustering of L₂₄DAP in lipid bilayers, the effects of L₂₄DAP may be further attenuated by the formation of peptide clusters especially in PE membranes where lipid-lipid interactions tend to be preferred over lipid-peptide interactions. Interestingly, although previous studies have shown that L₂₄ is only slightly more perturbing to gel-state bilayers than is L₂₄DAP (26), there was no evidence for major differences between L₂₄ and L₂₄DAP as regards their effects on the thermotropic phase behavior of either PC or PG bilayers (26, 27). Most probably this is because the electrostatic and H-bonding networks at the surfaces of PC and PG bilayers are considerably weaker than in PE bilayers and the differential effects of lysine and DAP in modulating these forces are not so obvious as in PE bilayers. Nevertheless, these results do highlight the potential importance of lysine snorkeling in the interactions of these model peptides with PE bilayers.

Our studies also show that the effect of WL₂₂W on the thermotropic phase behavior of PE bilayers is somewhat weaker than that of L₂₄. Given the arguments raised above (see previous paragraph), it does appear that the replacement of a leucine residue at each end of the hydrophobic core of L₂₄ by tryptophan residues attenuates the capacity of the terminal lysine residues to interact with or otherwise perturb the electrostatic and H-bonding network at the surfaces of PE bilayers. This could be an indication that the tryptophan residues are forming cation- π interactions with adjacent lysine residues, as suggested in our previous studies of the interaction of WL₂₂W with anionic PG bilayers (27). Indeed, if these cation- π interactions do occur between lysine and tryptophan residues, then the lysine residues may not be able to compete as effectively as those of L₂₄ for positively charged and H-bonding donor groups on adjacent lipids for electrostatic

and/or H-bonding acceptor sites. However, despite its having a weaker effect on the thermotropic phase behavior of PE bilayers than L_{24} , it is clear that the effects of both peptides are of comparable magnitude and are both much greater than that of L_{24} DAP. Thus, the effect of the cation- π interactions between lysine and tryptophan residues is considerably less effective than the lysine snorkeling effect in regulating lipid-peptide interactions in lipid bilayers.

In these studies we also observe small decreases in the frequency of peptide amide I band maxima at the gel/liquid-crystalline phase transitions of their lipid bilayer hosts, and that the magnitude of these frequency shifts decrease with increases in lipid hydrocarbon chain length. Similar results have been reported in studies of these peptides with PC and PG bilayers (26, 27) and in studies of the interaction of P_{24} with PC and PE bilayers (19, 25). As noted previously, these changes seem to arise from a lipid phase state-induced decline in populations giving rise to amide I absorption centered near 1660-1665 cm^{-1} and a concomitant increase in populations giving rise to amide I absorptions centered near 1645-1650 cm^{-1} , and have been assigned to conformational changes in the deuterium-exchanged N- and C-termini of these peptides (26). However, we also find that these lipid phase state-induced decreases in peptide amide I band maxima are consistently smaller in L_{24} DAP-containing PE membranes than observed with the either L_{24} -containing or $WL_{22}W$ -containing membranes. These observations are consistent with the idea that interactions of L_{24} DAP with PE bilayers are weaker than those of the peptides L_{24} and $WL_{22}W$. Moreover, they also suggest that unlike L_{24} - and $WL_{22}W$ -containing PE membranes, lipid phase transitions in L_{24} DAP-containing PE-containing membranes have relatively little effect on the conformation of the guest peptide. Given that the energetic

barriers against peptide clustering in L₂₄DAP-containing are probably weaker than those of the corresponding L₂₄- and WL₂₂W-containing lipid membranes (see above), these relative insensitivity of L₂₄DAP to the gel/liquid phase transitions of its PE host membrane may be indicative of significant clustering of L₂₄DAP in these PE bilayers.

In conclusion, our current studies highlight the importance of the H-bond interactions and electrostatic attractions between the lipid polar headgroups and the terminal lysine and/or tryptophan residues in peptide-lipid interactions. Our studies also indicate an important role of terminal lysine snorkeling in the interactions of these model peptides with zwitterionic PE bilayers and greatly extend our understanding of the role of interfacially localized lysine residues in natural membrane proteins. Further structural and computer modeling investigations may help to elucidate the detailed mechanism of how the terminal lysine and/or tryptophan residues may interact with adjacent lipid headgroups at the membrane polar/apolar interface.

References

1. Yeagle, P.L. (1993) *The Membranes of Cells*, Academic Press, pp 166-201, San Diego
2. Daum, G. (1985) Lipids of mitochondria, *Biochim. Biophys. Acta.* 822,1-42.
3. Devaux, P.F., and Seigneuret, M. (1985) Specificity of lipid-protein interaction as determined by spectroscopic techniques, *Biochim. Biophys. Acta.* 822,63-125.
4. Verkleij, A.J., Zwaal, R.F., Roelofsen, B., Comfurius, P., Kastelijn, D., and van Deenen, L.L. (1973) The asymmetric distribution of phospholipids in the human red cell membrane, *Biochim. Biophys. Acta.* 323,178-193.
5. Kleinschmidt, J.H. (2003) Membrane proteins—introduction, *Cell.Mol.Life Sci.*60, 1527-1528.
6. Bogdanov, M., and Dowhan, W. (1998) Phospholipid-assisted protein folding: phosphatidyl-ethanolamine is required at a late step of the conformational maturation of the polytopic membrane protein lactose permease, *EMBO J.* 17, 5255–5264.
7. Zhang, W., Bogdanov, M., Pi, J., Pittard, A.J., and Dowhan, W. (2003) Reversible topological organization within a polytopic membrane protein is governed by a change in membrane phospholipid composition, *J. Biol. Chem.* 278: 50128-50135
8. Svensson-Ek, M., Abramson, J., Larsson, G., Törnroth, S., Brzezinski, P., and Iwata, S. (2002) The X-ray crystal structures of wild-type and EQ(I-286) mutant cytochrome *c* oxidases from *Rhodobacter sphaeroides*, *J.Mol.Biol.* 257, 3032-3038.

9. Jones, M.R., Fyfe, P.K., Roszak, A.W., Isaacs, N.W., and Cogdell, R. J. (2002) Protein-lipid interactions in the purple bacterial reaction center, *Biochim Biophys. Acta* 1565, 206-214.
10. Pomorski T, Lombardi R, Riezman H, Devaux PF, van Meer G, and Holthuis, J.C.M. (2003) Drs2p-related P-type ATPases Dnf1p and Dnf2p are required for phospholipid translocation across the yeast plasma membrane and serve a role in endocytosis, *Mol.Biol.Cell* 14, 1240-1254.
11. http://blanco.biomol.uci.edu/Membrane_Proteins_xtal.html.
12. Gennis, R.B. (1989) Membrane dynamics and protein-lipid interactions, in *Biomembranes: Molecular Structure and Function*, Springer-Verlag, pp 166-198, New York.
13. Selinsky, B.S. (1992) Protein-lipid interactions and membrane function, in *The Structure of Biological Membranes* (Yeagle, P), pp 603-651, CRC Press, Boca Raton.
14. Marsh, D., and Horváth, L.I. (1998) Structure, dynamics and composition of the lipid-protein interface. Perspectives from spin-labelling, *Biochim. Biophys. Acta.* 1376, 267-296.
15. Davis, J.H., Clare, D.M., Hodges, R.S., and Bloom, M. (1983) Interaction of a synthetic amphiphilic polypeptide and lipids in a bilayer structure, *Biochemistry* 22, 5298-5305.
16. de Planque, M.R.R., and Killian, J.A. (2003) Protein-lipid interactions studied with designed transmembrane peptides: role of hydrophobic matching and interfacial anchoring, *Mol.Mem.Biol.* 20, 271-284.

17. Ren, J., Lew, S., Wang, Z., and London, E. (1997) Transmembrane orientation of hydrophobic α -helices is regulated both by the relationship of helix length to bilayer thickness and by the cholesterol concentration, *Biochemistry* 36, 10213-10220.
18. Zhang, Y.-P., Lewis, R.N.A.H., Hodges, R.S., and McElhaney, R.N. (1992) FTIR spectroscopic studies of the conformation and amide hydrogen exchange of a peptide model of the hydrophobic transmembrane α -helices of membrane proteins, *Biochemistry* 31, 11572-11578.
19. Zhang, Y.-P., Lewis, R.N.A.H., Hodges, R.S., and McElhaney, R.N. (1992) Interaction of a peptide model of a hydrophobic transmembrane α -helical segment of a membrane protein with phosphatidylcholine bilayers: differential scanning calorimetric and FTIR spectroscopic studies, *Biochemistry* 31, 11579-11588.
20. Axelsen, P.H., Kaufman, P.H., McElhaney, R.N., and Lewis, R.N.A.H. (1995) The infrared dichroism of transmembrane helical polypeptides, *Biophys. J.* 69, 2770-2781.
21. Huschilt, J.C., Millman, B.M., and Davis, J.H. (1989) Orientation of alpha-helical peptides in a lipid bilayer, *Biochim Biophys. Acta.* 979, 139-141.
22. Bolen, E.J., and Holloway, P.W. (1990) Quenching of tryptophan fluorescence by brominated phospholipid, *Biochemistry* 29, 9638-9643.
23. Huschilt, J.C., Hodges, R.S., and Davis, J.H. (1985) Phase equilibria in an amphiphilic peptide-phospholipid model membrane by deuterium nuclear magnetic resonance difference spectroscopy, *Biochemistry* 24, 1377-1386.

24. Morrow, M.R., Huschilt, J.C., and Davis, J.H. (1985) Simultaneous modeling of phase and calorimetric behavior in an amphiphilic peptide/phospholipid model membrane, *Biochemistry* 24, 5396-5406.
25. Zhang, Y.-P., Lewis, R.N.A.H., Hodges, R.S., and McElhaney, R.N. (1995) Interaction of a peptide model of a hydrophobic transmembrane α -helical segment of a membrane protein with phosphatidylethanolamine bilayers: differential scanning calorimetric and FTIR spectroscopic studies, *Biophys. J.* 68, 847-857.
26. Liu, F., Lewis, R.N.A.H., Hodges, R.S., and McElhaney, R.N. (2002). Effect of variations in the structure of a poly-leucine-based α -helical transmembrane peptide on its interaction with phosphatidylcholine bilayers, *Biochemistry* 41, 9197-9207.
27. Liu, F., Lewis, R.N.A.H., Hodges, R.S., and McElhaney, R.N. (2004). Effect of variations in the structure of a poly-leucine-based α -helical transmembrane peptide on its interaction with phosphatidylglycerol bilayers, *Biochemistry* 43, 3679-3687.
28. Zhang, Y-P., Lewis, R.N.A.H., Hodges, R.S., and McElhaney, R.N. (2001) Peptide models of the helical hydrophobic transmembrane segments of membrane proteins: Interactions of acetyl-K₂-(LA)₁₂-K₂-amide with phosphatidylethanolamine bilayer membranes, *Biochemistry* 40, 474-482 .
29. Pauls, K.P., MacKay, A.L., Soderman, O., Bloom, M., Taneja, A.K., and Hodges, R.S. (1985) Dynamic properties of the backbone of an integral membrane polypeptide measured by ²H-NMR, *Euro. Biophys. J.* 12, 1-11.
30. Subczynski, W.K., Lewis, R.N.A.H., McElhaney, R.N., Hodges, R.S., Hyde, J.S., and Kusumi, A. (1998) Molecular organization and dynamics of 1-palmitoyl-2-oleoyl-

- phosphatidylcholine bilayers containing a transmembrane α -helical peptide, *Biochemistry* 37, 3156-3164.
31. Subczynski, W.K., Pasenkiewicz-Gierula, McElhaney, R.N, Hyde, J.S., and Kusumi, A. (2003) Molecular organization and dynamics of 1-palmitoyl-2-oleoyl phosphatidylcholine bilayer membranes containing a transmembrane α -helical peptide with hydrophobic surface roughness, *Biochemistry* 42, 3939-3948.
32. Killian, J. A. and von Heijne., G (2000) How proteins adapt to a membrane-water interface, *TIBS* 25, 429-434.
33. Segrest, J.P., De Loof, H., Dohlman, J.G., Brouillette, C.G., and Anantharamaiah, G.M. (1990) Amphipathic helix motif: classes and properties, *Proteins: Struct. Funct. Genet.* 8, 103-117.
34. Monne, M., Nilsson, I., Johansson, M., Elmhed, N., and van Heijne, G. (1998) Positively and negatively charged residues have different effects on the position in the membrane of a model transmembrane helix, *J. Mol. Biol.* 284, 1177-1183.
35. von Heijne, G. (1994) Membrane proteins: from sequence to structure, *Annu.Rev.Biophys.Biomol.Struct.* 23, 167-192.
36. Mantsch, H.H., Madec, C., Lewis, R.N.A.H., and McElhaney, R.N. (1985) The thermotropic phase behavior of model membranes composed of phosphatidylcholines containing isobranched fatty acids. II. Infrared and ^{31}P -NMR spectroscopic studies, *Biochemistry* 24, 2440-2446.

37. Lewis, R.N.A.H., and McElhaney, R.N. (1993) Calorimetric and spectroscopic studies of the polymorphic phase behavior of a homologous series of *n*-saturated, 1,2-diacyl phosphatidyl-ethanolamines, *Biophys. J.* 64,1081-1096.
38. Tamm, L. K., and Tatulian, S. A. (1997) Infrared spectroscopy of proteins and peptides in lipid bilayers, *Quart. Rev. Biophys.* 30,365-429.
39. Lewis, R. N. A. H., and McElhaney, R. N (1996). FTIR spectroscopy in the study of hydrated lipids and lipid bilayer membranes, in *Infrared Spectroscopy of Biomolecules* (Mantsch, H. H. & Chapman, D ,eds), pp 159-202, John Wiley & Sons, New York.
40. Lewis, R. N. A. H., and McElhaney, R. N (2002) Vibrational spectroscopy of lipids. in *The Handbook of Vibrational Spectroscopy* (J.M. Chalmers and P.R. Griffiths, Eds), Volume 5, pp. 3447- 3464, John Wiley & Sons, New York.
41. Chirgadze, Y.N., and Brazhnikov, E.V (1974) Intensities and other spectral parameters of infrared amide bands of polypeptides in alpha helical form, *Biopolymers* 13,1701-1712.
42. Rabolt, J.F., Moore, W. H., and Krimm, S. (1977) Vibrational analysis of peptides, polypeptides and proteins. 3. Alpha-poly(L-alaninr), *Macromolecules* 10,1065-1074.
43. Zhang, Y-P., Lewis, R. N. A. H., Hodges, R. S., and McElhaney, R. N. (1995) Peptide models of hydrophobic transmembrane segments of membrane proteins. 2. Differential scanning calorimetric and FTIR spectroscopic studies of the interaction of Ac-K₂-(LA)₁₂-K₂-amide with phosphatidylcholine bilayers, *Biochemistry* 34, 2362-2371.

44. Lewis, R. N. A. H., Mak, N., and McElhaney, R. N. (1987) A differential scanning calorimetric study of the thermotropic phase behavior of model membranes composed of phosphatidylcholines containing linear saturated acyl chains, *Biochemistry* 26, 6118-6126.
45. Zhang, Y-P., Lewis, R. N. A. H., and McElhaney, R. N. (1997) Calorimetric and spectroscopic studies of the thermotropic phase behavior of the *n*-saturated 1,2-diacylphosphatidylglycerols, *Biophys. J.* 72, 779-793.
46. Boggs, J. M. (1980) Intermolecular hydrogen bonding between lipids: influence on organization and function of lipids in membranes, *Canad. J. Biochem.* 58, 755-770.
47. Boggs, J. M. (1986) Effect of lipid structural modifications on their intermolecular hydrogen bonding interactions and membrane function, *Biochem. Cell Biol.* 64, 50-67.
48. Boggs, J. M. (1987) Lipid intermolecular hydrogen bonding: influence on structural organization and membrane function, *Biochim. Biophys. Acta* 906, 353-404.

Table 1

Table 1: Hydrophobic Thicknesses of the Bilayer Formed by Various Phosphatidylethanolamines

PE	Hydrophobic thickness (Å) ^a		Mean ^b
	Gel phase	Liquid-crystalline phase	
12:0	29.3	19.7	24.5
14:0	34.2	22.8	28.5
16:0	39.5	26.3	32.9
18:0	44.7	29.8	37.3

^aHydrophobic thicknesses were estimated using the equations used by Sperotto and Mouritsen (1988) to calculate the hydrophobic thicknesses of PC bilayers.

^bMean of the hydrophobic thicknesses of the gel and liquid-crystalline phases.

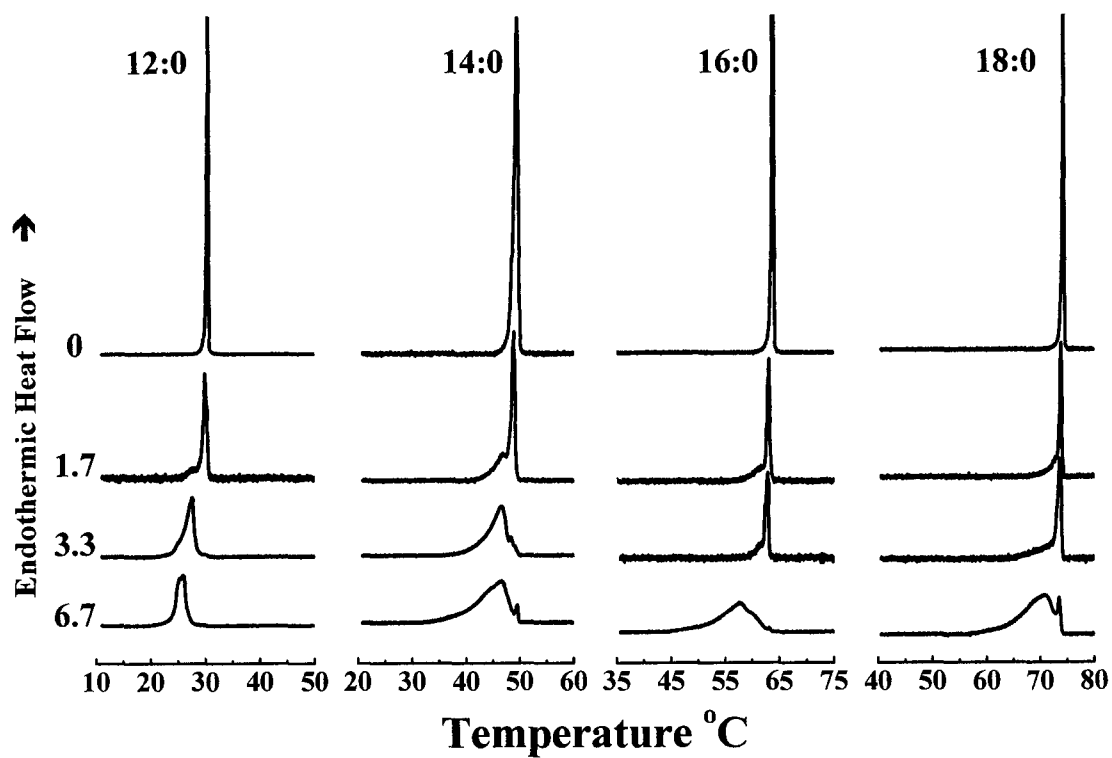


FIGURE 1. Effect of L₂₄ on the DSC thermograms of a series of *n*-saturated diacyl-PEs. Thermograms are shown as a function of the acyl chain length (*N*:0) of the lipids, at the peptide concentrations (mole percent) indicated.

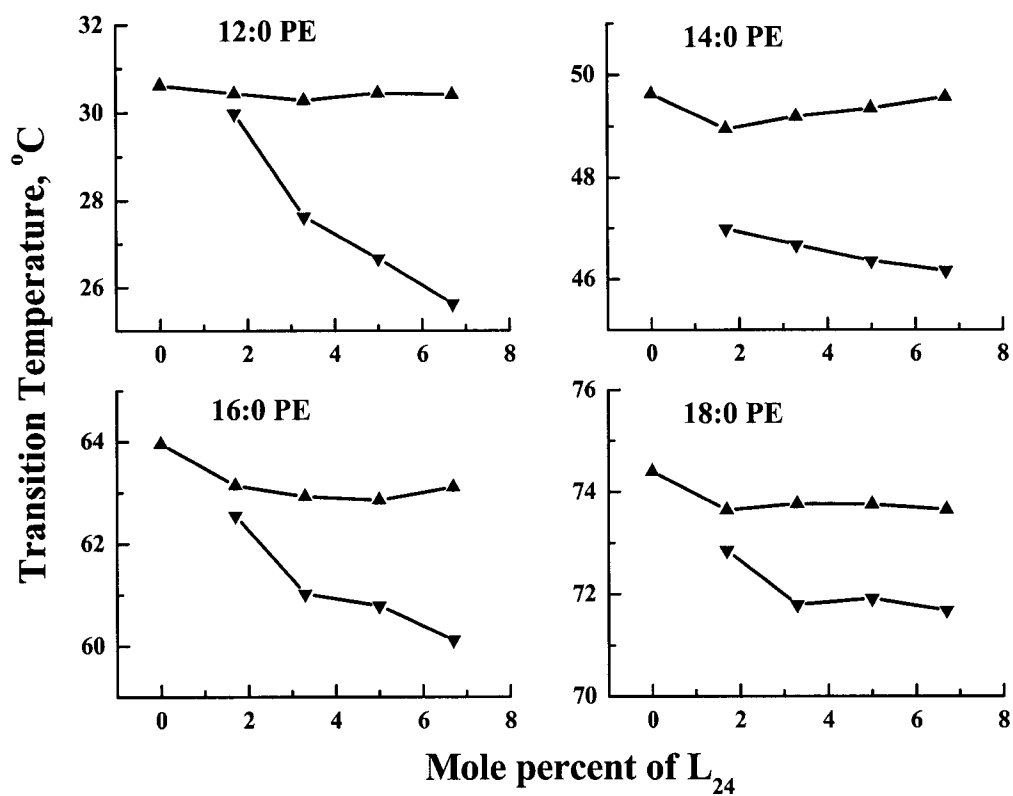


FIGURE 2. Effect of L₂₄ concentration on the peak temperatures of the two components of the DSC thermograms exhibited by the mixtures of L₂₄ and the *n*-saturated diacyl-PEs. Data are presented for the sharp (▲) and broad (▼) components of the DSC endotherms.

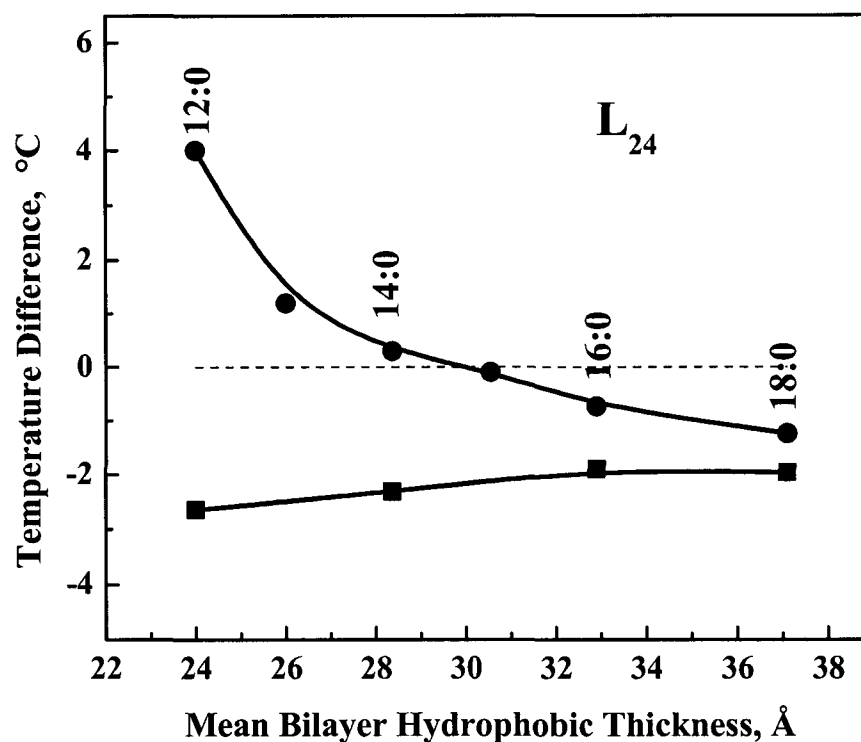


FIGURE 3. Hydrocarbon chain length dependence of the differences (ΔT) between the transition temperatures of the peptide-rich and the peptide-poor PE components of DSC thermograms exhibited by L_{24} /PE mixtures at a peptide concentration of 3.3 mol% (■). To facilitate comparison, comparable data obtained from studies of L_{24} with PC bilayers (●) are also shown.

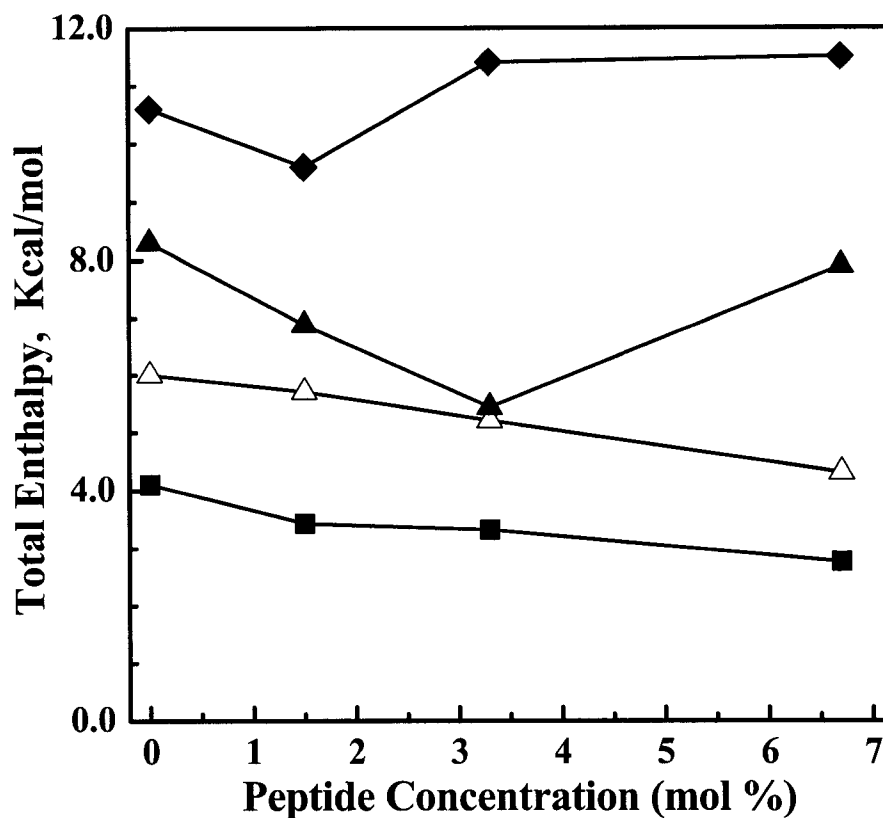


FIGURE 4. Peptide-concentration dependent changes in the enthalpy of the thermotropic transitions exhibited by L_{24} -containing PE bilayers. The data presented represents the total enthalpy change measured for mixtures of L_{24} with 12:0PE (—■—), 14:0 PE (—△—), 16:0 PE (—▲—) and 18:0 PE (—◆—).

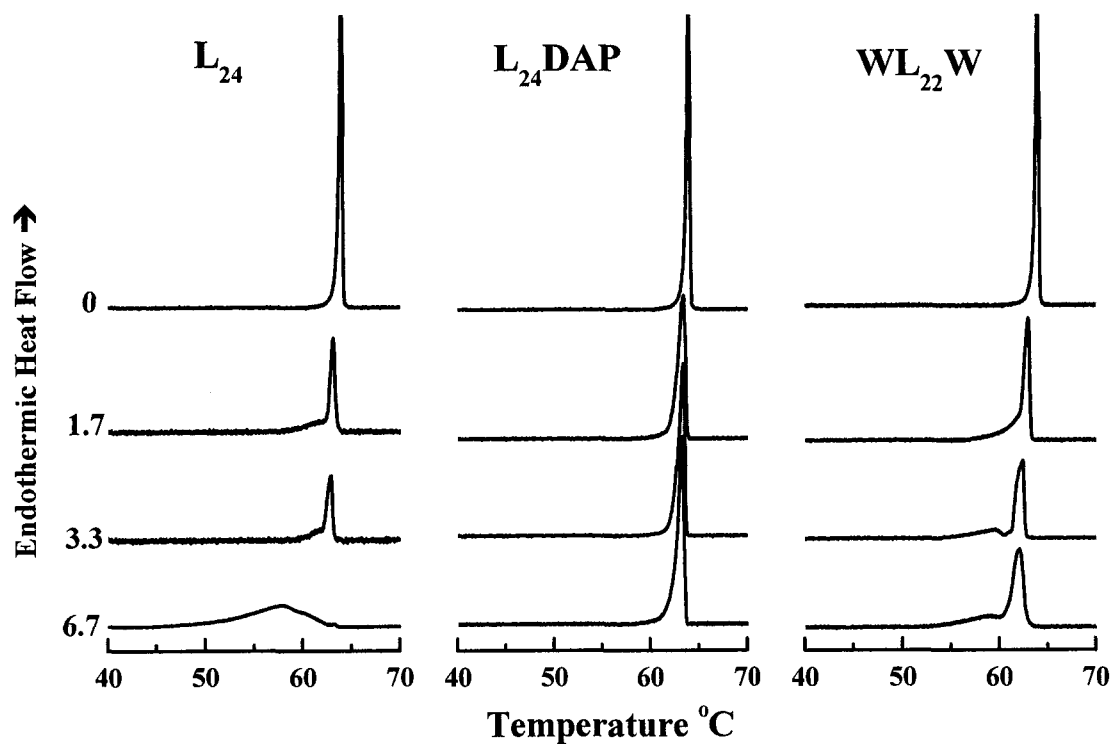


FIGURE 5. A comparison of the effects of L_{24} , $L_{24}DAP$ and $WL_{22}W$ on the DSC thermograms of 16:0 PE. The thermograms shown were obtained at the peptide concentrations (mole percent) indicated.

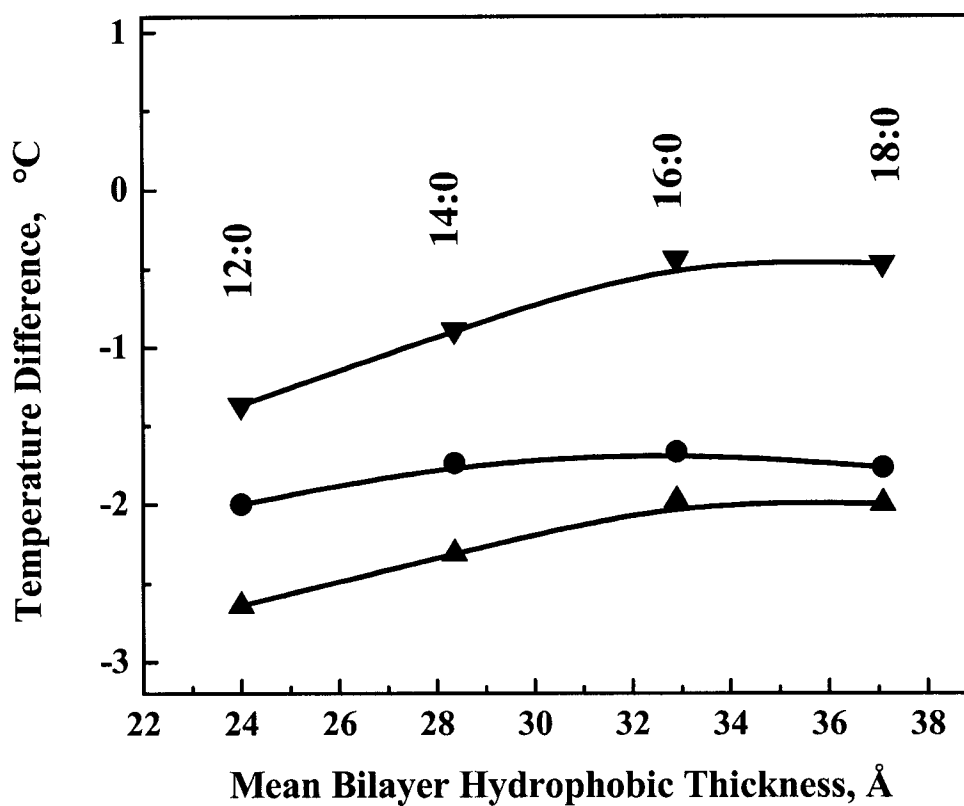


FIGURE 6. Hydrocarbon chain length dependence of the differences (ΔT) between the transition temperatures of the peptide-rich and the peptide-poor PE components of DSC thermograms exhibited by Peptide/PE mixtures at a peptide concentration of 3.3 mol%. Data are presented for mixtures of PE with L₂₄ (▲), WL₂₂W (●), and L₂₄DAP (▼).

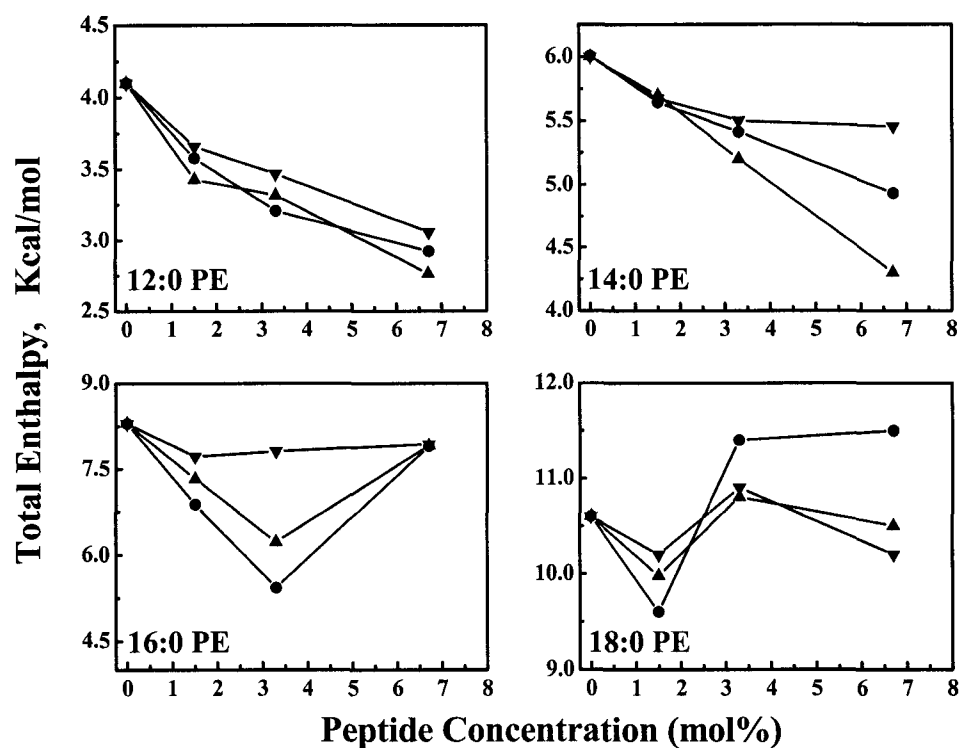


FIGURE 7. Effects of L₂₄ (▲), WL₂₂W (●), and L₂₄DAP (▼) concentration on the total transition enthalpies of 12:0, 14:0, 16:0, and 18:0 PE bilayers.

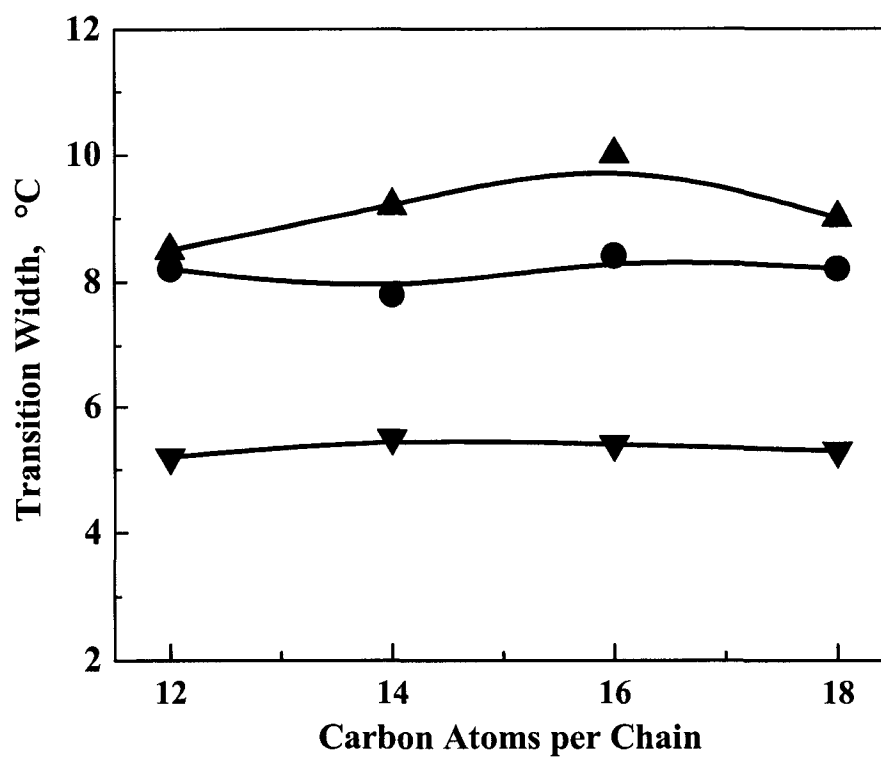


FIGURE 8 Plot of the transition width versus the hydrophobic chain length of the lipid bilayer at a peptide concentration of 3.3 mol%. Data are presented for mixtures of PE with L₂₄ (▲), WL₂₂W (●), and L₂₄DAP (▼).

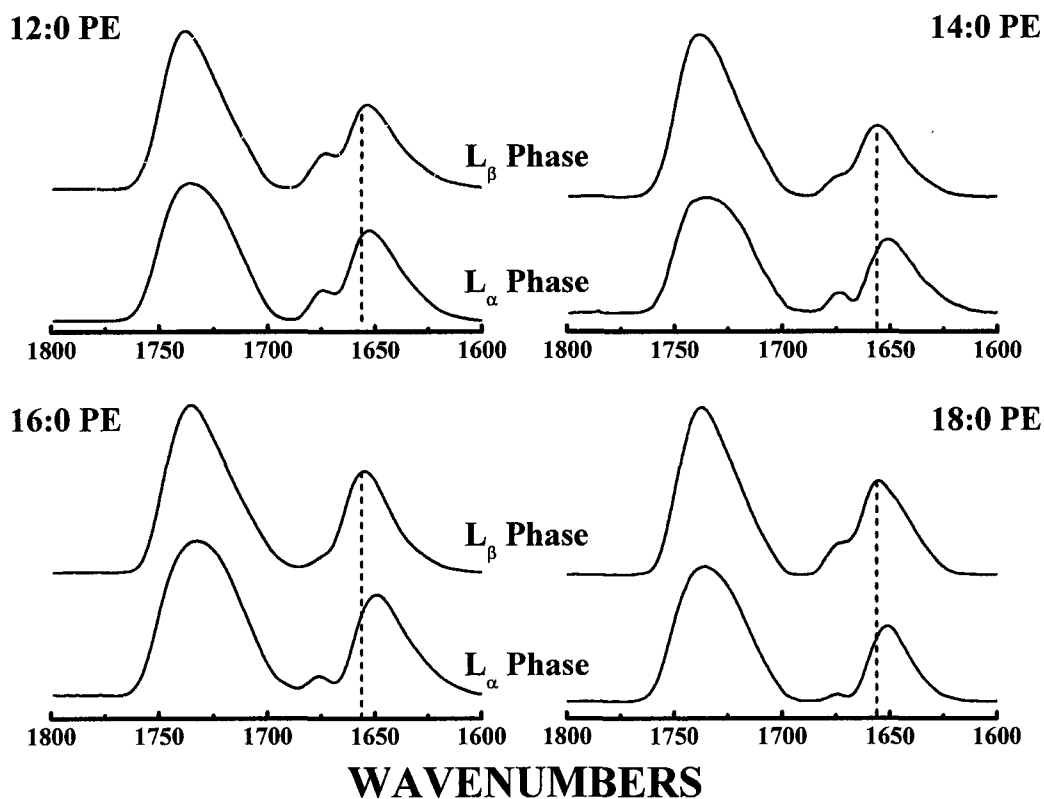


FIGURE 9. The C=O stretching and amide-I bands of the FTIR spectra exhibited by L_{24} -containing PE bilayers. The absorbance spectra shown were acquired with mixtures containing 3.3 mol% L_{24} under conditions where the lipid bilayer hosts are in the gel (L_{β} -phase) and liquid-crystalline (L_{α} -phase) states. The dashed lines mark the absorption maxima (1656 cm^{-1}) of the amide I absorption bands arising from fully proteated α -helical peptide domains. The small absorption bands centered near 1670 cm^{-1} arise from small amounts of trifluoroacetate counterions which were not completely removed during sample preparation.

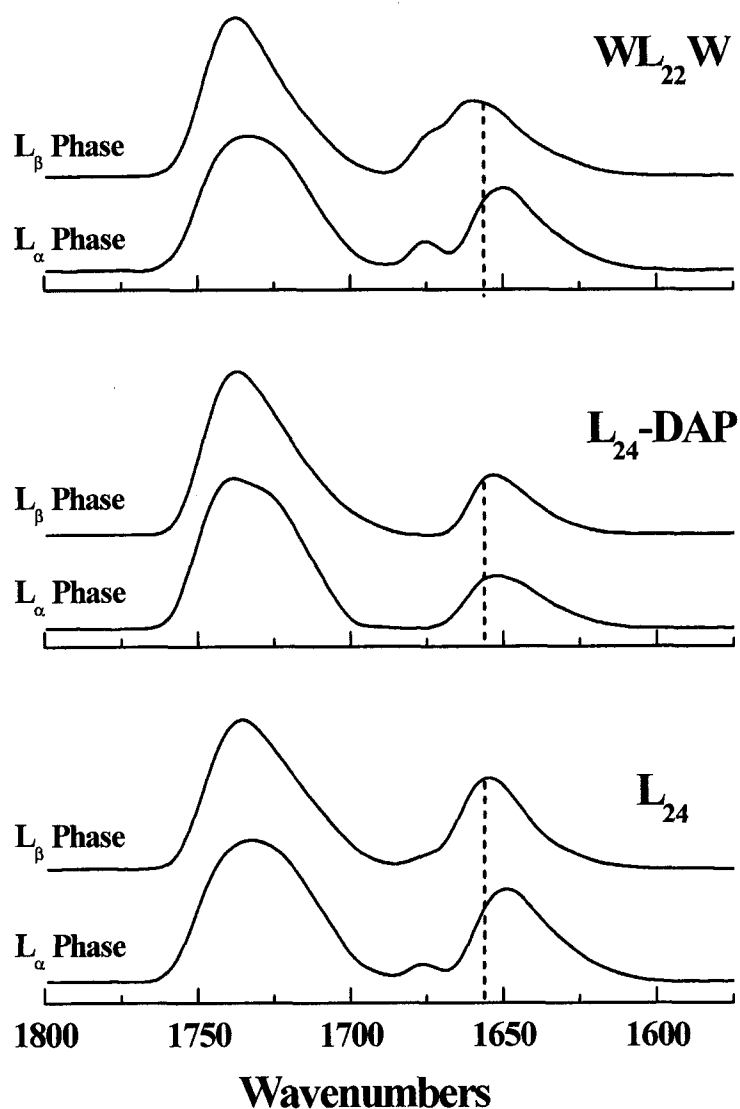


FIGURE 10. The C=O stretching and amide-I bands of the FTIR spectra exhibited by peptide-containing 16:0 PE bilayers. The absorbance spectra shown were acquired with mixtures containing 3.3 mol% of the peptides indicated under conditions where the lipid bilayer hosts are in the gel (L_{β} -phase) and liquid-crystalline (L_{α} -phase) states. The dashed lines mark the absorption maxima (1656 cm^{-1}) of the amide I absorption bands arising from fully proteated α -helical peptide domains. The small absorption bands centered near 1670 cm^{-1} arise from small amounts of trifluoroacetate counterions which were not completely removed during sample preparation.

CHAPTER V. A Differential Scanning Calorimetric and ^{31}P -NMR Spectroscopic Study of the Effect of Transmembrane α -Helical Peptides on the Lamellar/Reversed Hexagonal Phase Transition of Phosphatidylethanolamine Model Membranes

Introduction

The complex mixture of lipids present in prokaryotic and eukaryotic cell membranes typically forms only a liquid-crystalline lamellar (L_{α}) phase under physiologically relevant conditions (1-2). However, the individual lipid classes present in such membranes can form either lamellar or nonlamellar phases when dispersed in excess water (3-5). In prokaryotic cell membranes, the uncharged diglycosyl diacylglycerol and anionic phosphatidylglycerol and cardiolipin components prefer the lamellar phase, their uncharged monoglycosyl diacylglycerol and zwitterionic PE components prefer inverted hexagonal and cubic phases, and certain anionic phosphorylated glycolipid components prefer the normal micellar phase (6,7). Similarly, in eukaryotic membranes the zwitterionic PC and sphingomyelin components and the anionic phosphatidylserine prefer the lamellar phase, the zwitterionic phospholipid PE prefers the H_{II} phase, while the anionic, complex glycosphingolipid (ganglioside) components prefer the normal micellar phase at neutral pH and physiological ionic strength. A considerable body of evidence has now accumulated indicating that these nonlamellar phase-preferring lipid components, as well as the various lamellar phase-preferring lipid components, perform

A version of this chapter has been published. Liu, F., Lewis, R.N.A.H., Hodges, R.S., and McElhaney, R.N. (2001) *Biochemistry* 40, 760-768

important structural and functional roles in eucaryotic membranes (8).

The phase that a fully hydrated membrane lipid prefers under a given set of conditions can be rationalized by considering the geometric packing of lipid molecules in various aggregates, which can in turn be described by a packing parameter or shape factor characteristic of the lipid molecule under these conditions (see refs. 9 and 10). For a series of different phospholipids having the same number and type of hydrocarbon chains, this parameter is in turn determined primarily by the optimal area occupied by the polar headgroup at the lipid/water interface. If the conformations of the various phospholipid polar headgroups are generally similar, the optimal area occupied by the polar headgroups should be approximately proportional to headgroup size (7, 11-13). However, second-order but nevertheless potentially important interactions can also effect the optimal headgroup area and thus the effective shape of the lipid molecule, including attractive hydrogen-bonding and electrostatic interactions with adjacent polar headgroups. With liquid-crystalline PE bilayers, the combination of the relatively small size of the polar headgroups and their capacity for electrostatic and hydrogen-bonding attraction to adjacent polar headgroups results in significant negative curvature stress, which is the driving force behind their propensity to form H_{II} phases at higher temperatures. The modulation of both lipid packing and curvature stress by inclusions, such as proteins and peptides can markedly affect the lamellar/nonlamellar phase behavior of lipid membranes (for reviews ,see refs. 13 and 14).

The synthetic peptide P_{24} and its analogues have been successfully used as a model of the hydrophobic transmembrane α -helical segments of the integral membrane proteins (15,16). These peptides are composed of a long sequence of hydrophobic leucine residues capped at both the N- and the C-termini by two positively charged, relatively polar lysine

residues. The poly-leucine core of these peptides forms a hydrophobic α -helix that is intended to span the lipid bilayer, while the somewhat polar positively charged lysine residues at the N- and the C-termini serve to anchor these termini to the bilayer surface and to inhibit lateral aggregation. The α -helical conformation and transbilayer orientation of these peptides within lipid bilayers have been proved by a combination of CD (4), FTIR (17-19), X-ray diffraction (20) and fluorescence quenching (21) measurements. DSC (15,17) and ^2H -NMR spectroscopic (15, 22,23) studies also indicate that the incorporation of these peptides into PC and PE bilayers broaden the gel/liquid-crystalline phase transition and reduce its enthalpy. It has also been demonstrated that the effects of these peptides on PC bilayers are dependent on both the sign and the magnitude of the mismatch between peptide hydrophobic length and membrane hydrophobic thickness (17). However, comparable hydrophobic mismatch effects were not observed when P₂₄ was incorporated into PE bilayers (24). In addition, ^2H -NMR spectroscopic studies (25) have shown that the rotational motion of P₂₄ about its long axis perpendicular to the membrane plane is severely restricted in gel state but quite rapid in the liquid-crystalline state. Finally, ESR (26) results show that a closely related peptide, L₂₄, exists at least primarily as a monomer in liquid-crystalline PC bilayers, even at relatively high peptide concentrations.

In this study, the synthetic phospholipid DEPE was used as the primary matrix lipid to study the transmembrane peptide-lipid interactions generally and the effect of these peptides on the L _{α} /H_{II} phase equilibrium in particular. This lipid is well suited for these studies because its L _{β} /L _{α} and L _{α} /H_{II} phase transition temperatures occur at experimentally convenient temperatures [~ 37 and $\sim 65^\circ\text{C}$, respectively (3)], and because its hydrocarbon chain length closely matches that of the most common lipid species present in most

eukaryotic and prokaryotic membranes (1). Many previous studies have shown that DEPE is an excellent matrix for investigating the relative effects of lipophilic additives on lipid lamellar/nonlamellar phase behavior (see ref 12 and references therein). Other studies have shown that naturally occurring peptides such as alamethicin, gramicidin A, and gramicidin S all promote nonlamellar phase formation when incorporated into DEPE dispersions (27-30). Moreover, recent experiments with the WALP peptides have shown that synthetic α -helical transmembrane peptides may have a profound effect on the lamellar/nonlamellar phase behavior of DEPE, depending on the mismatch between the hydrophobic length of the peptide and the hydrophobic thickness of DEPE bilayers (31).

In this study, we investigate the effects of the α -helical transmembrane peptide L₂₄ and other structurally related peptides on the L _{α} /H_{II} phase equilibrium of a DEPE matrix. The examined structural derivatives were used to evaluate several hypotheses related to the effects of peptide/lipid hydrophobic mismatch on the lamellar/nonlamellar phase behavior of phospholipid model membranes. First, with the peptide L₂₄-DAP, the two pairs of capping lysine residues at the end of L₂₄ have been replaced with the lysine analogues DAP, in which three of the four side chain methylene groups have been removed. This peptide was used to test the so-called snorkel model first suggested by Segrest et al. (32) to explain the behavior of positively charged residues in the amphipathic helices present at the surfaces of blood lipoproteins and later extended to transmembrane α -helices by von Heijne et al (33). According to the transmembrane peptide version of the snorkel model, the long, flexible hydrophobic side chains of lysine or arginine can extend along the transmembrane helix so that the terminal charged moiety can reside in the lipid polar headgroup region while the α -carbon of the amino acid residue remains well below (or possibly above) the membrane/water interface, even when

the hydrophobic length of the peptide is considerably different from that of the host lipid bilayer. Because of the shorter spacer arms between the charged group and the α -carbon of DAP, the peptide L₂₄-DAP is expected to be less accommodating to hydrophobic mismatch and any effects of such mismatch on the phase behavior of its host lipid bilayer should be exaggerated.

Second, to investigate the importance of interfacially located tryptophan residues with respect to the effects of transmembrane peptides on their host lipid bilayer, we have examined the effect of the peptide W-L₂₂-W on the lamellar/nonlamellar phase behavior of DEPE membranes. W-L₂₂-W is an L₂₄ derivative in which the residues Leu-3 and Leu-26 are replaced by tryptophans. The preference of tryptophan and tyrosine residues for membrane polar-apolar interfaces is found to be one of the common features of natural membrane proteins (34). Previous studies have shown that interfacially localized tryptophan residues are necessary for the promotion of H_{II} phases by the peptide gramicidin A and that N-formylation of these tryptophan residues completely and reversibly blocks the capacity of gramicidin A to induce H_{II} phase formation in dioleoylphosphatidylcholine model membranes (35-37). In addition, recent studies of the WALP model transmembrane peptides (for details on the structures of these peptides see refs. 39 and 45) have shown that these peptides can promote the formation of inverted nonlamellar phases in PC and PE model membranes and that interfacially localized tryptophans markedly enhance their capacity to do so (32, 38-40).

Finally, to address more directly the issue of peptide-lipid hydrophobic mismatch on membrane lamellar/nonlamellar phase behavior, we have studied the effect of the peptide P₁₆ on the lamellar nonlamellar phase equilibrium of DEPE, and have also examined the effect of the longer peptides such as L₂₄ on the lamellar/nonlamellar phase behavior of

DPEPE. The peptide P₁₆ is a structural analog of P₂₄, with a shorter hydrophobic polyleucine core (16 rather than 24 leucine residues), and DPEPE is a shorter chain homologue of DEPE which forms bilayers with a reduced hydrophobic thickness. In contrast to previous findings with the WALP and KALP transmembrane peptides, we find no evidence for hydrophobic mismatch effects playing the major role in determining the effects of L₂₄ and related peptides on the L_α-H_{II} phase equilibrium of the host PE matrix.

Materials and methods

The peptides P₁₆, L₂₄, L₂₄DAP and W-L₂₂-W were synthesized and purified using the solid-phase synthetic methodology and the high-performance liquid chromatographic procedures described by Zhang *et al* (41). Phospholipids were obtained from Avanti Polar Lipids Inc. (Birmingham, AL) and used without further purification. Lipid/peptide vesicle suspensions were prepared as follows. The lipid and peptide were codissolved in methanol in a clean glass test tube in proportions appropriate for the required lipid:peptide ratio. The solution was concentrated with a stream of nitrogen to a small volume (~0.1 ml) and approximately 4 ml of benzene were added. The sample was then frozen with dry ice and acetone and lyophilized in vacuo overnight. The powdery sample obtained was hydrated by vigorous vortexing in a buffer [50 mM Tris and 100mM NaCl (pH 7.4)] at temperatures near 50°C. For the DSC experiments, 0.5 ml samples containing 2 mg of lipid were analyzed with a Microcal-VP-DSC high-sensitivity microcalorimeter (Microcal Inc., Northampton, MA) operating at scan rates near 30°C per hour except where noted. Data were normally acquired during three cycles of heating and cooling scans and were analyzed with the Origin software package (Microcal Software

Inc., Northampton, MA). The reported transition midpoints represent the temperatures at which 50% conversion occurs based on the area of the DSC peaks. All of the DSC experiments reported here were carried out twice, and the results of each set of experiments were very similar. For the ^{31}P NMR spectroscopic experiments, samples typically containing 10 mg of lipid were dispersed in the same buffer used for the DSC experiments by three cycles of vigorous vortexing at temperatures near 50°C and cooling to 0°C . Samples were then cooled to temperatures near 0°C prior to initial data acquisition in the heating mode. ^{31}P -NMR spectra were recorded with Varian Unity 300 spectrometer (Varian Instruments, Palo Alto, CA) operating at 121.42 MHz for ^{31}P . Data were recorded and processed using the data acquisition and data processing parameters described by Lewis *et al.* (42) and were plotted with the Origin software package.

Results

DSC thermograms illustrating the thermotropic phase behavior of aqueous dispersions of DEPE are shown in Figure 1. In the heating mode, two fairly cooperative endothermic phase transitions occur. The more energetic phase transition centered near 37°C corresponds to the L_β - L_α phase transition, and the less energetic phase transition centered near 65°C corresponds to the L_α - H_{II} phase transition (see ref.3 and references therein). In the cooling mode, the H_{II} - L_α phase transition of DEPE exhibits considerable hysteresis, being centered near 58°C , whereas the L_α - L_β phase transition exhibits less hysteresis but is split into two overlapping components, as reported previously (43). The splitting of the cooling exotherm of the L_α - L_β phase transition has also been observed with the linear saturated PEs (44-45) and appears to be the result of domain inhomogeneities in the sample (45). Although we will briefly discuss the effects of

incorporating the various transmembrane peptides studied on the L_{β} - L_{α} phase transition, the focus of this study is on the effects of these peptides on the L_{α} - H_{II} phase transition.

DSC heating thermograms illustrating the general effects of these transmembrane peptides on the L_{β} - L_{α} phase transition of aqueous dispersions of DEPE are shown in Figure 2. The thermograms were obtained from preparations composed of DEPE and the peptide L_{24} and are typical of those exhibited by mixtures of DEPE with all of the peptides used in this study. It is clear that the incorporation of increasing quantities of L_{24} progressively decreases the midpoint temperature and enthalpy and markedly increases the width (i.e. decreases the cooperativity) of the L_{β} - L_{α} phase transition of DEPE. Essentially identical effects on the L_{β} - L_{α} phase transition of DEPE were observed upon incorporation of peptides L_{24} -DAP and W- L_{22} -W (data not presented). These results are qualitatively similar to those observed upon incorporating comparable amounts of the closely related peptide P_{24} into linear saturated PC and PE bilayers (16,25) and thus confirm that the three peptides being studied here are being efficiently incorporated into the PE matrix.

DSC thermograms illustrating the general effects of these transmembrane peptides on the L_{α} - H_{II} phase transition of DEPE are shown in Figure 3. Again, the thermograms were obtained from preparations of DEPE and the peptide L_{24} and are typical of those exhibited by mixtures of DEPE with L_{24} -DAP and W- L_{22} -W as well. It is clear that the incorporation of these peptides into DEPE vesicles results in a progressive decrease in the T_h as well as a marked decrease in the enthalpy (see Figure 4) and in the cooperativity of the L_{α} - H_{II} phase transition. The effects of these peptides on the T_h of DEPE directly

reflect their effects on the lamellar/nonlamellar phase-forming propensity of their lipid hosts and are the primary focus of this study.

The effect of variations in peptide concentration on the T_h of the DEPE matrix is presented in Figure 5. With the peptides L_{24} , L_{24} -DAP and W - L_{22} - W , the T_h observed upon heating decreases fairly sharply at low (≤ 0.25 mol %) levels of peptide incorporation, and less sharply at the higher peptide concentrations that were studied (0.25-1.5 mol %), where the decreases in T_h are a nearly linear function of peptide content. In the cooling mode, the initial decreases in T_h observed at low peptide concentrations are smaller than observed upon heating, but the incremental decreases in T_h observed at higher peptide concentrations are comparable to those observed upon heating. Consequently, the overall decreases in T_h observed upon cooling are smaller than those observed in the corresponding heating experiment. It is thus clear that these transmembrane peptides all destabilize the L_α phase of DEPE relative to its H_{II} phase, thus promoting the formation of the inverted nonlamellar phase at lower temperatures. It is also apparent that in both heating or cooling mode experiments, these three transmembrane peptides all induce comparable decreases in the T_h of the host lipid throughout the entire range of peptide concentrations that were examined. Thus the characteristic effects of this class of α -helical transmembrane peptides on both the gel-liquid-crystalline and lamellar-nonlamellar phase transitions of DEPE dispersions are general and are not significantly affected by the structural variations of the L_{24} peptide examined here.

Previous studies have demonstrated that a significant peptide-induced enhancement in membrane nonlamellar phase-forming propensity occurs when the lipid hydrophobic thickness significantly exceeds the hydrophobic length of the embedded transmembrane

peptides (35, 36, 39, 40,46-49). The effects of varying peptide length and lipid bilayer thickness on the lamellar/nonlamellar phase behavior of peptide-containing PE vesicles were thus examined to determine whether comparable hydrophobic mismatch effects are involved in the phenomena reported here. One series measurements involved an examination of the effect of the peptide P₁₆ on the L_α-H_{II} phase transition of DEPE. The mean hydrophobic length of P₁₆, expressed as the length of the polyleucine sequence measured at any point along the helix surface, is about 20-21Å, approximately ²/₃ of that of the peptides L₂₄, W-L₂₂-W and L₂₄-DAP (30-31 Å), and the hydrophobic length of P₁₆ should therefore be much shorter than the expected hydrophobic thickness of liquid-crystalline DEPE bilayers (~29Å; see ref. 50). DSC thermograms illustrating the effect of the peptide P₁₆ on the L_α-H_{II} phase transition of DEPE are shown in Figure 6 (left panel). As observed with the other peptides studied here, the incorporation of increasing quantities of P₁₆ into DEPE results in considerable broadening of the L_α-H_{II} phase transition endotherm. Moreover, T_h generally decreases as the peptide concentration increases, and as observed with the other peptides, this decrease is more pronounced at low peptide concentrations. However, the reduction of T_h observed with the P₁₆/DEPE mixtures are significantly smaller than those of DEPE mixtures containing the longer peptides. This latter observation indicates that despite being significantly shorter than its host DEPE membrane, the peptide P₁₆ is not as efficient at inducing nonlamellar phase formation in its host lipid membrane as are the longer peptides used in this study.

The second series of measurements involved an examination of the effect of the peptides L₂₄, W-L₂₂-W and L₂₄-DAP on the L_α-H_{II} transition of DPEPE, a shorter chain homologue of DEPE. In these experiments, the peptide hydrophobic length (30-31Å) will more greatly exceed the lipid hydrophobic thickness (~25Å; see ref 50) when compared

with the corresponding experiments using DEPE so that effects arising from this type of hydrophobic mismatch should be exaggerated. DSC thermograms which illustrate the effect of the peptides L_{24} , $W-L_{22}-W$ and $L_{24}-DAP$ on the L_{α} - H_{II} phase transition of DPEPE are shown in the left panel of Figure 7. DPEPE exhibits its L_{β} - L_{α} phase transition at temperatures near 20°C and its L_{α} - H_{II} phase transition at temperatures near 92°C (51). The incorporation of these peptides into DPEPE vesicles also causes a marked lowering of the T_h of the DPEPE lipid matrix as well as a decrease in the enthalpy and the cooperativity of the lipid L_{α} - H_{II} phase transition, results qualitatively similar to those observed with the corresponding DEPE/peptide mixtures. Also, the peptide-concentration dependence of the peptide-induced decreases in the T_h of DPEPE is phenomenologically similar to that exhibited by the corresponding DEPE/peptide mixtures (Figure 7, left panel), although the magnitude of the decrease in T_h is considerably greater with the DPEPE-peptide mixtures. We also note that peptide-induced decreases in the L_{β} - L_{α} phase transition temperatures were also observed with the DPEPE/peptide mixtures examined here. However, unlike with the L_{α} - H_{II} phase transition, the magnitude of the changes observed were comparable to those observed with the corresponding DEPE/peptide mixtures (data not shown).

Additional calorimetric experiments were performed to evaluate the possible influence of kinetic artifacts on the observations reported above. This possibility was suggested by the substantial cooling hysteresis which occurs at the H_{II} - L_{α} phase transition of DEPE (see Figure 1) and by previous indications that the kinetics of L_{α} - H_{II} phase transitions can be relatively slow because of the requirement for an interconversion between a two-dimensional and a three-dimensional lipid phase (52). These issues are

particularly relevant to this work because the detection and accurate measurement of the thermodynamic properties of broad, weakly energetic phase transitions, such as the L_{α} - H_{II} phase transitions exhibited by many of the peptide-containing PE preparations that were examined, requires relatively rapid heating or cooling of the sample. Thus, to determine whether our results may have been affected by any differential effect of the incorporated transmembrane peptide on the kinetics, and thus the apparent temperature, of the L_{α} - H_{II} phase transition as measured by DSC, we carried out a series of experiments in which the scan-rate dependence of the T_h of peptide-free and peptide-containing DEPE samples were compared and the results of such an experiment are shown in Figure 8. A comparison of the scan-rate dependencies of the calorimetrically determined T_h values of peptide-free and peptide-containing DEPE vesicles is presented in Figure 9. With pure DEPE vesicles, increases in the heating scan rate ranging from 10 to 50°C/h produce a relatively small increase ($\sim 1^{\circ}\text{C}$) in the calorimetrically determined T_h values. Slightly larger decreases in T_h ($\sim 2^{\circ}\text{C}$) are observed when the scan rate was varied in the cooling mode (see Figure 9). With the lipid/peptide mixtures, the same increases in heating scan rate result in a relatively small decrease ($\sim 0.5^{\circ}\text{C}$) in the apparent T_h of the lipid/peptide mixture, and somewhat larger decreases in apparent T_h in the corresponding cooling experiments (Figure 9). These results do indicate that there is a small kinetic component to calorimetrically determined T_h values recorded for DEPE and its mixtures with the transmembrane peptides. However, the magnitude of this effect is similar for peptide-free and peptide-containing DEPE dispersions and is clearly smaller than the observed peptide-induced changes in T_h . We therefore conclude that the observed peptide-induced decreases in T_h are the result of real shifts in the L_{α} - H_{II} phase equilibrium and not the result of kinetic artifacts.

^{31}P NMR spectroscopic measurements were also performed to determine the nature of the various lamellar-nonlamellar phase transitions exhibited by the peptide-containing vesicles examined in this study. As illustrated in Figure 10A, aqueous dispersions of DEPE exhibit so-called axially symmetric ^{31}P NMR powder patterns at temperatures below the onset of the L_{α} - H_{II} phase transition of the lipid. Such powder patterns are typical of those exhibited by phospholipid bilayers in which the phosphate headgroup reorientational motions are fast and axially symmetric on the ^{31}P NMR timescale (53). At temperatures above the calorimetrically determined L_{α} - H_{II} phase transition, the powder pattern narrows significantly and its shape changes abruptly to one characteristic of phospholipid headgroups undergoing fast orientational motions in an inverted hexagonal assembly (54). As expected, these results are consistent with the conversion of a L_{α} phase to a H_{II} phase at temperatures coinciding with the calorimetrically observed heating endotherm near 65°C. Figure 10 also shows that the DEPE/peptide mixtures that were examined begin to exhibit ^{31}P NMR signatures of H_{II} phases at lower temperatures than with pure DEPE dispersions, in a peptide concentration-dependent manner. Thus, with mixtures containing 0.5 mol % peptide, ^{31}P NMR signatures consistent with the retention of lamellar structures are observed at temperatures near 55°C and powder patterns consistent with complete conversion to the H_{II} phase are observed at temperatures near 60°C (Figure 10B). At peptide concentrations near 1.5 mol %, our ^{31}P NMR spectroscopic data also show that the onset of H_{II} phase formation occurs at temperatures near 55°C and is substantially complete at temperatures near 60°C (Figure 10C), observations in excellent agreement with the results of our DSC experiments. However, the data also show that the ^{31}P NMR spectra of the peptide-containing samples also contain nontrivial contributions from a resonance peak at the so-called isotropic

frequency (Figures 10B, C), and that the relative intensity of this peak increases with increasing peptide concentration. The structural basis of the appearance of this signal is unclear at this time but could, in principle, be an indication of the presence of small fast tumbling vesicular structures or three dimensionally ordered lipid structures such as inverted cubic phases (54), most likely the latter. Nevertheless, it is clear that such structures form only a small fraction of the overall phospholipid population throughout most of the range of peptide concentrations that were examined and that the dominant structural change being monitored in our calorimetric experiments is in fact the L_{α} - H_{II} phase transition of the DEPE matrix, even at the highest peptide concentrations tested.

Discussion

The most important finding of this study is that small amounts of the three α -helical transmembrane peptides L_{24} , W- L_{22} -W, and L_{24} -DAP significantly lower the L_{α} - H_{II} phase transition temperature of the PE matrices into which they insert and that this effect is qualitatively and quantitatively comparable when each of these three peptides are incorporated into the same PE matrix. Peptide-induced promotion of lipid nonlamellar phase formation has been the subject of many theoretical considerations (see refs 35, 36, 55, and 56 and references therein) and has been observed experimentally in lipid bilayers containing the amphipathic α -helical peptide alamethicin (28), the channel-forming antimicrobial peptide gramicidin A (refs 15, 35, 36, and 49 and references therein), and the cyclic β -sheet-forming antimicrobial peptide gramicidin S (29), and has recently been observed in lipid bilayers containing a number of synthetic tryptophan-anchored transmembrane peptides, the “WALP” peptides (46-48). In addition, peptide-induced demotion of lipid nonlamellar phase formation has also been observed in lipid bilayers

containing apolipoprotein class A amphipathic helices (57) and the pore-forming antimicrobial peptide Magainin 2 (58). However, the mechanism(s) whereby such peptides affect the formation of nonlamellar phases in their host lipid matrices is currently unknown, and it is not clear whether our experimental observations are mechanistically comparable to any of the previously reported instances of peptide-induced enhancement of lipid nonlamellar phase formation. The mechanistic basis for the peptide-induced enhancement of lipid nonlamellar phase-forming propensity is an unresolved issue which is under active investigation in many laboratories.

It is interesting to compare the general findings of these studies with the spectroscopic and X-ray diffraction studies of Killian and co-workers, who examined the effects of various ditryptophan-anchored (40, 46-48), and dilysine-anchored (39) transmembrane peptides on the lamellar/nonlamellar phase behavior of phospholipid bilayers. These authors demonstrated that the tryptophan-anchored (WALP) peptides markedly enhance the nonlamellar phase-forming propensities of their host membranes under conditions where lipid bilayer hydrophobic thickness significantly exceeds the hydrophobic length of the peptide (40, 46-48), observations similar to those reported in comparable studies of the interaction of gramicidin A with phospholipid bilayers (15, 35, 36, 49). They also demonstrated that the peptides WALP-27 and WALP-31 were considerably less efficient at promoting nonlamellar phase formation in DEPE and DOPE/DOPG membranes (40,48), presumably because their hydrophobic lengths more closely match the hydrophobic thickness of the lipid matrix. There were also indications that WALP-31 (the longest of the WALP peptides used) may not be completely miscible with the L_{α} and H_{II} phases of dielaidoyl or dioleoyl phospholipids, presumably because its hydrophobic length greatly exceeds the probable hydrophobic thickness of these

lipids, especially at temperatures above the T_h (40,48). In these respects, the behavior of the WALP peptides contrast sharply with that of our dilysine-anchored peptides, which cause a significant enhancement of the nonlamellar phase forming propensities of their host PE membranes under conditions where peptide hydrophobic length is either comparable to or significantly greater than the expected hydrophobic thickness of the liquid-crystalline lipid membrane hosts. Interestingly, Killian and co-workers also demonstrated that some dilysine-anchored model transmembrane peptides (KALPs) can also induce the formation of nonlamellar phases under conditions where membrane hydrophobic thickness greatly exceeds peptide hydrophobic length (39). However, the KALP peptides were shown to be less potent inducers of nonlamellar phase formation than the corresponding WALP analogues, and evidence of nonlamellar phase formation was only obtained when the KALP peptides were incorporated into membranes composed of unsaturated phospholipids with very long chains. The authors therefore concluded that the induction of nonlamellar phases by the WALP and KALP series of peptides was driven by the hydrophobic mismatch stress which occurs when membrane hydrophobic thickness significantly exceeds peptide hydrophobic length, and the difference between the nonlamellar phase-inducing properties of comparable WALP and KALP peptides was ascribed to differences in the affinities of the anchoring tryptophan and lysine residues for the polar-apolar interfacial regions of their membrane hosts (39). In these studies, we also demonstrate that dilysine-anchored transmembrane peptides can enhance the nonlamellar phase-forming propensity of their PE membrane hosts. However, as shown below, our data cannot be rationalized within the framework of the hydrophobic mismatch effects described by Killian and co-workers.

We have clearly demonstrated here that our dilysine-anchored peptides, L₂₄, W-L₂₂-W and L₂₄-DAP, significantly enhance the lamellar/nonlamellar phase-forming propensity of DEPE model membranes under conditions where peptide hydrophobic length exceeds membrane hydrophobic thickness. Moreover, the magnitude of this effect increases when these same peptides are incorporated into a thinner membrane (see Figure 7, right panel) and decreases when a shorter peptide is incorporated into the DEPE matrix (see Figure 6, right panel). These observations are the opposite of the hydrophobic mismatch effects reported by Killian and co-workers. The basis of these phenomenological differences between our results and those obtained in studies of gramicidin A and of the WALP and KALP series of peptides is not clear. However, some of these differences could arise, in part, from the different methodologies employed in the different laboratories. For example, the decreases in the T_h of DEPE observed in our DSC experiments (~6-8°C at peptide concentrations near 1.5 mol%) are smaller than the temperature resolution of the comparable ³¹P NMR spectroscopic studies performed by Killian and co workers (~10°C, see ref. 40), and it is therefore possible that the peptides WALP-27 and WALP-31 could have had effects comparable to those observed by us that were not detected in these earlier studies. Whether these differences are the cause of, or significant contributors to, the phenomenological differences noted above remains to be determined.

Our studies also show that the extent of destabilization of the L_α phase relative to the H_{II} phase of DEPE is not affected by the replacement of each of the leucine residues at the ends of the hydrophobic core of L₂₄ with tryptophan residues, or by replacing each of the two positively charged lysine residues at the two ends of L₂₄ with the shorter side chain but still positively charged amino acid analog DAP. Thus, the alteration of the

lamellar-inverted nonlamellar phase equilibrium of the DEPE matrix stems from the general overall structure of these peptides and is apparently insensitive to the modifications tested here. However, with peptides such gramicidin A, seemingly small modifications of the chemical structure of the peptide (e.g. formylation of the terminal tryptophans) completely abolishes the capacity to induce formation of lipid nonlamellar phases (37,38). Also, Killian and co-workers have shown that a change in the nature of amino-acid residues anchoring an alternating stretch of leucine and alanine residues (note the differences between the WALP and KALP series of peptides) can also markedly alter their capacity to induce nonlamellar phases in their membrane hosts (39). An obvious difference between our work and those involving gramicidin A and the WALP and KALP series of peptides is the fact that the polyleucine cores of the helical peptides used here are intrinsically more hydrophobic and more conformationally stable than the poly-(Leu-Ala) cores of the WALP and KALP series of peptides (see ref. 41). It is therefore possible that the greater hydrophobicity and conformational stability which the polyleucine core confers upon our peptides may make their nonlamellar phase-inducing properties less sensitive to the “end-group” modifications employed in these studies.

A common feature of our results and some of the data presented elsewhere (48) is the fact that the incorporation of relatively small amounts of transmembrane peptide can induce seemingly disproportionately large decreases in the T_h of the host membrane. We have shown in this study that the enthalpy of the L_α - H_{II} phase transition is also markedly and disproportionately reduced at very low peptide concentrations. Recently, Morein *et al.* (48) suggested that peptide concentrations near 0.25 mol % are probably insufficient to globally alter the spontaneous curvature or packing properties of the lipid membrane to an extent consistent with the magnitude of the observed depression in T_h , and that the

mechanistic basis of the changes in nonlamellar phase behavior observed at low peptide concentrations may not be the same as that operating at higher concentrations. Our ^{31}P -NMR spectroscopic studies also show that concomitant with the peptide-induced lowering of the L_{α} - H_{II} phase transition temperature, there was a small co-existing phospholipid population undergoing fast isotropic motion on the ^{31}P -NMR timescale (possibly a cubic phase), and that the size of this population increases with increases in peptide concentration. The possibility that our lipid/peptide preparations may preferentially form cubic phases instead of H_{II} phases at higher peptide concentrations is consistent with the suggestions of Morein *et al.* (48).

Finally, we note that our experimental results provide neither positive nor negative evidence for the so-called “snorkel effect” of the terminal lysine residues in modulating the effects a hydrophobic mismatch between peptide hydrophobic length and membrane hydrophobic thickness, mainly because the effects of our peptides on the lamellar/nonlamellar phase behavior of their host membrane do not appear to be primarily governed by hydrophobic mismatch effects in any case. Consequently, these experiments do not provide a crucial test of whether the flexible side chains of lysine residues near the ends of transmembrane peptide helices can alter the effective hydrophobic lengths of such peptides.

References

1. Gennis, R. B. (1989) The structures and properties of membrane lipids, in *Biomembranes. Molecular Structure and Function*, pp36-84, Springer-Verlag, New York.
2. Yeagle, P. (1992) *The Structure of Biological Membranes*, CRC Press, Boca Raton.
3. Lewis, R. N. A. H., Mannock, D. A., and McElhaney, R. N. (1997) Membrane lipid molecular structure and polymorphism, in *Current Topics in Membranes* (Epanand, R. M., Ed.) Vol. 44, pp 25-102, Publ. Academic Press, New York.
4. Rilfors, L., Lindblom, G., Wieslander, A., and Christiansson, A. (1984) Lipid bilayer stability in biological membranes, in *Membrane Fluidity* (Kates, M., and Manson, L. A., Eds.) pp 205-245, Plenum Press, New York.
5. Thurmond, R. L., and Lindblom, G. (1997) NMR studies of membrane lipid properties, in *Lipid Polymorphism and Membrane Properties* (Epanand, R. M., Eds.) pp 103-166, Academic Press, San Diego.
6. Lewis, R. N. A. H., and McElhaney, R. N. (1995) *Acholeplasma laidlawii* B membranes contain a lipid (glycerylphosphoryldiglucoyl diacylglycerol) which forms micelles rather than lamellar or reversed phases when dispersed in water, *Biochemistry* 34, 13818–13824.
7. Foht, P. J., Tran, Q. M., Lewis, R. N. A. H., and McElhaney, R. N. (1995) Quantitation of the phase preferences of the major lipids of the *Acholeplasma laidlawii* membrane, *Biochemistry* 34, 13811-13817.
8. Hui, S. W. (1997) Curvature stress and biomembrane function, in *Lipid Polymorphism and Membrane Properties* (Epanand, R. M., Eds.) pp 541-563, Academic Press, San Diego.

9. Israelachvili, J. (1992) *Intermolecular and Surface Forces*, Academic Press, San Diego.
10. Cevc, G., and Marsh, D. (1987) Nonbilayer phases, in *Phospholipid Bilayers. Physical Principles and Models*, pp407-425, John Wiley and Sons, New York.
11. Lee, Y. C., Zheng, Y. O., Taraschi, T. F., and Janes, N. (1996) Hydrophobic alkyl headgroups strongly promote membrane curvature and violate the headgroup volume correlation due to "headgroup" insertion, *Biochemistry* 35, 3677-3684.
12. Lee, Y-C., Taraschi, T. F., and Janes, N. (1993) Support for the shape concept of lipid structure based on a headgroup volume approach, *Biophys. J.* 65, 1429-1432.
13. Janes, N. (1996) Curvature stress and polymorphism in membranes, *Chem. Phys. Lipids* 81, 133-150.
14. Epanand, R. M. (1997) Modulation of lipid polymorphism by peptides, in *Lipid Polymorphism and Membrane Properties* (Epanand, R. M., Ed.) Vol. 44, pp 237-252, Publ. Academic Press, New York.
15. Davis, J. H., Clare, D. M., Hodges, R. S., and Bloom, M. (1983) Interaction of a synthetic amphiphilic polypeptide and lipids in a bilayer structure, *Biochemistry* 22, 5298-5305.
16. Killian, J. A. (1998) Hydrophobic mismatch between proteins and lipids in membranes, *Biochim. Biophys. Acta* 1376, 401-416.
17. Zhang, Y.-P., Lewis, R. N. A. H., Hodges, R. S., and McElhaney, R. N. (1992) Interaction of a peptide model of a hydrophobic transmembrane α -helical segment of a membrane protein with phosphatidylcholine bilayers: differential scanning calorimetric and FTIR spectroscopic studies, *Biochemistry* 31, 11579-11588.

18. Zhang, Y.-P., Lewis, R. N. A. H., Hodges, R. S., and McElhaney, R. N. (1992) FTIR spectroscopic studies of the conformation and amide hydrogen exchange of a peptide model of the hydrophobic transmembrane α -helices of membrane proteins, *Biochemistry* 31, 11572-11578
19. Axelsen, P. H., Kaufman, B. K., McElhaney, R. N., and Lewis, R. N. A. H. (1995) The infrared dichroism of transmembrane helical polypeptides, *Biophys. J.* 69, 2770-2781.
20. Huschilt, J. C, Millman, B. M, and Davis, J. H. (1989) Orientation of alpha-helical peptides in a lipid bilayer, *Biochim.Biophys.Acta* 979, 139-141.
21. Bolen, E. J., and Holloway, P. W. (1990) Quenching of tryptophan fluorescence by brominated phospholipid, *Biochemistry* 29, 9638-9643.
22. Huschilt, J. C, Hodges, R. S, and Davis, J. H.(1985) Phase equilibria in an amphiphilic peptide-phospholipid model membrane by deuterium nuclear magnetic resonance difference spectroscopy, *Biochemistry* 24, 1377-1386.
23. Morrow, M. R., Huschilt ,J. C, and Davis, J. H.(1985) Simultaneous modeling of phase and calorimetric behavior in an amphiphilic peptide/phospholipid model membrane, *Biochemistry* 24, 5396-5406.
24. Zhang, Y.-P., Lewis, R. N. A. H., Hodges, R. S., and. McElhaney, R. N (1995) Interaction of a peptide model of a hydrophobic transmembrane α -helical segment of a membrane protein with phosphatidylethanolamine bilayers: differential scanning calorimetric and FTIR spectroscopic studies, *Biophys. J.* 68, 847-857.
25. Pauls, K. P., MacKay, A. L., Soderman, O., Bloom, M., Taneja, A. K., and Hodges, R. S. (1985) Dynamic properties of the backbone of an integral membrane polypeptide measured by ^2H -NMR, *Eur. Biophys. J.* 12, 1-11.

26. Subczynski, W. K., Lewis, R. N. A. H., McElhaney, R. N., Hodges, R. S., Hyde, J. S., and Kusumi, A. (1998) Molecular organization and dynamics of 1-palmitoyl-2-oleoyl-phosphatidylcholine bilayers containing a transmembrane α -helical peptide, *Biochemistry* 37, 3156-3164.
27. Keller, S. L., Gruner, S. M., and Gawrisch, K. (1996) Small concentrations of alamethicin induce a cubic phase in bulk phosphatidylethanolamine mixtures, *Biochim. Biophys. Acta* 1278, 241-246.
28. Prenner, E. J., Lewis, R. N. A. H., Neuman, K. C., Gruner, S. M., Kondejewski, L. H., Hodges, R. S., and McElhaney, R. N. (1997) Nonlamellar phases induced by the interaction of gramicidin S with lipid bilayers. A possible relationship to membrane-disrupting activity, *Biochemistry* 36, 7906-7916.
29. van Eetheld, C. J. A., van Strigt, R., de Kruijff, B., Leunissen-Bijvelt, J., Verkleij, A. J., and De Geir, J. (1981) Gramicidin promotes formation of the hexagonal H_{II} phase in aqueous dispersions of phosphatidylethanolamine and phosphatidylcholine, *Biochim. Biophys. Acta* 648, 287-291.
30. Killian, J. A. and de Kruijff, B. (1985) Thermodynamic, motional, and structural aspects of gramicidin-induced hexagonal H_{II} phase formation in phosphatidylethanolamine, *Biochemistry* 24:7881-7890.
31. van der Wel, P. C. A., Pott, T., Morein, S., Greathouse, D. V., Koeppe, R. E., and Killian, J. A. (2000) Tryptophan-anchored transmembrane peptides promote formation of nonlamellar phases in phosphatidylethanolamine model membranes in a mismatch-dependent manner, *Biochemistry* 39, 3124-3133.

32. Segrest, J. P., De Loof, H., Dohlman, J. G., Brouillette, C. G., and Anantharamaiah, G. M. (1990) Amphipathic helix motif: classes and properties, *Proteins: Struct. Funct. Genet.* 8, 103-117.
33. Monne, M., Nilsson, I., Johansson, M., Elmhed, N., and von Heijne, G. (1998) Positively and negatively charged residues have different effects on the position in the membrane of a model transmembrane helix, *J. Mol. Biol.* 284, 1177-1183.
34. Preusch, P. C., Norvell, J. C., Cassatt, J. C., and Cassman, M. (1998) Progress away from 'no crystals, no grant', *Nat. Struct. Biol.* 5, 12-14.
35. Killian, J. A., and de Kruijff, B. (1988) Proposed mechanism for H_{II} phase induction by gramicidin in model membranes and its relation to channel formation, *Biophys. J.* 53, 111-117.
36. Killian, J. A. (1992) Gramicidin and gramicidin-lipid interactions, *Biochim. Biophys. Acta* 1113, 391-425.
37. Killian, J. A., Timmermans J. W., Keur, S., and de Kruijff, B. (1985) The tryptophans of gramicidin are essential for the lipid structure modulating effect of the peptide, *Biochim. Biophys. Acta* 820, 154-156.
38. Aranda, F. J., Killian, J. A., and de Kruijff, B. (1987) Importance of the tryptophans of gramicidin for its lipid structure modulating activity in lysophosphatidylcholine and phosphatidylethanolamine model membranes. A comparative study employing gramicidin analogs and a synthetic alpha-helical hydrophobic polypeptide, *Biochim. Biophys. Acta.* 901, 217-228.

39. de Planque, M. R. R., Keuijtzter, J. A. W., Liskamp, R. M. J., Marsh, D., Greathouse, D. V., Koeppe, R. E., de Kruijff, B., and Killian, J. A. (1999) Different membrane anchoring positions of tryptophan and lysine in synthetic transmembrane α -helical peptides, *J. Biol. Chem.* 274, 20839-20846.
40. Van der Wel, P. C. A., Pott, T., Morein, S., Greathouse, D. V., Koeppe, R. E., and Killian, J. A. (2000) Tryptophan-anchored transmembrane peptides promote formation of nonlamellar phases in phosphatidylethanolamine model membranes in a mismatch-dependent manner, *Biochemistry* 39, 3124-3133.
41. Zhang, Y.-P., Lewis, R. N. A. H., Henry, G. D., Sykes, B. D., Hodges, R. S., and McElhaney, R. N. (1995) Peptide models of helical hydrophobic transmembrane segments of membrane proteins. I. Studies of the conformation, intrabilayer orientation and amide hydrogen exchangeability of Ac-K₂-(LA)₁₂-K₂ amide, *Biochemistry* 34, 2348-2361.
42. Lewis, R. N. A. H., Sykes, B. D., and McElhaney, R. N. (1988) The thermotropic phase behavior of model membranes composed of phosphatidylcholines containing *cis*-monounsaturated acyl chain homologues of oleic acid: Differential scanning calorimetric and ³¹P-NMR studies, *Biochemistry* 27, 880-887.
43. Epand, R.M., and Epand, R.F. (1988) Kinetic effects in the differential scanning calorimetry cooling scans of phosphatidylethanolamines, *Chem.Phys.Lipids* 49, 101-104.
44. Lewis, R. N. A. H., and McElhaney, R. N. (1993) Calorimetric and spectroscopic studies of the polymorphic phase behavior of a homologous series of *n*-saturated 1,2-diacyl phosphatidylethanolamines, *Biophys. J.* 64, 1081-1096.

45. Yao, H., Hatta, I., Koynova, R., and Tenchov, B. (1992) Time-resolved X-ray diffraction and calorimetric studies at lower scan rates. II on the fine structure of the phase transitions in hydrated dipalmitoylphosphatidylethanolamine, *Biophys. J.* *61*, 683-693.
46. Killian, J. A., Salemink, I., De Planque, M. R. R., Lindblom, G., Koeppe, R. E., and Greathouse, D. V. (1996) Induction of nonbilayer structures in diacylphosphatidylcholine model membranes by transmembrane α -helical peptides: importance of hydrophobic mismatch and proposed role of tryptophans, *Biochemistry* *35*, 1037-1045.
47. Morein, S., Strandberg, E., Killian, J. A., Persson, S., Arvidson, G., Koeppe, R. E., and Lindblom, G. (1997) Influence of membrane-spanning alpha-helical peptides on the phase behavior of the dioleoylphosphatidylcholine/water system, *Biophys. J.* *73*, 3078-3088.
48. Morein, S., Koeppe, R. E., Lindblom, G., de Kruijff, B., and Killian, J. A. (2000) The effect of peptide/lipid hydrophobic mismatch on the phase behavior of model membranes mimicking the lipid composition in *Escherichia coli* membranes, *Biophys. J.* *78*, 2475-2485.
49. Watnick, P. I., Chan, S. I., and Dea, P. (1990) Hydrophobic mismatch in gramicidin A'/lecithin systems, *Biochemistry* *29*, 6215-6221.
50. Harper, P. E., Lewis, R. N. A. H., Mannock, D. A., McElhaney, R. N., and Gruner, S. M. (2000) X-ray diffraction structures of some phosphatidylethanolamine lamellar and inverted hexagonal phases, *Biophys. J.* *81*, 2693-2706.

51. Silvius, J. R., Lyons, M., Yeagle, P. L., and O'Leary, T. J. (1985) Thermotropic properties of bilayers containing branched-chain phospholipids. Calorimetric, Raman, and ^{31}P NMR studies, *Biochemistry* 24, 5388-5395.
52. Caffrey, M. (1985) Kinetics and mechanism of the lamellar gel/lamellar liquid-crystal and lamellar/inverted hexagonal phase transition in phosphatidylethanolamine: a real-time X-ray diffraction study using synchrotron radiation, *Biochemistry* 24, 4826-4844.
53. Seelig, J. (1978) ^{31}P nuclear magnetic resonance and the head group structure of phospholipids in membranes, *Biochim. Biophys. Acta* 515, 105-140.
54. Tilcock, C. P. S., Cullis, P. R., and Gruner, S. M (1986) On the validity of ^{31}P -NMR determinations of phospholipid polymorphic phase behaviour, *Chem. Phys. Lipids* 40, 47-56.
55. Cornell, B. A., and Separovic, F. (1988) A model for gramicidin A'-phospholipid interactions in bilayers, *Eur. Biophys. J.* 16, 299-306.
56. May, S., and Ben-Shaul, A. (1999) Molecular theory of lipid-protein interaction and the L_{α} - H_{II} transition, *Biophys. J.* 76, 751-767.
57. Tytler, E.M., Segrest, J.P., Epanand, R.M., Nie, S.Q., Epanand, R.F., Mishra, V.K., Venkatachalapathi, Y.V., and Anantharamaiah, G.M. (1993) Reciprocal effects of apolipoprotein and lytic peptide analogs on membranes. Cross-sectional molecular shapes of amphipathic alpha helices control membrane stability, *J.Biol.Chem.* 268, 22112-22118.
58. Matsuzaki, K., Sugishita, K., Ishibe, N., Ueha, M., Nakata, S., Miyajima, K., and Epanand, R.M. (1998) Relationship of membrane curvature to the formation of pores by magainin 2, *Biochemistry* 37, 11856-63.

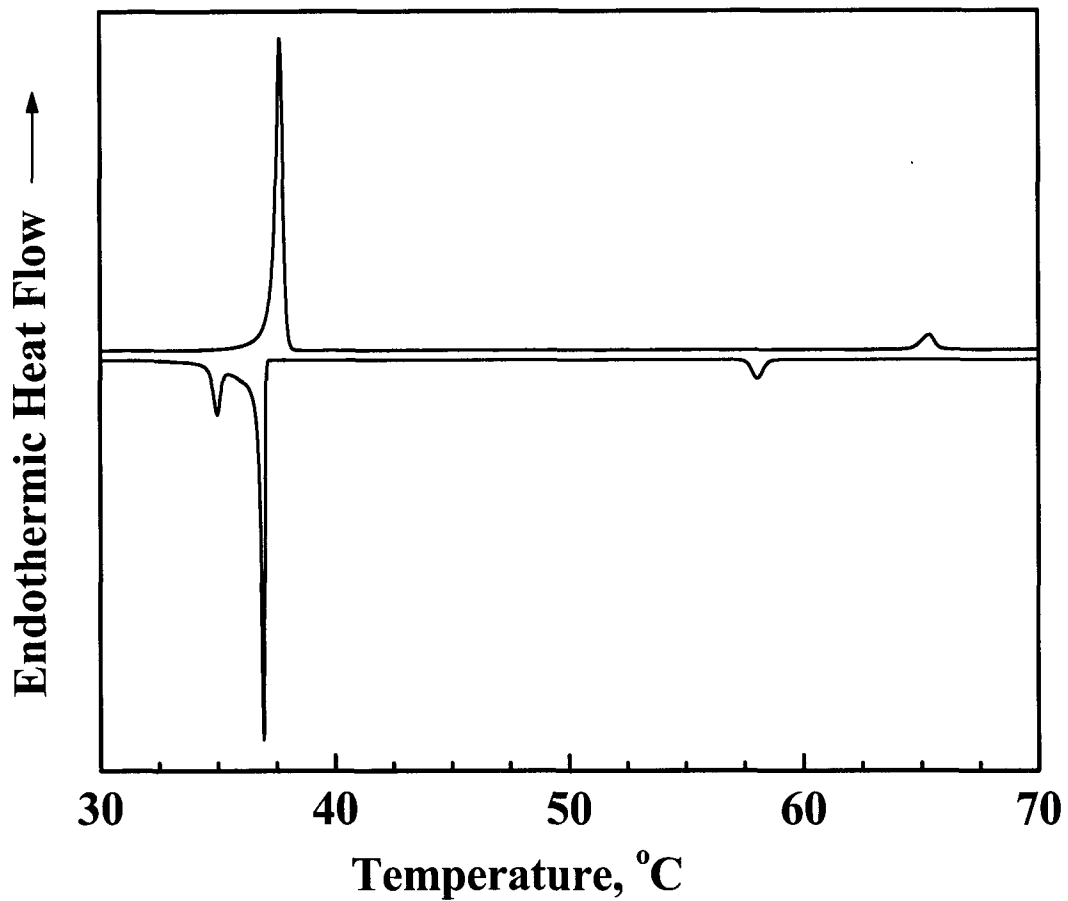


FIGURE 1. DSC heating (top) and cooling (bottom) thermograms illustrating the thermotropic phase behavior of aqueous dispersions of DEPE in the absence of peptide. The thermograms that are shown were acquired at scan rates of 30°C/h.

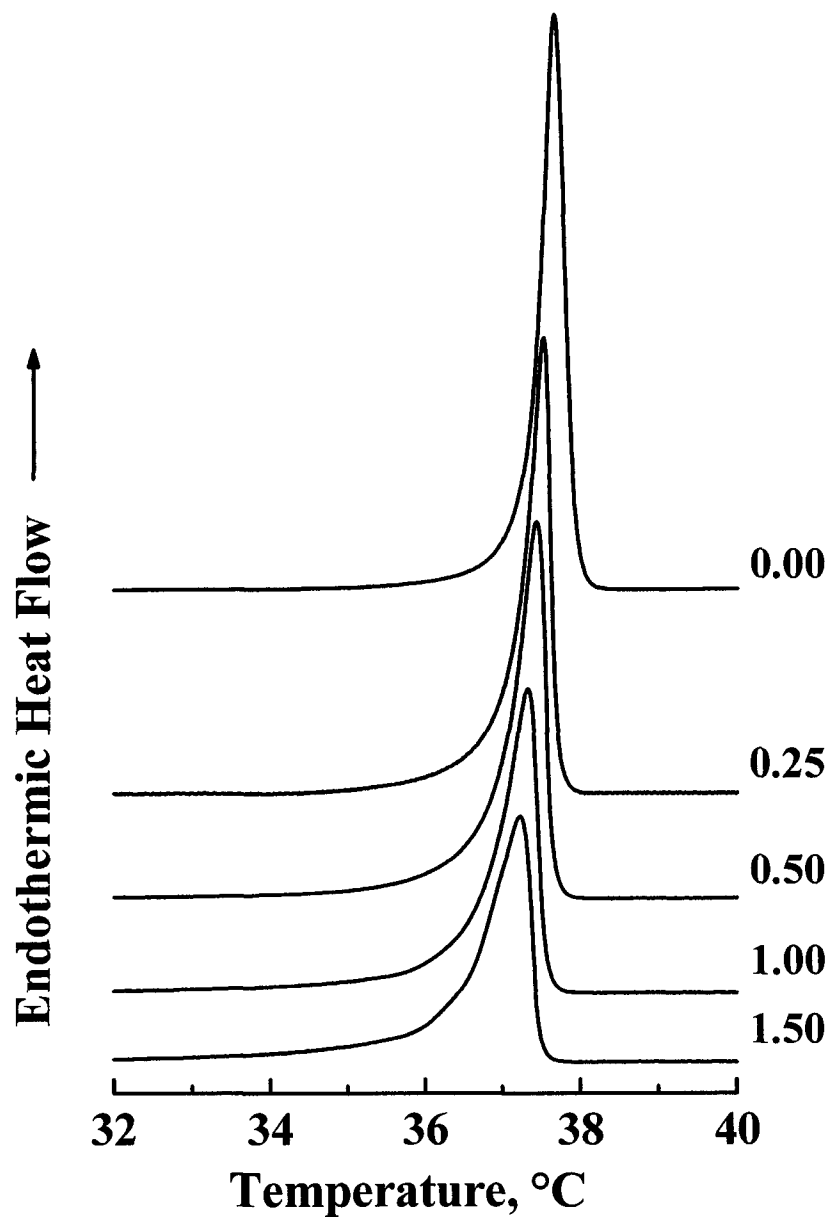


FIGURE 2. DSC heating thermograms illustrating the effect of incorporation of the peptide L₂₄ on the L_β-L_α phase transition of DEPE. The thermograms that are shown were acquired at the indicated peptide concentrations (mol percentage) and at a scan rate of 30°C/h.

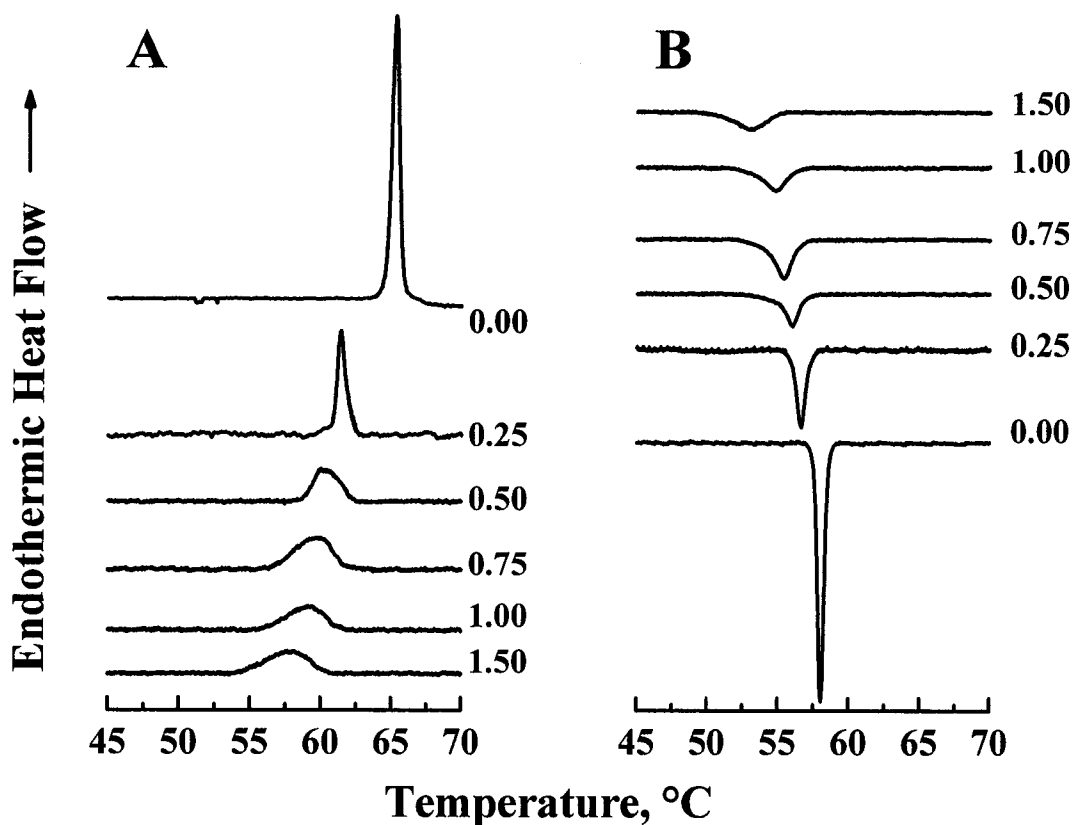


FIGURE 3. DSC heating (A) and cooling (B) thermograms illustrating the effect of the incorporation of peptide L_{24} on the L_{α} - H_{II} phase transition of DEPE. The thermograms that are shown were acquired at scan rates of $30^{\circ}\text{C}/\text{h}$ and at the indicated peptide concentrations (mol percentage).

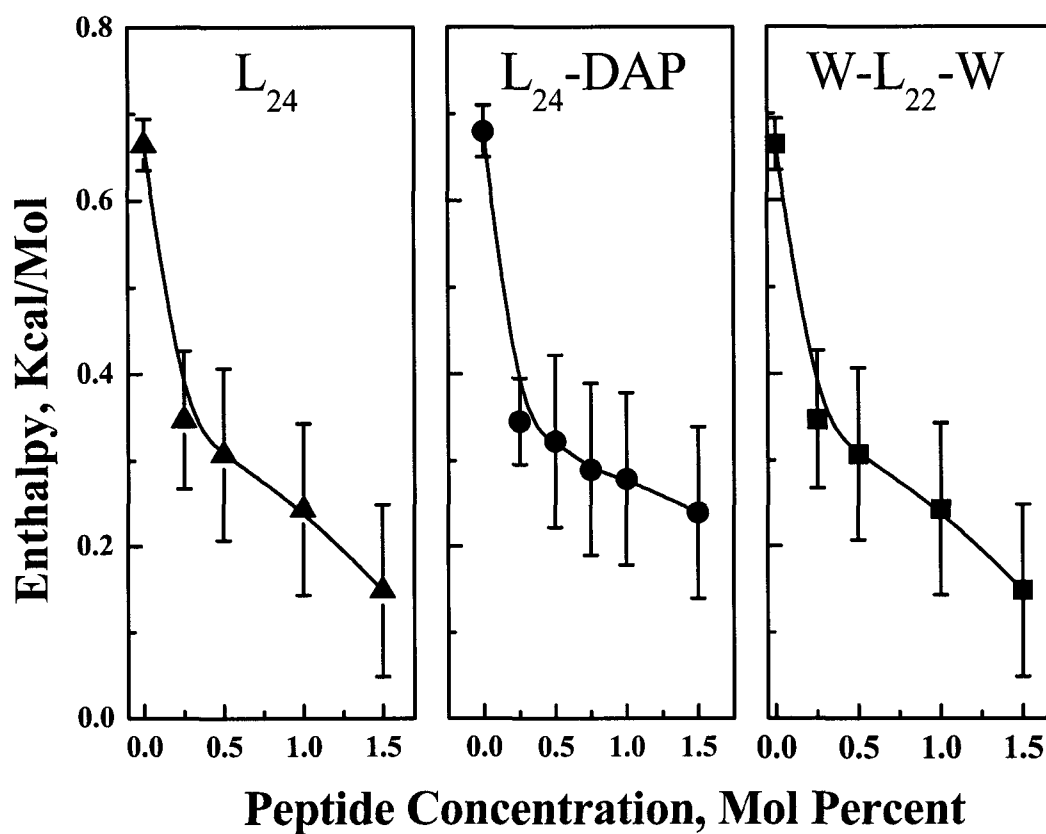


FIGURE 4. Effect of peptide concentration on the enthalpy of the L_{α} - H_{II} phase transition of DEPE. The enthalpy values that are shown were derived from DSC heating thermograms obtained using a scan rate of $30^{\circ}\text{C}/\text{h}$. The enthalpy values that are shown are the average and standard error from three determinations each on two independent prepared samples, The symbols used for mixtures of DEPE with each peptides are L_{24} (▲), L_{24} -DAP (●), and W - L_{22} - W (■).

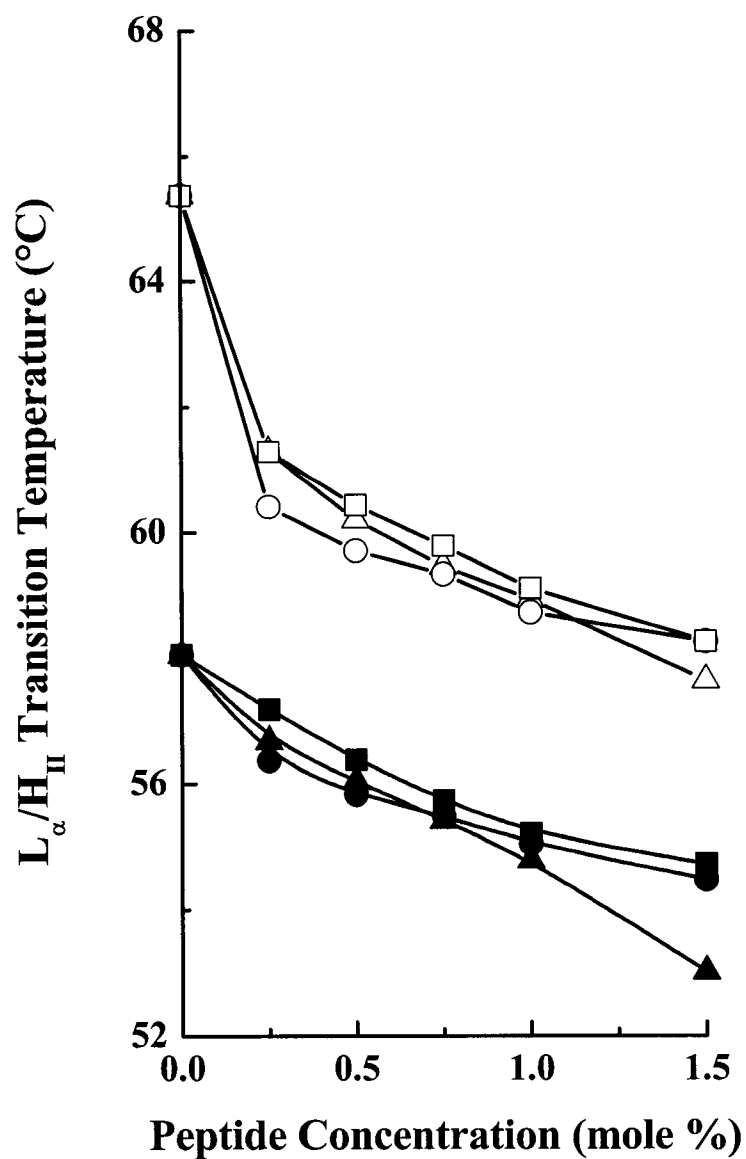


FIGURE 5. Effects of peptide concentration on the L_{α} - H_{II} phase transition temperature of DEPE. The data were obtained from heating (white symbols) and cooling (black symbols) thermograms acquired at scan rates near 30°C/h. The symbols used for mixtures of DEPE with each peptides are L_{24} (\blacktriangle or \triangle), L_{24} -DAP (\bullet or O), and W - L_{22} - W (\blacksquare or \square).

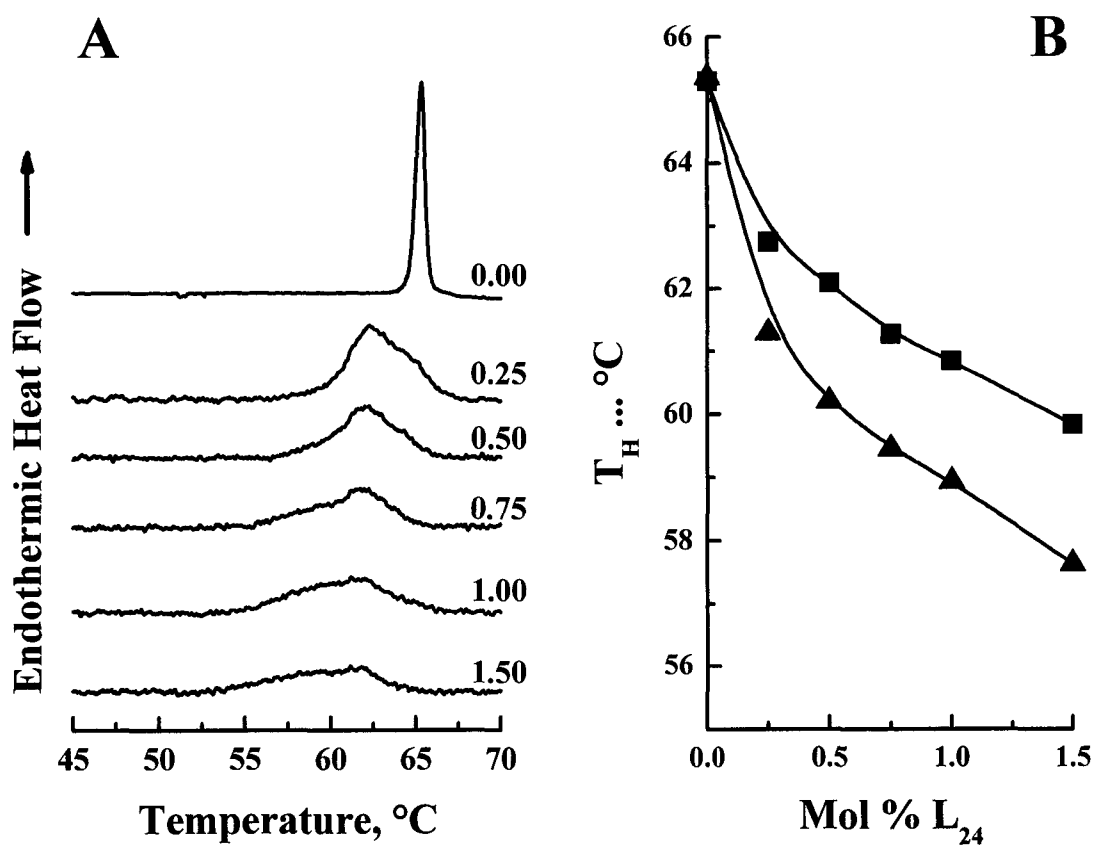


FIGURE 6. Effect of the incorporation of peptide P₁₆ on the L_α-H_{II} phase transition of DEPE. Panel A shows DSC heating thermograms of the L_α-H_{II} phase transitions exhibited by vesicles composed of DEPE and the peptide P₁₆. The thermograms that are shown were acquired at scan rates of 30°C/h at the indicated peptide concentrations (mol percentage). Panel B shows a comparison of the concentration dependent changes in the T_h of DEPE induced by the peptides P₁₆ (■) and L₂₄ (▲).

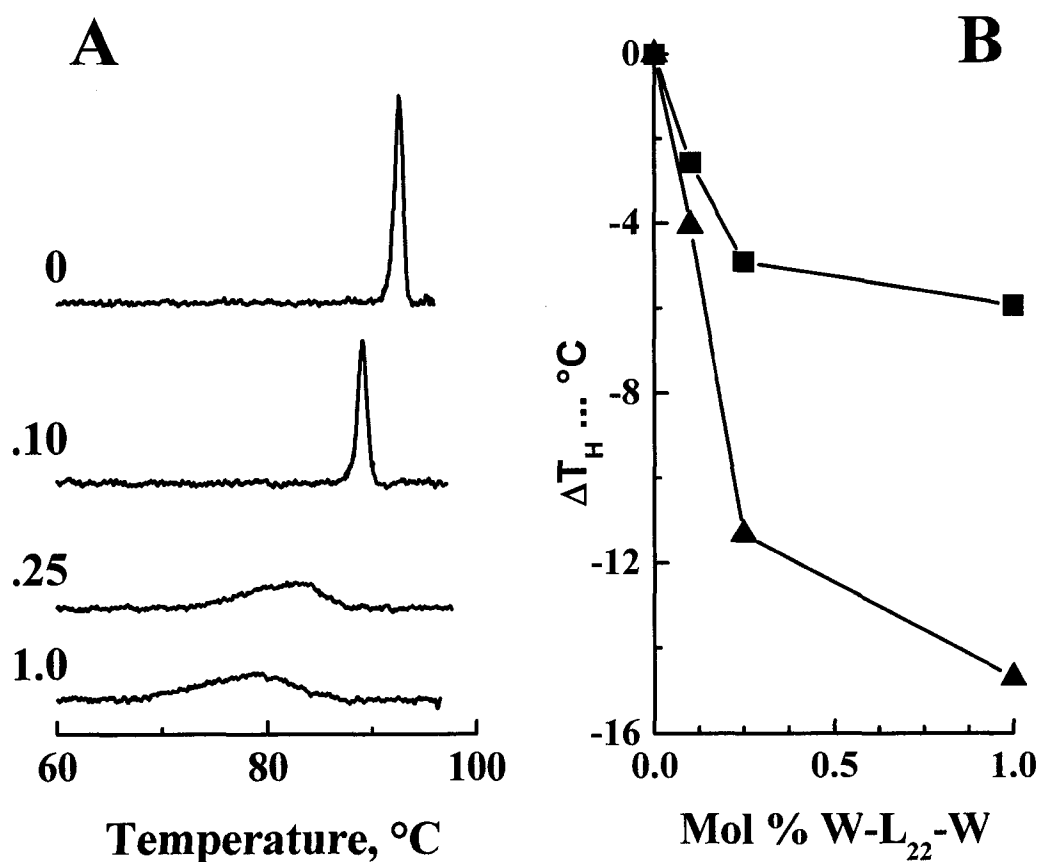


FIGURE 7. Effects of peptide incorporation on the L_α - H_{II} phase transition of DPEPE. Panel A shows DSC heating thermograms of the L_α - H_{II} phase transitions exhibited by vesicles composed of DPEPE and the peptide W-L₂₂-W. The thermograms that are shown were acquired at scan rates of 30°C/h at the indicated peptide concentrations (mol percentage). Panel B shows a comparison of the peptide-induced depression in the T_h of DPEPE (▲) and DEPE (■).

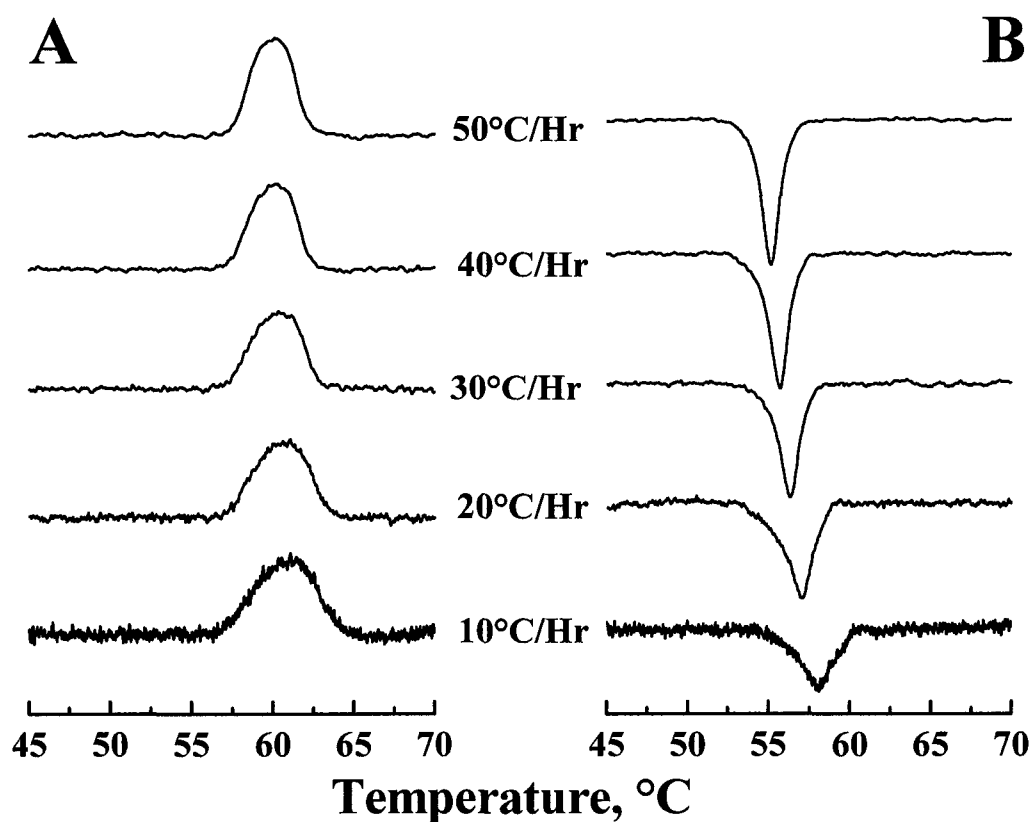


FIGURE 8. DSC heating (A) and cooling (B) thermograms illustrating the effect of scan rate on the L_{α} - H_{II} phase transitions that were examined. The thermograms that are shown were acquired at the indicated scan rates using DEPE samples containing 0.5 mol% of the peptide L_{24} . The areas under the DSC thermograms have been normalized to reflect variations in the scan rate that was utilized.

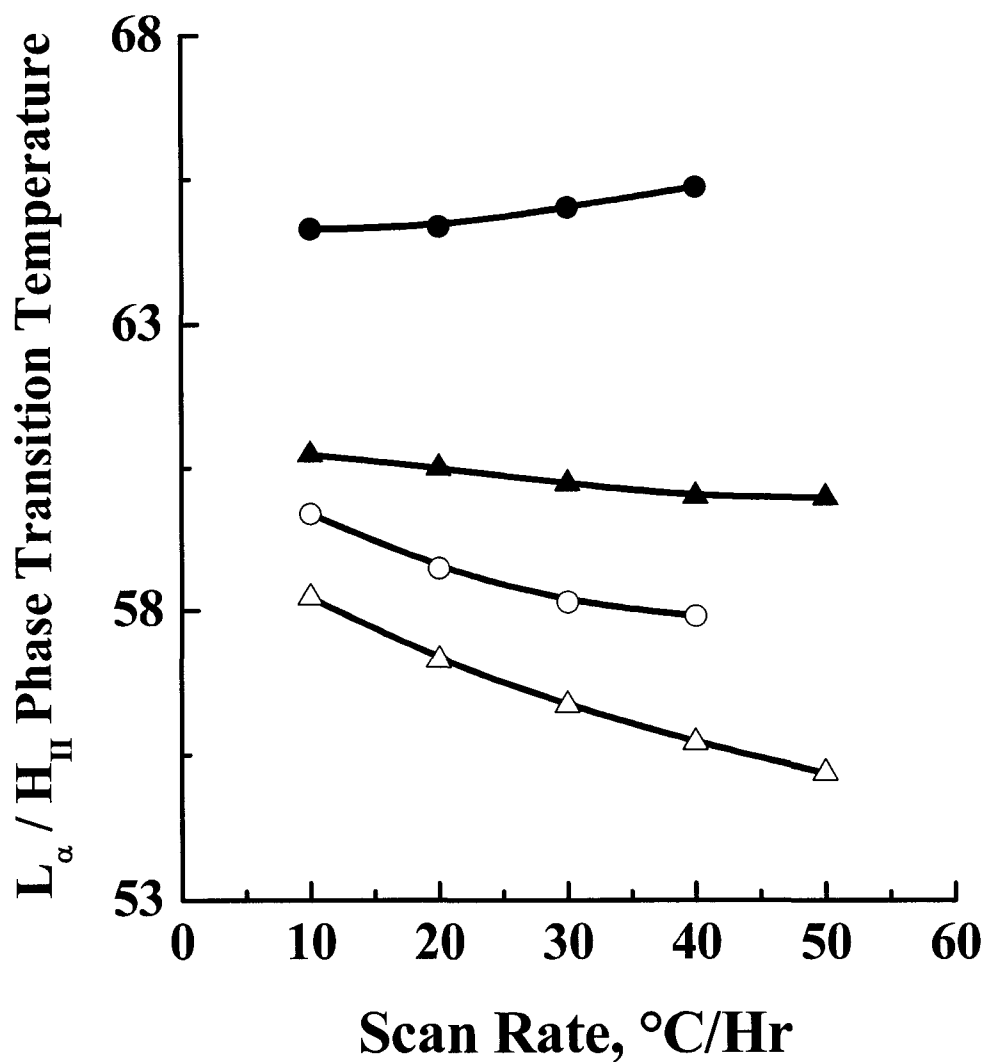


FIGURE 9. Effect of scan rate on the L_{α} - H_{II} phase transition temperatures of peptide-free (\bullet and \circ) and peptide-containing (\blacktriangle and \triangle) DEPE vesicles. The data were acquired from both heating (black symbols) and cooling (white symbols) experiments. The peptide-containing DEPE sample contained 0.5 mol % L_{24} .

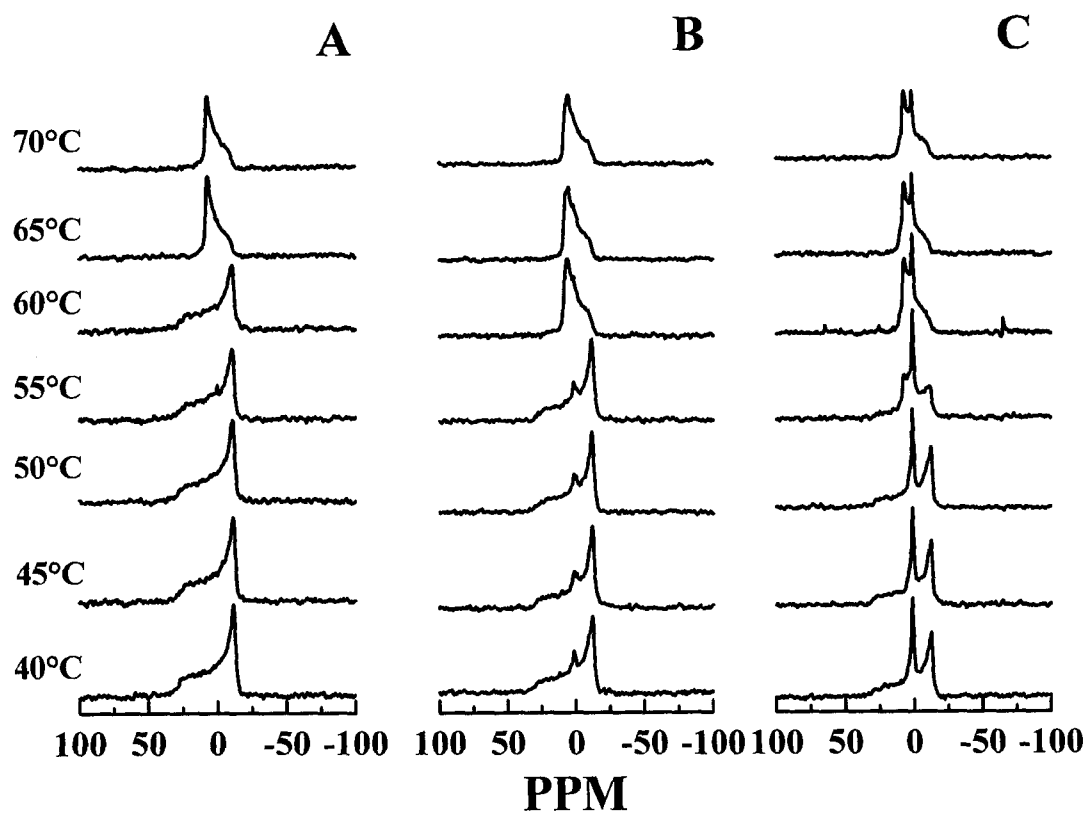


FIGURE 10. Proton decoupled ^{31}P NMR spectra exhibited by peptide-free (A) and peptide-containing (B and C) DEPE preparations. Sample B contained 0.5 mol% L₂₄, and sample C contained 1.5 mol% L₂₄. The spectra that are shown were acquired in the heating mode at the indicated temperatures.

CHAPTER VI. General Discussion

Integral membrane proteins generally traverse the membrane with hydrophobic transmembrane α -helical segments that are normally flanked by aromatic and charged residues (1). Numerous studies have shown that the activities and stabilities of many integral membrane proteins are dependent on the physical properties of lipid bilayers such as their physical state, fluidity, bilayer thickness, and lamellar/nonlamellar phase-preference (2-5). However, because of the complexity of the biological membrane systems, the molecular mechanisms by which lipid bilayers influence the protein structure and functions remain largely unknown. To investigate these mechanisms, simple model membrane systems made up of single phospholipid species and synthetic polypeptide models of the hydrophobic transmembrane α -helical segments of integral membrane proteins have been widely applied to study the protein-lipid interactions at molecular level (6-9). In this thesis, to further explore the roles of flanking aromatic and charged residues in integral membrane proteins, we have synthesized three model peptides (L_{24} , $L_{24}DAP$ and $WL_{22}W$) and studied their interactions with phospholipids with different polar headgroups and hydrocarbon chain structures using various biophysical techniques. The objectives of the work described in this thesis are to establish how the lipid-peptide interactions are affected by the nature and magnitude of the peptide-lipid hydrophobic mismatch and the H-bonding and electrostatic interactions between the lipid polar headgroups and those flanking aromatic and charged residues.

Hydrophobic mismatch between peptides and phospholipids

In this thesis, I have demonstrated that the effects of L_{24} and its analogues on the T_m s of zwitterionic PC and anionic PG bilayers are primarily determined by the hydrophobic

mismatch between the peptide and the lipid bilayer. In particular, in PC bilayers, when the mean hydrophobic thickness of the lipid bilayer is less than the hydrophobic length of the model peptide, the peptide-associated lipids melt at higher temperature than the peptide-poor lipids and *vice-versa*. Thus, the fact that the L₂₄-associated di-15:0 PC melts almost at the same temperature as L₂₄-poor di-15:0 PC indicates that the hydrophobic length of L₂₄ is very close to the mean hydrophobic thickness of di-15:0 PC (about 30.7Å) (7). This observation strongly supports the use of the average effective hydrophobic length (AEHL) for the calculation of peptide hydrophobic length. The AEHL is measured at any point on a single face of the α -helix and is one-half turn less at each terminus than the maximum hydrophobic length of the model peptide ($1.5\text{\AA} \times \text{number of hydrophobic residues}$). Thus, the AEHL of L₂₄ is $24 \times 1.5\text{\AA} - 2 \times 0.5 \times 5.4\text{\AA} = 30.6\text{\AA}$, which is very close to the mean hydrophobic thickness of di-15:0 PC. Moreover, our ²H-NMR studies show that L₂₄ increases the orientational order of the hydrocarbon chains of liquid-crystalline DPPC-d₆₂ bilayers. This is understandable since the AEHL of L₂₄ (30.6Å) is longer than the hydrophobic thickness of DPPC bilayers in the liquid-crystalline state (26.3Å). Similar hydrophobic mismatch-dependent effects on the orientational order and thus the bilayer thickness have also been observed in the ²H-NMR studies of WALP-containing PC bilayers (10). WALP is a model peptide with a hydrophobic core of alternating leucine and alanine residues that is flanked at both ends by two tryptophans. It was found that WALP16 (the number here is the total number of the amino acids) causes an increase of 0.6 and 0.4Å, no effect, and a decrease of 0.4Å in the bilayer thickness of di-12:0 and 14:0 PC, di-16:0 PC, and di-18:0 PC in the liquid-crystalline state while WALP19 causes an increase of 1.4, 0.6, 0.2Å, and no effect in the

bilayer thickness of di-12:0, 14:0, and 16:0 PC, and di-18:0 PC in the liquid-crystalline state. Thus the incorporation of WALP peptides produces systematic changes in the bilayer thickness dependent on the hydrophobic mismatch between the peptides and the lipid bilayer. Moreover, these results indicate that the hydrophobic length of WALP16 is very close to the hydrophobic thickness of liquid-crystalline di-16:0 PC bilayer (26.3Å), which is obviously larger than that predicted by its AEHL ($10 \times 1.5\text{Å} - 2 \times 0.5 \times 5.4\text{Å} = 9.6\text{Å}$). To explain this discrepancy, one should note that WALP and L_{24} have different hydrophobic core and different flanking residues that may have different interactions with the lipid bilayers. Indeed, WALP23 was found to induce a much larger increase in the bilayer thickness of di-14:0 PC (1.0Å) than did KALP23 (0.2Å) (KALP has the same hydrophobic core as WALP, but has two pairs of lysines instead of tryptophans as its flanking residues) (11), indicating that the tryptophan-flanked peptides may have a larger effective hydrophobic length than the lysine-flanked peptides with the same hydrophobic core.

H-bonding and electrostatic interactions between peptides and lipids

I have also demonstrated that the lipid-peptide interactions are affected by the nature and magnitude of the H-bonding interactions between the peptide terminal lysine residues and the lipid polar headgroups. In PC bilayers, because of the bulky choline group, the quaternary nitrogen atoms can not come closer to the phosphate than approximately 4.5Å. The PC molecules can only form indirect H-bonds between adjacent phosphate groups through the mediation of water molecules (12). It is thus likely that the peptide incorporation does not significantly change the weak intermolecular H-bonding interactions in PC bilayers. In the case of PG bilayers, the lipid polar headgroups contain

several H-bond donors and acceptors, including the glycerol hydroxyls and the phosphate group, which can form direct intermolecular H-bonding interactions. Previous studies have shown that the binding of water-soluble cationic peptides usually produces an increase in T_m due to a partial alleviation of the electrostatic repulsion between adjacent anionic phosphate groups (13). In contrast, this study shows that the incorporation of cationic L₂₄ and its analogues actually produces a decrease in the T_m . This suggests that peptide incorporation causes a larger disruptive effect in the H-bond network in PG bilayers compared to its alleviation of the electrostatic repulsions between anionic phosphate groups, thus on balance decreasing the relative stability of gel state bilayers. However, the fact that peptide incorporation produces a hydrophobic mismatch-dependent decrease in the T_m of PG bilayers suggest that the hydrophobic mismatch between the peptide and the lipid bilayer still plays a significant role here. In the case of PE bilayers, the polar headgroups can form more direct H-bonding interactions between adjacent phosphate and ethanolamine groups than those of PC bilayers, which is responsible for the much higher T_m of PE bilayers than that observed for PC bilayers (14). The DSC measurements presented here show that peptide incorporation produces a progressive and more significant reduction in the T_m of PE bilayers in a manner largely independent of the hydrophobic mismatch between the peptide and the lipid bilayer. This result was explained by assuming that peptide incorporation disrupts the H-bond network in gel state PE bilayers to a greater extent than in it does in gel-state PG and PC bilayers, which can efficiently mask the hydrophobic mismatch between the peptide and the lipid bilayer. It is obvious from the above that the H-bonding interactions between the peptide and the lipid polar headgroups play an increasingly important role in lipid-peptide

interactions when one proceeds from peptide-PC systems to peptide-PG systems and then to peptide-PE systems.

The measurements presented here show that the incorporation of cationic model peptides L₂₄ and its analogues only changes the T_ms of zwitterionic PC and PE bilayers to a small magnitude ($\leq 2^\circ\text{C}$), indicating that the electrostatic interactions between the peptides and the lipid polar headgroups are probably not significantly different from that between the lipid polar headgroups. In anionic PG bilayers, the alleviation of the electrostatic repulsion between adjacent anionic phosphate groups by the incorporation of the cationic peptides plays a less important role in determining the nature of peptide-lipid interactions than the peptide disruption of the inter-lipid H-bond interactions, as discussed above. Moreover, these studies show that the increase of salt concentration has only small effects on the temperatures, enthalpies and cooperativities of the main phase transition of di-16:0 PG bilayers containing 3.3 mol% L₂₄, which again indicates that the peptide-PG interactions are mainly determined by forces other than the electrostatic interactions between peptide terminal lysine residues and lipid anionic headgroups.

Are L₂₄ and its analogues good transmembrane model peptides?

The DSC measurements presented here show that the incorporation of L₂₄, L₂₄DAP and WL₂₂W progressively decreases the enthalpy and the cooperativity of the L _{β} -L _{α} phase transitions of PC bilayers and affects the T_m in a manner dependent on the hydrophobic mismatch between the peptides and the PC bilayers. All of these characteristic effects are very similar to that of their parent peptide P₂₄ (7). Previous studies have shown that P₂₄ forms a very stable α -helix that assumes a transbilayer orientation with the N- and C-termini exposed to the aqueous environment and the

hydrophobic poly-leucine core embedded in the hydrocarbon core of the lipid bilayer when reconstituted in various PCs (6,7,15-17). Thus, we assume that L₂₄, L₂₄DAP and WL₂₂W can form similar α -helical conformations and transbilayer orientations as P₂₄. Indeed, the FTIR measurements show that L₂₄ and its two analogues exhibit sharp amide I bands at around 1654 cm⁻¹, indicating the formation of a stable α -helical conformation for these peptides. Moreover, the amide I band frequency for these peptides shows a small downshift (< 3 cm⁻¹) at the L _{β} -L _{α} phase transitions of PC bilayers, which is similar to that reported by P₂₄ (7). A close inspection of the contours of these amide I bands in the gel state longer-chain PCs indicates that they actually consist of three components: two major components centered near 1653 cm⁻¹ and 1658-1660 cm⁻¹, and one minor component centered near 1645-1649 cm⁻¹. At the L _{β} -L _{α} phase transition, the intensity of the lower frequency component near 1645-1649 cm⁻¹ increases at the expense of the higher frequency component centered near 1658-1660 cm⁻¹, whereas the intensity of the major component centered near 1653 cm⁻¹ remains relatively unchanged. As a result, the overall frequency of the amide I band was shifted down. As suggested by previous studies, the amide I band frequencies near 1655 cm⁻¹ are typical of α -helices with fully protonated peptide amide bonds, whereas amide I band frequencies near 1645-1650 cm⁻¹ are normally observed when these bonds are fully deuterium-exchanged (18-20). By comparing the relative intensity of these three amide I band components, we can estimate that no more than 30% of the total amide protons are deuterium-exchanged, and that those exchanged protons are likely to be located near the N- and C-termini of the peptide. Thus, it seems likely that most of the peptide amide bonds are protected from H-D exchange, suggesting a predominantly transmembrane orientation for these peptides in

PC bilayers. A similar pattern of amide I bands is also observed when these peptides are incorporated into PE or PG bilayers. It seems logical to conclude that when reconstituted in PC, PE, and PG bilayers, these peptides fulfill two basic requirements to be effective transmembrane model peptides: an α -helical conformation and a transbilayer orientation in lipid bilayers.

This laboratory has previously studied the aggregation state of L₂₄ and its analogues in phospholipid bilayers directly by ESR and here, I have studied peptide aggregation indirectly by DSC. Previous ESR studies found that at pH 7.0, L₂₄ exists primarily as monomers in L _{α} POPC bilayers, even at a peptide to lipid mole ratio of 1 to 10 (21). Although I have not performed ESR studies of other peptide-phospholipid mixtures, the DSC measurements presented here indirectly support the idea that L₂₄, L₂₄DAP and WL₂₂W are dispersed relatively well in PG and PC bilayers at pH 7.4 without significant peptide aggregation. Interestingly, the DSC endotherms exhibited by either di-16:0 PG or di-16:0 PC bilayers containing 3.3 mol% L₂₄ at pH 11.5 are much sharper than similar samples measured at pH 7.5, indicating that some populations of peptides either are aggregating or are squeezed out from the lipid bilayers (unpublished data). Because the pK_a of the free amino group on a lysine residue occurs at pH 10.5, it seems reasonable to suggest that the deprotonation of the lysine amino group, and thus the weakening of the electrostatic repulsion between the model peptides, is responsible for their reduced effects on the thermotropic phase behavior of both di-16:0 PG or di-16:0 PC bilayers at pH 11.5. Interestingly, some unpublished ESR measurements from this laboratory of samples containing L₂₄ at pH 11.5 also showed a reduced effect of the peptide on the POPC hydrocarbon chain order parameter and motional rates. Moreover, this hypothesis is

supported by the fluorescence studies of polyLeu-Trp by London and coworkers (22). PolyLeu-Trp is a di-lysine-flanked polyleucine model peptide with a tryptophan residue at the center of the leucine stretch. These authors found that above pH 10-11, the λ_{\max} of the tryptophan of polyLeu-Trp is shifted up by several nanometers, whereas fluorescence quenching indicates that the peptide is still in a transmembrane state. It was also suggested that the deprotonation of the lysine residues weakens the electrostatic repulsion between model peptides and increases peptide aggregation, thus increasing the polarity of the environment in which tryptophan resides. Altogether, these studies strongly suggest that the electrostatic repulsions between the positively-charged lysine residues at the peptide termini may be required to prevent peptide aggregation in lipid bilayers. In addition, the lack of electrostatic repulsions between the peptide termini could be one reason why WALP peptides experience some degree of aggregation when the peptide is too short or too long relative to the bilayer thickness, as shown by the FTIR spectroscopic and sucrose density gradient centrifugation experiments (23,24). This suggests that one of the advantages of L₂₄ and its analogues over WALP peptides is the presence of positively-charged lysine residues at their termini to avoid peptide aggregation.

Role of lysine snorkeling in peptide-lipid interactions

In this thesis, I have studied the effects of lysine snorkeling on peptide-lipid interactions by comparing the effects of L₂₄ with that of L₂₄ DAP on the phase properties of phospholipids with different polar headgroups and hydrocarbon chain structures. First, I have studied the effects of L₂₄ and L₂₄DAP on the L_β-L_α phase transitions of zwitterionic PC and anionic PG bilayers. Because of the shorter spacer arms between the charged amino group and the α -carbon of DAP compared with that of lysine residue, the

peptide L₂₄DAP is expected to be less accommodating to the hydrophobic mismatch between the peptide and the lipid bilayer than L₂₄, and any effects of such mismatch on the thermotropic phase behavior of its host lipid bilayer should be exaggerated. In contrast to this predication, the measurements presented here actually showed that replacing the terminal lysine residues of L₂₄ by DAP attenuates the hydrophobic mismatch effects of the peptide on the thermotropic phase behavior of zwitterionic PC and anionic PG bilayers. These results are explained by postulating that the DAP residues are too short to engage in significant electrostatic interactions with the polar headgroups of the host phospholipid bilayer, as discussed in chapter 2 and 3. However, the magnitude of the variations of ΔT with changes in hydrocarbon chain length produced by L₂₄DAP incorporation relative to that by L₂₄ is only slightly smaller in PC than in PG bilayers, which strongly suggests that the magnitude of the attractive electrostatics interactions between the positively charged lysine, or DAP residues at the peptide termini and the negatively charged phosphate groups of PG and PC bilayers are not greatly different.

Second, I have demonstrated that lysine snorkeling plays an important and possibly indispensable role in the interactions of L₂₄ with zwitterionic PE bilayers. The DSC measurements show that L₂₄ DAP is much less effective than L₂₄ in reducing the T_m of zwitterionic PE bilayers. Moreover, the DSC endotherms exhibited by L₂₄DAP-containing PE bilayers are much sharper than those of L₂₄-containing PE bilayers at the same peptide concentration. Interestingly, such a marked difference between L₂₄ and L₂₄ DAP was not observed in their effects on the T_m and cooperativity of comparable zwitterionic PC bilayers. Thus, it seems reasonable to suggest that the different effects of L₂₄ and L₂₄ DAP on the phase properties of PE bilayers are not determined by their

different electrostatic interactions with zwitterionic headgroups. From the above discussions, gel-state PE bilayers appear to have much stronger intermolecular H-bonding interactions than gel-state PC bilayers. Because DAP has a much shorter spacer arm between its α -carbon and amino group, it is possible that the extension of its side chain away from the helix surface will be less disruptive to the H-bond network in PE bilayers than that of L₂₄, and that this may reasonably explain their different effects on the phase properties of PE bilayers.

Summarizing, I have clearly demonstrated that lysine snorkeling not only affects the hydrophobic mismatch between the peptide and the lipid bilayer, but also affects the electrostatic and H-bonding interactions between the peptide and the lipid polar headgroups. Moreover, these studies indicate that the lysine snorkeling is probably required for the interactions of hydrophobic transmembrane α -helices with zwitterionic PE bilayers, which may be one possible function for the lysine residues at the ends of hydrophobic transmembrane α -helix in natural integral membrane proteins.

Role of interfacially-localized tryptophan residues in peptide-lipid interactions

In this thesis, I have also studied the effects of another model peptide, WL₂₂W, in which residues Leu-3 and Leu-26 at the ends of the hydrophobic poly-leucine core of L₂₄ are replaced with tryptophans, on the phase properties of various phospholipids. One advantage of WL₂₂W over WALP is that WL₂₂W contains both lysine and tryptophan at its N- and C- termini, whereas WALP contains only tryptophan as its flanking residues. Statistical analysis has shown that the hydrophobic transmembrane α -helices of integral membrane proteins are normally flanked by aromatic residues, such as tryptophan or

tyrosine, and that positively charged lysine or arginine residues are found adjacent to these aromatic residues (1). This suggests that WL₂₂W more closely mimics the interfacial properties of integral membrane proteins than WALP peptides.

The measurements presented here demonstrate that the replacement of two leucine residues at the ends of the hydrophobic core of L₂₄ by tryptophan residues does not significantly alter the nature of the peptide-lipid interactions. In particular, WL₂₂W produces a hydrophobic mismatch-dependent decrease in the T_m of zwitterionic PC and anionic PG bilayers, while producing a hydrophobic mismatch-independent decrease in the T_m of zwitterionic PE bilayers. All these characteristic effects of WL₂₂W are qualitatively similar to that reported by L₂₄ in respective phospholipids, which does not support the idea that tryptophan interacts strongly with the polar/apolar interface of the phospholipids. In contrast, previous studies of WALP peptides strongly suggest that the tryptophan residue has a specific affinity for a well-defined site near the lipid carbonyl region (25). For example, the effect of WALP¹⁶₂₆ [Ac-(GA)₃-WW-(LA)₅-WW-(AG)₃-Etn] on the orientational order of the hydrocarbon chains of di-14:0 PC is similar to that of WALP16 and is significantly smaller than that of WALP23. It was suggested that the lipid adaptations are not primarily directed to avoid a peptide-lipid hydrophobic mismatch, but to prevent displacement of the tryptophan side chains from the polar/apolar interface of phospholipids. To explain this obvious discrepancy between WL₂₂W and WALP, one needs to note that WALP peptides contain only tryptophans as flanking residues while WL₂₂W contains both lysines and tryptophans as its flanking residues. Thus, in WL₂₂W, lysine can compete with tryptophan to interact with the phospholipid polar/apolar interface. Moreover, as suggested by the FTIR studies of the

PG/ WL₂₂W mixtures, tryptophan residues may form cation- π interactions with lysine residues, which is also supported by computer modeling studies of model peptides containing adjacent tryptophan and lysine residues (26). Because of the possible formation of cation- π interactions between tryptophan and lysine, tryptophans in WL₂₂W will be less efficient in forming specific interactions with the phospholipid polar/apolar interface than tryptophans in the WALP peptides. However, compared with that of WALP peptide, the tryptophan residues in WL₂₂W are actually more close to the interfacially localized tryptophan residues in natural integral membrane proteins, since they are located adjacent to positively-charged amino acid residues.

It is instructive to compare these results on WL₂₂W with that reported by London and coworkers on polyLeu-Trp (1,27). It was found that the transmembrane orientation of polyLeu-Trp was well maintained when the peptide hydrophobic length matches the hydrophobic thickness of PC bilayers. When the peptide is too short to span the PC bilayer, it will move to a non-transmembrane orientation close to the polar/apolar interface. When the model peptide is longer than necessary to span the PC bilayer, it can still maintain a transmembrane orientation but with increased levels of self-association. Interestingly, such variations of lipid/peptide stoichiometry were not observed in the interactions of WL₂₂W with PC bilayers with different hydrocarbon chain lengths. The DSC and FTIR measurements presented in this thesis indicate that WL₂₂W is incorporated well into PC bilayers and retains a stable α -helical conformation and a transbilayer orientation when the acyl chain length of PC bilayers is increased from 13 to 19 carbon atoms. One possible explanation for this marked difference between WL₂₂W and polyLeu-Trp is that the tryptophan residues in WL₂₂W are close to the peptide

termini while the tryptophan residue in polyLeu-Trp is at the center of its hydrophobic core. Previous studies have shown that about 25% of model peptide Lys₂-Gly-Leu₁₆-Lys-Ala-Amide lost its transbilayer orientation in POPC small unilamellar vesicles after the introduction of a tryptophan at the center of polyleucine core (28). Thus, it is likely that some populations of polyLeu-Trp can intrinsically adopt a non-transmembrane orientation in lipid bilayers, regardless of the conditions of the peptide-lipid hydrophobic mismatch. In addition, the behaviors of polyLeu-Trp were studied in *cis*-unsaturated diacyl PC bilayers, whereas those of WL₂₂W were studied in saturated diacyl PC bilayers. The *cis*-unsaturated PC with a chain length of 18 carbons or smaller has a T_m below -10°C (29). Therefore its hydrocarbon chains are highly disordered at room temperature. Because of this highly disordered state of acyl chains and the presence of a permanent kink formed by a single double bonds in each hydrocarbon chain, one might expect that the van der Waals interactions between polyLeu-Trp and *cis*-unsaturated PCs would be much weaker than those between WL₂₂W and saturated PCs. As a result, polyLeu-Trp will transform more easily from a transmembrane orientation to a non-transmembrane orientation in *cis*-unsaturated diacyl PC bilayers than WL₂₂W in saturated diacyl PC bilayers. There is also some question as to whether the fluorescence techniques used by these authors are able to accurately measure the peptide orientation in lipid bilayers. In these studies, the emission λ_{max} of the tryptophan of polyLeu-Trp was shifted to longer wavelength when incorporated into shorter or longer acyl chains, which they suggested was an indication of the transformation from a transmembrane orientation to a non-transmembrane orientation of the model peptide. However, the λ_{max} of tryptophan is actually determined by the polarity of the environment in which tryptophan resides which

can be influenced by many other factors, such as the state of peptide aggregation, as shown by the studies of polyLeu-Trp in relatively short chain PCs (27). Given these shortcomings, it is worthwhile to point out that the studies of polyLeu-Trp indicate that a hydrophobic transmembrane model peptide containing a tryptophan at the center of its hydrophobic core may be much less tolerant to the peptide-lipid hydrophobic mismatch than a model peptide containing tryptophans near its termini, such as WL₂₂W, and that this may be one reason why tryptophan residues are found mostly in a position corresponding to the membrane polar/apolar interface in integral membrane proteins.

Effects of peptides on the L_α/H_{II} phase transition of DEPE matrix

I have demonstrated that L₂₄ and its analogues promote the formation of nonlamellar phases in DEPE model membranes. In particular, the incorporation of small amounts of L₂₄ (≤1.5mol%) significantly decreases the temperature, enthalpy and cooperativity of the L_α-H_{II} phase transition of DEPE model membranes despite the fact that the peptide hydrophobic length (30.6Å) is longer than the lipid hydrophobic thickness (~29Å). Moreover, the magnitude of this effect decreases when a shorter peptide (P₁₆) is incorporated into DEPE matrix and increases when L₂₄ and its analogues are incorporated into DPEPE membranes with a shorter hydrophobic thickness (~25Å). These observations are the opposite of those reported by Killian and coworkers, which showed that WALP peptides promote the formation of nonlamellar phases in a DEPE matrix when the peptide hydrophobic length is shorter than the lipid hydrophobic thickness (30). These authors found that the incorporation of 2 mol% of relatively short peptides, WALP14-17, lowers the L_α-H_{II} phase transition temperatures of the DEPE matrix, while relatively long peptides, WALP19-27, induces Q_{II} phase formation in the DEPE matrix.

Interestingly, ^{31}P -NMR measurements from this laboratory have found that the incorporation of a relatively high concentration of L₂₄ (1.5 to 4 mol%) also results in the formation of Q_{II} phases in DEPE model membranes. These results probably reflect the different geometry-related constraints on peptide accommodation in the H_{II} and Q_{II} phases (31). In the H_{II} phase, the N- and C- termini of transmembrane model peptides are required to be located in contact with water. Because of the high intrinsic curvature of the H_{II} phase, the distribution and thus the amount of peptide that can be accommodated into a H_{II} phase are severely limited. In contrast, the Q_{II} phase has a lower intrinsic curvature and tends to present fewer geometry-related constraints on the amounts of peptides which can be accommodated. Therefore, mixtures of DEPE model membranes with transmembrane peptides may form a Q_{II} phase in preference to a H_{II} phase at relatively high peptide concentrations. Moreover, ^{31}P -NMR measurements by Killian and coworkers found that KALP23 lowered the L_α-H_{II} phase transition temperature, whereas WALP23 induced the formation of a Q_{II} phase in the DEPE matrix (32). These results suggest that the effects of a model peptide on the lamellar/nonlamellar phase-preference of the DEPE matrix are probably affected by the flanking residues of the peptide, such as tryptophans in WALP, or lysines in KALP and L₂₄. However, it is not possible to provide a detailed comparison between the data reported on the lipid/WALP mixtures and that on the lipid/L₂₄ mixtures because different techniques have been employed in these studies. One difficulty is that the decreases of about 6~8°C in the T_h of DEPE observed at 1.5 mol% peptide concentration in our DSC studies are smaller than the temperature interval of 10 °C used in the comparable ^{31}P -NMR spectroscopic studies of WALP peptides (32).

Our studies show that both $WL_{22}W$ and $L_{24}DAP$ have qualitatively similar effects on the temperature, enthalpy, and cooperativity of the L_{α} - H_{II} phase transition of DEPE matrix as L_{24} . Thus, the characteristic effects of L_{24} on the nonlamellar phase-forming properties of DEPE model membranes are not greatly altered by the replacement of residues Leu-3 and Leu-26 at the ends of the hydrophobic polyleucine core of L_{24} by tryptophans and the replacement of the lysine residues at the ends of L_{24} with the DAP residues. In chapter 5, I have suggested that the greater hydrophobicity and conformational stability which the polyleucine core confers upon the above peptides may have their nonlamellar phase-inducing properties less sensitive to the “end group” modifications described above. However, Killian and coworkers found that KALP23 and an analogue, K'ALP23, which has the same hydrophobic core as KALP23, but has two DAPs instead of lysines as its flanking residues, have essentially identical effects in promoting nonlamellar phase-formation in DEPE matrix (31). This observation does not support the above hypothesis since the nonlamellar phase-promoting properties of KALP23, with a hydrophobic core of alternating leucine and alanine residues that is less hydrophobic than the polyleucine core of L_{24} , is also insensitive to the replacement of lysine by DAP residues. However, it is also possible that the difference between KALP23 and K'ALP23 in promoting nonlamellar phase formation in DEPE is once again smaller than the temperature interval of ^{31}P -NMR spectroscopic studies used by Killian and coworkers (31).

Future directions

It is obvious from above that the work described in this thesis greatly extends our knowledge on the nature and magnitude of the hydrophobic mismatch and the H-bonding

and electrostatic interactions between transmembrane α -helical model peptides and the lipid matrix. These studies may also help to elucidate the roles of lysine and tryptophan residues that normally flank the transmembrane α -helices in many integral membrane proteins. However, one needs to note that the studies described above also have their limitations. Although the long hydrophobic polyleucine core of L₂₄ and its analogues confers these peptides with a stable α -helicity and a transbilayer orientation, it also makes these peptides less sensitive to the “end-group” modifications such as the replacement of lysine residues at the peptide termini by DAP residues and the leucine 3 and leucine 26 of L₂₄ by tryptophan residues. In addition, although a previous attenuated total reflectance (ATR) FTIR study indicates that the long axis of L₂₄ is predominantly oriented normal to the bilayer plane of the di-15:0 PC (33), the exact nature of the peptide tilt in other phospholipid bilayers remains to be determined. To overcome these limitations of our model systems, I propose to carry out future experiments in the following directions. First, ²H-NMR may be used to study the effects of L₂₄ and its analogues on the orientational order of PC bilayers with varying chain length. This study may help to resolve the obvious discrepancy between L₂₄ and WALP in their hydrophobic mismatch with PC bilayers. Second, ATR-FTIR may be used to study the tilt of L₂₄ and its analogues in phospholipid bilayers with different headgroups and hydrocarbon chain structures. The results obtained may be used to adjust the extent of hydrophobic mismatch between peptides and lipid bilayers, especially in some shorter chain phospholipids. Third, one may synthesize analogues of (LA)₁₂ in which the two pairs of lysine residues at the termini of (LA)₁₂ are replaced by DAP residues or the leucine 3 and alanine 26 of (LA)₁₂ are replaced by tryptophan residues. It is possible that

this set of model peptides will be more sensitive than L₂₄ and its analogues for the study of lysine snorkeling and the role of aromatic tryptophans. Fourth, one may synthesize analogues of L₂₄ in which the two pairs of lysine residues at its termini are replaced with negatively charged aspartic acids or polar but uncharged amino acids such as asparagines. These model peptides may help to further examine the nature and magnitude of the electrostatic and H-bonding interactions between the peptide terminal residues and the lipid polar headgroups. Fifth, one may synthesize analogues of L₂₄ in which the two pairs of lysine residues at its termini are replaced with lysine analogues with a side chain of two or three methylene groups. The minimum side chains requirements for lysine snorkeling in PE bilayers can be determined by studying the interactions of these two peptides with PE bilayers by DSC and ESR. Finally, one could synthesize analogues of WL₂₂W that contain two tryptophan residues at positions 4 and 25, 5 and 24, and so on. By moving the tryptophan residue away from lysine residue in the model peptide, one could determine the effects of their interval distance and their relative positions in helical wheel on the formation of cation- π interactions between lysine and tryptophan residues. Moreover, with this set of model peptides, one could eventually separate the effects of tryptophan from that of lysine so that their respective flanking properties for membrane polar/apolar interface may be determined.

References

1. Killian, J.A., and von Heijne, G. (2000) How proteins adapt to a membrane–water interface, *TIBS* 25,429-434.
2. Silvius, J.R., and McElhaney, R.N. (1980) Membrane lipid physical state and modulation of the (Na⁺, Mg²⁺)-ATPase activity in *Acholeplasma laidlawii* B, *Proc. Natl. Acad. Sci. U.S.A.* 77,1255-1259.
3. Silvius, J.R., and McElhaney, R.N. (1982) Membrane lipid fluidity and physical state and the activity of the Na⁺, Mg²⁺-ATPase of *Acholeplasma laidlawii* B, *Biophys. J.* 37, 36-38.
4. George, R., Lewis, R.N.A.H., Mahajan, S., and McElhaney, R.N. (1989) Studies on the purified, lipid-reconstituted (Na⁺+Mg²⁺)-ATPase from *Acholeplasma laidlawii* B membranes: Dependence of enzyme activity on lipid headgroup and hydrocarbon chain structure, *J. Biol. Chem.* 264, 11598-11604.
5. Brown, M.F. (1997) Influence of nonlamellar-forming lipids on rhodopsin, in *Lipid Polymorphism and Membrane Properties* (Eppand, R.M), pp 285-356, Academic Press, San Diego, CA.
6. Davis, J.H., Clare, D.M., Hodges, R.S., and Bloom, M. (1983) Interaction of a synthetic amphiphilic polypeptide and lipids in a bilayer structure, *Biochemistry* 22, 5298-5305.
7. Zhang, Y.-P., Lewis, R.N.A.H., Hodges, R.S., and McElhaney, R.N. (1992) Interaction of a peptide model of a hydrophobic transmembrane α -helical segment of a membrane protein with phosphatidylcholine bilayers: differential scanning calorimetric and FTIR spectroscopic studies, *Biochemistry* 31, 11579-11588.

8. Ren, J., Lew, S., Wang, Z., and London, E. (1997) Transmembrane orientation of hydrophobic α -helices is regulated both by the relationship of helix length to bilayer thickness and by the cholesterol concentration, *Biochemistry* 36, 10213-10220.
9. de Planque, M.R.R., and Killian, J.A. (2003) Protein-lipid interactions studied with designed transmembrane peptides: role of hydrophobic matching and interfacial anchoring, *Mol. Mem. Biol.* 20, 271-284.
10. de Planque, M.R.R., Greathouse, D.V., Koeppe, II, R.E., Schäfer, H., Marsh, D., and Killian, J.A. (1998) Influence of lipid/peptide hydrophobic mismatch on the thickness of diacylphosphatidylcholine bilayers. A ^2H -NMR and ESR study using designed transmembrane α -helical peptides and gramicidin A, *Biochemistry* 37, 9333-9345.
11. de Planque, M.R.R., Kruijtzter, J.A.W., Liskamp, R.M.J., Marsh, D., Greathouse, D.V., Koeppe II, R.E., de Kruijff, B., and Killian, J.A. (1999) Different membrane anchoring positions of tryptophan and lysine in synthetic transmembrane α -helical peptides, *J. Biol. Chem.* 274, 20839-20846.
12. Hauser, H., Pascher, I., Pearson, R.H., and Sundell, S. (1981) Preferred conformation and molecular packing of phosphatidylethanolamine and phosphatidylcholine, *Biochim. Biophys. Acta* 650, 21-51.
13. McElhaney, R.N. (1986) Differential scanning calorimetric studies of lipid-protein interactions in model membrane systems, *Biochim. Biophys. Acta* 864, 361-421.
14. Lewis, R.N.A.H., and McElhaney R.N. (1993) Calorimetric and spectroscopic studies of the polymorphic phase behavior of a homologous series of n-saturated 1,2-diacyl phosphatidylethanolamines, *Biophys. J.* 64, 1081-96.

15. Zhang, Y.-P., Lewis, R.N.A.H., Hodges, R.S., and McElhaney, R.N. (1992) FTIR spectroscopic studies of the conformation and amide hydrogen exchange of a peptide model of the hydrophobic transmembrane α -helices of membrane proteins, *Biochemistry* 31, 11572-11578.
16. Axelsen, P.H., Kaufman, P.H., McElhaney, R.N., and Lewis, R.N.A.H. (1995) The infrared dichroism of transmembrane helical polypeptides, *Biophys. J.* 69, 2770-2781.
17. Huschilt, J.C., Millman, B.M., and Davis, J.H. (1989) Orientation of α -helical peptides in a lipid bilayer, *Biochim. Biophys. Acta* 979, 139-141.
18. Chirgadze, Y.N., and Brazhnikov, E.V. (1974) Intensities and other spectral parameters of infrared amide bands of polypeptides in the α -helical form, *Biopolymers* 13, 1701-1712.
19. Rabolt, J.F., Moore, W.H., and Krimm, S. (1977) Vibrational analysis of peptides, polypeptides, and proteins. 3. α -Poly(L-alanine), *Macromolecules* 10, 1065-1074.
20. Dwivedi, A.M. and Krimm, S. (1984) Vibrational analysis of peptides, polypeptides, and proteins. XVIII. Conformational sensitivity of the α -helix spectrum: α I- and α II-poly (L-alanine), *Biopolymers* 23, 923-943
21. Subczynski, W.K., Lewis, R.N.A.H., McElhaney, R.N., Hodges, R.S., Hyde, J.S., and Kusumi, A. (1998) Molecular organization and dynamics of 1-palmitoyl-2-oleoyl-phosphatidylcholine bilayers containing a trans-membrane α -helical peptide, *Biochemistry* 37, 3156-3164.
22. Lew, S., Ren, J., and London, E. (2000) The effects of polar and/or ionizable residues in the core and flanking regions of hydrophobic helices on transmembrane conformation and oligomerization, *Biochemistry* 39, 9632-9640.

23. Killian, J.A., Salemink, I., de Planque, M.R.R., Lindblom, G., Koeppe II, R.E., and Greathouse, D.V. (1996) Induction of nonbilayer structures in diacylphosphatidylcholine model membranes by transmembrane α -helical peptides: importance of hydrophobic mismatch and proposed role of tryptophans, *Biochemistry* 35, 1037–1045.
24. de Planque, M.R.R., Goormaghtigh, E., Greathouse, D.V., Koeppe II, R.E., Kruijtzter, J.A.W., Liskamp, R.M.J., de Kruijff, B., and Killian, J.A. (2001) Sensitivity of single membrane-spanning α -helical peptides to hydrophobic mismatch with a lipid bilayer: effects on backbone structure, orientation, and extent of membrane incorporation, *Biochemistry* 40, 5000–5010.
25. de Planque, M.M.R., Bonev, B.B., Demmers, J.A.A., Greathouse, D.V., Koeppe, II, R.E., Separovic, F., Watts, A., and Killian, J.A. (2003) Interfacial anchor properties of tryptophan residues in transmembrane peptides can dominate over hydrophobic matching effects in peptide-lipid interactions, *Biochemistry* 42, 5341–5348.
26. Jensen, M., and Nielsen, C. (2004) Effects of interfacial tryptophan residues on protein interactions with lipid bilayers, *Biophys. J.* 86, 561a.
27. Ren, J., Lew, S., Wang, J., and London, E. (1999) Control of the transmembrane orientation and interfacial interactions within membranes by hydrophobic helix length, *Biochemistry* 38, 3905–3912.
28. Bolen, E.J., and Holloway, P.W. (1990) Quenching of tryptophan fluorescence by brominated phospholipid, *Biochemistry* 29, 9638-9643.

29. Silvius, J.R. (1982) Thermotropic phase transitions of pure lipids in model membranes and their modifications by membrane proteins, in *Lipid-Protein Interactions*, vol 2, pp 239-281, John Wiley & Sons, Inc., New York.
30. van der Wel, P.C.A., Pott, T., Morein, S., Greathouse, D.V., Koeppe II, R.E., and Killian, J.A. (2000) Tryptophan-anchored transmembrane peptides promote formation of nonlamellar phases in phosphatidylethanolamine model membranes in a mismatch-dependent manner, *Biochemistry* 39, 3124-3133.
31. Lewis, R.N.A.H., Prenner, E.J., Liu, F., and McElhaney, R.N. (2004) The accommodation of transmembrane and interfacially located amphipathic peptides in lamellar and inverted nonlamellar lipid assemblies: geometric considerations and implications, *Biophys. J.* 86, 558a.
32. Strandberg, E., Morein, S., Rijkers, D.T.S., Liskamp, R.M.J., Van der Wel, P.C.A., and Killian, J.A. (2002) Lipid dependence of membrane anchoring properties and snorkeling behavior of aromatic and charged residues in transmembrane peptides, *Biochemistry* 41, 7190-7198.
33. Zhang, Y.-P., Lewis, R.N.A.H., Henry, G.D., Sykes, B.D., Hodges, R.S., and McElhaney, R.N. (1995) Peptide models of helical hydrophobic transmembrane segments of membrane proteins. I. Studies of the conformation, intrabilayer orientation and amide hydrogen exchangeability of Ac-K₂-(LA)₁₂-K₂ amide, *Biochemistry* 34, 2348-2361.



ELSEVIER

Biochimica et Biophysica Acta 1511 (2001) 60–73



www.bba-direct.com

Differential scanning calorimetry and ^2H nuclear magnetic resonance and Fourier transform infrared spectroscopy studies of the effects of transmembrane α -helical peptides on the organization of phosphatidylcholine bilayers

Chantal Paré ^a, Michel Lafleur ^{a,*}, Feng Liu ^b, Ruthven N.A.H. Lewis ^b,
Ronald N. McElhaney ^b

^a *Département de Chimie and Groupe de Recherche en Transport Membranaire, Université de Montréal, C.P. 6128, succursale Centre-ville, Montréal, Québec H3C 3J7, Canada*

^b *Department of Biochemistry, University of Alberta, Edmonton, Alberta T6G 2H7, Canada*

Received 20 September 2000; received in revised form 17 November 2000; accepted 21 November 2000

Abstract

We have studied the effects of the incorporation of the α -helical transmembrane peptides Ac-K₂-L₂₄-K₂-amide (L₂₄) and Ac-K₂-(L-A)₁₂-K₂-amide ((LA)₁₂) on the thermotropic phase behavior of 1,2-dipalmitoyl-d₆₂-sn-glycero-3-phosphocholine (DPPC-d₆₂) and 1-palmitoyl-d₃₁-2-oleoyl-sn-glycero-3-phosphocholine (POPC-d₃₁) lipid bilayer model membranes by differential scanning calorimetry (DSC) and the conformational and orientational order of the phospholipid chains by Fourier transform infrared (FTIR) spectroscopy and ^2H nuclear magnetic resonance (^2H -NMR) spectroscopy, respectively. Our DSC and FTIR spectroscopic studies indicate that the peptides L₂₄ and (LA)₁₂ both decrease the temperature and enthalpy of the gel/liquid-crystalline phase transition of DPPC-d₆₂ bilayers, with (LA)₁₂ having the greater effect in this regard. An examination of the frequencies of the CH₂ and CD₂ symmetric stretching bands of the infrared spectra of liquid-crystalline states of the peptide-free and peptide-containing DPPC-d₆₂ and POPC-d₃₁ samples, and a comparison with the orientational order as measured by ^2H -NMR spectroscopy as well as with the chain order as measured by electron spin resonance spectroscopy, lead us to conclude that the CH₂ (or CD₂) stretching frequencies of lipid hydrocarbon chains are not a reliable measure of chain conformational order in lipid bilayers containing significant amounts of peptides or other lipophilic inclusions. In contrast, the results of our ^2H -NMR spectroscopic studies present a consistent picture in which both L₂₄ and (LA)₁₂ increased in a similar way the time-averaged orientational order of the lipid chains of their liquid-crystalline lipid bilayer hosts. The comparison of the effects L₂₄ and (LA)₁₂ on phosphatidylcholine bilayers indicates that the gel-to-liquid-crystalline phase transition appears to be more sensitive to small changes in transmembrane peptide surface topology

Abbreviations: CD, circular dichroism; DPPC, 1,2-dipalmitoyl-sn-glycero-3-phosphocholine; DPPC-d₆₂, 1,2-dipalmitoyl-d₆₂-sn-glycero-3-phosphocholine; DSC, differential scanning calorimetry; ESR, electron spin resonance; FTIR, Fourier transform infrared; Hepes, *N*-[2-hydroxyethyl]piperazine-*N'*[2-ethanesulfonic acid]; ^2H -NMR, ^2H nuclear magnetic resonance; L₂₄, Ac-K₂-L₂₄-K₂-amide; (LA)₁₂, Ac-K₂-(L-A)₁₂-K₂-amide; MLV, multilamellar vesicles; P₂₄, Ac-K₂-G-L₂₄-K₂-A-amide; PC, phosphatidylcholine; POPC, 1-palmitoyl-2-oleoyl-sn-glycero-3-phosphocholine; POPC-d₃₁, 1-palmitoyl-d₃₁-2-oleoyl-sn-glycero-3-phosphocholine; $\nu_{\text{C-DS}}$, symmetric CD₂ stretching band; $\nu_{\text{C-HS}}$, symmetric CH₂ stretching band

* Corresponding author. Fax: +1-514-343-7586; E-mail: michel.lafleur@umontreal.ca

0005-2736/01/\$ – see front matter © 2001 Elsevier Science B.V. All rights reserved.

PII: S0005-2736(00)00382-5

than hydrocarbon carbon chain orientational order in the liquid-crystalline state. © 2001 Elsevier Science B.V. All rights reserved.

Keywords: Transmembrane peptide; Lipid; IR spectroscopy; NMR spectroscopy; Lipid chain order

1. Introduction

The mutual interactions of lipids and proteins are of fundamental importance for both the structure and the function of all biological membranes (see [1,2]). In particular, the chemical composition and physical properties of the host lipid bilayer can markedly influence the activity and thermal stability of a large number of integral membrane proteins in both model and biological membrane systems (see [1–5]). For this reason there have been many studies of the interactions of membrane proteins with their host lipid bilayers, in both biological and reconstituted model membrane systems, employing a wide range of different physical techniques (see [6–10]). However, our understanding of the physical principles underlying lipid-protein interactions remains incomplete and the actual molecular mechanisms whereby associated lipids actually alter the activity, and presumably also the structure and dynamics, of integral membrane proteins are largely unknown. This situation is due in part to the fact that most transmembrane proteins are relatively large, multidomain macromolecules of complex and often unknown three dimensional structure and topology, that can interact with lipid bilayers in complex, multifaceted ways (see [1–10]). To overcome this problem, a number of workers have designed and synthesized peptide models of specific regions of natural membrane proteins and have studied their interactions with model lipid membranes of defined composition (see [11–13]). Physical studies of such relatively tractable model membrane systems have already significantly advanced our understanding of the molecular basis of lipid-protein interactions.

The synthetic peptide Ac-K₂-G-L₂₄-K₂-A-Amide (P₂₄) and its analogs have been successfully utilized as a model of the hydrophobic transmembrane α -helical segments of integral membrane proteins (see [12,13]). These peptides contain a long sequence of hydrophobic and strongly α -helical promoting leucine residues capped at both the N- and C-termini

with two positively charged, relatively polar lysine residues. Moreover, the normally positively charged N-terminus and the negatively charged C-terminus have both been blocked in order to provide a symmetrical tetracationic peptide which will more faithfully mimic the transbilayer region of natural membrane proteins. The central poly-leucine region of these peptides was designed to form a maximally stable α -helix, particularly in the hydrophobic environment of the lipid bilayer core, while the dilysine caps were designed to anchor the ends of these peptides to the polar surface of the lipid bilayer and to inhibit the lateral aggregation of these peptides. In fact, circular dichroism (CD) [13] and Fourier transformed infrared (FTIR) [14–16] spectroscopic studies of P₂₄ have shown that it adopts a very stable α -helical conformation both in solution and in lipid bilayers, and X-ray diffraction [17], fluorescence quenching [18] and FTIR spectroscopic [14–16] studies have confirmed that P₂₄ and its analogs assume a transbilayer orientation with the N- and C-termini exposed to the aqueous environment and the hydrophobic poly-leucine core embedded in hydrocarbon core of the lipid bilayer when reconstituted with various phosphatidylcholines. Differential scanning calorimetry (DSC) [13,15,19,20] and ²H nuclear magnetic resonance (²H-NMR) spectroscopic [13,19,20] studies have shown that P₂₄ broadens the gel/liquid-crystalline phase transition and reduces its enthalpy. The phase transition temperature is shifted either upward or downward, depending on the degree of mismatch between the hydrophobic length of the peptide and the hydrophobic thickness of phosphatidylcholine lipid bilayers [15]. As well, small distortions of the α -helical conformation of P₂₄ are also observed in response to peptide-lipid hydrophobic mismatch [15]. ²H-NMR [21] and electron spin resonance (ESR) [22] spectroscopic studies have shown that the rotational diffusion of P₂₄ about its long axis perpendicular to the membrane plane is rapid in the liquid-crystalline state of the bilayer and that a closely related peptide, Ac-K₂-L₂₄-K₂-amide (L₂₄),

exists at least primarily as a monomer in liquid-crystalline 1-palmitoyl-2-oleoyl-*sn*-glycero-3-phosphocholine (POPC) bilayers, even at relatively high peptide concentrations.

A related peptide, Ac-K₂-(L-A)₁₂-K₂-amide (LA)₁₂, in which the poly-leucine core of P₂₄ is replaced by alternating Leu and Ala residues, has also been investigated to examine whether the replacement of one half of the leucine residues by smaller and less hydrophobic alanine residues would influence the stability of the helical form of the peptide and if the surface topology of transmembrane peptides would affect its influence on lipid bilayers. The application of a variety of physical techniques has revealed that the behavior of (LA)₁₂ in solution or in lipid micelles or bilayers is generally similar to that of P₂₄ [23,24]. However, (LA)₁₂ perturbs the gel/liquid-crystalline phase transition of phosphatidylcholine (PC) bilayers to a greater extent than does P₂₄ at comparable concentrations, as inferred from the greater decrease of the temperature and enthalpy of the gel-to-liquid-crystalline phase transition, possibly due to its rougher surface topology. However, the influence of the hydrophobic mismatch between the peptide and the host lipid bilayer on the shift in the phase transition temperature is less pronounced for (LA)₁₂ than for L₂₄, possibly due in part to the greater conformational plasticity of (LA)₁₂ in response to alterations of the bilayer thickness [24].

In general, the results from the various studies of P₂₄ and related peptides obtained by different physical techniques agree rather well with one another. However, the results of several spectroscopic studies of the effects of the incorporation of these transmembrane α -helical peptides on the order of the hydrocarbon chains of the host PC bilayer do not. For example, ²H-NMR studies indicate that the incorporation of P₂₄ into 1,2-dipalmitoyl-d₆₂-*sn*-glycero-3-phosphocholine (DPPC-d₆₂) bilayers substantially decreases the time-averaged orientational order of the hydrocarbon chains in the gel and increases slightly their orientational order in the liquid-crystalline state in a manner proportional to the peptide concentration [13,19]. Similarly, a ²H-NMR study reported an ordering of the hydrocarbon chains by P₂₄ in 1-palmitoyl-d₃₁-2-oleoyl-*sn*-glycero-3-phosphocholine (POPC-d₃₁) bilayers in the liquid-crystalline state [25]. Moreover, a subsequent ESR study of the

effect of the closely related peptide L₂₄ on POPC bilayers also indicated a substantial increase in hydrocarbon chain order and a decrease in chain motional rates in proportion to the amount of peptide incorporated into the bilayer [22]. However, FTIR spectroscopic studies of the effects of P₂₄ on DPPC-d₆₂ bilayers indicate only a slight disordering of the lipid hydrocarbon chains in the gel state and essentially no effect on conformational order in the liquid-crystalline state [15]. Moreover, a complementary FTIR spectroscopic study indicated that the peptide (LA)₁₂ significantly decreases the conformational order of the lipid acyl chains in both the gel and the liquid-crystalline phases PCs [24]. However, ESR studies of the peptide (LA)₁₂ in POPC bilayers suggests that this peptide is slightly more effective than is L₂₄ in increasing the orientational order and dampening the motion of POPC hydrocarbon chains in the liquid-crystalline state (W.K. Subczynski, A. Kusumi, personal communication).

In order to resolve these discrepancies in the literature, we have undertaken a combined ²H-NMR and FTIR spectroscopic study of the effects of L₂₄ and (LA)₁₂ on the acyl chain order of both DPPC-d₆₂ and POPC-d₃₁ bilayers over a range of temperatures in their liquid-crystalline states, and have supplemented such studies with a high-sensitivity DSC analysis of these binary peptide-lipid systems. The use of lipids bearing one or two fully deuterated palmitoyl chains was indeed required to perform the ²H-NMR spectroscopy but also has the advantage, in FTIR spectroscopy, of having the methylene stretching bands shifted to a region where the transmembrane peptides do not contribute, preventing potential spectral interference. In order to insure maximum reliability and reproducibility, all three techniques were applied to the same samples, which contained a relatively high concentration of peptide (a lipid/peptide molar ratio of 20:1). This approach allows us to directly compare the effect of the two peptides on the chain order of liquid-crystalline PC bilayers under exactly the same conditions, which was not the case in previous studies. Our study indicates that both the ESR and ²H-NMR techniques provide reliable and almost comparable results indicating that both peptides order liquid-crystalline PC bilayers. On the other hand, the relative frequencies of the methylene symmetric stretching band moni-

tored by FTIR spectroscopy suggests variable effects of these peptides on hydrocarbon chain conformational order. Thus the CH₂ and CD₂ symmetric stretching frequencies do not appear to provide a reliable indication of relative hydrocarbon chain orientational order in these peptide–lipid systems.

2. Materials and methods

2.1. Materials

The peptides L₂₄ and (LA)₁₂ were synthesized exactly as previously described [23]. POPC-d₃₁ and DPPC-d₆₂ were purchased from Avanti Polar Lipids (Alabaster, AL). Deuterium-depleted water and *N*-[2-hydroxyethyl]piperazine-*N'*[2-ethanesulfonic acid] (Hepes) were obtained from Aldrich (Milwaukee, WI) and Sigma Chemical Co. (St. Louis, MO), respectively.

2.2. Preparation of peptide-containing membranes

The lipid–peptide mixtures used were prepared by co-solubilizing 30 mg of lipid and the appropriate amount of peptide in methanol and subsequently evaporating the solvent with a gentle stream of nitrogen gas. The samples were placed under vacuum for about 16 h to remove residual traces of solvent. The film was subsequently hydrated with a Hepes buffer (20 mM Hepes, with 100 mM NaCl, 2 mM EDTA (pH 7.0) in deuterium-depleted water) to obtain a final concentration of about 15% (w/w) in total lipid. The procedure involved vigorous agitation of the sample at temperatures some 10°C above the gel/liquid-crystalline phase transition temperature of the pure lipid followed by at least five freeze/thaw cycles between liquid-nitrogen temperatures and about 10°C above the gel-to-liquid-crystalline phase transition of the pure phospholipid.

2.3. Differential scanning calorimetry

Samples were prepared for DSC by diluting the NMR samples with buffer to obtain lipid concentrations near 0.5 mg/ml. The various samples were analyzed using a MicroCal VP-DSC instrument (Microcal, Northampton, MA) operating at heating

and cooling scan rates of 20°C h⁻¹. The data acquired were analyzed and plotted using the Origin software package (MicroCal Software, Northampton, MA).

2.4. ²H nuclear magnetic resonance spectroscopy

The NMR samples were transferred into a home-made Teflon sample holder of 5 mm of diameter and the ²H-NMR spectra were recorded on a Bruker DSX-300 spectrometer operating at 46 MHz for ²H and equipped with a static probe with a 5-mm coil. Data acquisition involved the acquisition of 20 000 transients using a quadrupolar echo pulse sequence in which the 90° and refocusing pulses were separated by an interpulse delay of 35 μs, and with a recycle delay of 0.5 s. A total of 8192 points were collected in the quadrature mode with a dwell time of 0.5 μs. The dePacking of the spectra obtained and interpretation of the dePacked spectra in terms of smoothed segmental order profiles were achieved using previously published procedures [26]. Sample temperature was controlled with a Bruker variable temperature unit.

2.5. Fourier transform infrared spectroscopy

For FTIR spectroscopy experiments, an aliquot of the sample freshly hydrated or an aliquot of the NMR sample which had been lyophilized and subsequently rehydrated was squeezed between the CaF₂ windows of a heatable, demountable liquid cell equipped with a 5-μm Teflon spacer. Spectra were recorded at a resolution of 2 cm⁻¹ using previously published data acquisition protocols [27] with a BioRad FTS-25 spectrometer (BioRad, Cambridge, MA) equipped with an MCT detector. Sample temperature was controlled with thermopumps using a home-made controller [28]. The contribution of water was subtracted using a least-square fitted polynomial simulating the edge of the water O–H stretching band around 3400 cm⁻¹ in the C–H stretching region or by subtracting the buffer spectrum recorded at the same temperature to eliminate the contribution of the association band of water at 2070 cm⁻¹ in the C–D stretching region. The band maxima reported in this paper correspond to the centers of gravity calculated on the top 5% of the bands.

3. Results

3.1. Differential scanning calorimetry studies

DSC heating thermograms of aqueous dispersions of DPPC- d_{62} alone, or of L_{24} - or $(LA)_{12}$ -DPPC- d_{62} mixtures at a lipid-peptide ratio of 20:1, are presented in Fig. 1. The heating and cooling (not shown) scans of DPPC- d_{62} alone reveal two phase transitions, a lower temperature, less energetic pretransition and a higher temperature main phase transition. The pretransition, which occurs at about 30°C on heating and which exhibits a transition enthalpy of 0.9 kcal/mol on heating or cooling, corresponds to the transition from the planar gel (L_{β}') to the rippled gel (P_{β}') phase and exhibits appreciable hysteresis on cooling. The main phase transition, which occurs at 37.0°C on heating and which exhibits a transition enthalpy of 8.4 kcal/mol on heating or cooling, corresponds to the transition from the P_{β}' to the lamellar liquid-crystalline (L_{α}) phases and exhibits only a small degree of hysteresis. These results agree well

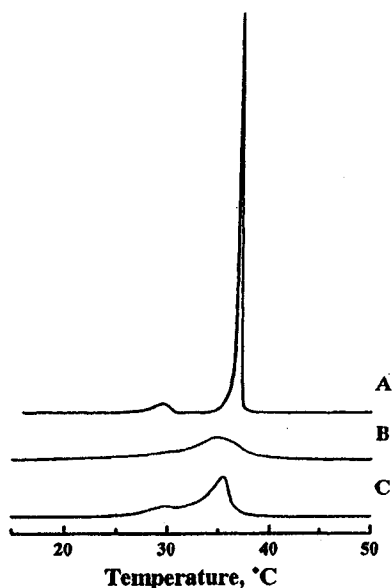


Fig. 1. DSC heating thermograms illustrating the thermotropic phase behavior of (A) DPPC- d_{62} and its mixtures with the peptides (B) L_{24} and (C) $(LA)_{12}$.

with those of most previous studies of DPPC- d_{62} large multilamellar vesicles (MLVs) (see Lipid Data Base). A subtransition was not observed here as these samples were not incubated at low temperatures for the long periods of time required for subgel phase formation (see [29]).

The incorporation of either peptide into the DPPC- d_{62} MLVs generally results in a decrease of the enthalpy but not in the temperature of the pretransition, which nevertheless persists at the peptide concentration studied here, and a reduction in the temperature, enthalpy and cooperativity of the main phase transition. When the contribution of the pretransition, present as a lower temperature, hysteresis-exhibiting shoulder on the heating and cooling endotherms, is subtracted, we find that the temperature corresponding to the mid-point of the main phase transition and enthalpy of the L_{24} - and $(LA)_{12}$ -containing samples are reduced to about 34°C and 33°C and 7.7 and 7.1 kcal/mol, respectively. The more pronounced reduction in the temperature and enthalpy of the gel/liquid-crystalline phase transition temperatures of DPPC- d_{62} MLVs by $(LA)_{12}$ as compared to L_{24} agrees well with previous DSC studies of $(LA)_{12}$ and P_{24} in 1,2-dipalmitoyl-*sn*-glycero-3-phosphocholine (DPPC) MLVs [15, 24], and with the results of the FTIR studies to be discussed below.

DSC studies were also attempted with pure and peptide-containing POPC- d_{31} MLVs. By employing cooling scans to supercool the aqueous phase and thus to delay ice formation, we were able to detect a sharp exotherm for POPC- d_{31} at -7.5°C prior to the onset of the large ice formation exotherm. However, using the same approach, we could not detect discrete exotherms for the peptide-containing POPC- d_{31} samples. A reduction in the temperature, enthalpy and cooperativity of the POPC- d_{31} MLVs exotherm by the presence of these peptides apparently precluded an accurate determination of their thermotropic phase behavior by DSC.

3.2. FTIR spectroscopy

The thermotropic phase behavior of DPPC- d_{62} and of its mixtures with the peptides L_{24} and $(LA)_{12}$ were examined by monitoring the temperature-dependent changes in the symmetric CD_2

stretching band (ν_{C-Ds}) of the phospholipid hydrocarbon chains which is centered near 2090 cm^{-1} . The frequency of this methylene symmetric stretching vibrational mode is known to be sensitive to changes in the conformational order of lipid hydrocarbon chains and it can therefore be used to monitor the progress of lipid gel/liquid-crystalline phase transitions [30]. Fig. 2A shows that DPPC- d_{62} undergoes a highly cooperative hydrocarbon chain-melting phase transition, as indicated by an abrupt increase in the ν_{C-Ds} frequency from values near 2089 cm^{-1} at temperatures below the transition temperature to values near 2094 cm^{-1} at higher temperatures, respectively. These frequency changes are also accompanied by the significant broadening of the overall band envelope (data not shown). Such changes are typical of hydrocarbon chain-melting phase transitions such as occurs at the gel/liquid-crystalline phase transitions of hydrated lipid bilayers [30]. Fig. 2A also shows that comparable temperature-induced changes in ν_{C-Ds} band frequency also occur with the L_{24} - and $(LA)_{12}$ -containing DPPC- d_{62} mixtures, but these changes are observed at a lower temperatures and span a broader temperature range than with the pure lipid, observations in qualitative agreement with the DSC data presented above. Moreover, an examination of the first derivatives of these temperature-induced frequency changes (Fig. 2B) shows that the estimated midpoint temperatures of the gel/liquid-crystalline phase transitions of the pure lipid, L_{24} -containing and $(LA)_{12}$ -containing MLVs occur at temperatures near 38°C , 37°C and 34°C , respectively, values in reasonable but not exact agreement with the calorimetrically derived values. Comparable studies of the thermotropic phase behavior of POPC- d_{31} and its peptide-containing mixtures were not performed because of problems arising from the freezing of the aqueous phase at the low temperatures at which POPC- d_{31} exhibits its gel/liquid-crystalline phase transition.

The IR data also display the relative effects of the incorporated peptide on the symmetric stretching frequencies of the CD_2 or CH_2 bands exhibited by MLVs. The data shown in Fig. 2A indicate that at low temperatures, the ν_{C-Ds} frequencies exhibited by the L_{24} - and $(LA)_{12}$ -containing DPPC- d_{62} preparations are comparable and are both higher than those of the pure lipid. These results are consistent with the

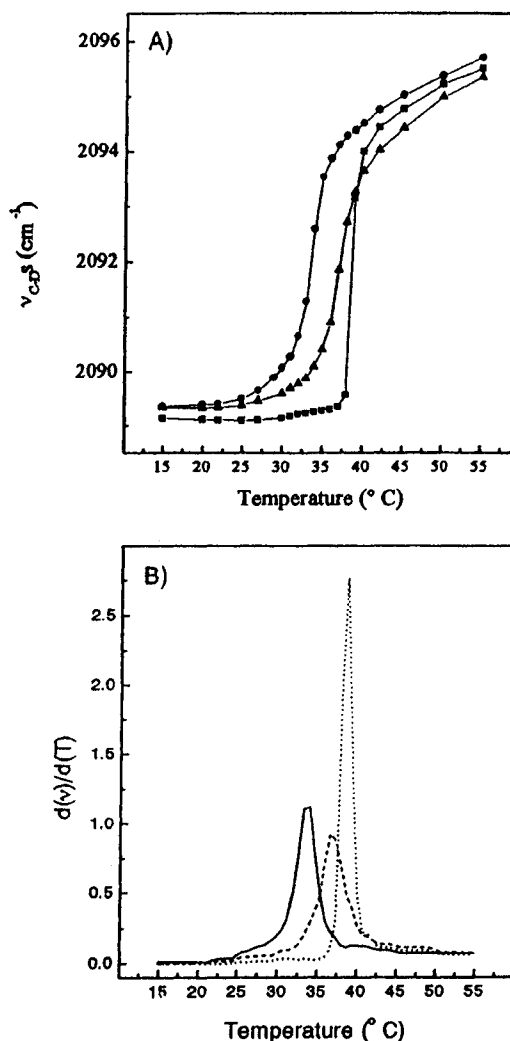


Fig. 2. (A) Thermotropic phase behavior of pure DPPC- d_{62} (■), and DPPC- d_{62}/L_{24} (▲) and DPPC- $d_{62}/(LA)_{12}$ (●) mixtures (lipid/peptide molar ratio of 20:1), as probed by the position of the C-D methylene symmetric stretching band. (B) First derivatives of the curves shown in A. (—) Pure DPPC- d_{62} ; (---) DPPC- d_{62}/L_{24} mixture; (····) DPPC- $d_{62}/(LA)_{12}$ mixture.

increased frequency of the symmetric CH_2 stretching band (ν_{C-Hs}) observed in gel-phase DPPC bilayers upon incorporation of $(LA)_{12}$ [24] and the analog P_{24} [15], an experimental observation that was interpreted as a slight disorder of the all-*trans* hydrocar-

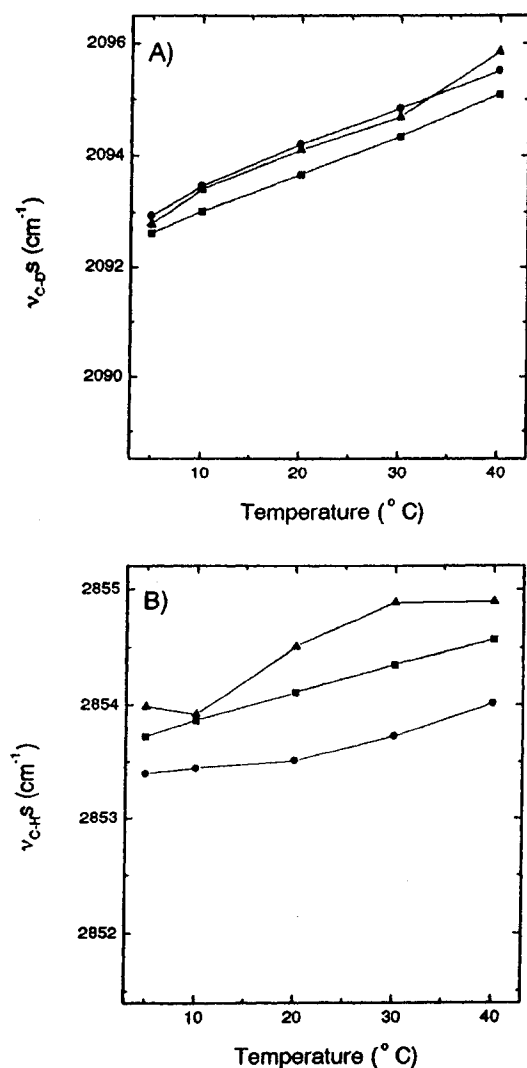


Fig. 3. (A) Position of the CD₂ symmetric stretching (ν_{C-D_S}) band of pure POPC-d₃₁ (■), and POPC-d₃₁/L₂₄ (▲) and POPC-d₃₁/(LA)₁₂ (●) mixtures (lipid/peptide molar ratio of 20:1). (B) Position of the C-H methylene symmetric stretching (ν_{C-H_S}) band of pure POPC-d₃₁ (■), and POPC-d₃₁/L₂₄ (▲) and POPC-d₃₁/(LA)₁₂ (●) complexes (lipid/peptide molar ratio of 20:1). The y-axis of both graphs has been scaled to obtain an equivalent relative amplitude of a gel-to-liquid-crystalline phase transition.

bon chains of DPPC gel-state bilayers caused by these peptides. At temperatures above the transition temperature, our results indicate that the ν_{C-D_S} frequencies exhibited by the (LA)₁₂-containing samples are higher than those exhibited by the pure lipid which, in turn, are higher than those exhibited by the L₂₄-containing mixtures. (Fig. 2A). The observations related to (LA)₁₂ are consistent with previous results indicating an increased of ν_{C-H_S} frequency upon incorporation of (LA)₁₂ in perhydrogenated DPPC fluid bilayers [24]. However, it was shown that the addition of the analog P₂₄ has practically no effect on the position of the ν_{C-H_S} or ν_{C-D_S} frequency of DPPC or DPPC-d₆₂, respectively [15]. These spectral changes were interpreted as suggesting that whereas (LA)₁₂ incorporation conformationally disorders liquid-crystalline DPPC-d₆₂ bilayers, L₂₄ incorporation has no effect on DPPC-d₆₂ conformational order at temperatures above the transition temperature.

With the POPC-d₃₁-based system, data were only available for the liquid-crystalline phase. With these samples, however, one can compare the relative effects of the incorporated peptide on the conformational order of the oleoyl and perdeuterated palmitoyl chains separately by examining the frequencies of the CH₂ and CD₂ symmetric stretching bands, respectively. The data shown in Fig. 3A indicate that throughout the temperature range examined, the frequencies exhibited by the L₂₄- and (LA)₁₂-containing POPC-d₃₁ preparations are comparable and are both higher than the those exhibited by the pure lipid. If these spectral changes are strictly interpreted in terms of conformational order, they would suggest that the two peptides cause a comparable disordering of the palmitoyl chains of liquid-crystalline POPC bilayers. In contrast, an examination of the CH₂ symmetric frequencies of the same sample (Fig. 3B) suggests that, whereas the peptide L₂₄ disorders the oleoyl chains of POPC, the peptide (LA)₁₂ orders those chains. These FTIR spectroscopic results are apparently internally inconsistent, and, as will be shown below, they are also inconsistent with the results of our ²H-NMR spectroscopic studies. The possible basis of these observations will be examined later.

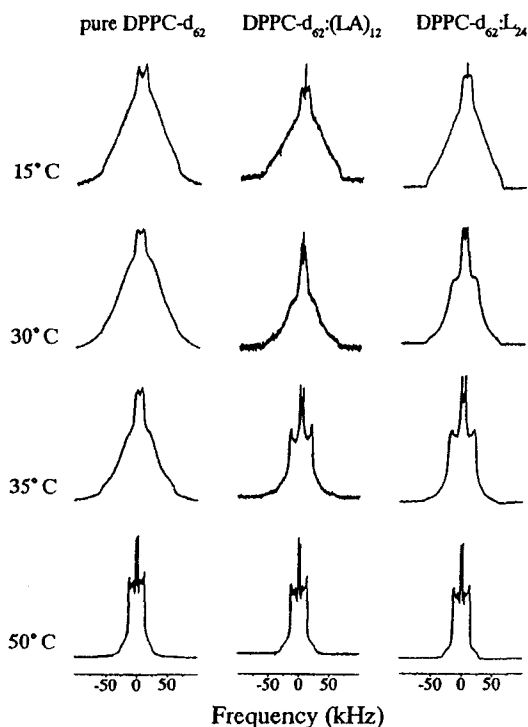


Fig. 4. ^2H -NMR spectra of pure DPPC- d_{62} and DPPC- d_{62}/L_{24} and DPPC- $d_{62}/(LA)_{12}$ mixtures (lipid/peptide molar ratio of 20:1). The temperatures are indicated on the left.

3.3. ^2H -NMR spectroscopy

Illustrated in Fig. 4 are the ^2H -NMR spectra obtained with DPPC- d_{62} in the presence and absence of the transmembrane peptides. At temperatures near 15°C, the spectra of pure DPPC- d_{62} and its mixtures with the peptides all show powder patterns typical of gel-phase bilayers [31]. Upon heating, a component typical of fluid-phase bilayers, composed of overlapping powder patterns associated with axially symmetric systems, appears in the spectra of the lipid-peptide mixtures. The shift of the gel-to-fluid phase transition towards the low temperatures caused by the presence of the peptides, as detected by FTIR spectroscopy and DSC, can also be observed in the NMR spectra at 35°C, since the spectrum of pure DPPC- d_{62} still shows exclusively a typical gel-phase profile whereas the spectra of the peptide-containing

samples display a significant proportion of a fluid component, indicating that, in these conditions, lipids form a two-phase (gel and fluid) system. Similar spectra were obtained for the complex DPPC- $d_{62}:L_{24}$ (31:1) by Huschilt et al. [19]. At 50°C, the spectra of pure DPPC- d_{62} and DPPC- d_{62} in the presence of L_{24} or $(LA)_{12}$ are typical of the lamellar liquid-crystalline phase and the presence of the peptides leads to an increase of the spectral width. Thus, for example, the

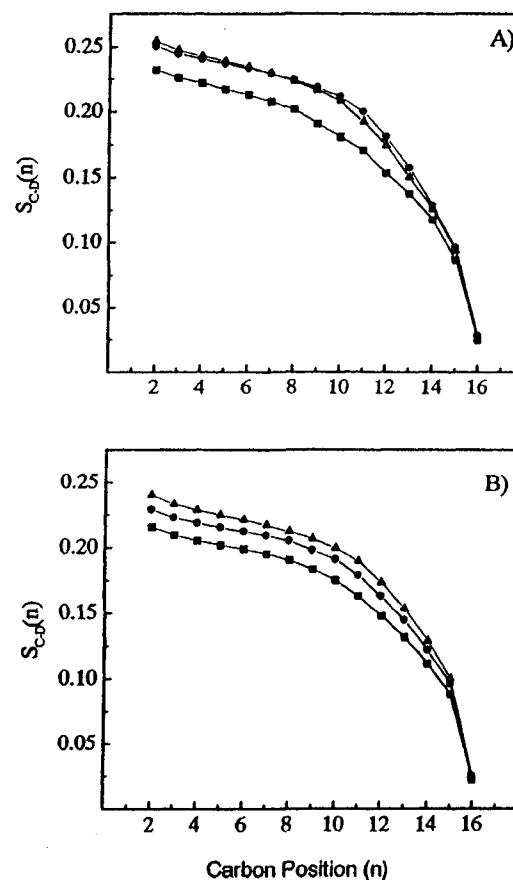


Fig. 5. (A) Smoothed order profiles determined for pure POPC- d_{31} (■), and POPC- d_{31}/L_{24} (▲) and POPC- $d_{31}/(LA)_{12}$ (●) mixtures (lipid/peptide molar ratio of 20:1), at 15°C. (B) Smoothed order profiles determined for pure DPPC- d_{62} (■), and DPPC- d_{62}/L_{24} (▲) and DPPC- $d_{62}/(LA)_{12}$ (●) mixtures (lipid/peptide molar ratio of 20:1), at 50°C.

quadrupolar splittings associated with lipid CD₂ groups located near to the bilayer polar/apolar interface increases from values near 24.6 kHz with the pure phospholipid samples to values near 26.3 and 27.2 kHz with the (LA)₁₂- and L₂₄-containing samples, respectively. A similar increase of orientational order caused by the peptide P₂₄ has been already reported from an increase of the first moment of the spectra [19]. The smoothed segmental order profiles constructed from spectra obtained at 50°C (see Fig. 5B) show that throughout the entire length of the fatty acyl chain, segmental order parameters derived from the L₂₄- and (LA)₁₂-containing membranes are both higher than those derived from the pure lipid preparations, except possibly for the terminal CD₃ groups, whose mobility is strongly influenced by the free rotation along the CD₂–CD₃ bond. The order parameters obtained with the L₂₄-containing samples appears to be consistently higher than those obtained with the (LA)₁₂-containing preparations (Fig. 5B), suggesting that L₂₄ may exert a greater ordering effect on liquid-crystalline DPPC hydrocarbon chains than does (LA)₁₂. As illustrated in Fig.

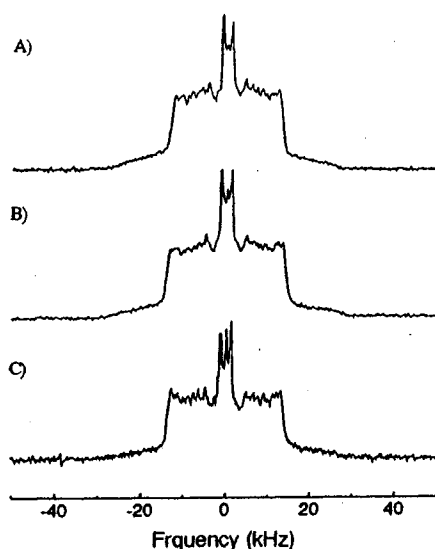


Fig. 6. ²H-NMR spectra of (A) pure POPC-d₃₁, and (B) POPC-d₃₁/L₂₄ and (C) POPC-d₃₁/(LA)₁₂ mixtures (lipid/peptide molar ratio of 20:1), recorded at 30°C.

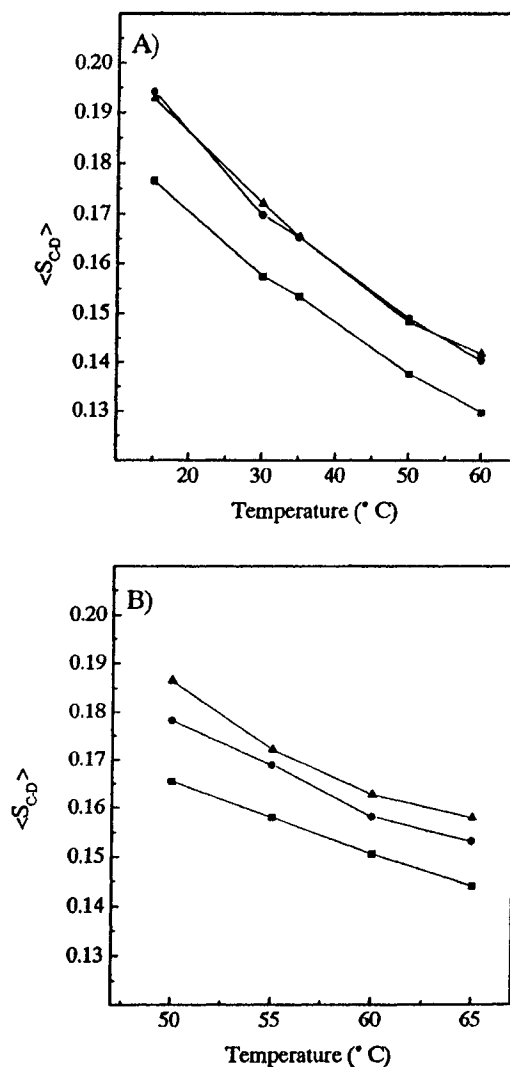


Fig. 7. Plots of chain-averaged order parameters as a function of temperature. (A) POPC-d₃₁ (■), POPC-d₃₁/L₂₄ (▲) and POPC-d₃₁/(LA)₁₂ (●) mixtures at a lipid/peptide molar ratio of 20:1. (B) DPPC-d₆₂ (■), DPPC-d₆₂/L₂₄ (▲) and DPPC-d₆₂/(LA)₁₂ (●) mixtures at a lipid/peptide molar ratio of 20:1.

7B, this effect is observed at all temperatures examined where the lipid is in the liquid-crystalline state.

The effect of (LA)₁₂ and L₂₄ on the orientational order of the lipid acyl chains was also determined in

POPC-d₃₁ bilayers. Fig. 6 displays ²H-NMR spectra obtained for pure POPC-d₃₁ and its mixtures with (LA)₁₂ and L₂₄ at a molar lipid/peptide ratio of 20:1 at temperatures near 30°C. Because the gel/liquid-crystalline phase transitions of these samples occur at temperatures below 0°C, these three samples all exhibit exclusively axially symmetric powder patterns typical of lipids in the lamellar liquid-crystalline phase throughout the entire temperature range examined (5–60°C) and, as observed with the DPPC-d₆₂-based mixtures, quadrupolar splittings exhibited by the peptide-containing preparations are higher than those observed by the pure lipid. Thus, for example, the splitting of the widest doublet increases from values near 24.4 kHz with pure POPC-d₃₁ to values near 25.9 and 26.6 kHz for the (LA)₁₂- and L₂₄-containing mixtures, respectively. The smoothed segmental order profiles derived from the spectra (see Fig. 5A) indicate that with the both the L₂₄- and (LA)₁₂-containing preparations, a comparable peptide-induced increase of the orientational order occurs at all positions along the acyl chain, except the terminal CD₃ group and, as illustrated in Fig. 7A, this effect is observed at all temperatures examined. These peptide-induced increases in CD₂ segmental order parameters are comparable to those observed in previous ²H-NMR spectroscopic studies of P₂₄-containing POPC membranes [25], and are consistent with the L₂₄-induced orientational ordering of POPC observed in previous reported ESR spectroscopic studies [22]. The present results suggest that both L₂₄ and (LA)₁₂ tend to order hydrocarbon chains in POPC bilayers to a comparable extent.

4. Discussion

An objective of the present work was to evaluate the impact of two transmembrane peptides with different surface topology on the lipid acyl chains of fluid PC bilayers. Our ²H-NMR spectroscopic results clearly indicate that the incorporation of both L₂₄ and (LA)₁₂ significantly increase the time-averaged orientational order of hydrocarbon chains in liquid-crystalline DPPC-d₆₂ and POPC-d₃₁ bilayers, an effect observed at all positions along the hydrocarbon chain and at all temperatures examined. The results

with L₂₄ are consistent with those of previous ²H-NMR spectroscopic studies where increases in hydrocarbon chain orientational order were observed when the structurally related peptide P₂₄ was incorporated into liquid-crystalline DPPC-d₆₂ [13,19] and POPC-d₃₁ [25] bilayers. The present work reveals that (LA)₁₂ also orders PC bilayers. This finding is supported by our ESR spectroscopic studies in progress, where the incorporation of L₂₄ and (LA)₁₂ into liquid-crystalline POPC bilayers causes an increase in the orientational order and a decrease in the rates of motion of the lipid hydrocarbon chains ([22]; W.K. Subczynski, A. Kusumi, personal communication). However, these findings are not in accord with the FTIR spectroscopic results of the present and previous work [15,24], where in most cases, increases in the frequencies of CH₂ and CD₂ stretching bands are observed, and these spectral changes have been empirically associated with a disordering of the lipid chains in the liquid-crystalline state by these peptides.

The puzzling and often inconsistent conclusions derived from FTIR spectroscopic data raises the issue of the reliability of the widespread practice of using CH₂ and CD₂ stretching frequencies as indicators of relative hydrocarbon chain conformational order or disorder. This molecular interpretation is empirically based on the fact that the gel to liquid/crystalline phase transition temperature is accompanied by an increase (typically 2–5 cm⁻¹) in the frequency of the CH₂ (or CD₂) symmetric stretching vibrations because of the conversion of the conformationally highly ordered all-*trans* hydrocarbon chains characteristic of the gel state into the conformationally disordered chains characteristic of the liquid-crystalline state (see [29,32]). Moreover, the relative frequency of the CH₂ (or CD₂) symmetric stretching vibration in the liquid-crystalline state seems to be quantitatively related to the relative degree of hydrocarbon order in many, but not in all, phospholipid model membrane systems (see [29,32,33]). For this reason, shifts in the CH₂ (or CD₂) symmetric stretching frequencies have often been used to assess the effects of the addition of cholesterol [34,35], peptides [15,24] or proteins (see [36]) on hydrocarbon chain conformational order in the gel and liquid-crystalline states of the host lipid bilayer. However, it has been shown that other phenomena,

such as changes in interchain coupling and librotorsional motions, can also induce shifts in the frequency of the methylene stretching bands, even in the absence of changes in hydrocarbon chain conformational order [37]. For example, interchain coupling is significant enough even in fluid lipid bilayers that its alteration by isotopic dilution can lead to a ν_{C-D} frequency shift of more than 2 cm^{-1} [37]. The incorporation of transmembrane peptides in the lipid bilayer is likely to affect the interchain coupling in addition to its potential effect on lipid chain order. In addition, the CH_2 stretching band should also contain contributions from the amino acid side chains of the peptide; such potential spectral interference, that is dependent on the side chain composition, is difficult to correct adequately and can alter the absolute value of the frequency of the measured for the band maximum. Given this, the molecular interpretation of a shift in the frequency of these bands exclusively in terms of hydrocarbon chain conformational order is probably not justified. We also note that there are other examples in the literature in which the frequency of the CH_2 symmetric stretching mode also does not appear to be well correlated with lipid hydrocarbon chain order (e.g. [34,35,38]).

The ^2H -NMR and IR measurements do not probe the chain order in the same way. As discussed elsewhere [1,33], the two techniques do not report the same type of order (conformational versus orientational), do not respond on the same time scale, and do not express the order distribution along the acyl chain the same way. The order parameters in ^2H -NMR spectroscopy are primarily sensitive to *trans/gauche* isomerization, as is the case of FTIR spectroscopy, even though the wobbling of the director axis associated with the lipid fast rotation may play some role in the averaging of the NMR quadrupolar interactions [33]. Thus the increased ^2H -NMR order parameters caused by the transmembrane peptides are almost certainly a consequence of reduced segmental motions along the lipid acyl chains resulting from a decrease of rotational isomerism. Therefore, the contradictory and unreliable molecular interpretation drawn from the frequency of the methylene stretching modes in IR spectroscopy are likely attributed to the sensitivity of the band position to phenomena other than *trans/gauche* isomerization such as the interchain coupling and the

contribution of peptide in the methylene and methyl stretching regions.

A key factor which may influence the effect of α -helical transmembrane peptides on the orientational order of lipid hydrocarbon chains is the degree of mismatch between the length of the hydrophobic segment of the peptide and the intrinsic hydrophobic thickness of the host lipid bilayer. The effect of such hydrophobic mismatch has been considered in the so-called mattress model [39], which postulates that the phospholipid chains will either extend (become more ordered) or shorten (become more disordered) in order to match their length as closely as possible to the hydrophobic segment of the peptide, so as to minimize contact between water and hydrophobic surfaces on the lipid or peptide [25,39]. Thus, if one assumes that the peptides L_{24} and $(LA)_{12}$ are oriented perpendicular to the lipid bilayer [17,24], then the actual and effective lengths of their 24-amino-acid hydrophobic core should be about 30–31 Å [15,24], a value larger than the ~ 26 Å expected for liquid-crystalline DPPC and POPC bilayers at temperatures just above their gel/liquid-crystalline phase transition temperatures [40]. Given these observations, hydrophobic mismatch considerations would predict that with the systems studied here, both peptides should induce some lengthening (i.e., ordering) of the phospholipid hydrocarbon chains at temperatures above T_m as observed. Such an ordering has been observed previously for P_{24} in POPC [25] and DPPC- d_{62} bilayers [13,19]. The present study extends the observation of this behavior to the analog L_{24} peptide and to a peptide composed of alternating Ala and Leu residues, leading to a rougher surface topology. It should be mentioned that $(LA)_{12}$, the peptide with the more compositionally complex transmembrane core and rougher surface topology, seems to exert a smaller ordering effect on liquid-crystalline DPPC bilayers than does L_{24} , but its overall effect is still a considerable ordering of the lipid chains. Interestingly, the introduction of peptides containing an alternating leucine and alanine segment flanked on both sides with tryptophan residues (WALP peptides) in PC membranes has also shown systematic changes of bilayer thickness related to the hydrophobic mismatch [41].

It is not yet established how the surface topology of the helix surface influences the order of the neigh-

boring lipid chains. The set of data presented here provides some insights into this aspect since the effect of two peptides with different surface topology on lipid chain order has been examined in the same conditions. We have found that despite the replacement of one half of the leucine residues by smaller and less hydrophobic alanine, there is no considerable difference in their chain stiffening effect, suggesting that the different surface topology of the two investigated transmembrane helices does not have a considerable effect on fluid-lipid chain order. The primary sequence variations between L_{24} and $(LA)_{12}$ are relatively modest, but one should note that they are sufficient to have a marked effect on the stability of the helical structure of the peptide [23]. Moreover, the surface topology effects may also explain why L_{24} causes smaller reductions in the temperature and enthalpy of the gel/liquid-crystalline phase transition of DPPC bilayers than does $(LA)_{12}$. The DSC and FTIR spectroscopic results presented here indicate that the incorporation of $(LA)_{12}$ into DPPC- d_{62} MLVs produces a greater reduction in the lipid gel/liquid-crystalline phase transition temperature and enthalpy than does the incorporation of a comparable amount of L_{24} . These findings are consistent with the results of previous calorimetric studies of the effects of the peptides $(LA)_{12}$ and P_{24} on DPPC and other linear saturated PC bilayers [14,24]. Since the peptides L_{24} and $(LA)_{12}$ have roughly comparable ordering effects in the liquid-crystalline states of both DPPC and POPC bilayers, we presume that the greater reduction in the gel/liquid-crystalline phase transition temperature and enthalpy by $(LA)_{12}$ arises primarily from exerting a greater destabilizing effect on of the gel state of PC bilayers. The results of previous FTIR spectroscopic studies of the peptides P_{24} and $(LA)_{12}$ in PC bilayers [15,24] would seem to support this conclusion. However, since our present findings indicate that the CH_2 and CD_2 symmetric stretching frequencies are not reliable indicators of hydrocarbon chain conformational order in these systems, firm conclusions about the effect of these peptides on lipid chains in gel-state bilayers cannot be drawn from this and previous FTIR spectroscopic studies; additional studies using more reliable techniques will be required to address this question adequately.

In biological membranes, it has been reported that

the presence of integral transmembrane proteins either does not alter hydrocarbon chain orientational order in the liquid-crystalline state [42] or may orientationally disorder liquid-crystalline phospholipid chains [43]. The evolutionary selection of proteins for which the match between the length of their apolar transmembrane segments and the hydrophobic section of the membrane that are inserted in is good has been proposed to be at the origin of the very limited effect of membrane proteins on the lipid chain order observed on various bacterial membranes [39]. Other phenomena like peptide tilting could also take place to compensate for the hydrophobic mismatch when the length of the peptide exceeds the hydrophobic thickness of the host lipid bilayers [12]. Moreover, previous studies have shown that the transmembrane α -helical peptides P_{24} and $(LA)_{12}$ may not behave as rigid cylinders in lipid bilayers, as often assumed in theoretical studies, but may exhibit some changes in helical conformation in response to changes in the hydrophobic thickness of the host bilayer [15,24]. In addition, the more compositionally complex peptide $(LA)_{12}$ appears to be more conformationally flexible than is the more compositionally homogenous peptide L_{24} . It is therefore possible that the very compositionally heterogeneous transmembrane α -helices of natural membrane proteins may more readily alter their conformation in order to match their hydrophobic thickness with that of the host lipid bilayer, which could, in turn, attenuate their ordering effect on the hydrocarbon chains of adjacent lipid molecules. The idea of membrane lipid thickness-induced conformational distortions of the transmembrane segments of membrane proteins is compatible with the so-called squishy protein hypothesis [44] which proposes that the surface of transmembrane helical protein segments is fairly soft and malleable, leading to a smooth interfacing of the peptide and the lipid bilayer [44]. The limited effect of the peptide surface topology on lipid chain order presented here is compatible with the squishy protein hypothesis [44]. However, natural transmembrane proteins and these α -helical transmembrane peptides may display important differences in their surface topologies. Unlike peptides such as P_{24} , L_{24} , or even $(LA)_{12}$, which have a rather compositionally homogenous hydrophobic core and consequently relatively smooth cylindrically symmetrical

surface topologies, the transmembrane segments of natural transmembrane proteins are compositionally heterogeneous entities with rougher and more varied surface topologies, which may therefore interact differently with adjacent lipids. In this regard one should note that in a recent ^2H -NMR and ESR spectroscopic study of a series of synthetic transmembrane α -helical peptides and gramicidin A, it was concluded that both the effective hydrophobic length and the structure of the peptide surface can affect hydrocarbon chain order in liquid-crystalline phosphatidylcholine bilayers [41]. It would clearly be valuable to extend the ^2H -NMR spectroscopic experiments reported here to a series of PCs of widely varying hydrocarbon chain length in order to better quantify any hydrophobic mismatch effects between a single transmembrane peptide and phospholipid bilayers of different thicknesses, and to transmembrane peptides with more pronounced changes in amino acid composition to separate this effect from any surface topology effects.

Acknowledgements

This work was supported by the Natural Sciences and Engineering Research Council of Canada (M.L.), by the Québec Fonds FCAR (M.L.), by operating and major equipment grants from the Medical Research Council of Canada (R.N.M.), and by a major equipment grant from the Alberta Heritage Foundation for Medical Research (R.N.M.).

References

- [1] R.B. Gennis, *Biomembranes: Molecular Structure and Function*, Springer, New York, 1989.
- [2] P. Yeagle, *The Structure of Biological Membranes*, CRC Press, Boca Raton, FL, 1992.
- [3] H. Sandermann, *Biochim. Biophys. Acta* 515 (1978) 209–237.
- [4] R.N. McElhaney, in: S. Razin, S. Rottem (Eds.), *Current Topics in Membranes and Transport*, vol. 17, Academic Press, New York, 1982, pp. 317–380.
- [5] R.N. McElhaney, in: R.A. Aloia, J.M. Boggs (Eds.), *Membrane Fluidity in Biology*, vol. 4, Academic Press, New York, 1985, pp. 147–208.
- [6] R.N. McElhaney, *Biochim. Biophys. Acta* 864 (1986) 361–421.
- [7] A. Watts, J.J.H.M. De Pont (Eds.), *Progress in Lipid-Protein Interactions*, vol. 1, Elsevier, Amsterdam, 1986.
- [8] A. Watts, J.J.H.M. De Pont (Eds.), *Progress in Lipid-Protein Interactions*, vol. 2, Elsevier, Amsterdam, 1986.
- [9] D. Marsh, L.I. Horváth, *Biochim. Biophys. Acta* 1376 (1998) 267–296.
- [10] A. Watts, *Biochim. Biophys. Acta* 1376 (1998) 297–318.
- [11] S.H. White, W.C. Wimley, *Biochim. Biophys. Acta* 1376 (1998) 339–352.
- [12] J.A. Killian, *Biochim. Biophys. Acta* 1376 (1998) 401–416.
- [13] J.M. Davis, D.M. Clare, R.S. Hodges, M. Bloom, *Biochemistry* 22 (1983) 5298–5305.
- [14] Y.-P. Zhang, R.N.A.H. Lewis, R.S. Hodges, R.N. McElhaney, *Biochemistry* 31 (1992) 11572–11578.
- [15] Y.-P. Zhang, R.N.A.H. Lewis, R.S. Hodges, R.N. McElhaney, *Biochemistry* 31 (1992) 11579–11588.
- [16] P.H. Axelsen, B.K. Kaufman, R.N. McElhaney, R.N.A.H. Lewis, *Biophys. J.* 69 (1995) 2770–2781.
- [17] J.C. Huschilt, B.M. Millman, J.H. Davis, *Biochim. Biophys. Acta* 979 (1989) 139–141.
- [18] E.J. Bolen, P.W. Holloway, *Biochemistry* 29 (1990) 9638–9643.
- [19] J.C. Huschilt, R.S. Hodges, J.H. Davis, *Biochemistry* 24 (1985) 1377–1386.
- [20] M.R. Morrow, J.C. Huschilt, J.H. Davis, *Biochemistry* 24 (1985) 5396–5406.
- [21] K.P. Pauls, A.L. MacKay, O. Soderman, M. Bloom, A.K. Taneja, R.S. Hodges, *Eur. Biophys. J.* 12 (1985) 1–11.
- [22] W.K. Subczynski, R.N.A.H. Lewis, R.N. McElhaney, R.S. Hodges, J.S. Hyde, A. Kusumi, *Biochemistry* 37 (1998) 3156–3164.
- [23] Y.-P. Zhang, R.N.A.H. Lewis, G.D. Henry, B.D. Sykes, R.S. Hodges, R.N. McElhaney, *Biochemistry* 34 (1995) 2348–2361.
- [24] Y.-P. Zhang, R.N.A.H. Lewis, R.S. Hodges, R.N. McElhaney, *Biochemistry* 34 (1995) 2362–2371.
- [25] F.A. Nezil, M. Bloom, *Biophys. J.* 61 (1992) 1176–1183.
- [26] M. Lafleur, B. Fine, E. Sternin, P.R. Cullis, M. Bloom, *Biophys. J.* 56 (1989) 1037–1041.
- [27] M. Lafleur, *Can. J. Chem.* 76 (1998) 1501–1511.
- [28] M. Pérolet, B. Boulé, D. Bourque, *Rev. Sci. Instrum.* 54 (1983) 1364–1367.
- [29] H.L. Casal, H.H. Mantsch, *Biochim. Biophys. Acta* 779 (1984) 381–402.
- [30] R.N.A.H. Lewis, R.N. McElhaney, in: H.H. Mantsch, D. Chapman (Eds.), *Infrared Spectroscopy of Biomolecules*, Wiley-Liss, New York, 1996, pp. 159–202.
- [31] J.H. Davis, *Biophys. J.* 27 (1979) 339–358.
- [32] H.H. Mantsch, R.N. McElhaney, *Chem. Phys. Lipids* 57 (1991) 213–216.
- [33] V.R. Kodati, M. Lafleur, *Biophys. J.* 64 (1993) 163–170.
- [34] T.P.W. McMullen, R.N.A.H. Lewis, R.N. McElhaney, *Biophys. J.* 66 (1994) 741–752.
- [35] L. Senak, D. Moore, R. Mendelsohn, *J. Phys. Chem.* 96 (1992) 2749–2754.
- [36] R. Mendelsohn, H.H. Mantsch, in: A. Watts, J.J.H.M. De

- Pont (Eds.), *Progress in Lipid-Protein Interactions*, vol. 2, Elsevier, Amsterdam, 1986, pp. 103–146.
- [37] V.R. Kodati, R. El Jastimi, M. Lafleur, *J. Chem. Phys.* 98 (1994) 12191–12197.
- [38] K. Brandenburg, S.S. Funari, M.H.J. Koch, U. Seydel, *J. Struct. Biol.* 128 (1999) 175–186.
- [39] O.G. Mouritsen, M. Bloom, *Biophys. J.* 46 (1984) 141–153.
- [40] M.M. Sperotto, O.G. Mouritsen, *Eur. Biophys. J.* 16 (1988) 1–10.
- [41] M.R.R. de Planque, D.V. Greathouse, R.E. Koeppel, H. Schafer, D. Marsh, J.A. Killian, *Biochemistry* 37 (1998) 9333–9345.
- [42] M. Bloom, I.C.P. Smith, in: A. Watts, J.J.H.H.M. DePont (Eds.), *Progress in Lipid-Protein Interactions*, vol. 1, Elsevier, Amsterdam, 1985, pp. 61–88.
- [43] D. Marsh, in: A. Watts, J.J.H.H.M. DePont (Eds.), *Progress in Lipid-Protein Interactions*, vol. 1, Elsevier, Amsterdam, 1985, pp. 143–173.
- [44] M. Bloom, *Can. J. Phys.* 57 (1979) 2227–2230.